TRIESKOVÉ A BEZTRIESKOVÉ OBRÁBANIE DREVA 2022

CHIP AND CHIPLESS WOODWORKING PROCESSES 2022

Vedecký časopis // Scientific journal

Technická univerzita vo Zvolene // Technical University in Zvolen
Drevárska fakulta // Faculty of Wood Sciences and Technology
Katedra obrábania dreva // Department of Woodworking

TECHNICKÁ UNIVERZITA VO ZVOLENE // TECHNICAL UNIVERSITY IN ZVOLEN
DREVÁRSKA FAKULTA // FACULTY OF WOOD SCIENCES AND TECHNOLOGY
KATEDRA OBRÁBANIA DREVA // DEPARTMENT OF WOODWORKING

TRIESKOVÉ A BEZTRIESKOVÉ OBRÁBANIE DREVA 2022

CHIP AND CHIPLESS WOODWORKING PROCESSES 2022

Vedecký časopis // Scientific journal

drevársky
kongres

Trieskové a beztrieskové obrábanie dreva (ISSN 2453-904X (print), ISSN 1339-8350 (online)) je vedecký časopis uverejňujúci recenzované pôvodné vedecké práce, z oblasti technického a technologického výskumu trieskového delenie a obrábanie dreva, procesu tvorby triesky, kvality vytváraného povrchu a fyzikálno-mechanických vlastnostiach triesky. Súčasťou zamerania časopisu je i problematika termickej a hydrotermickej úpravy drevnej hmoty teplom a realizácie týchto procesov. Časopis vychádza s dvojročnou periodicitou v elektronickej a printovej forme.

Chip and chipless woodworking processes (ISSN 2453-904X (print), ISSN 1339-8350 (online)) is a scientific journal publishing the reviewed original scientific works focusing on the technical and technological research of chip separation and wood processing, the process of making chips, the quality of created surface as well as the physico-mechanical chips characteristics. The journal focuses also on the issue of thermal and hydrothermal modification of the wood pulp by heat and how these processes are realized. The journal is published in a two-year periodicity in an electronic and a print form.

Redakčná rada/Editorial Board

Predseda redakčnej rady/Editorial Board Chief
Ladislav DZURENDA

Členovia edičnej rady/Editorial Board Members
Vladimír GOGLIA, Zhivko GOCHEV, Mikuláš SIKLIENKA, Kazimierz A. ORLOWSKI, Grzegorz KOWALUK, Alena OČKAJOVÁ, Zdeněk KOPECKÝ, Tomasz ROGOZIŃSKI

Zodpovední vedeckí redaktori/Responsible scientific editors
Ladislav DZURENDA
Adrián BANSKI

Technický redaktor/Technical Editor
Silvia NEMCOVÁ

Redakcia/Editorial office
Technická univerzita vo Zvolene/ Technical university in Zvolen
Drevárska fakulta/ Faculty of Wood Sciences and Technology
Katedra obrábania dreva/ Departmen of Woodworking
T. G. Masaryka 24
960 01 Zvolen

Vydavateľ/Publisher
Technická univerzita vo Zvolene/Technical university in Zvolen,
T. G. Masaryka 24
960 01 Zvolen, IČO 00397440, 2022
Náklad(Circulation) 75 výtlačkov, rozsah (Pages) 188 strán
Tlač (Printed by) Vydavateľstvo Technickej univerzity vo Zvolene.
Vydanie I. – september
Periodikum s periodicitou raz za dva roky.
Za odbornú úroveň tejto publikácie zodpovedajú autori.
Všetky práva vyhradené. Nijaká časť textu ani ilustrácie nemôžu byť použité na ďalšie šírenie akoukoľvek formou bez predchádzajúceho súhlasu autorov alebo vydavateľa.
© Technická univerzita vo Zvolene
ISSN 2453-904X (print), ISSN 1339-8350 (online)

CONTENTS

Section Mechanical Woodworking

DUDIAK Michal – BANSKI Adrián:
Density of heartwood and sapwood beech wood 7

HANINCOVÁ Luďka – VRÁBLÍK Michal – KOPECKÝ Zdeněk – NOVÁK Vít – ROGOZIŃSKI Tomasz:
Change of cutting parameters and their influence on the particle size distribution when sanding thermally modified material 13

HORTOBÁGYI Áron – KOLEDA Peter – KMINIAK Richard:
Workpiece gripper vibration measurement for nesting milling 19

HRISTODOROVA Desislava – STANEVA Nelly – GENCHEV Yancho:
Static analysis of an upholstered furniture skeleton at heavy-service load by FEM 25

CHUCHALA Daniel – KARPINSKA Sandra – SUCHTA Aleksandra – ORLOWSKI Kazimierz A.:
Preliminary studies on the effect of feed speed on the colour change of wood 31

JÚDA Martin – ŠUSTEK Ján – KRIŠŤÁK Ľuboš:
Granulometric characteristics of MDF and particleboard by varying technological parameter feed speed using a CNC milling router 39

KOCZAN Grzegorz Marcin – KOZAKIEWICZ Paweł:
Rectangular-triangular and reference trapezoidal bending models versus measurement results of three species of exotic wood 51

KOLEDA Pavol – HRČKOVÁ Mária:
Sawdust analysis using Matlab 59

KOVATCHEV Georgi – ATANASOV Valentin – RADKOVA Izabela:
Influence of mechanical oscillations on the accuracy of making grooves in solid wood 65

KWIDZIŃSKI Zdzisław – DREWCZYŃSKI Marcin – ROGOZIŃSKI Tomasz – PĘDZIK Marta:
Energy efficiency in mass customized production of wooden doors 71

OČKAJOVÁ Alena – KUČERKA Martin – BANSKI Adrián:
Sustainable manufacturing process in wood machining 75

PAŁUBICKI Bartosz – ORLIKOWSKI Dariusz – JARECKI Witold – WIADEREK Krzysztof – MATWIEJ Łukasz – WIERUSZEWSKI Marek:
Provenance dependent optimization of Pine timber processing in wooden bad frame production 81

ROHANOVÁ Alena:
The influence false heartwood on the quality of beech structural timber 87

STENKA Dawid – ORLOWSKI Kazimierz A. – CHUCHAŁA Daniel:
Overall set of bandsaw teeth versus methods of measurements 95

VITCHEV Pavlin – GOCHEV Zhivko – HALIM Engindzhan:
Milling of plywood with a shaper origin handheld CNC router 101

Section Thermal Treatment of Wood

BORYSIUK Piotr – AURIGA Radosław:
Thickness Swelling and water absorption of PLA-based composites filled with bark 113

DELIISKI Nencho – DZURENDA Ladislav – VITCHEV Pavlin – TUMBARKOVA Natalia – ANGESKI Dimitar:
Change in the energy for warming up of wooden prisms during autoclave steaming at dispatching interferences in production of veneer 123

DZURENDA Ladislav:
Granulometric composition of chip from the process of machining steamed and unmammed beech wood on the CNC machining center 129

GOCHEV Zhivko – VITCHEV Pavlin:
The effect of CO2 laser engraving on the colour modifications of birch plywood in different modes of use 137

JURKOVIČ Peter – SEDLIAČIK Ján – NOVÁK Igor – MATYAŠOVSKÝ Ján – KLEINOVÁ Angela:
Study of maple wood modified by saturated water steam 147

KLEMENT Ivan – VILKOVSKÝ Peter – VILKOVSKÁ Tatiana – BARAŃSKI Jacek – SUCHTA Aleksandra:
Effect of press drying on dimension stability and density of beech wood 151

KUČERKA Martin – OČKAJOVÁ Alena – KMINIAK Richard:
Influence of heat treatment of Wood on chip size during milling 161

MATYAŠOVSKÝ Ján – SEDLIAČIK Ján – NOVÁK Igor – JURKOVIČ Peter – DUCHOVIČ Peter – SEDLIAČIKOVÁ Mariana:
Wood-beech panels with low formaldehyde emission 169

RAJKO Ľubomír – KOLEDA Peter – BARCÍK Štefan – GOGLIA Vlado:
Effect of hydrothermal treatment on surface quality of beech wood after plane milling 175

SEDLIAČIK Ján – JURKOVIČ Peter – NOVÁK Igor – Igor KRUPA – MATYAŠOVSKÝ Ján:
Evaluation of properties of date palm wood composites with polyolefin 183

SECTION

MECHANICAL WOODWORKING

Chip and chipless woodworking processes, 13(1): 7–11, 2022
Zvolen, Technical University in Zvolen, ISSN 1339-8350 (online), ISSN 2453-904X (print)

DENSITY OF HEARTWOOD AND SAPWOOD BEECH WOOD

Michal Dudiak – Adrián Banski

Abstract

The paper deals with the issue of determining the density of absolutely dry sapwood beech wood and wood with false heartwood using a new method of determining wood density using a KIT 128 digital densitometer. The density of false heartwood beech wood is higher on average by 12.2 kg.m^{-3} compared to sapwood beech wood. But it does not exceed the natural variability of the density of beech wood stated in the professional literature, i.e. it is not necessary to take into account the change in the density of the false heartwood of beech wood in technical applications in the production of furniture, etc. It was proven that the new method of determining the density of absolutely dry wood achieves relevant results comparable to the values in the professional literature, while eliminating and especially simplifying laboratory work, as well as shortening the measurement time and increasing the accuracy of wood density measurement.

Keywords: *density wood, beech wood, false heartwood, sapwood*

INTRODUCTION

The Beech wood belongs to the scattered-porous coreless woods with the possibility of forming a false heartwood. Sapwood beech wood is medium heavy, flexible, easily split. It has good mechanical properties, it is plasticized, bent and machined very well. Thanks to its high permeability, it is well impregnated, stained and dyed. Beech wood is used for the production of furniture, floors, sports equipment, toys and small useful household items. Sapwood beech wood has a light white-gray color with a yellow tinge. Beech wood is used for the production of furniture, floors, sports equipment, toys and small useful household items.

A false beech heartwood is a growth defect that results from air-wood reactions in the sapwood zone. The primary cause of a false heartwood is injury to the tree trunk or branches, which allows air to enter the tree trunk. The oxygen contained in the air will cause the oxidation of soluble carbohydrates and starch (contained in living or partially dead parenchymal cells), resulting in brown-colored polyphenolic compounds that penetrate into the neighboring tissues and color them Bauch – Koch (2001), Račko – Čunderlík (2010). According to the appearance of the false heartwood in the tree trunk and its shape on the cross-section of the trunk, the false heartwood is divided into: Round, Mosaic Star-shaped, Flaming (eccentric, centric) Mahler – Höwecke (1991). In comparison to sapwood and mature wood, the wood of the false heartwood has a lower moisture content in the growing tree, and according to the work of Babiak *et al.* (1990) lower fluid permeability.

Technical University in Zvolen, T. G. Masaryka 24, 960 01 Zvolen
e-mail: xdudiak@tuzvo.sk, banski@tuzvo.sk

The density of wood in a dry state is one of the basic physical properties of wood. The density of wood is influenced by factors such as the growing conditions of the tree, the elemental composition of the wood, the moisture content of the wood or the position in the tree trunk, etc. According to the authors Požgaj *et al.* (1993), the density of absolutely dry beech wood in the Central European area (locality Carpathians) Makovíny (2010), Klement et al. (2010), Dzurenda – Dudiak (2020) in the range $\rho_0 = 490$ to 880 $kg.m^{-3}$.

The aim of the work is to determine the density of the false heartwood of beech wood and to compare the density of the false heartwood with the density of sapwood beech wood.

MATERIAL AND METHODS

From beech lumber with false heartwood, test bodies were made from the zone of sapwood and false heartwood to determine the density of wood with dimensions: thickness h = 15 mm; width w = 50 mm; length l = 100 mm in the number of 30 pieces from each group. The produced test bodies were dried in a laboratory oven (MEMMERT UM110m) at a temperature of t = 103 ± 2 °C to a constant weight. After drying, the samples were placed in a desiccator, and then, after cooling, the wood density was measured.

Determination of the density of samples of sapwood beech wood or false heartwood in the dry state was carried out using a digital density meter: Set for determining the density of solid substances KIT 128 from the company RADWAG (Poland).

The measurement of wood density was carried out in accordance with STN 49 0108 *"Wood, Determination of density"* and Internal methodical procedure IMP-3/2019 *Determination of the density of wood in a dry state* according to STN 49 0108 developed at the Department of Woodworking - DF Technical University in Zvolen after consultations with the representative RADWAG company. Verification of the procedure for measuring the density of bodies with a density lower than $\rho \leq 1000$ $kg.m^{-3}$ was performed by representatives of the RADWAG company. The determination itself consists of determining the weight of an absolutely dry sample by weighing it in air m0 and then determining the weight in distilled water m_0* (Fig. 1). According to Archimedes' law, *"A body immersed in a liquid is overburdened by a hydrostatic buoyant force, the magnitude of which is equal to the weight of the liquid with the same volume as the volume of the immersed part of the body"*, the volume of the wood sample "V" is balanced from the balance of the sample weights:

m_0 = weight determined by trapping the sample in air [kg]

$m_0^* = m_0 - V . \rho_{H_2o} . g$ = weight determined by weighing the sample in water [kg] (1)

$$V = \frac{m_0 - m_0^*}{\rho_{H_2o} \cdot g} \quad [m^3] \qquad (2)$$

$$\rho_0 = \frac{m_0}{V} = \left(\frac{m_0}{m_0 - m_0^*}\right) . \left(\rho_{H_2o} . g\right) \quad [kg.m^{-3}] \qquad (3)$$

The densitometer has a built-in software that automatically determines the density of wood from the data measured and confirmed by the operator, it is compatible with the computer software Excel 2019, where it transfers and tabulates all entered and measured density data of a given wood sample Dudiak (2021).

The values of the density of sapwood and false heartwood of beech wood are given in the form of $\bar{x}$ notation: of the average measured value and sx of the standard deviation.

$$x = \bar{x} \pm s_x \ [kg.m^{-3}] \qquad (4)$$

The degree of dispersion of the density values of false heartwood and sapwood is evaluated through the coefficient of variation:

$$v_x = \frac{s_x}{\bar{x}} \cdot 100 \ [\%] \qquad (5)$$

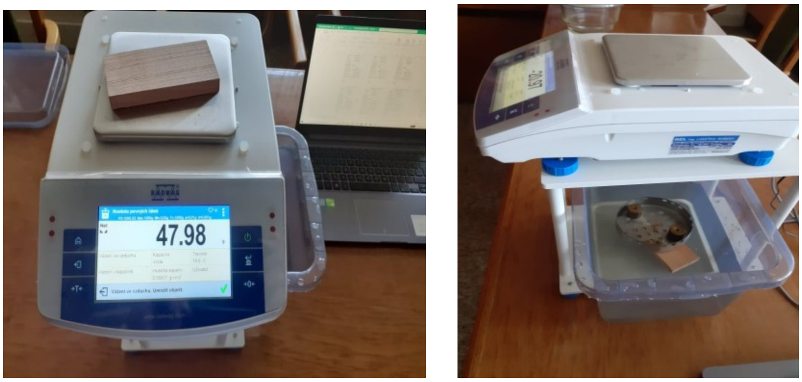

Fig. 1 Course of determination of wood density

RESULTS AND DISCUSSION

The measured values of the wood density of false heartwood and sapwood beech wood in an absolutely dry state are given in Table 1.

Tab. 1 Density values of sapwood and false heartwood of beech wood

Beech wood	Number of measurements	Wood density	Variation coefficient
false heartwood	30	$\rho_0 = 695.7 \pm 28.4$ kg.m^{-3}	4.08 %
sapwood	30	$\rho_0 = 683.5 \pm 29.1$ kg.m^{-3}	4.25 %

From the measured values of the density of sapwood beech wood and false heartwood in an absolutely dry state, the graph shown in Fig. 2

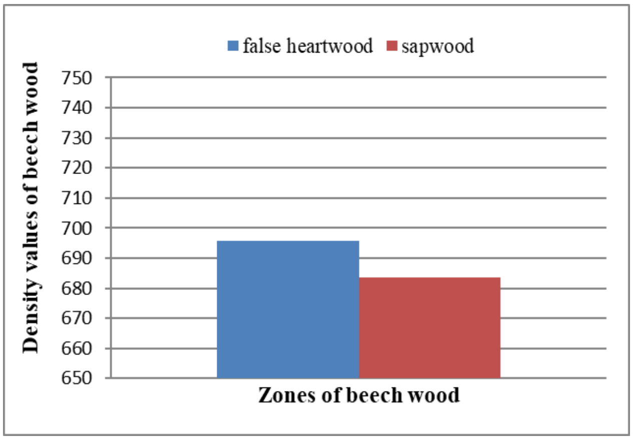

Fig. 2 Density of beech wood in individual zones

The values of the density of absolutely dry beech wood in individual zones measured using a digital densitometer KIT 128 show that the density in individual zones of beech wood (false heartwood or sapwood) is not uniform. The value of the density of sapwood beech wood is higher on average by 12.2 kg.m^{-3}.

The degree of dispersion of the values of the density of false heartwood and sapwood beech wood evaluated through the coefficient of variation shows a low percentage of variability of the measured data, which indicates a good accuracy of measuring the density of beech wood. The value of the coefficient of variation in the density of sapwood beech wood compared to wood with a false heartwood was higher by 0.17 %, which can be attributed to the higher variability of sapwood beech wood.

Since, the mentioned difference in the density of the false heartwood of beech wood compared to sapwood beech wood is not greater than the natural variability of the density of sapwood beech wood mentioned in the professional literature of Požgaj *et al.* (1993), Makovíny (2010), Klement *et al.* (2010) Dzurenda – Dudiak (2020) it is not necessary to take into account the change in the density of the false heartwood of beech wood in technical applications in the production of furniture or construction and carpentry products used in the interior.

The determination of the density of the wood of the false heartwood was carried out using a digital densitometer KIT 128 according to IMP-3/2019 "*Determination of the density of wood in a dry state*" developed at Department of Woodworking in 2019 as part of the solution of the project APVV 17-0456 *"Thermal modification of wood with saturated water steam for the purpose of targeted and stable color change of wood material"* to determine the influence of wood steaming on the change in wood density by the steaming process. The mentioned method of determining the density of wood brings time, technically and practically acceleration and precision of the measurement of wood density, where it is possible to determine the density of wood of irregular shapes and sizes.

CONCLUSION

Based on the laboratory measurements of the density of absolutely dry beech wood in individual zones using the presented method, I came to the conclusion that the density of the false heartwood of beech wood is higher on average by 12.2 kg.m^{-3} compared to sapwood beech wood, but does not exceed the natural variability density of beech wood mentioned in professional literature.

By introducing the measurement of the density of wood in the dry state using a digital densitometer KIT 128 according to: IMP-3/2019 Determination of the density of wood in the dry state in accordance with STN 49 0108, laboratory work in determining one of the basic characteristics of wood was not only removed and simplified, but also the time was shortened measurements and the accuracy of wood density measurement increased. The acquired knowledge and skills during the implementation of the mentioned methodology at the workplace were used in the measurement of the density of beech wood (false heartwood and sapwood), as well as other wood species.

REFERENCES

Babiak, M., Čunderlík, I., Kúdela, J. 1990. Permeability and structure of beech wood. *IAWA bulletin*, 11(2): 115.

Bauch, J., Koch, G. 2001. Biologische und chemische Untersuchungen über Holzverfarbungen der Rotbuche (*Fagus sylvatica* L.) und Möglichkeiten vorbeugender Maßnahmen. *Abschlussbericht, Bundesforschungsanstalt für Forst- und Holzwirtschaft, Universität Hamburg*. Vol. 216(2001), p. 84.

Dudiak, M., 2021. Modification of maple wood colour during the process of thermal treatment with saturated water steam. *Acta facultatis xylologiae Zvolen*. 63(1). s. 25−34. Zvolen: Technická univerzita vo Zvolene DOI: 10.17423/afx.2021.63.1.03

Dzurenda, L., Dudiak, M. 2020. Changes in wood tree species *Fagus sylvatica* L. and characteristics of the thermal process of modifying its color with saturated water steam. *Advances in ecological and environmental research*. pp. 142-156. ISSN 2517-9454.

Klement, I., Réh, R., Detvaj, J. 2010. Basic characteristics of forest trees - processing of wood raw material in the wood processing industry. Zvolen: NLC. 82 p.

Mahler, G., Höwecke, B. 1991. Verkernungserscheinungen bei der Buche in Baden-Württemberg in Abhängigkeit von Alter, Standort und Durchmesser. Schweiz. Z. *Forstwes*. 142: 375−390.

Makovíny, I. 2010. Useful properties and use of different types of wood. Zvolen: Technical University in Zvolen. 104 p.

Požgaj, A., Chovanec, D., Kuriatko, S., Babiak, M. 1993. Structure and properties of wood. I. edition. Bratislava: Príroda a.s. 485 p. ISBN 80-07-00600-1.

Račko, V., Čunderlík, I. (2010). Zrelé drevo ako limitujúci faktor vzniku nepravého jadra buka (*Fagus sylvatica* L.). [Sapwood as a limiting factor for the formation of a false heardwood beech (*Fagus sylvatica* L.)] *Acta facultatis xylologiae Zvolen*, 52 (1): 15 – 24.

Acknowledgement:

This experimental research was prepared within the grant project: *APVV-21-0051 Research of false heartwood and sapwood of Fagus sylvatica* L. *wood in order to eliminate color differences by the process of thermal treatment with saturated water steam* as the result of work of author and the considerable assistance of the APVV agency.

CHIP AND CHIPLESS WOODWORKING PROCESSES, 13(1): 13–18, 2022
Zvolen, Technical University in Zvolen, ISSN 1339-8350 (online), ISSN 2453-904X (print)

CHANGE OF CUTTING PARAMETERS AND THEIR INFLUENCE ON THE PARTICLE SIZE DISTRIBUTION WHEN SANDING THERMALLY MODIFIED MATERIAL

Luďka Hanincová[1] – Michal Vráblík[1] – Zdeněk Kopecký[1] – Vít Novák[1] – Tomasz Rogoziński[2]

Abstract

The research was focused on wood dust generated during the sanding of native pine wood and two types of heat-treated pine wood (Thermo-S and Thermo-D). The aim of the research was to assess the effect of feed speed and type of workpiece on the generation of wood dust. The experiment was performed on a Buldog 7 wide belt sander. The dust generated during sanding was subjected to particle size analysis by means of Retsch AS 200-digit apparatus on a set of sieves with mesh sizes 1000, 500, 250 and 100 µm. The laser particle sizer Analysette 22 Microtec Plus was used to determine the size distribution of dust particles smaller than 100 µm. The obtained results showed the influence of thermal modification and feed speed on the generation of wood dust. The heat-treated wood produces more fine dust than native wood. The higher the modification temperature, the higher the fine dust content. It has been found that the fine dust content increases with decreasing feed speed.

Key words: *heat-treated wood, sanding, dustiness, sieve analysis, laser particle sizer*

INTRODUCTION

Wood dust is generated as a waste in most woodworking operations. However, due to its properties, it is undesirable and there is an effort to eliminate it as much as possible and reduce dust at work. It is dangerous in many respects, such as an increased risk of slipping in the workplace, a greater risk of fire, as dust settles on all surfaces in the immediate vicinity of the source. Another very serious problem connecting with dustiness is respiratory problems and irritating effects on humans.

The technology of thermal modification makes it possible to obtain new materials based on solid wood. This technology changes the mechanical and physical properties of the wood. The advantages of wood modified by heat, water, and steam include the absence of harmful chemicals, the reduction of moisture absorption, dimensional stability, biological resistance, and others. Wood acquires different physical-mechanical properties resulting in the improved performance of material. The advantages of thermal modified wood include the reduced moisture absorption, dimensional stability, and biological resistance. Thermal processes also have several disadvantages; changes in physical properties of the thermally

---

[1] Mendel University in Brno, Faculty of Forestry and Wood Technology, Department of Wood Science and Technology, Zemědělská 3, Brno, 613 00, Czech Republic

[2] Poznań University of Life Sciences, Faculty of Forestry and Wood Technology, Department of Furniture Design, Wojska Polskiego 28, 60-637 Poznań, Poland

modified wood (decreases in weight and density), reduction of mechanical properties (dynamic stability, bending and toughness), which results in increased fragility of wood.
The aim of the research was to assess the effect of feed speed and temperature of thermal modification of pine wood on the particle size distribution.

MATERIAL AND METHODS

The material used for the experiment was made directly by Finnish manufacturer Lunawood from pine wood. Two types of this material have been investigated:
1) The material Thermo-S (the heat treatment was performed at a temperature of 190 °C),
2) The material Thermo-D (the heat treatment of the wood was performed at a temperature of 212 °C). These heat-treated materials were compared with native pine wood.

Table 1: Material description

	Pine	Thermo-S (190 °C)	Thermo-D (212 °C)
Length [mm]	3000	3000	3000
Thickness [mm]	26	26	26
Width [mm]	90	90	90
Moisture content [%]	5	7	8
Density [kg/m^3]	410	450	500

Sanding experiment was performed on a Buldog 7 wide belt sander (Houfek, Czech Republic). Before sanding, it was necessary to seal all the exhaust systems from the machine space. This step was necessary to prevent the examined sanding dust from being sucked out. The suction device remained switched off throughout the sanding process. The experiment was performed on sanding belt with a grain size of 100 (Napoleon Abrasives spa, Italy). The required sanding parameters can be found in Table 2:

Table 2: Sanding parameters

Cutting speed [m/s]	18
Grit of sanding belt	100
Number of sandings	5
Depth of cut [mm]	0.2
Feed speed [m/min]	3, 6, 9, 12

The material was placed on a feed belt and sanded by 0.2 mm thickness by passing through a wide belt sander. After passing through the sander, the material on the feed belt shifted by its width, thus ensuring even wear of the sanding belt. This procedure was repeated 5 times, then a Bosch GAS 35 M AFC Professional industrial vacuum cleaner was used to remove dust. This device ensured a near-total collection efficiency of dust. After complete cleaning of the sander, the dust from the vacuum cleaner poured into a plastic bag. This procedure was repeated for all investigated feed speeds and all materials.
The granulometric composition of wood dust was determined by sieving on a Retsch AS 200 (Verder, Germany) the sieving machine. Set of sieves with a mesh size of 1 mm, 0.5 mm, 0.25 mm, and 0.1 mm was used. The sieve vibration amplitude was set to A = 1.5 and the time for the sieve analysis t = 20 min. The granulometric composition was obtained by weighing the percentages remaining on the sieves after sieving on an electronic laboratory

scale Vibra AJ-420-CE (Shinko Denshi, Japan) with weighing accuracy of 0.001 g. Five repetitions were performed for each variant; and the results are given as their average values.

The laser particle sizer Analysette 22 Microtec Plus (Fritsch, Germany) was used to determine the size distribution of dust particles collected in the bottom collector (size was smaller than 100 µm). The sizer automatically measures particle size according to predetermined SOP (Standard Operating Procedure) and theoretical assumptions.

RESULTS AND DISCUSSION

Fig. 1 shows the results of the particle size distribution of dry sawdust which were generated during sanding of native pine wood and heat-treated materials. The results were obtained by the sieving method.

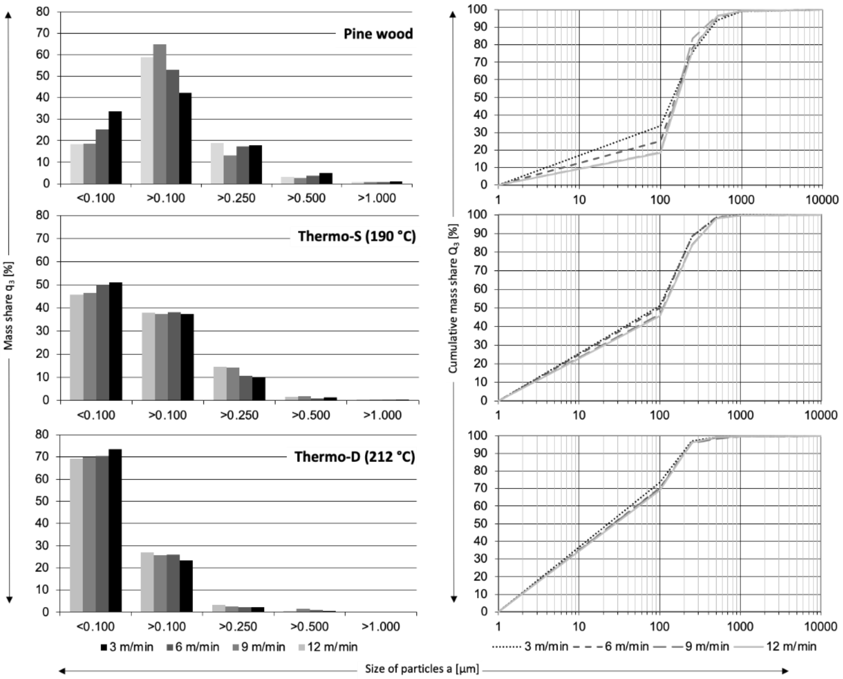

Figure 1: Mass share and cumulative particle-size distribution of tested dust

From the comparison of mass shares and cumulative mass shares in Figure 1, it is obvious that with increasing modification temperature, the proportion of fine dust particles smaller than 100 micrometers increases. It can also be seen that the proportion of dust particles decreases with increasing feed speed. For native pine wood, the proportion of these particles is a maximum of 32 %, for Thermo-S 51 % and for Thermo-D 72 %.

Reinprecht and Vidholdová (2008), Dzurenda et al. (2010), Piernik et al. (2018) state that the machining of heat-treated wood is accompanied by an increased content of fine particles. These materials become more brittle and produce a higher content of fine dust. The increased fragility of heat-treated wood is caused by nanocracks and microcracks in the cell wall. Majka et al. (2022) state that heat-treated beech wood produces more fine dust (particles smaller than 80 µm) than native beech wood. The authors explain increased dustiness of heat-treated wood due to changes in the microscopic structure of wood. Most of the mechanical properties of heat-treated wood decrease (bending strength by up to 50 %). Hill (2006) states that increasing temperature causes degradation of polymers in cell walls. At temperatures above 140 °C, the polymer chains begin to break, and dehydration reactions take place in the wood. Hemicelluloses are the least resistant and their degradation already occurs at a temperature of 170 °C (Horáček, 1998). In the case of pine wood, the result can also be supported by the anatomical structure of the wood itself, where the high resin content is removed from the wood during thermal modification.

As the feed speed decreases, the content of fine particles increases. As the feed speed decreases, the chip thickness decreases, which increases the concentration of fine dust particles. Ugulino and Hernández (2017) and Hlásková et al. (2016) publish very similar results in their work, when they focused on the effect of feed speed on the content of fine dust particles when cutting two-side-laminated particleboards.

Figure 2 shows a comparison of a fine dust content of less than 100 μm. From this comparison, the highest fine dust content is for all feed speeds for Thermo-D, followed by Thermo-S and pine wood. Furthermore, we can notice a gradual increase in the content of fine dust as the feed speed decreases. These results correspond to the known fact that, as the feed speed decreases, a larger amount of fine dust is generated.

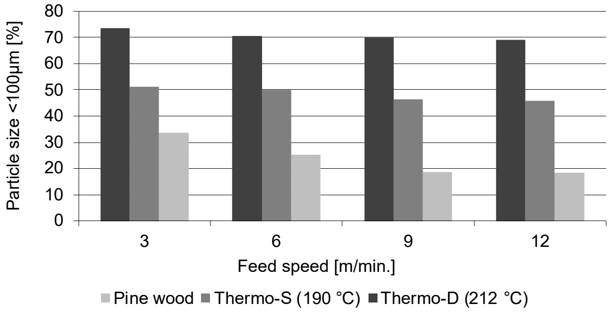

Figure 2: Comparison of particles smaller than 100 μm

Table 3 shows the results of cumulative particle-size distribution of analyzed dust sampled from the bottom collector of the sieving machine. The dust particles below 100 μm represent almost 82 to 100 % of the analyzed material. These results indicate that the content of fine particles in the tested dust of material Thermo-D created during sanding is higher than in case material Thermo-S or native pine wood. Očkajová et al. (2014) described the share of beech wood dust particles with a diameter of ≤80 μm in the range of 89.21–96.29 %.

Table 3: Cumulative particle-size distribution of dust sampled from the bottom collector

Mass rate in the smallest sieving fraction [%]												
Feed speed	3 m/min			6 m/min			9 m/min			12 m/min		
Upper limit [μm]	Pine	Thermo-S	Thermo-D	Pine	Thermo-S	Thermo-D	Pine	Thermo-S	Thermo-D	Pine	Thermo-S	Thermo-D
2.5	2.61	2.82	3.04	2.02	2.94	1.71	1.82	3.11	2.86	2.81	2.52	2.59
4	2.63	3.33	3.41	2.09	3.23	2.09	1.93	3.43	3.66	2.95	2.78	3.11

10	5.55	15.31	16.81	6.33	15.31	10.22	2.64	15.14	19.15	10.46	12.89	16.44
20	22.33	46.16	50.74	23.46	47.41	32.04	9.85	47.96	54.03	37.14	43.47	47.85
30	41.12	69.28	74.53	40.41	71.22	50.14	21.56	72.16	77.27	60.63	67.57	70.31
40	56.46	83.20	87.71	53.98	85.23	62.72	33.95	86.14	89.65	76.52	82.46	83.64
50	68.05	91.29	94.41	64.06	92.82	71.46	45.54	93.43	95.67	86.53	90.93	90.96
60	76.67	95.57	97.65	71.73	96.74	77.58	55.61	97.12	98.36	92.63	95.55	94.83
70	82.96	97.76	99.16	77.51	98.61	81.88	64.21	98.82	99.45	96.11	97.93	96.81
80	87.44	98.84	99.64	81.92	99.32	85.07	71.32	99.55	99.83	98.05	99.06	97.75
90	90.73	99.22	99.73	85.23	99.69	87.39	77.14	99.76	99.92	99.06	99.55	98.16
100	93.22	99.41	99.82	87.95	99.78	89.12	81.93	99.86	99.99	99.57	99.72	98.39

Table 4 shows the results of total contents of particles with the expected size limits of <2.5 µm, 2.5–4 µm, 4–10 µm, 10–20 µm and further in the analyzed dust, which were calculated based on the particle-size distribution obtained by the laser diffraction method and considering the mass share of the fraction <100 µm determined by the sieving method.

Table 4: Total contents of particles with the expected size limits

Mass rate in the total dust [%]												
Feed speed	3 m/min			6 m/min			9 m/min			12 m/min		
Upper limit [µm]	Pine	Ther mo-S	Ther mo-D	Pine	Ther mo-S	Ther mo-D	Pine	Ther mo-S	Ther mo-D	Pine	Ther mo-S	Ther mo-D
2.5	0.87	1.44	2.22	0.43	1.43	1.17	0.34	1.01	1.95	0.51	0.66	1.70
4	0.87	1.67	2.52	0.44	1.61	1.39	0.35	1.19	2.51	0.53	0.83	2.11
10	1.85	7.84	12.36	1.52	7.67	7.16	0.49	6.13	11.36	1.90	2.05	11.34
20	7.49	23.59	37.27	5.81	23.71	22.59	1.82	19.11	37.75	6.77	4.38	33.04
30	13.80	35.41	54.76	10.10	35.63	35.31	4.00	29.26	54.04	11.07	6.45	48.57
40	18.94	42.58	64.48	13.48	42.65	44.23	6.31	35.77	62.72	13.99	8.29	57.72
50	22.83	46.64	69.43	16.04	46.45	50.38	8.45	39.71	66.92	15.82	10.02	62.81
60	25.71	48.85	71.79	17.97	48.40	54.67	10.33	42.04	68.81	16.92	11.67	65.52
70	27.83	49.99	72.82	19.43	49.33	57.74	11.93	43.38	69.57	17.56	13.29	66.89
80	29.34	50.52	73.20	20.53	49.71	59.94	13.25	44.08	69.82	17.91	14.86	67.51
90	30.45	50.76	73.33	21.38	49.85	61.59	14.34	44.45	69.88	18.09	16.40	67.78
100	31.27	50.85	73.36	22.04	49.90	62.89	15.23	44.62	69.90	18.18	17.91	67.88

The average content of particles smaller than 10 µm in dust from tested materials did not exceed 12.36 %, and the highest content was observed for combination material Thermo-D and feed speed 3/min. In other cases, the content of this dust fraction was lower, and the dust produced by sanding pine wood by feed speed 9 m/min had the smallest content of the fraction <10 µm, i.e., 0.49 %. The occurrence of these particles is undesirable in working environments, as it is a large amount of dust, which might pollute a huge volume of air at the acceptable limit of dust concentration. These particles can penetrate the alveoli and be the source of serious diseases.

CONCLUSION

Based on findings and the obtained results, it can be concluded that the amount of fine dust generated during sanding heat-treated wood increases with the temperature of wood modification and decreasing feed speed. These materials have a changed microscopic structure of wood, which causes deterioration of mechanical properties, heat-treated materials thus become more brittle and produce a higher content of fine dust.

AKNOWLEDGEMENT

The research was supported by the Specific University Research Fund MENDELU IGA-LDF-22-TP-004: „Advanced tool materials and their influence on the parameters of CNC machining of wood-based materials“ and by the project MENDELU international development II (CZ.02.2.69/0.0/0.0/18_053/0016930).

REFERENCES

[1] Dzurenda, Ladislav, Kazimierz Orlowski, and Marek Grzeskiewicz. "Effect of thermal modification of oak wood on sawdust granularity." Drvna industrija 61.2 (2010): 89-94.
[2] Hill, Callum AS. Wood modification: chemical, thermal and other processes. John Wiley & Sons, 2007.
[3] Hlásková, Luďka, Tomasz Rogoziński, and Zdeněk Kopecký. "Influence of Feed Speed on the Content of Fine Dust during Cutting of Two-Side-Laminated Particleboards." Wood Industry/Drvna Industrija 67.1 (2016).
[4] Horáček, P. "Fyzikální a mechanické vlastnosti dřeva 1. vyd.[Physical and Mechanical Properties of Wood,]." (1998).
[5] Majka, Jerzy, et al. "Quantifying the finest particles in dust fractions created during the sanding of untreated and thermally modified beech wood." BioResources 17 (2021): 7-20.
[6] Očkajová, Alena, et al. "The granularity of dust particles when sanding wood and wood-based materials." Advanced Materials Research. Vol. 1001. Trans Tech Publications Ltd, 2014.
[7] Piernik, Magdalena, et al. "The influence of the thermal modification of pine (Pinus sylvestris L.) wood on the creation of fine dust particles in plane milling." Journal of Occupational Health 61.6 (2019): 481-488.
[8] Reinprecht, Ladislav, and Zuzana Vidholdová. Termodrevo: príprava, vlastnosti a aplikácie. TU Zvolen, 2008.
[9] Ugulino, B., and R. E. Hernández. "Effect of cutting parameters on dust emission and surface roughness during helical planing red oak wood." Wood Fiber Sci 49.3 (2017): 323-331.

CHIP AND CHIPLESS WOODWORKING PROCESSES, 13(1): 19–24, 2022
Zvolen, Technical University in Zvolen, ISSN 1339-8350 (online), ISSN 2453-904X (print)

Workpiece gripper vibration measurement for nesting milling

Áron Hortobágyi – Peter Koleda – Richard Kminiak

Abstract

This article shows part of study into vibrations measured on workpiece dripping points as a potential signal for adaptive control of CNC mill. In the experiment, medium density fiberboards and particle boards were cut with diamond and spiral mills with feed rates 2 m/s, 6m/s, 10 m/s and tool rotations 10 000/min and 20 000/min. Accelerometer output show amplitudes changing with tool movement. On MDF, with spiral mill, part of board furthest from gripping points shows amplitude rise. This is less visible with use of diamond mill. In all cases, "z" axis amplitudes are higher than "x" axis. When same parameters were used, amplitudes were higher on particle boards. Movement of tool is also visible on comparison of amplitudes od different grippers – the further tool is from gripper, registered amplitudes seem as lower. Fourier transform shows prominent frequencies of 333 Hz and its multiples.

Key words: *Milling, vibration, CNC, MDF*

INTRODUCTION

While the topic of adaptive control of CNC machine is a current topic, it is not an entirely new concept. It was already discussed as early as the 1980s. Experiments on CNC lathe were conducted by (Bedini, Pinotti, 1982). The description of development of adaptive control tools with its concept was described in publication of (Ulsoy et al., 1983). Process of deep hole drilling and its adaptive control was studied by (Kavaratzis, Maiden, 1990). During this period, adaptive control in the grinding process was also addressed (Rowe et al., 1991).

Research on adaptive control for the milling process continued (Huang et al., 2010), with use of neural networks (Zuperl, Cus, 2011), high-speed interpolation (Zang et al., 2011), schemes of closed loop servo drive control (Ye, Hu, 2012) and discrete algorithms on the principle of sigmoid function for change in feed rate (Wang, Cao, 2012). Multiple topics were addressed, such as the introduction of STEP and STEP-NC standards (Ridwan, Xu, 2013) to enable optimization during machining, adaptive control systems for drilling machines by a program were developed in C++ (Mikolajczyk et al., 2013), but also active vibration control of CNC milling machines was addressed (Ford et al., 2013).

Most publications dealt with metalworking, but the process of milling wood and its composites was also addressed, with result in the design of adaptive control for the grooving process, dependent on the wear and tear of the material (Ohuchi et al., 2006). As part of wood processing, the development was directed to adaptive control responding to tool wear when milling MDF boards with use of machine vision (Laszewicz et al., 2013).

Technical University in Zvolen, T. G. Masaryka 24, 960 01 Zvolen
e-mail: xhortobagyi@is.tuzvo.sk

MATERIAL AND METHODS

The measurement took place in the laboratories of the Technical University in Zvolen at the CNC centre SCM Tech Z5 from Höchsmann corporation. Its parameters are summarized in Table 1.

Table 1 Parameters of the CNC center SCM TECH 5

Workspace parameters along axes X–Y–Z [mm]:	3050 x 1550 x 160
Vector velocity of the axis X–Y [m·min^{-1}]:	83
Engine power (S1) [kW]:	11
Max. rotations [min^{-1}]:	20 000
Number of positions in the tool changer:	12

Source: (Höchsmann, 2014)

MDF board was used for experiments, cut to 500 x 300 x 18 mm. Particle board of same size was used as control sample.
The board was clamped on four vacuum grippers measuring 120 x 120 mm with a clamping force 16 kg/cm^2.

The picoscope 3-output NVH interface kit, with two TA143 MEMS accelerometers were used to measure vibrations. Accelerometers were magnetically clamped to pneumatic grippers (Fig. 1 a), which were modified to allow such attachment. Picoscope allowed simultaneous measurement of four axes. These were colour coded as shown in (Fig. 1 b).

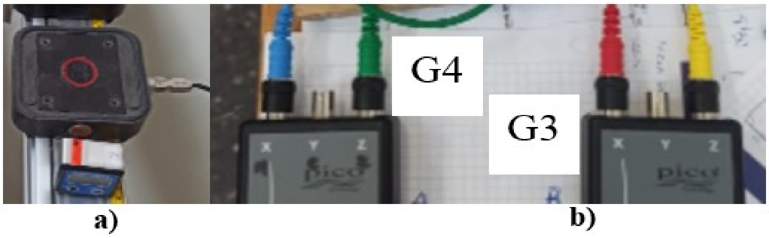

Fig. 1 a) pneumatic gripper with accelerometer b) color coding of measured axes

First, vibrations were measured on three axes of each gripper. This was done on MDF board, with feed rate 6 m/min and tool rotating 20 000/min. Results were processed in Matlab via fast Fourier Transform. As a part of processing, signal length was cut off. This was due to fact that measurement started before and was stopped after the milling process took part. Example of result is shown in Fig. 2.

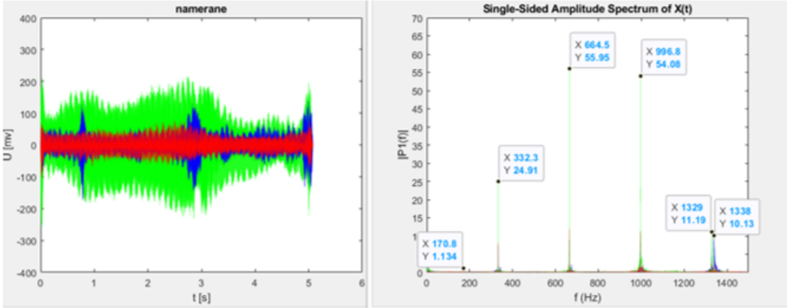

a) b)

Fig. 2) Example of first measurements, from Griper 1. a) accelerometer output b) Fast Fourier Transform result

Assessment of these measurements showed that “y” axis has the smallest amplitude. Also, amplitudes on grippers 3 and 4 reached higher values than those on grippers 1 and 2. Therefore, it was decided that the methodology should be changed. Instead of one, two grippers would be monitored simultaneously.

Placement of the board and accelerometers is shown in Fig. 3.

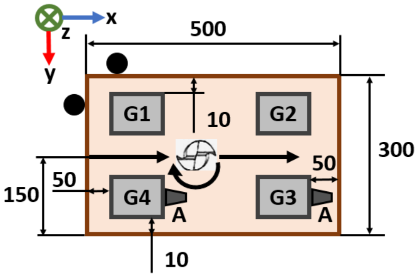

Fig. 3. Placement of board on and accelerometers (A) on grippers (G1 – G4), tool movement and accelerometer orientation (x,y,z).

Since Picoscope can measure four channels, it was decided that “y” axis would be excluded. Final matrix of measurements is shown in Fig. 4. These were performed on both MDF and DTD boards. During experiments, various tools, feed rates and tool rotations were used. Each cutting process was repeated three times.

Number of measurments			vf [m/min]									
			2			6			10			
tool	n	grip.	x	y	z	x	y	z	x	y	z	
spiral mill	10 000/min	1	-	-	-	-	-	-	-	-	-	
		2	-	-	-	-	-	-	-	-	-	
		3	3	-	3	3	-	3	3	-	3	
		4	3	-	3	3	-	3	3	-	3	
	20 000/min	1	-	-	-	3	3	3	-	-	-	
		2	-	-	-	3	3	3	-	-	-	
		3	3	-	3	3	3	3	3	-	3	
		4	3	-	3	3	3	3	3	-	3	
diamond mill	10 000/min	1	-	-	-	-	-	-	-	-	-	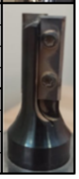
		2	-	-	-	-	-	-	-	-	-	
		3	3	-	3	3	-	3	3	-	3	
		4	3	-	3	3	-	3	3	-	3	
	20 000/min	1	-	-	-	-	-	-	-	-	-	
		2	-	-	-	-	-	-	-	-	-	
		3	3	-	3	3	-	3	3	-	3	
		4	3	-	3	3	-	3	3	-	3	

Fig. 4. Marix of measurements for MDF and DTD boards.

RESULTS

Results were first visible in Picoscope software. Example of these is shown in Fig. 5.

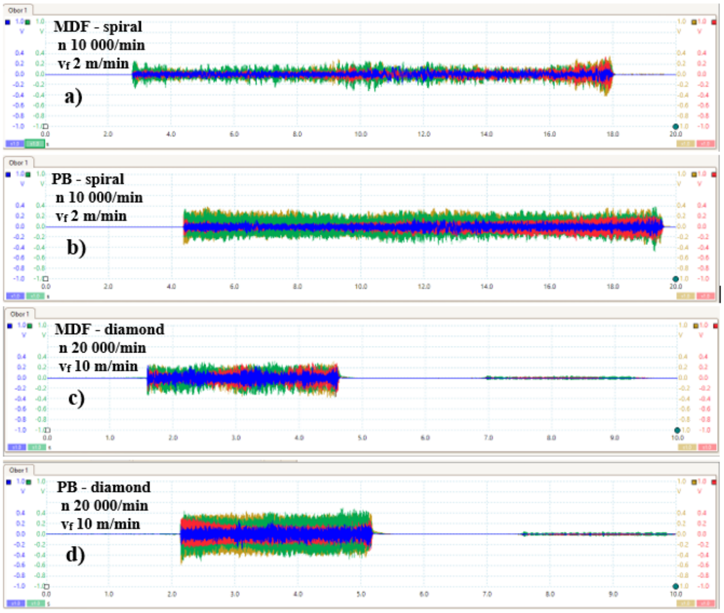

Fig. 5 example of Picoscope firmware output.

The part with highest amplitudes refers to the milling process. Color coding is same as in Fig. 1. It is easy to notice, movement of tool in Fig. 5a), 5b) as by time increase, amplitudes from gripper 4 decrease and amplitudes measured on gripper 3 rise. However, there is part of charts which should not be included in final analysis – before and after milling. There is another part with higher amplitudes in charts with v_f 10 m/min. This corresponds to spindle returning to idle position.

Then, amplitudes and their Fourier transforms were assessed in Matlab. Part of results is shown in Fig. 6. To reach these results, scripts were developed, to cut unwanted parts, perform Fourier transform, plot charts and summarize multiple measurements in .xlsx format.

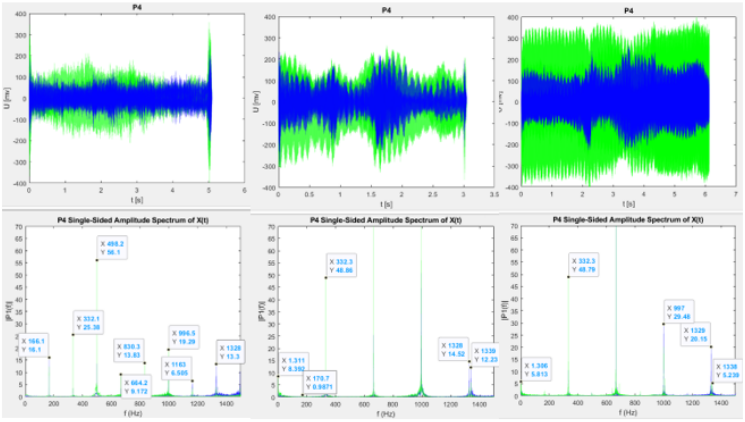

a) **MDF** **n 10 000/min** **v_f 6 m/min**

b) **MDF** **n 20 000/min** **v_f 6 m/min**

c) **MDF** **n 20 000/min** **v_f 6 m/min**

Fig. 6: Comparison of amplitudes on „x“ (blue) and „z“ (green) axis on gripper 4 with various milling parameters, done with spiral mill - a), b) and diamond mill - c)

DISCUSSION

As shown in Fig. 5, change of parameters, tools ald material are all visible in ampitudes. When Fig 5 a) and Fig. 5 b) are compared, vibration in „z“ axix is noticably more prominent when particle board was used.

In all four cases of Fig. 5, there is a slight amplitude increase in middle part of chart. This represents mill moving through part of board with highest distance from grippers, therefore it can oscilate more.

In Fig. 6, already shortened signals are shown with fourier transforms. In Fig. 6 a) and 6 b), rise of amlitude with higher cutting speed is visible. This is in contradiction with expectation that either slower feed rate or faster cutting speed would result in lower amplitudes. Fig. 6 c) seems completely different, aplitudes are higher, but their change during the process is smaller. This is due to use of another tool.

CONCLUSION

The study is oriented on question, whether vibrations on grippers would be suitable data for adaptive control of milling process on CNC mill.

So far, results show, how a change in cutting parameters affects accelerometer output. Fourier transforms in Fig. 6 show prominent frequency arround 333 Hz, and multiples of this frequency.

Although measurements have already been done, the assesment of most requires further work. Algorithms in Matlab have to be changed, as during first tests, only prominent amplitudes, were those caused by milling process, as in Fig. 5 a). Therefore, it is necessary to either cut import data manually, or change scripts to recognize unwanted section as those in Fig. 5 c). Also, surface roughness of cut samples is yet to be analysed, to achieve more complex results.

ACKNOWLEDGMENTS

The paper was written with the support of project APVV-20-0403, “FMA analysis of potential signals suitable for adaptive control of nesting strategies for milling wood-based agglomerates,“ and thanks to support under the Operational Program Integrated Infrastructure for the project: National infrastructure for supporting technology transfer in Slovakia II – NITT SK II, co-financed by the European Regional Development Fund.

REFERENCES

1. Bedini, R. and Pinotti, P. C. (1982). Experiments on Adaptive Constrained Control of a CNC Lathe. Journal of Engineering for Industry, [online] Volume 104(2), p. 139. Available at: doi:10.1115/1.3185809 [Accessed 6 Apr. 2022].
2. Ford, D., Myers, A., Haase, F., Lockwood, S., & Longstaff, A. (2013). Active vibration control for a CNC milling machine. In: Proceedings of the Institution of Mechanical Engineers, Part C: Journal of Mechanical Engineering Science, [online] Volume 228(2) , p. 230-245. Available at: doi:10.1177/0954406213484224 [Accessed 25 Jan. 2022].
3. Höchsmann (2014). SCM TECH z 5. [online]. Available at: https://wtp.hoechsmann.com/cz/lexikon/22803/scm_tech_z_5 [Accesed 30 Jan. 2022]
4. Kavaratzis, Y. and Maiden, J. D. (1990). Real time process monitoring and adaptive control during CNC deep hole drilling. International Journal of Production Research, [online] Volume 28(12), p. 2201–2218. Available at: doi:10.1080/00207549008942862 [Accessed 12 Mar. 2022].
5. Laszewicz, K., Górski, J., Wilkowski, J. (2013). Long-term accuracy of MDF milling process—development of adaptive control system corresponding to progression of tool wear. European Journal of Wood and Wood Products, [online] Volume 71(3), p. 383-385. Available at: doi:10.1007/s00107-013-0679-2 [Accessed 29 Jan. 2022].
6. Ohuchi, T. and Murase, Y. (2006). Milling of wood and wood-based materials with a computerized numerically controlled router V: development of adaptive control grooving system corresponding to progression of tool wear. Journal of Wood Science, [online] Volume 52(5), p. 395-400. Available at: doi:10.1007/s10086-005-0779-7 [Accessed 1 Feb. 2022].
7. Pico Technology (2008). PicoDiagnostics NVH kits. [online]. Available at: https://www.picoauto.com/products/noise-vibration-and-balancing/nvh-overview [Accesed 30.1.2022].
8. Rowe, W. B., Allanson, D. R., Pettit, J. A., Moruzzi, J. L., & Kelly, S. (1991). Intelligent CNC for Grinding. Proceedings of the Institution of Mechanical Engineers, Part B: Journal of Engineering Manufacture, [online] Volume 205(4), p. 233–239., Available at: https://doi.org/10.1243/PIME_PROC_1991_205_075_02 [Accessed 12 Mar. 2022].
9. Ulsoy, A. G., Koren, Y., Rasmussen, F. (1983). Principal Developments in the Adaptive Control of Machine Tools. Journal of Dynamic Systems, Measurement, and Control, [online] Volume 105(2), p. 107. Available at: doi:10.1115/1.3149640 [Accessed 6 Apr. 2022].

CHIP AND CHIPLESS WOODWORKING PROCESSES, 13(1): 25–30, 2022
Zvolen, Technical University in Zvolen, ISSN 1339-8350 (online), ISSN 2453-904X (print)

STATIC ANALYSIS OF AN UPHOLSTERED FURNITURE SKELETON AT HEAVY-SERVICE LOAD BY FEM

Desislava Hristodorova – Nelly Staneva – Yancho Genchev

Abstract

Two 3D geometric models of one-seat upholstered furniture skeleton with staple corner joints are created - without and with strengthening details under the rails of the seat. A linear static analysis is carried out with CAE system Autodesk Simulation Mechanical® by the method of finite elements (FEM) simulating heavy-service loading of the skeleton. The orthotropic material characteristics of pine solid wood (Pinus Sylvestris L.) for the rails and particle boards (PB) for the side plates are considered in the analysis. The analysis was performed with regard to laboratory derived coefficients of rotational stiffness of used staple corner joints. As results the distribution of displacements, stresses (principal), equivalent strains and factors of safety of upholstered furniture skeleton with staple corner joints are presented and analyzed. It has established the probability of failure of the corner joints between the rear rails of the seat and side plates in the model without strengthening details under the rails of the seat on heavy service load - the bending strength of the side plate material (PB) has 2 times exceeded and factor of safety is critical one – 0.47.

Key words: *upholstered furniture skeleton, staple joints, PB, heavy-service load, FEM*

INTRODUCTION

Upholstered furniture frames have to be both strong and stiff enough to bear especially the heavy-service loads.

The literature study revealed a limited number of publications on skeleton studies of upholstered furniture with side plates made of PB and staple corner joints under heavy-service loads.

Wang [4] has investigated 3D models by beam finite elements of three-seat sofa frame made of OSB simulating light- (1334N), medium- (1779N) and heavy-service (2669N) one seat loads with SAP 2000. She has modeled three constructions of a sofa frame with rigid and semi-rigid connections and two types of connectors: screws and metal plates; staples and metal plates. Wang has established that either screw or staple joints between front rail with stretcher and back rail with stretcher on the bottom had difficulty to hold the medium force and these joints should be reinforced. The frame can’t serve heavy-service load because of the exceeding bending strength of the frame material.

Langova et al. [3] have focused on the latest worldwide problem – growing of the count of overweight people that affect especially sitting furniture design. They have investigated the ultimate load-carrying (up to 110 kg and 150 kg user weight) capacity of flexible chairs made of laminated furniture panels and have established that designed

---

University of Forestry, blvd. “Kl. Ohridsky” 10, 1797 Sofia
e-mail: nelly_staneva@yahoo.com

constructions fail to meet the requirements for weight gain of a population. The authors concluded that current standards (110 kg) must be re-evaluated.

The aim of this study was to define and analyze the displacements and stresses of one-seat skeleton of upholstered furniture with side plates of PB and staple joints *at heavy-service load* by CAD/CAE using the method of finite elements (FEM).

MATERIALS AND METHODS

Three dimensional (3D) model of one-seat upholstered furniture skeleton (rails with cross section 25x50 mm and side plates with thickness 16 mm) was created with Autodesk Inventor Pro® – Fig.1. Two 3D discrete models of the skeleton were created [2] - without (*model A*) and with strengthening details under the rails of the seat (*model B*) – Fig.1. The generated midplane mesh has 5130 orthotropic plate finite elements and 33616 DOF's for *model A* and 5230 orthotropic plate finite elements and 34096 DOF's for *model B*.

A linear static analysis of discrete models (*A* and *B*) of the upholstered furniture skeleton was carried out with CAE system Autodesk Simulation Mechanical® by FEM. Support conditions were set: bottom front rail – no translation on *y* direction and bottom rear rail no translation on *x*-, *y*- and *z* direction – Fig.1. Orthotropic materials characteristics of Scots pine (*Pinus sylvestris L.*) for rails and strengthening details and particleboards (PB) for side plates were introduced in the FEA and are given in our previous publication [2]. Semi-rigid connections between rails and side plates of the skeleton were simulated and detailed described in [1, 2]. The both discrete skeleton models (*A* and *B*) were loaded with a total heavy-service load of 2400 N distributed only between rails of the seat with application point of 100 mm in front of the rear rail (Fig.1).

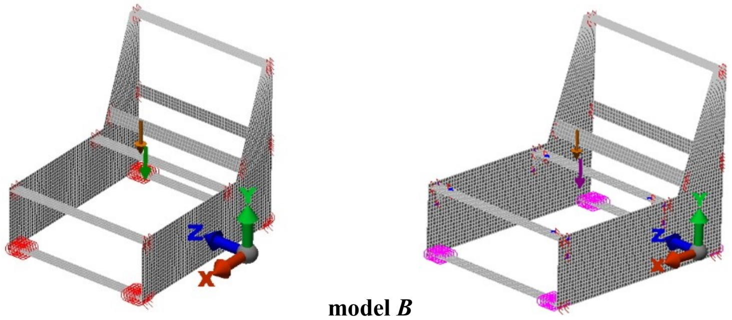

model *A* **model *B***

Figure 1. 3D skeleton discrete models *A* and *B* and loading.

The static factor of safety (FOS) was calculated for the construction for both discrete models under heavy-service loading by the following equation [5]:

$$FOS = \frac{\sigma_{allowable}}{\sigma_{working}} \geq 1,$$

where $\sigma_{allowable}$ is the allowable stress of the material,

$\sigma_{working}$ – working stress of the material.

The changed angle γ between the joint shouders at rails of the seat was mesuared by vectors in the program.

RESULTS AND DISCUSSION

The results of static analysis for linear displacemets u, nodal rotations θ, maximum principal stresses σ_1,minimum principal stresses σ_3, von Mises stresess $\sigma_{vonMises}$ and equivalent strains $\varepsilon_{vonMises}$, as well as the changed angle γ between the joint shouders at the rails of the seat are shown in Table 1, and in Fig.2 to Fig.4 for the skeleton and for the side plates of the skeleton for models *A* and *B,* respectively. The visualizations of the deformed model are shown with a scale factor 3% of model size for the skeleton and with a scale factor 5% of model size for the side plates.

In Fig. 2 the distribution of resultant linear displacement for both models is presented. The maximal resultant displacement for both models was received in the middle of the rear rail of the seat (10.04 mm for *model A* and 7.54 for *model B*) and is determined mainly by the y-displacement (u_y) – Table 1. The strengthening of the upper rail of the seat leads to reducing of the resultant linear displacements of front and rear rails of the seat 1.4 times.

Table 1. Maximal displacements and strains of the whole model and in the side plates.

Parameter	**Location whole model**	***Model A***	***Model B***	**Location side plates**	***Model A***	***Model B***
$u_x.10^{-3},[m]$	side plates	0.67 -2.20	0.75 -0.20	backrest rear upper rail	0.67 0.27	0.75 0.28
$u_y.10^{-3},[m]$	front upper rail rear upper rail	-4.99 -10.04	-3.57 -7.54	front upper rail rear upper rail	0.47 -0.64	0.29 -0.42
$u_z.10^{-3},[m]$	side plates	1.58	2.87	base rear upper rail	1.54 -0.44	2.85 -0.27
θ_{res},[°]	rear upper rail	6.76	5.31	front upper rail rear upper rail	1.39 2.42	0.81 1.72
θ_x, [°]	rear upper rail	2.96	2.11	front upper rail rear upper rail	-1.13 -2.13	-0.62 -1.69
θ_y,[°]	side plates	0.74	0.93	rear upper rail	0.54 -0.75	0.64 -0.92
θ_z, [°]	front upper rail rear upper rail	6.04 -6.76	5.07 -5.35	front upper rail rear upper rail	1.19 -0.78	0.75 -0.45
$\sigma_{vonMises}.10^6$, [N/m^2]	front upper rail rear upper rail	15.34 - 29.85	16.84 32.93 25.03	front upper rail rear upper rail	13.83 20.73	9.08 8.39
$\sigma_1.10^6$, [N/m^2] Max Principal stress	front upper rail rear upper rail	13.63 - 29.13	11.64 26.68 23.92	front upper rail rear upper rail	11.48 7.68	8.30 7.28
$\varepsilon_{vonMises}$, [m/m]	side plates	0.0357	0.0226	front upper rail	0.0356	0.0218
γ,[°]	front upper rail rear upper rail	89.24 88.75	89.81 89.76	-	-	-

In the side plates the maximal resultant linear displacement was established in the base of side plates for both models as for *model B* is 1.84 times greater (absolute value of 1.31 mm) and dissolution of the side plates were established due to the redistribution of the load – Fig. 2. In the side plates the maximal resultant linear displacement for *model B* in the field of rear rail of the seat decreases 1.4 times and in the field of upper front rail - 1.5 times.

The maximal values of the nodal rotations θ are given in Table 1. The maximal resultant nodal rotations for *model A* and for *model B* are located in the rear rail for both models. They are determined manly by rotations around z-axis. The strengthening of the rails of the seat leads to decreasing of the nodal rotations of front and rear rails of the seat 1.3 times.

The change in the angle γ between the joint shouders at the front and rear rails of the seat is also greater for *model A* than the same in the *model B* although insignificant – Table 1.

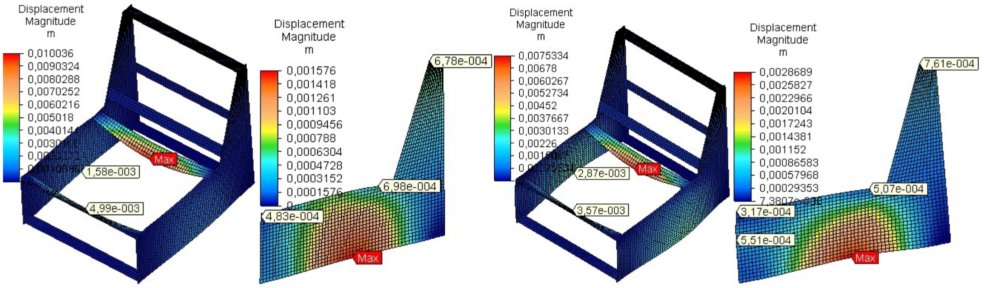
Displacement
Magnitude
m
0,010036
0,0090324
0,0080288
0,0070252
0,0060216
0,005018
1,58e-003
Max
4,99e-003
Displacement
Magnitude
m
0,001576
0,001418
0,001261
0,001103
0,0009456
0,000788
0,0006304
0,0004728
0,0003152
6,78e-004
6,98e-004
4,83e-004
Max
Displacement
Magnitude
m
0,0075334
0,00678
0,0060267
0,0052734
0,00452
0,0037667
0,0030133
0,00226
2,87e-003
Max
3,57e-003
Displacement
Magnitude
m
0,0028689
0,0025827
0,0022966
0,0020104
0,0017243
0,0014381
0,001152
0,00086583
0,00057968
0,00029353
7,61e-004
5,07e-004
3,17e-004
5,51e-004
Max

Figure 2. Distribution of linear resultant displacements for *model A and model B*

The maximum value of von Mises stress in *model A* is concentrated in the rear rail of the seat as *model B* is concentrated in the strengthening details – Table 1. In the rear rail the maximal values of von Mises stress are 1.1 times greater for model A. The maximum value of von Mises stress in *model A* is concentrated in the rear rail of the seat as *model B* is concentrated in the strengthening details – Table 1. In the rear rail the maximal values of von Mises stress are 1.1 times greater for model A. In *model A* the maximal value of maximum principal stress σ_1 (tension) of 29.13 N/mm^2 and minimum principal stress σ_3 (compression) of 29.89 N/mm^2 are located in the middle of the rear rail of the seat, on the bottom and on the top, respectively - Fig. 3.

In *model B* the maximal values of maximum principal stress σ_1 and minimum principal stress σ_3 of 31.11 N/mm^2 are located in the strengthening details of the rear rail of the seat. In the middle of the rear rail in the *model B* maximum principal stress and minimum principal stress are 1.2 times less than the same in *model A* - *F*ig. 3 and Table 1.

In the side plates maximal value of von Mises stress in *model A* is concentrated in the field of rear rail of the seat as in *model B* maximal value of von Mises stress is concentrated in the field of front rail of the seat.

Maximum value of tension stresses in the side plates of the skeleton is located in the field of front rail of the seat for both models (11.48.10^6 N/m^2 for *model A*), as for *model B* it decreases 1.4 times –Table 1.

In the side plates maximal values of compression stresses are located in the field of rear rail of the seat for both models (23.47.10^6 N/m^2 for *model A*), as for *model B* it decreases 2.5 times – Table 1 and Fig.3.

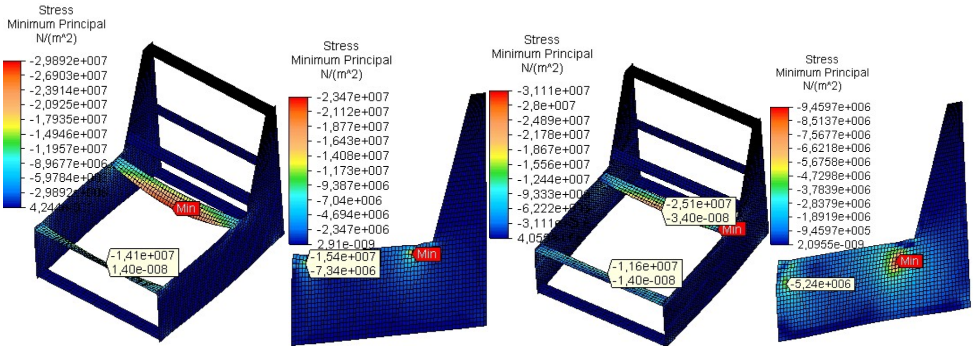
Stress
Minimum Principal
N/(m^2)
-2,9892e+007
-2,6903e+007
-2,3914e+007
-2,0925e+007
-1,7935e+007
-1,4946e+007
-1,1957e+007
-8,9677e+006
Min
-1,41e+007
1,40e-008
Stress
Minimum Principal
N/(m^2)
-2,347e+007
-2,112e+007
-1,877e+007
-1,643e+007
-1,408e+007
-1,173e+007
-9,387e+006
-7,04e+006
-4,694e+006
-2,347e+006
2,91e-009
-1,54e+007
-7,34e+006
Min
Stress
Minimum Principal
N/(m^2)
-3,111e+007
-2,8e+007
-2,489e+007
-2,178e+007
-1,867e+007
-1,556e+007
-1,244e+007
-2,51e+007
-3,40e-008
Min
-1,16e+007
-1,40e-008
Stress
Minimum Principal
N/(m^2)
-9,4597e+006
-8,5137e+006
-7,5677e+006
-6,6218e+006
-5,6758e+006
-4,7298e+006
-3,7839e+006
-2,8379e+006
-1,8919e+006
-9,4597e+005
2,0955e-009
Min
-5,24e+006

Figure 3. Distribution of minimum principal stresses for *model A and model B*

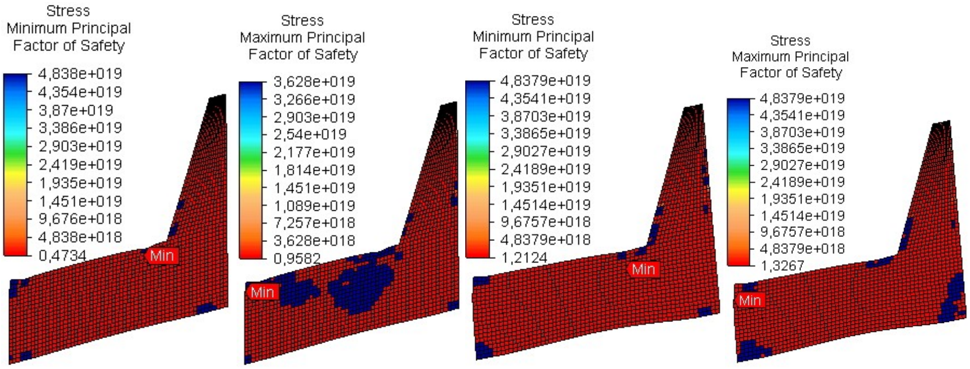
Stress
Minimum Principal
Factor of Safety
4,838e+019
4,354e+019
3,87e+019
3,386e+019
2,903e+019
2,419e+019
1,935e+019
1,451e+019
9,676e+018
4,838e+018
0,4734
Min
Stress
Maximum Principal
Factor of Safety
3,628e+019
3,266e+019
2,903e+019
2,54e+019
2,177e+019
1,814e+019
1,451e+019
1,089e+019
7,257e+018
3,628e+018
0,9582
Min
Stress
Minimum Principal
Factor of Safety
4,8379e+019
4,3541e+019
3,8703e+019
3,3865e+019
2,9027e+019
2,4189e+019
1,9351e+019
1,4514e+019
9,6757e+018
4,8379e+018
1,2124
Min
Stress
Maximum Principal
Factor of Safety
4,8379e+019
4,3541e+019
3,8703e+019
3,3865e+019
2,9027e+019
2,4189e+019
1,9351e+019
1,4514e+019
9,6757e+018
4,8379e+018
1,3267
Min

Figure 4. Distribution of factor of safety (FOS) in the side plates for *model A and model B*

At heavy-service load the tension and especially compression stresses in the side plates of skeleton *model A* reach and exceed bending strength of the board of PB.

The maximal equivalent strain ε is located in the field of front rail of the side plates for both models but for *model B* is 1.6 times less that in the *model A* – Table 1.

It was established that *under heavy-service load* the critical values of the minimum principal stress factor of safety of 0.47 for *model A* and 1.21 for *model B* are received in the field of rear rails of the side plates made of PB (Fig.4). The critical values of the maximum principal stress factor of safety 0.96 for *model A* and 1.33 for *model B* are received in the field of front rails of the side plates.

CONCLUSIONS

Under heavy-service load the critical joints were established – the corner joints between rear rail and the side plates especially for non-strengthening skeleton (*model A*). The most loading field of the side plates is the field of joining of rear rail of the seat, where the maximum values of stresses exceed 2 times the bending strength of PB for *model A*.

The strengthening of the rails of the seat improves the deformation and strength characteristics of the upholstered furniture skeleton under heavy-service load – linear displacements in the upper rails of the seat decrease about 25-28%, nodal rotations – 21%, principal stresses – 16-17%. In the field of upper rails of the side plates the linear displacements decrease about 27%, principal stresses almost 60%.

The probability of failure of the corner joints between the rear rails of the seat and side plates in *model A* is possible during prolonged operation at heavy service load. The established critical values of the factor of safety 0.47 in the side plates made of PB under heavy-service load show that in order to observe safety requirements, skeletons with side plates of PB in case of joints with staples and glue have to be produced of boards with thickness of 18 mm or to be further strengthened.

REFERENCES

1. HRISTODOROVA D., (2019): Stiffness Coefficients in Joints by Staples of Skeleton Upholstered Furniture, Innovation in Woodworking Industry and Engineering Design (INNO), 16 (2), 27-33.
2. STANEVA, N., YA. GENCHEV, D. HRISTODOROVA, (2018b): Approach to designing an upholstered furniture frame by the finite element method. In Acta Facultatis Xylologiae Zvolen, 60 (2), 61−69. doi:10.17423/ afx.2018.60.2.06.
3. LANGOVA, N., R. REH, R. IGAZ, L. KRIST’AK, M. HITKA, AND P. JOSCAK, (2019): Construction of Wood Based Lamella for Increased Load on Seating Furniture. Forests, 10, 525, 1-16; doi:10.3390/f10060525.
4. WANG, X., (2007): Designing, Modeling and Testing of Joints and Attachment Systems for the Use of OSB in Upholstered Furniture Frames, PhD thesis, University Laval, Quebec, Canada.
5. www.autodesk.com - Autodesk Simulation Mechanical – user manual.

CHIP AND CHIPLESS WOODWORKING PROCESSES, 13(1): 31–37, 2022
Zvolen, Technical University in Zvolen, ISSN 1339-8350 (online), ISSN 2453-904X (print)

PRELIMINARY STUDIES ON THE EFFECT OF FEED SPEED ON THE COLOUR CHANGE OF WOOD

Daniel Chuchala – Sandra Karpinska – Aleksandra Suchta – Kazimierz A. Orlowski

Abstract

This paper presents the results of preliminary analyses of the effect of cutting parameters on changes in the colour of wood. Beech wood cut with use circular saw was analysed. The cutting parameter tested was the feed speed, represented by the feed per tooth. Sawing processes with different feed per tooth ranging from 0.0008 mm to 0.09 mm were analysed. It was observed that over the entire range of feed rate per tooth analysed, the colour of the wood changed noticeably, while at certain values the change was very large. However, from a certain limit of feed per tooth, the values of total colour change begin to stabilise. The observed phenomena need to be analysed more extensively and confirmed using other wood sawing processes.

Key words: *sawing process, beech wood, feed speed, colour changes, circular sawing*

INTRODUCTION

Wood is natural and renewable resource has been popular by humans life for millennia. Currently, the wood usage is increasing in modern architecture (SEKULARAC *et al.* 2016) and civil construction (AHMED AND AROCHO 2021; BUKAUSKAS *et al.* 2019) because wood has the specific mechanical and physical properties and is very good storage of carbon (BRUNET-NAVARRO *et al.* 2021).

The wood properties can be changed by use different technological processes. VILKOVSKÝ *et al.* (2021) showed that the storage conditions have an affect on mechanical properies of beech and oak wood. Mechanical properties also change during the wood drying process. The scale of these changes depends on the drying process type used as showed by CHUCHALA *et al.* (2020). Whereas, KLEMENT *et al.* (2020) showed that the contact-drying process affects the physical properties of beech wood. Also, the impregnation process of wood affects its mechanical properties (SINN *et al.* 2020) and physical properties (LICOW *et al.* 2020). Thermal treatments such as drying or steaming of wood, as well as impregnation of wood, also affect to some extent the granulation of chips and dust produced during the machining processes (ROGOZINSKI *et al.* 2021; KMINIAK *et al.* 2020; ORLOWSKI *et al.* 2019). Thermal treatment processes for wood significantly vary the colour of the treated wood. This is noticeable both for drying processes (BARANSKI *et al.* 2020; KLEMENT *et al.* 2019) and in steaming processes using higher temperatures (DZURENDA 2022; GEFFERT *et al.* 2017). In addition, the structural structure of the wood also influences the colour differences (KLEMENT and

Gdansk University of Technology, Faculty of Mechanical Engineering and Ship Technology, Institute of Manufacturing and Materials Technology, Narutowicza 11/12, 80-233 Gdansk, Poland
e-mail: danchuch@pg.edu.pl, sandrakarpi@wp.pl, alekonop@pg.edu.pl, korlowsk@pg.edu.pl

VILKOVSKÁ 2019). Therefore, it can be concluded that the process temperature has a noticeable effect on the colour changes of the wood. However, KONOPKA *et. al.* (2021) showed that colour change of beech wood during kiln drying process and steaming process is only on very thin external layer of wood.

The wood colour is more important an aesthetic property. Machining processes are often the last processes in the manufacturing process of wooden components. The parameters of the machining processes affect the cutting forces (CHUCHALA *et al.* 2020; SINN *et al.* 2020), noise during the process (LICOW *et al.* 2020) as well as the granulation of chips and dust (ORLOWSKI *et al.* 2019; ROGOZINSKI *et al.* 2021; KMINIAK *et al.* 2020). The cutting parameters also have a significant effect on the temperature in the cutting zone (IGAZ *et al.* 2019). The heat generated during the cutting process can affect the wood and consequently change its colour. A change in colour during the cutting process can be an aesthetically undesirable effect on the finished product.

The aim of the research was to carry out preliminary tests to verify how the feed speed of the sawing process affects the colour change of beech wood.

MATERIALS AND METHODS

Materials

The beech wood (*Fagus sylvatica* L.) was a analysed material. The analysed wood was obtained from the regions of southern Austria. For the analysis, 11 rectangular samples of (wood blocks W = 30 mm × H = 20 mm × L = 200 mm) were prepared, cut from beams coming from one log. The test material was free from defects that could affect the colour change, e.g. false heartwood, reaction wood etc. One of the samples was selected as a reference sample (no. 0), which was not subjected to sawing tests. The surface of the reference sample created by the sawmilling process was handly sanded to remove a layer of wood, which colour may have changed as a result of the sawmilling process.

Machine tool, tools and cutting process

Cutting tests of the analysed wood were carried out under industrial conditions on a SERON CNC milling machine dedicated to wood processing. The cutting tool used for the tests was a saw milling cutter PI-401 from FABA S.A. (Poland) with cemented carbide teeth and straight cutting edges in GM shape. The applied cutting tool was sharp, the cutting edges and other basic dimensions as follows: overall set (kerf width) (S_t), 4 mm; saw blade thickness (s), 3 mm; diameter (D), 125 mm; number of teeth (z), 24; tool side rake (γ_f), 15°.

The cutting process was conducted with one and constant value of cutting speed for all samples, v_c = 50 m·s^{-1} The only varying cutting parameter was feed speed (v_f), which was adopted in the range from 115 mm·min^{-1} to 16509 mm·min^{-1}, divided into 10 steps (Table 1).

Table 1. Cutting parameters used in tests

Sample number	Cutting speed, v_c	Feed speed, v_f	Feed per tooth, f_z
	$m \cdot s^{-1}$	$mm \cdot min^{-1}$	mm
1	50	154	0.0008
2	50	384	0.002
3	50	768	0.004
4	50	1152	0.006
5	50	1536	0.008
6	50	1834	0.01
7	50	5503	0.03
8	50	9172	0.05
9	50	12840	0.07
10	50	16509	0.09

Colour measurement and analysis

Colour measurements were carried out using a portable Konica Minolta CR-10 Colour Reader spectrometer. The newly created surfaces as a result of cutting through each sample at different feed speeds were subjected to colour measurements at 10 equally spaced points. Changes in wood colour were analysed using the CIELAB system (ISO 11664-2:2007; ISO 11664-4:2019):

$$\Delta E = \sqrt{(L_i - L_0)^2 + (a_i - a_0)^2 + (b_i - b_0)^2}[-] \qquad (1)$$

where L_0, a_0, b_0 are the values of color spectra for reference sample without sawing, and L_i, a_i, b_i are the values of color spectra for each sawing samples, where $i = 1,\ldots,10$.

In addition, colour changes were assessed according to the scale proposed by CIVIDINI *et al.* (2007), as follows:

$\Delta E < 0.2$: invisible colour change;
$2 > \Delta E > 0.2$: slight change of colour;
$3 > \Delta E > 2$: colour change visible in high filter;
$6 > \Delta E > 3$: colour changes visible with the average quality of the filter;
$12 > \Delta E > 6$: high colour change;
$\Delta E > 12$: different colour.

RESULTS

The results of the measured colour change parameters during the sawing process with different feed rates per tooth are shown in Table 2. Sample number 0 shows the results of the measurement of the colour parameters for the reference sample, while the subsequent numbers from 1 to 10 represent measurements for successive cutting processes with different values of one of the main parameters of the cutting process, which is the feed speed v_f. In this case this parameter is represented by the basic parameter such as feed per tooth f_z.

Table 2. Color change measurement results after sawing process with different values of feed per tooth

Number of sample	Feed per tooth, mm	Statistic values	L	a	b	ΔE [%]
0	-	average value	66.61	11.01	16.80	-
		SD	0.18	0.08	0.29	
1	0.0008	average value	63.39	10.72	15.87	2.30
		SD	4.33	0.69	0.21	
2	0.002	average value	66,17	11.00	17.01	3.55
		SD	0.97	0.34	0.19	
3	0.004	average value	67.31	10.98	17.01	4.62
		SD	0.59	0.45	0.41	
4	0.006	average value	66.48	11.10	16.06	3.99
		SD	0.92	0.51	0.21	
5	0.008	average value	65.83	11.63	16.37	3.15
		SD	0.18	0.29	0.24	
6	0.01	average value	66.62	11.03	16.84	3.97
		SD	0.17	0.09	0.30	
7	0.03	average value	67.97	10.29	17.00	5.48
		SD	0.39	0.22	0.32	
8	0.05	average value	66.15	10.89	17.23	3.56
		SD	0.70	0.38	0.16	
9	0.07	average value	66.00	10.83	16.58	3.54
		SD	0.63	0.29	0.24	
10	0.09	average value	65.91	11.36	17.02	3.17
		SD	0.14	0.13	0.33	
Legend: L, a, b – colour changes parameters measured for reference sample without sawing process and for samples after sawing process, ΔE - total colour change, SD – standard deviation						

When observing the individual values of the colour parameters (L, a, b), the large differences are not visible in the results. However, if observing the values of the total colour change parameter ΔE, can be notice that the values in the characteristic points reach almost the values of high colour change according to CIVIDINI *et al.* (2007), i.e. up to 6 % (sample no 3 and sample no 7).

Almost all used values feed per tooth resulted in achieving a total colour change ΔE of more than 3%. Only the value of f_z = 0.0008 mm produced a lower total colour change (ΔE = 2.30%). Which is an interesting phenomenon, as IGAZ *et al.* (2019) showed that at lower feed per tooth, the cutting process temperatures are higher than at larger feed per tooth values. Figure 1 shows the course of the total colour change as a function of the feed per tooth used in the sawing process. It can be observed that the total colour change values start be stabilised as feed per tooth of f_z = 0.05 mm. However, it still maintains values above 3% which indicates a noticeable change in colour.

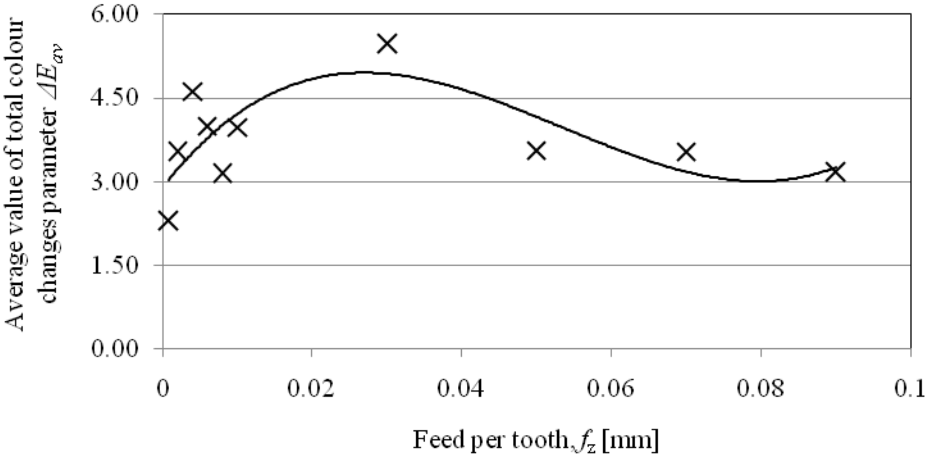

Figure 1. Average value of total colour changes parameter ΔE_{av} in relation to feed per tooth.

CONCLUSIONS

The analysis carried out to investigate the effect of the feed speed during the sawing process on the colour change of beech wood has allowed the following conclusions:

- the sawing process noticeably changes the colour of the beech wood over a wide range of feed speeds used. The parameter of total colour change ΔE in almost the whole range of tested feed speeds reached values above 3%;
- for the circular sawing process analysed, the highest values of the total colour change parameter were observed for feed per tooth of 0.03 mm, $\Delta E = 5.48\%$. It is very close value to limit of high colour change;
- The issue of the effect of the cutting process parameters on the colour change of wood needs to be analysed in greater depth. Both an enlargement of the range of analysed feed per tooth values for the circular sawing process and an analysis of other cutting processes and other cutting parameters, such as cutting speed.

ACKNOWLEDGEMENTS

This work was supported by Polish National Agency for Academic Exchange (NAWA Poland), grant no BPN/BSK/2021/1/00033 and the Slovak Research and Development Agency under the contract no. SK-PL-21-0059 are kindly acknowledged.

The authors would also like to acknowledge the company STOLMACH from Nowy Dwor Gdanski, Poland, for sharing the machine tool and their assistance with the sawing tests.

REFERENCES

AHMED, S., AROCHO, I., 2021. Analysis of cost comparison and effects of change orders during construction: Study of a mass timber and a concrete building project. Journal of Building Engineering 33, 101856. DOI: 10.1016/j.jobe.2020.101856

BARANSKI, J., KONOPKA, A., VILKOVSKÁ, T., KLEMENT, I., VILKOVSKÝ, P., 2020. Deformation and surface color changes of beech and oak wood lamellas resulting from the drying process. Bioresources, 15(4), 8965–8980. DOI:10.15376/biores.15.4.8965-8980.

BRUNET-NAVARRO, P., JOCHHEIM, H., CARDELLINI, G., RICHTER, K., MUYS, B., 2021. Climate mitigation by energy and material substitution of wood products has an expiry date. Journal of Cleaner Production 303, 127026. DOI: 10.1016/j.jclepro.2021.127026

BUKAUSKAS, A., MAYENCOURT, P., SHEPHERD, P., SHARMA, B., MUELLER, C., WALKER, P., BREGULLA, J., 2019. Whole timber construction: A state of the art review. Construction and Building Materials, 213, 748–769, DOI: 10.1016/j.conbuildmat.2019.03.043

CHUCHALA, D., SANDAK, J., ORLOWSKI, K.A., MUZINSKI, T., LACKOWSKI, M., OCHRYMIUK, T., 2020. Effect of the Drying Method of Pine and Beech Wood on Fracture Toughness and Shear Yield Stress. Materials, 13, 4692. DOI: 10.3390/ma13204692

CIVIDINI, R., TRAVAN, L., ALLEGRETTI, O., 2007. White beech: A tricky problem in drying process. Proceedings of 7th ISCHP (International Scientific Conference on Hardwood Processing), 24-26 September 2007, Quebec City, Canada

DZURENDA, L. 2022. Range of color changes of beech wood in the steaming process. BioResources 17(1): 1690-1702.

GEFFERT, A., VÝBOHOVÁ, E., GEFFERTOVÁ, J., 2017. Characterization of the changes of colour and some wood components on the surface of steamed beech wood. Acta Facultatis Xylologiae Zvolen, 59(1), 49–57. DOI:10.17423/afx.2017.59.1.05.

IGAZ, R., KMINIAK, R., KRIŠÁK, L., NĚMEC, M., GERGEĽ, T., 2019. Methodology of temperature monitoring in the process of CNC machining of solid wood. Sustainability, 11, 95. DOI:10.3390/su11010095

ISO 11664-2 (2007) Colorimetry – Part 2: CIE Standard Illuminants (Geneva: International Organization for Standardization)

ISO 11664-4 (2019) Colorimetry — Part 4: CIE 1976 L*a*b* Colour Space (Geneva: International Organization for Standardization)

KLEMENT, I., VILKOVSKÁ, T., BARANSKI, J., KONOPKA, A., 2019. The impact of drying and steaming processes on surface color changes of tension and normal beech wood. Drying technology, 37(12), 1490-1497. DOI: 10.1080/07373937.2018.1509219

KLEMENT, I., VILKOVSKÁ, T., 2019. Color characteristics of red false heartwood and mature wood of beech (Fagus sylvatica L.) determining by different chromacity coordinates. Sustainability, 11(3), 690. DOI: 10.3390/su11030690

KLEMENT, I., VILKOVSKÝ, P., VILKOVSKÁ, T., 2020. The effect of contact-drying on physical properties of European beech (Fagus sylvatica L.). Forests 11(8), 890. DOI: 10.3390/f11080890

KMINIAK, R., ORLOWSKI, K.A., DZURENDA, L., CHUCHALA, D., BANSKI, A., 2020. Effect of Thermal Treatment of Birch Wood by Saturated Water Vapor on Granulometric Composition of Chips from Sawing and Milling Processes from the Point of

View of Its Processing to Composites. Applied Sciences-Basel, 10, 7545. DOI: 10.3390/app10217545

KONOPKA, A., CHUCHALA, D., ORLOWSKI, K.A., VILKOVSKÁ, T., KLEMENT, I., 2021. The effect of beech wood (Fagussylvatica L.) steaming process on the colour change versus depth of tested wood layer, Wood Material Science & Engineering, AHEAD-OF-PRINT, 1-9. DOI: 10.1080/17480272.2021.1942200

LICOW, R., CHUCHALA, D., DEJA, M., ORLOWSKI, K.A., TAUBE, P., 2020. Effect of pine impregnation and feed speed on sound level and cutting power in wood sawing. Journal of Cleaner Production, 272, 122833. DOI: 10.1016/j.jclepro.2020.122833

ORLOWSKI, K.A., CHUCHALA, D., MUZINSKI, T., BARANSKI, J., BANSKI, A., ROGOZIŃSKI, T., 2019. The effect of wood drying method on the granularity of sawdust obtained during the sawing process using the frame sawing machine. Acta Facultatis Xylologiae Zvolen, 61, 83-92. DOI: 10.17423/afx.2019.61.1.08

ROGOZINSKI, T., CHUCHALA, D., PĘDZIK, M., ORLOWSKI, K.A., DZURENDA, L., MUZIŃSKI, T., 2021. Influence of drying mode and feed per tooth rate on the fine dust creation in pine and beech sawing on a mini sash gang saw. European Journal of Wood and Wood Products (HOLZ ALS ROH-UND WERKSTOFF), 79, 91-99. DOI: 10.1007/s00107-020-01608-8

SEKULARAC, J.I., TOVAROVIC, J.C., SEKULARAC, N., 2016. Application of wood as an element of façade cladding in construction and reconstruction of architectural objects to improve their energy efficiency. Energy and Buildings, 115, 85–93. DOI: 10.1016/j.enbuild.2015.03.047

SINN, G., CHUCHALA, D., ORLOWSKI, K.A., TAUBE, P., 2020. Cutting model parameters from frame sawing of natural and impregnated Scots pine (Pinus sylvestris L.). European Journal of Wood and Wood Products (HOLZ ALS ROH-UND WERKSTOFF), 78, 777-784. DOI: 10.1007/s00107-020-01562-5

VILKOVSKÝ, P., VILKOVSKÁ, T., KLEMENT, I., ČUNDERLÍK, I., 2021. Impact of storage conditions on shear strength of beech (Fagus sylvatica L.) and sessile oak (Quercus petraea (Matt.) Liebl.). Forests 12(8), 1025. DOI: 10.3390/f12081025

CHIP AND CHIPLESS WOODWORKING PROCESSES, 13(1): 39–49, 2022
Zvolen, Technical University in Zvolen, ISSN 1339-8350 (online), ISSN 2453-904X (print)

GRANULOMETRIC CHARACTERISTICS OF MDF AND PARTICLEBOARD BY VARYING TECHNOLOGICAL PARAMETER FEED SPEED USING A CNC MILLING ROUTER

Martin Júda – Ján Šustek – Ľuboš Krišťák

Abstract

The object of this study is to compare granulometric characteristics of wood dust generated by milling using a CNC milling machine of two wood-based materials: medium-density fibreboard (MDF) and particleboard. Selected specimens were milled at a constant depth of cut $e = 4$ mm and revolutions of cutting tool at $n = 18\,000$ rev·min^{-1} using three various feed speeds $v_f = 4$, 6, and 8 m·min^{-1}. Characteristics of wood dust generated by defined conditions were evaluated by sieve analysis which represents the total percentage weight share of a fraction collected at a defined sieve mesh. Sieving analysis showed that the smallest chips and the finest dust are created during the milling of medium-density fibreboard. The granulometric analysis showed that a high percentage of so-called fine fractions (84%) was generated during the milling of MDF panels with the depth of cut $e = 4$ mm and feed speed $v_f = 4$ m·min^{-1}. In combination the depth of cut $e = 4$ mm and feed speed $v_f = 8$ m·min^{-1} the percentage weight share decreased to 46% of the total weight share. In the case of particleboard, a high percentage of generated fractions were in the range of the so-called medium-coarse fraction. In the so-called fine fraction, the highest number was achieved at the total weight share of 37% in the same combination as in the previous case the depth of cut $e = 4$ mm and feed speed $v_f = 4$ m·min^{-1}. At the depth of cut $e = 4$ mm and feed speed $v_f = 8$ m·min^{-1} the so-called fine fraction decreased to 22% of the total weight share.

Key words: *Respirable dust, Granulometric analysis, Sieve analysis, Feed speed, Medium-density Fiberboard, Particleboard.*

INTRODUCTION

Medium-density fibreboard (MDF) and particleboard are the most frequently used wood-based materials in furniture or cabinet manufacturing industries. This statement corresponds to a survey [1] published in the year 2019, stating that the world's medium-density fibreboard output surpassed 104 million m^3 and particleboards 98 million m^3. After sawing, milling is the most comprehensive method of secondary moulding of wood-based materials. During the milling process of wood-based materials, massive quantities of dust are generated while those materials are cut and milled in industrial woodworking processing operations. This dust is likely to be inhaled by workers and can cause serious non-reversible diseases. In many sources [2-8], it is mentioned that exposure to wood dust is associated with an increased risk of nasal and sino-nasal cancer. Recent studies [9-12] in

Technical University in Zvolen, T. G. Masaryka 24, 960 01 Zvolen
e-mail: xjuda@is.tuzvo.sk, sustek@tuzvo.sk, kristak@tuzvo.sk

several woodworking factories found that approximately 30% of collected dust formed by machining MDF, was respirable. In the source [13] it is mentioned that this number is even 30 times higher than previous studies showed. It has been issued by the International Agency for Research on Cancer that wood dust is one of the carcinogens to humans (Group 1) and induces nasal and paranasal sinus malignancies according to extensive epidemiological evidence [14]. The recent European Union (EU) directives also classified hardwood dust as carcinogenic to humans and set an occupational exposure limit (OEL) of 2 $mg \cdot m^{-3}$ of inhalable hardwood dust fraction calculated or measured for a reference 8-h period with a transitional limit value of 3 $mg \cdot m^{-3}$ until January 2023 [21]. Wood dust presents a serious occupational hazard not just to human health, but also to the environment. Due to its good flammability and its small size with a large surface contact area if wood dust conducts a spark it can lead to fire and explosion [15-17].

The development of an effective dust reduction technique in wood machining processes is essential and thus it is necessary to investigate the granulometric characteristic of dust generated from woodworking machinery and to clarify the effect of machining conditions on the properties of wood dust. The Authors [9] reported that MDF can generate 6 times higher mass concentration than solid wood (pine or beech). The Authors [18] mentioned the source [19] reported that the milling of MDF generates 27 times more airborne dust than solid pine. Other authors [20] reported that the milling of MDF generates 30 times and 8 times more airborne dust than solid pine and particleboard, respectively. To this date, most reported studies focused on comparing the dust emission rate of different tree (wood) specimens and wood-based products. It can be stated that medium-density fibreboard, particleboard, and tropical hardwoods have a high rate of dust emission compared to softwood species [5, 18, 20]. As the author [22] noted the correlation between the chip thickness and mass concentration of airborne dust is complex and depends on the variation in depth of cut, feed speed, and rotation speed. When chip thickness is varied by changing the depth of cut and feed speed, dust emission is highly affected by chip thickness at a smaller depth of cut.

CNC milling machines are some of the widely used machines in the furniture and cabinet industry. If the workers are exposed to the wood dust which is not effectively removed by dust extractors, they can be seriously damaged by long exposure to the dust. Thus, it is necessary to investigate the granular characteristics of wood dust generated by MDF using a CNC milling machine with various technological parameters. In this study morphological characteristics of MDF and particleboard granulometry by sieve analysis is investigated.

WORK MATERIALS AND METHODOLOGY

CNC MACHINE:

The presented experiment was carried out using a 5-axis CNC machining centre SCM Tech Z5 manufactured by the company SCM Group, Headquarters Via Emilia 77, 47, 921 Rimini (RN), Italy. The basic parameters of the machining centre given by the manufacturer are provided in **Table 1** and **Table 2**.

Table 1 Technical and technological parameters of CNC machining centre SCM Tech Z5 used in the experiment

Useful desktop:	X = 3050 [mm], Y = 1300 [mm], Z = 300 [mm]
Speed axis:	X = 0 ÷ 70 [m·min^{-1}] Y = 0 ÷ 40 [m·min^{-1}] Z = 0 ÷ 15 [m·min^{-1}]
Vector rate:	0 ÷ 83 [m·min^{-1}]

Table 2 Parameters of the main spindle / electric spindle with HSK F63 connector

Rotation axis B:	320 [°]
Rotation axis C:	640 [°]
Revolutions n:	600 ÷ 24,000 [rev·min^{-1}]
Power P:	11 [kW], 24 000 [rev·min^{-1}]
Power - HSK P:	7.5 [kW], 10 000 [rev·min^{-1}]
Maximum tool diameter and length:	D = 160 [mm], L = 180 [mm]

TOOL PARAMETERS:

The characteristic of the tool used for the experiment is as follows: diamond router cutter (shank cutter) with two cutting blades (Diamond Router Cutter Economic Z2+1-D18x26L85S=20x50 (6DP+1HW)), manufactured by IGM Tools and Machines (Czech Republic). The basic technical data and technological parameters that are given by the manufacturer are shown in **Table 3**. A diamond shank cutter with two cutting blades was used for the experiment. It was chosen for its frequent usage in small woodworking companies due to its high tool lifetime and relatively low cost.

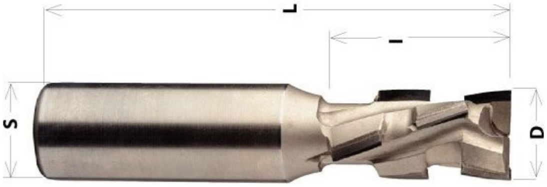

Figure 1 IGM Diamond Router Cutter Economic Z2+1-D18x26 L85 S=20x50 (6DP+1HW) (Source: IGM Tools and Machines)

Table 3 Technical parameters of the milling tool

Name of the milling tool	Working diameter D [mm]	Working length L [mm]	Diameter of the chucking shank S [mm]	Number of cutting blades	Material of the cutting edge
Router Cutter Econ. Z2+1	18	26	20	2+1 HW	Diamond

SPECIMENS:

The raw particleboard and medium-density fibreboard panels (manufactured by the company Kronospan Polska sp. Z o. o., street Warýnskiego 1, PL-78-400 Szczecinek, Poland) were used for the experiments. The processed MDF and particleboard blanks had those dimensions: thickness t = 18 mm, width w = 300 mm, and length l = 500 mm.

MILLING PARAMETERS:

The specimens were milled with the diamond shank milling cutter with the following technological parameters: constant depth of cut e = 4 mm; rotation speed of spindle with cutting tool n = 18.000 rev·min^{-1}; and feed speed v_f = 4, 6, and 8 m·min^{-1}. For each combination of parameters, six specimens in total were collected. The conventional milling (up-milling) method was used for carried experiment.

METHODOLOGY:

The particle size distribution (PSD) was determined by sieving analysis off-site in the laboratory. A special set of stacked sieves was used for this experiment. This set consists of various sieves in the interval (2mm, 1mm, 0.5mm, 0.25mm, 0.125mm, 0.063mm, 0.032mm, and the pan representing all sizes below 0.032mm), stacked on each other. Then this set was placed in the vibration stand of the screening device Retsch AS 200c (Retsch GmbH, Haan, Germany). In accordance with the standard ISO 3310-1 sieving parameters were sieve interruption frequency 20 sec, network deflection amplitude 2 mm·g^{-1}, screening time τ = 15 min, the weight of the specimen = 50 g.

The particle size distribution (PSD) was obtained by weighting. The proportions of the remaining fractions on the sieves after sieving were weighed on an electric laboratory balance weight Radwag 510/C/2 (Radwag Balances and Scales, Radom, Poland) with an accuracy of 0.001 g. The screening was performed on six specimens in total for each.

The results were worked out to a multi-factor statistical analysis of variance (ANOVA) to discern significant differences at 95% level of confidence, using a specialized SAS software program (version 9.2, Cary, NC, USA).

RESULTS AND DISCUSSION

In the presented study, the grain size distribution between the two wood-based materials during various milling conditions using a CNC milling machine was investigated by the weighting method. The results of weight share can be observed in **Table 4** for medium-density fibreboard (MDF) and **Table 5** for particleboard. In both cases, the tables demonstrate the average particle size distribution (PSD).

Table 4 Average particle size distribution of MDF according to individual combinations of technological parameters such as feed speed (v_f) and depth of cut (e)

Sieve Mesh [mm]	Fraction Type	**Medium-density fibreboard, thickness 18 mm**		
		I.	**II.**	**III.**
		vf4 - e/4	**vf6 - e/4**	**vf8 - e/4**
2.00	Coarse	0.03	0.01	0.01
1.00		0.06	0.08	0.14
0.500	Medium Coarse	0.29	4.78	21.10
0.250		16.00	37.00	32.59
0.125	Fine	31.44	25.50	18.72
0.063		28.57	17.04	14.12
0.032		20.02	14.17	12.74
<0.032		3.58	1.43	0.58
Σ of Fine %		**83.61**	**58.13**	**46.17**

Depth of cut – **e** [mm], Feed speed – $\mathbf{v_f}$ [m·min^{-1}]

Table 5 Average particle size distribution of particleboard according to individual combinations of technological parameters such as feed speed (v_f) depth of cut (e)

Sieve Mesh [mm]	Fraction Type	**Particleboard, thickness 18 mm**		
		I.	**II.**	**III.**
		vf4 - e/4	**vf6 - e/4**	**vf8 - e/4**
2.00	Coarse	0.01	0.05	0.09
1.00		3.66	4.87	6.71
0.500	Medium Coarse	21.65	28.07	34.38
0.250		37.75	38.23	36.42
0.125	Fine	28.08	22.30	17.87
0.063		7.83	5.75	3.97
0.032		1.01	0.72	0.56
<0.032		0.00	0.00	0.00
Σ of Fine %		**36.93**	**28.77**	**22.40**

Depth of cut – **e** [mm], Feed speed – $\mathbf{v_f}$ [m·min^{-1}]

Table 4 shows that the majority of share weight during milling of MDF material was formed by the so-called fine fraction. The highest percentage was achieved with combinations of feed speed $v_f = 4$ m·min^{-1} and depth of cut e = 4 mm. The proportions of fine particles, in this case, represent almost 84% of the total percentage weight share. Compared to the authors [23] the similar results that can be used for comparison (obtained with a combination of feed speed $v_f = 5$ m·min^{-1} and depth of cut e = 5 mm) during milling an MDF panels fine fraction representing in authors case 90% of the total percentage weight share.

In the case of the present paper, increased feed speed from v_f = 4 m·min^{-1} to v_f = 6 m·min^{-1} caused a reduction of the so-called fine fraction from 84% to 58% of the total percentage weight share. The lowest total percentage weight share of 46% was achieved with a combination of feed speed v_f = 8 m·min^{-1} and depth of cut e = 4 mm. It was found that during the milling of MDF panels using a CNC milling machine, no significant percentage of the total weight share of the so-called coarse fraction type was created.

In the case of particleboard (**Table 5**), most of the fraction type was formed by the so-called medium-coarse fraction. This total percentage share weight is in the range from 64% to 71%. The lowest total percentage weight share of the medium-coarse fraction was achieved with a combination of feed speed v_f = 4 m·min^{-1} and depth of cut e = 4 mm. However, in a combination of cutting parameters feed speed v_f = 4 m·min^{-1} and depth of cut e = 4 mm, the highest percentage of the so-called fine fracture types (37% of total percentage weight share) was achieved. In the combination of feed speed v_f = 8 m·min^{-1} and depth of cut e = 4 mm, the highest value of the medium-coarse fraction type peaked at 71%, and the lowest value of the so-called fine fraction botted at 22% of the total percentage weight share.

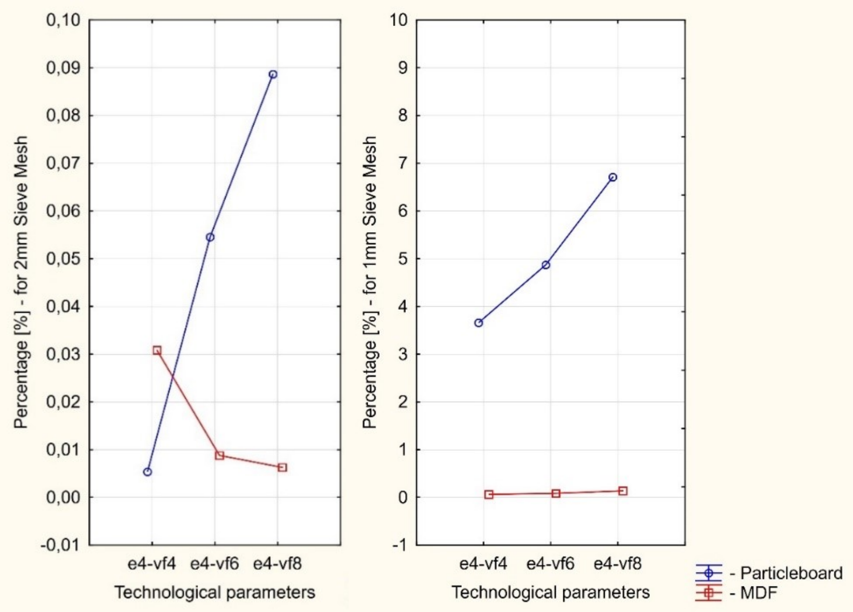

Depth of cut – **e** [mm], Feed speed – $\mathbf{v_f}$ [m·min^{-1}]

Figure 2 Comparison between Medium Density Fibreboard and Particleboard Granulometry of 2mm and 1mm Grain Size Grade

In terms of technological parameters, it can be seen in **Figure 2** that the so-called coarse fraction total weight share in the case of MDF was represented by a total percentage weight share ranging from 0.06% to 0.14% for 1 mm grain Size. It was found that increasing feed speed v_f from 4 m·min^{1} to 8 m·min^{-1} had no significant effect on the growth of coarse fraction total percentage weight share. A significant percentage total weight share was formed in particleboard ranging from 4% to 7%. Increasing feed speed from v_f = 4 m·min^{-1} to v_f = 8 m·min^{-1} had also no significant effect on the growth of the total percentage weight share. In this case, no total percentage weight share of 2 mm particle size was found.

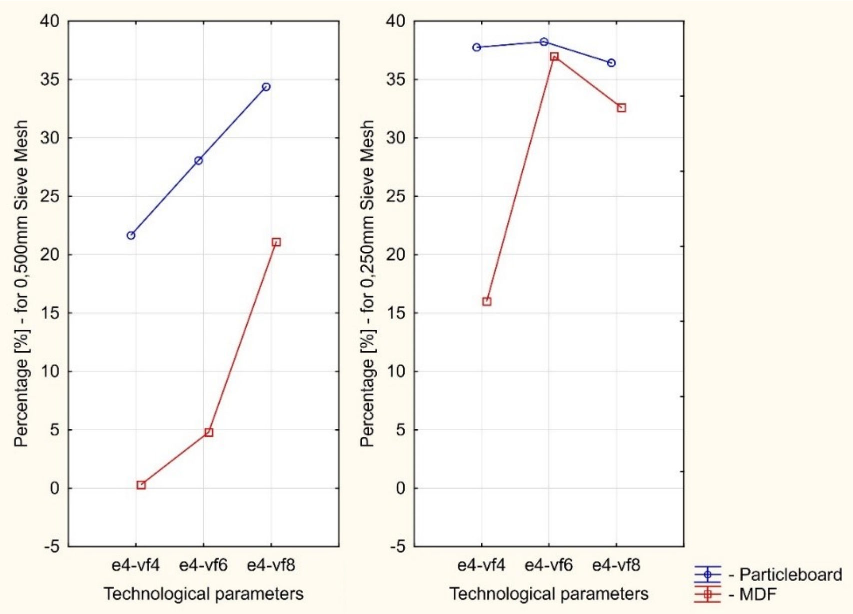

Depth of cut – **e** [mm], Feed speed – $\mathbf{v_f}$ [m·min^{-1}]

Figure 3 Comparison between Medium Density Fibreboard and Particleboard Granulometry of 0.5mm and 0.25mm Grain Size Grade

For the so-called medium coarse fraction, **Figure 3** shows that the MDF total percentage weight share ranged from 0% to over 20% for 0.5mm grain size. The grain size of 0.25mm ranged from 16% to 37% of the total weight share. The percentage weight share of 0.5mm grain size had grown as the feed speed was increasing. In this case, there was a steep growth in weight when the feed speed increased. For the grain size of 0.250mm, the results are mostly the same except for the feed speed $v_f = 8$ m·min^{-1} when the percentage value decreased. Similar results can be observed also in the case of particleboard, where 0.5mm the grain size was growing linearly as the feed speed was increasing. For the 0.25mm grain size, there was a slight growth in grain size, and at a feed speed of $v_f = 8$ m·min^{-1} the total percentual weight share decreased a bit.

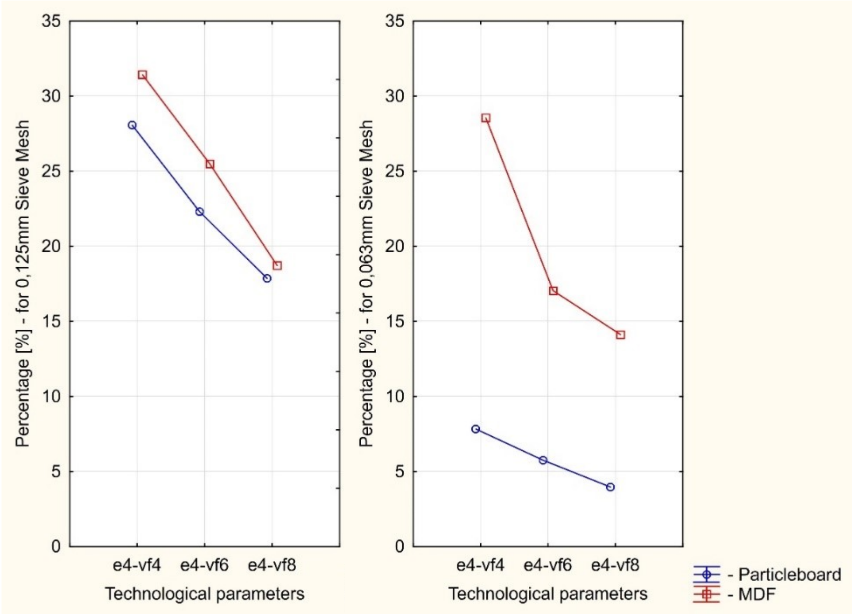

Depth of cut – **e** [mm], Feed speed – $\mathbf{v_f}$ [m·min^{-1}]

Figure 4 Comparison between Medium Density Fibreboard and Particleboard Granulometry of 0.125mm and 0.063mm Grain Size Grade

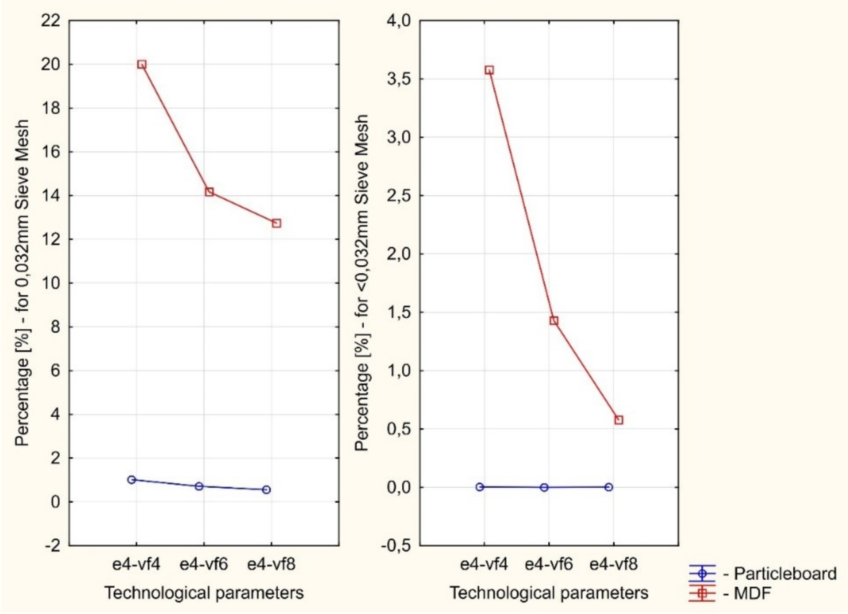

Depth of cut – **e** [mm], Feed speed – $\mathbf{v_f}$ [m·min^{-1}]

Figure 5 Comparison between Medium Density Fibreboard and Particleboard Granulometry of 0.032mm and lower than <0.032mm Grain Size Grade

Figure 4, and **Figure 5** represent the so-called fine fraction type. In the case of this type if fraction showed the most significant influence of increasing feed speed from $v_f = 4\ \text{m}\cdot\text{min}^{-1}$ to $v_f = 8\ \text{m}\cdot\text{min}^{-1}$ and a decrease in the amount of formed so-called fine fraction of MDF and particleboard. Can be observed for Grain size of 0.125mm in both cases of MDF and particleboard, increasing feed speed decreased the total percentage weight share of fine fraction. The same results can be observed in the grain size of 0.063mm. In the case of grain sizes, 0.032mm and <0.032mm MDF there was a decrease in total percentage weight share when the feed speed increased. No significant amount of fine fraction is formed by milling of particleboard.

CONCLUSION

The granulometric analysis of MDF and particleboard during milling using a CNC machine was investigated using the sieve analysis. The paper demonstrates a change in the granulometry composition of wood-based materials by modifying the technological parameter of feed speed. Based on the above, the obtained results can be summarized as follows:

- The majority of the so-called fine fractions 0.125mm and smaller ≤0.125mm are formed during the milling of medium-density fibreboard. The highest content of fine respirable particles reaches 84% in combination with the depth of cut e = 4 mm and feed speed $v_f = 4\ \text{m}\cdot\text{min}^{-1}$. Increasing the feed speed causes decrease in fine particle content during milling it bottoms at 46% when the depth of cut is e = 4 mm and feed speed is $v_f = 8\ \text{m}\cdot\text{min}^{-1}$ of medium-density fibreboard panels.
- In the case of particleboard, the number of fine inhalable particles formed during milling is significantly lower than compared to medium-density fibreboard. The total percentage weight share of fine inhalable particles is smaller than ≤0.125mm at 37% in combination with depth of cut e = 4 mm and feed speed $v_f = 4\ \text{m}\cdot\text{min}^{-1}$. Increase in the feed speed results in a decrease in the total percentage weight share of fine particles. It bottoms at 22% in combination with the depth of cut e = 4 mm and feed speed $v_f = 8\ \text{m}\cdot\text{min}^{-1}$. In both cases changing technological properties of feed speed v_f causes a decrease in the total percentage weight share value of fine particles formed during the milling of wood-based materials.

The obtained result could be used to optimise the CNC router to reduce the lower content of fine particles and thus, to reduce occupational exposure to harmful wood dust.

REFERENCES

[1] Food and Agriculture Organization of the United Nations (2019) FAO yearbook of forest products 2019. DOI: <https://www.fao.org/3/cb3795m/cb3795m.pdf> FAO, Geneva. ISBN 978-92-5-134118-6

[2] American Conference of Governmental Industrial Hygienists (ACGIH) (2016) *Threshold limit values for chemical substances and physical agents & biological exposure indices*. Cincinnati, OH: ACGIH.

[3] Siew, S.S. et al. (2017) *Occupational exposure to wood dust and risk of nasal and nasopharyngeal cancer: A case-control study among men in four Nordic countries -*

With an emphasis on nasal adenocarcinoma. Int. J. Cancer 2017, 141, 2430–2436. DOI: <https://doi.org/10.1002/ijc.31015>

[4] Hancock, D.G. et. al (2015) *Wood dust exposure and lung cancer risk: A meta-analysis*. Occup. Environ. Med. 2015, 72, 889–898. DOI <http://dx.doi.org/10.1136/oemed-2014-102722>

[5] Barcenas, CH. et al. (2005) *Wood dust exposure and the association with lung cancer risk*. Am. J. Ind. Med. 2005 Apr; 47(4), 349-357. DOI:<https://doi.org/10.1002/ajim.20137>. PMID: 15776474.

[6] Jayaprakash, V. et al. (2008) *Wood dust exposure and the risk of upper aero-digestive and respiratory cancers in males*. Occup. Environ. Med. 2008 Oct; 65(10), 647-54. DOI: <https://oem.bmj.com/content/65/10/647>. Epub 2008 Jan 8. PMID: 18182588.

[7] Kauppinen, T. et al. (2006) *Occupational exposure to inhalable wood dust in the member states of the European Union*. Ann. Occup. Hyg. 2006 Aug; 50(6), 549-561. DOI: <https://doi.org/10.1093/annhyg/mel013>. Epub 2006 Mar 29. PMID: 16571638.

[8] Scheeper B. et al. (1995) *Wood-dust exposure during wood-working processes*. Ann Occup. Hyg. 1995 Apr; 39(2): DOI: <https://pubmed.ncbi.nlm.nih.gov/7741413/> 141-154. PMID: 7741413.

[9] Palmqvist, J. et al. (1999) *Emission of dust in planing and milling of wood*. Holz als Roh-und Werkstoff 57, 164–170 (1999). DOI: <https://doi.org/10.1007/s001070050035>

[10] HSC (1998) Advisory Committee on Toxic Substances working group (WATCH), paper WATCH/28/98. Health and Safety Executive, London (available from WATCH Secretariat, Health and Safety Executive, Rose Court, 2, Southwark Bridge, London SE1 9HS, UK).

[11] Douwes J. et al. (2017) *Wood Dust in Joineries and Furniture Manufacturing: An Exposure Determinant and Intervention Study.* Annals of Work Exposure and Health, 2017, Vol. 61, No. 4, 416-428. DOI: <https://doi.org/10.1093/annweh/wxx016>

[12] Teixiera, R. et. al. (2017) *Evaluation of Airborne MDF Dust Concentration in Furniture Factories*. Floresa e Ambiente, 2017; 24: e00086514. DOI: <http://dx.doi.org/10.1590/2179-8087.086514> ISSN 2179-8087.

[13] Cui, Y. et al. (2022) *Spatial distribution characteristics of the dust emitted at different cutting speeds during MDF milling by image analysis*. J. Wood Sci. 68, 17 (2022). DOI: <https://doi.org/10.1186/s10086-022-02025-6>

[14] Nylander L.A. et al. (1993). *Carcinogenic effects of wood dust: review and discussion*. Am. J. Ind. Med. 24(5), 619–647. DOI: <https://doi.org/10.1002/ajim.4700240511>

[15] Calle S. et al. (2005) *Influence of the size distribution and concentration on wood dust explosion: experiments and reaction modelling*. Powder Technology. 157(1–3), 144–148. DOI: <https://doi.org/10.1016/j.powtec.2005.05.021>

[16] Pang ZH. et al. (2020) *Experimental investigation on explosion fame propagation of wood dust in a semi-closed tube*. J. Loss. Prev. Process Ind 63:10. DOI: <https://doi.org/10.1016/j.jlp.2019.104028>

[17] Guo, L. et. al., (2019). *Comparative Studies on the Explosion Severity of Different Wood Dusts from Fibreboard Production*. BioResources 14(2), 3182-3199 DOI: <https://doi.org10.15376/biores.14.2.3182-3199>

[18] Fujimoto, K. et. al. (2011) *Difference in the mass concentration of airborne dust during circular sawing of five wood-based materials*. J. Wood Sci. 57, 149–154 (2011). DOI: <https://doi.org/10.1007/s10086-010-1145-y>

[19] Hemmilä, P. et al. (1999) *Reducing the amount of noise and dust in NC-milling.* In: Proceedings of 14th International Wood machining Seminar. Epinal, pp 335-365

[20] Rautio, S. et. al. (2007) *Modelling of airborne dust emissions in CNC MDF milling*. Holz. Roh. Werkst. 65, 335-341 (2007). DOI: <https://doi.org/10.1007/s00107-007-0179-3>

[21] Directive (EU) 2017/2398 of the European Parliament and of the Council of 12 December 2017 amending Directive 2004/37/EC on the Protection of Workers from the Risks Related to Exposure to Carcinogens or Mutagens at Work. Available online: <http://data.europa.eu/eli/dir/2017/2398/oj> (accessed on 10 June 2022).

[22] Nasir, V. et. al. (2020) *Characterization, optimization, and acoustic emission monitoring of airborne dust emission during wood sawing*. Int. J. Adv. Manuf. Technol. 109, 2365–2375 (2020). DOI:<https://doi.org/10.1007/s00170-020-05842-5>

[23] Kminiak, R. et al. (2021) *Granulometric Characterization of Wood Dust Emission from CNC Machining of Natural Wood and Medium Density Fibreboard*. Forests **2021**, 12, 1039. DOI: <https://doi.org/10.3390/f12081039>

Acknowledgement:

This experimental research was prepared within the grant project by Ministry of Education, Science, Research and Sport of the Slovak Republic VEGA 1/0324/21 and by Slovak Research and Development Agency under contracts APVV-19-0269 and APVV-20-0403.

CHIP AND CHIPLESS WOODWORKING PROCESSES, 13(1): 51–58, 2022
Zvolen, Technical University in Zvolen, ISSN 1339-8350 (online), ISSN 2453-904X (print)

RECTANGULAR-TRIANGULAR AND REFERENCE TRAPEZOIDAL BENDING MODELS VERSUS MEASUREMENT RESULTS OF THREE SPECIES OF EXOTIC WOOD

Grzegorz Marcin Koczan[1a]– Paweł Kozakiewicz[1b]

Abstract

The bending models in which the graphs of compressive and tensile stresses have a triangular or rectangular shape were considered. All four such models were matched with the reference Thunell–Roš trapezoidal model. Models determine the bending strength of wood based on its compressive and tensile strength.

The results of the compressive, tension and bending strength of three exotic species are presented: wenge, merbau and white meranti. The wood was measured in parts with two different moisture classes of 12% and 8%, with the exception of white meranti which was only measured at a standard moisture of 12%.

Then the measurement results were compared with the predictions of the bending models. The measure of the model fit to the measurement results was the mean square relative error. Based on this measure, the ranking order of the five tested models was established. The article presents the so far unpublished part of the results of the author's doctoral dissertation. It was limited to the simplest piecewise straight rectangular-triangular models, supplemented with the R model with a triangular compressive stress and a rectangular tensile stress. In addition, it was limited to the results of exotic species for which models have not been separately ranked (or published) so far. The ranking criterion has also been slightly modified.

Key words: *Thunell–Roš bending model, bending R model, wenge, merbau, white meranti*

INTRODUCTION

The bending test of wood is a universal test in the sense that it combines compressive, tensile (and even shear) stresses. In the standard simple Euler–Bernoulli bending model, the stress in the cross-section of the bending beam is a linear function of the distance from the cross-section axis [6, 7]. Unfortunately, such a linear model is poorly suited to predicting the ultimate strength of a wooden beam [6, 8]. The best literature model for this purpose is the Thunell–Roš trapezoidal model (TR model). In this model, the compressive stress reaches the limit value (compressive strength *C*), and then it no longer increases its value, but the graph does not end (Fig. 1). On the tension side, the line diagram ends after reaching the ultimate tension strength *T* (rupture occurs).

---

[1] Institute of Wood Sciences and Furniture, Warsaw University of Life Sciences – SGGW,
166 Nowoursynowska St., 02–787 Warsaw, Poland
[a] Department of Mechanical Processing of Wood, ORCID ID: 0000-0003-3692-6270,
e-mail: grzegorz_koczan1@sggw.edu.pl
[b] Department of Wood Sciences and Wood Preservation, ORCID ID: 0000-0002-2285-2912,
e-mail: pawel_kozakiewicz@sggw.edu.pl

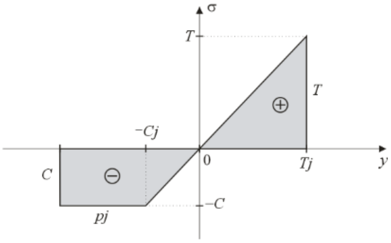

Fig. 1 Thunell-Roš trapezoidal reference bending TR model [16, 14, 9, 6]

It can be shown that the TR model, after simplifying calculations [6], predicts a relatively simple formula for the bending strength *B* (the subscript determines the model):

$$B_{\mathrm{TR}} = \frac{(3T-C)C}{T+C} \tag{1}$$

This TR model formula is taken as the reference model formula which should describe the bending strength of the wood fairly well. Nevertheless, alternative models with different formulas are analyzed. The simplest model (Fig. 2a) is the two-triangular Kocoń model (K model) [5], which leads to the following formula [6]:

$$B_{\mathrm{K}} = \frac{2TC}{T+C} \tag{2}$$

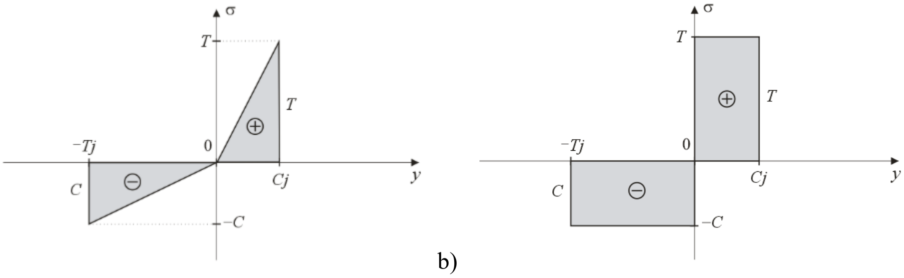

a) b)

Fig. 2 Stress graphs in the following bending models:
a) two-triangular Kocoń model (K model) [5, 6]
b) two-rectangular fully plasticized PP model [15, 6]

An extreme case is the two-rectangular PP model describing a completely plastic stress state (Fig. 2b). This model, although it appears in the figures of works (e.g. [15]), after calculations leads to the formula [6]:

$$B_{\mathrm{K}} = \frac{2TC}{T+C} \tag{2}$$

It turns out that the PP model predicting the highest bending strength predicts exactly one and a half times greater strength than the K model (i.e. the model with the lowest strength prediction).

Readers interested in deriving the formulas (1), (2), (3) are referred to the dissertation [6]. However, in the further part of this article, a formula will be derived for the next rectangular-triangular P model and the new triangular-rectangular R model (reversed model). Model P is the original dissertation model, while model R is novelty of this article. The R model does not seem to be physically justified in relation to the P model, but how can the model predict e.g. lower values for some reason more consistent with the measurements.

MATERIAL AND METHODS

Three species of exotic wood were tested. The first dark and striped species was wenge (*Millettia laurentii* De Wild.), and the second was heavy and hard merbau (*Intsia bijuga* Kuntze) wood. The third exotic species was a brighter and softer, but fibrous wood of white meranti (*Shorea bracteolata* Dyer). All three types of wood are deciduous, diffuse macroporous wood. The differences in the structure are that wenge has a wide stranded parenchyma and a stored structure [2, 11], merbau has a paratracheal wing parenchyma [1, 11] and white meranti has medium-sized wood rays [1].

Timber of all species was cut into 20 x 20 x 300 mm beams (90 wenge, 80 merbau, 64 white meranti). After selection, the beams were sorted into triples, so that every two samples from the triples with a good approximation could be treated as twins. Then, one of the three samples was used to test the bending strength (*B*) – these samples did not require further processing. The beams intended for the compressive strength test (*C*) had to be cut to length to the dimensions of 20 x 20 x 60 mm. However, the samples for the tension test were made in the process of turn milling and had a cylindrical base (Fig. 3). Cylindrical samples are developed and tested in cooperation with Zbigniew Karwat [3, 4].

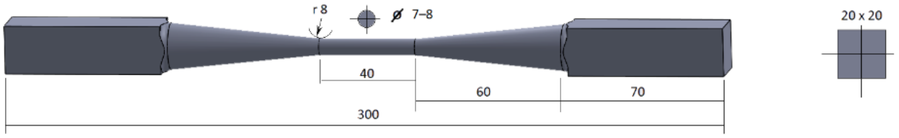

Fig. 3 Dimensions and shapes of the cylindrical samples for tension test [3, 4]

In addition, one part of samples of each species was seasoned at 65% air humidity (over a saturated $NaNO_2$ solution), which ensured an equivalent wood moisture close to the strength standard (12%). The second part of wenge and merbau samples was seasoned in air-dry room conditions, which led to a wood moisture content of about 8%. Due to the smaller number of samples, white meranti was tested only in the standard moisture content of 12%.

The measurement of the bending strength *B* was performed in the IV-point symmetrical bending test with the supports span of 240 mm and the load heads span of 80 mm in accordance with the standards [V, I]. The supports and load heads had a diameter of 30 mm. The compression test was carried out in conditions compliant with the standard [IV]. The cylindrical base tension specimen was not the standard specimen, but was an approximately scaled (1: 4) sample of the archetype of the Australian standard [VI]. However, the tension test itself was practically in accordance with the standards [II, III]. The speed of all tests was selected in such a way that the rupture of the samples occurred after an average of about 90 seconds. Finally, five sets of mean values of $\bar{C}, \bar{T}, \bar{B}$ measurements for exotic wood were obtained, taking into account two classes of moisture: wenge (12%), wenge (8%), merbau (12%), merbau (8%) and white meranti (12%).

The theoretical methodology for bending models assumed that when bending a rectangular beam, the area P_- of the compression stress graph should be equal to (in the sense of a positive value) the area P_+ of the tension stress graph ([6]: (32)):

$$P_- = P_+ \tag{4}$$

In addition, the graph of the compression stress should have a maximum absolute value equal to the compression strength *C*, and the diagram of the tension stress should reach the value of the tension strength *T*. For rectangular-triangular models, it is easy to adjust the sizes of the figures in advance to ensure that condition (4) is met. An example can be the graph of the P model (Fig.4a). For simplicity in graphs of this type, some conventional unit j is used with the length to stress ratio dimension.

The total moment of the stress state (bending moment of the force) is equal to the sum of the moments of the compression stress M_- and the tension stress M_+ calculated, for example, with respect to the neutral axis (per unit width of the beam). For example, for the P model (Fig.4a) these moments are calculated quite simply ([6]: (71)):

$$M_- = Tj/2 \cdot C \cdot \tfrac{1}{2} Tj/2 = \tfrac{1}{8} T^2 C j^2 \quad , \quad M_+ = \tfrac{1}{2} Cj \cdot T \cdot \tfrac{2}{3} Cj = \tfrac{1}{3} T C^2 j^2 \tag{5}$$

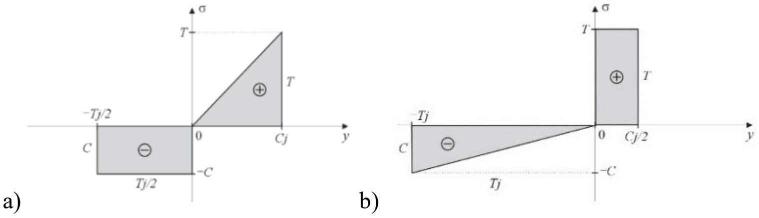

a) b)

Fig. 4 Stress graphs in the following bending models:
a) model P of rectangular (plastic) stress on the compression side [6]
b) triangular-rectangular bending model R which is a reversal of the P model

The knowledge of the bending moments enables the application of a general formula to calculate the bending strength predicted by a given model ([6]: (40)):

$$B(C,T) = \frac{6(M_- + M_+)}{h^2} \tag{6}$$

where: h – beam thickness (total width of the graph of compression and tension stresses). For example, in the P model (Fig. 5), the beam thickness is given by the formula:

$$h = Tj/2 + Cj \tag{7}$$

The dependence of h on C and T (similarly to the bending moments) is explained by the dependence on C and T in the formula (6). However, this relationship $B(C, T)$ is different in each model. Five models and five formulas are analyzed in this article: the TR reference model and four rectangular-triangular models K, PP, P and R.

For each of these five models based on the five exotic wood result sets can be calculated mean square relative error of model prediction:

$$\delta = \sqrt{\frac{1}{5} \sum_{i=1}^{5} \frac{\left(B(\bar{C}_i, \bar{T}_i) - \bar{B}_i\right)^2}{\bar{B}_i^2}} \tag{8}$$

This formula differs from the formula (133) from the dissertation [6] in calculating the relative error instead of the absolute error and in a smaller number 5 of measurement data sets, limited to exotic wood. Due to the use of the relative error, the measurements of the less strength species are included in the formula (8) with an appropriate weight. The model with the lowest δ value will be the best model for the considered measurements of the three exotic species.

RESULTS AND DISCUSSION

The results of the experimental part of the work are presented in Tab. 1. These results were supplemented (in relation to the dissertation [6]) with the number of samples used in each test. The three standard error values have also been corrected and agreed with the source files. The given results for exotic wood from the dissertation [6] have not been published so far. Currently, only the results for tension and compression of seven native species in the standard moisture content of 12% are published [4].

The results from Tab. 1 are visualized in the column diagram of Fig. 5. The density of the examined wood was within the ranges of typical densities of the selected species [1, 2, 10, 11, 12, 17]. The exception was the exceptionally dense merbau wood with a moisture content of 12%, which most likely resulted from the above-average content of non-structural compounds filling the vessels and parenchyma cells. In this case, higher density did not translate into higher strength. Merbau wood disrupted the regularity of the growing $C_{12\%}<C_{8\%}<B_{12\%}<B_{8\%}<T_{12\%}<T_{8\%}$ trend. It turned out that two significant different pieces of merbau sawn timber (I and II) were tested in two different moisture conditions. Surprisingly, the drier piece II of high-density merbau timber (1002 kg/m^3) showed all strength parameters lower than the wetter and lighter piece I of merbau wood. This state of affairs can be explained, firstly, by the waviness of the fibres of the heavy merbau II, secondly, by higher content of unstructured substances increasing the density in heavy merbau II.

Table 1 Strength measurements results *C*, *B*, *T* for three species of exotic wood for two moisture content classes (does not apply to white meranti)

± standard error	**Physical properties***		**Strength of mechanical tests**		
Wood species (moisture class)	**Absolute moisture**	**Density [kg/m^3]**	**Compression *C* [MPa]**	**Bending *B* [MPa]**	**Tension *T* [MPa]**
Wenge (12%) number of samples	10,34%	885	96,3±1,2 32	155,1±8,0 16	166,2±9,7 13 (from 16)
Wenge (8%) number of samples	8,23%	900	114,4±1,8 26	161,6±8,0 12	177,6±6,3 7 (from 12)
Merbau I (12%) number of samples	11,58%	871	91,33±0,94 16	141,3±3,9 9	143,1±4,6 8 (from 10)
Merbau II (8%) number of samples	9,18%	1002	83,9±1,4 14	96,5±4,5 8	111,1±5,1 7 (from 8)
White meranti (12%) number of samples	11,57%	627	59,80±0,48 17	101,4±1,0 17	162,1±6,6 16 (from 17)

* The median value of the mean values for tests *C*, *B*, *T* (the differences were slight)

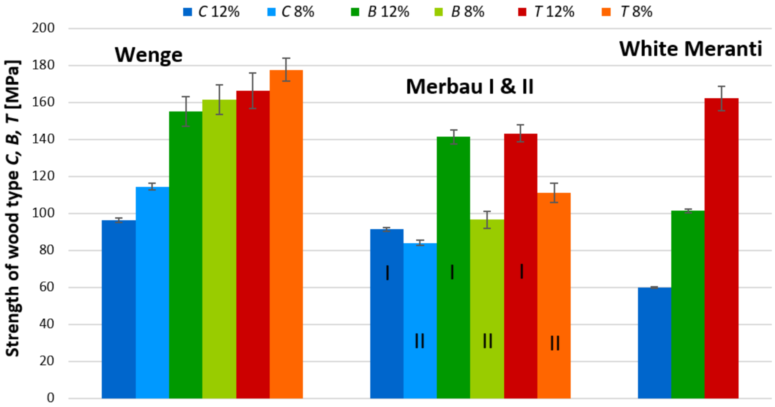

Fig. 5 Strength measurements results *C*, *B*, *T* for three exotic species in two classes of moisture content (12% and 8%)

The obtained mean values of strength in the present study are higher than the mean values available in the literature [1, 2, 10, 11, 12, 13, 17] which is most likely the result of very precise selection and excision of samples with no anatomical defects (except for merbau II).

The application of the theoretical aspects of the methodology leads to the formulas for bending strength predicted by the five models. For the TR, K and PP models, these formulas were already given in the introduction, respectively (1), (2), (3). Complementing the calculations from the methodological part leads to the formula for the P model:

$$B_{\mathrm{P}} = \frac{TC(3T+8C)}{(T+2C)^2} \tag{9}$$

However, for the R model (Fig. 4b), which is the reverse of the P model, it is enough to swap *T* with *C* or equivalently swap the coefficients at *T* and *C*:

$$B_{\mathrm{R}} = \frac{TC(8T+3C)}{(2T+C)^2} \tag{10}$$

The results of all bending strength formulas were compared with the measurements of exotic wood in Tab. 2. Apart from the measured and predicted values, the values of all relative errors were given along with their mean square δ.

Based on the error value δ, it was possible to arrange the models in the ranking order visualized in Fig. 6.

Table 2 Comparison of five mean values of exotic wood bending strength measurements with the predictions of five models

Wood species (moisture class)	**Bending strength *B*[MPa]**					
	Bending Test	**Model TR**	**Model R**	**Model P**	**Model K**	**Model PP**
Wenge (12%)	155,1	147,6	140,9	157,8	121,9	182,9
relative error	5,2%*	–4,8%	–9,1%	+1,7%	–21,4%	+17,9%
Wenge (8%)	161,6	163,9	162,5	178,1	139,2	208,7
relative error	5,0%*	+1,4%	+0,6%	+10,2%	–13,9%	+29,2%
Merbau I (12%)	141,3	131,7	130,1	142,8	111,5	167,2
relative error	2,8%*	–6,8%	–7,9%	+1,1%	–21,1%	+18,4%
Merbau II (8%)	96,5	107,3	113,5	120,4	95,6	143,4
relative error	4,7%*	+11,2%	+17,6%	+24,7%	–0,9%	+48,6%
White meranti (12%)	101,4	114,9	97,0	117,8	87,4	131,1
relative error	1,0%*	+13,4%	–4,3%	+16,2%	–13,8%	+29,2%
Mean squre error δ	4,0%*	8,7%	9,7%	14%	16%	31%

* The relative error of the measured test value relates to the standard error

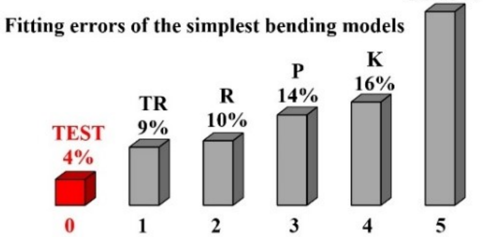

Fig. 6 Ranking of rectangular-triangular models, along with the reference trapezoidal bending model TR, based on the mean square of the relative errors of fit to the measurement results of exotic species (for comparison, the error of the reference tests was also marked)

CONCLUSION

Although the Thunell-Roš (TR) reference model slightly won in the confrontation of the simplest piecewise straight bending models, the results of the new R model are a surprise.

The triangular-rectangular R model was introduced somewhat artificially as a reverse of the P model, and turned out to be much better in strength predictions, than the other three rectangular-triangular models. It is difficult to say whether it is a random coincidence or whether this model somehow reflects the specificity of exotic wood. It is worth noting here that the compression of hard species of wood like wenge and merbau is not characterized by a very large range of plasticity as predicted by the TR model.

REFERENCES

[1] **Jankowska A., Kozakiewicz P.** [2021]: Atlas of exotic wood – Asia and Australia. The first edition. Publishing by SGGW, Warsaw

[2] **Jankowska A., Kozakiewicz P., Szczęsna M.** [2021]: Drewno egzotyczne – rozpoznawanie, właściwości i zastosowanie (Exotic wood – recognition, properties and application). Wydanie II. Wydawnictwo SGGW. Warszawa

[3] **Karwat Z., Koczan G.** [2018]: Making of tension testing samples by turning and milling in single process. Chip and Chipless Woodworking Processes, 11(1): 73–78, Zvolen

[4] **Karwat Z., Koczan G., Rębkowski B., Kozakiewicz P.** [2022]: Comparison beech wood tension strength parallel to grain of cylindrical samples with conical and funnel tapering versus standard rectangular cross section samples. Drewno 209 – in press

[5] **Kocoń J.** [1984]: Teoretyczne podstawy przesuwania strefy obojętnej w zginanych elementach drewnianych (Theoretical basis for moving the neutral zone in bending wooden elements). Scientific conference of WTD SGGW-AR. December 14–15 Warsaw

[6] **Koczan G.** [2020]: Badanie nieliniowych modeli wytrzymałościowych dla zginania drewna (Research of nonlinear strength models for wood bending). Doctoral dissertation. Warsaw University of Life Sciences, Institute of Wood Sciences and Furniture. www.researchgate.net/publication/358969612

[7] **Koczan G., Kozakiewicz P.** [2017]: The role of shear stress in the bending strength test of short and medium length specimens of clear wood. Drewno 199(60):161–175. DOI: 10.12841/wood.1644-3985.102.12

[8] **Koczan G., Kozakiewicz P.** [2018]: Unified anisotropic strength criterion rank two for fibrous materials like wood. Drewno 201(61):119–134. DOI: 10.12841/wood.1644-3985.259.11

[9] **Kollmann F.** [1951]: Technologie des Holzes und der Holzwerkstoffe (Technology of wood and wood-based materials). Vol. 1, 2nd edition. Springer Verlag. Berlin, Göttingen, Heidelberg, München

[10] **Kozakiewicz P.** [2006]: Merbau (Intsia sp.) – drewno egzotyczne z Azji i Oceanii (Merbau (Intsia sp.) – exotic wood from Asia and Oceania). Przemysł Drzewny 9: 21–24. Wydawnictwo Świat

[11] **Kozakiewicz P.** [2007]: Wenge (*Millettia laurentii* De Wild) – drewno egzotyczne z Afryki (Wenge (*Millettia laurentii* De Wild) – exotic wood from Africa). Przemysł Drzewny 5: 33–36. Wydawnictwo Świat

[12] **Kozakiewicz P.** [2010]: Effect of temperature and moisture content on compression strength parallel to the grain of selected species of wood with variable density and anatomical structures – 375. in Treatises and Monographs series of Publishing by SGGW, Warsaw

[13] **Kurowska A., Kozakiewicz P., Gładzikowski T.** [2016]: Ultrasonic waves propagation velocity and dynamic modulus of elasticity of European oak, European aspen, American cherry and wenge wood. Annals of Warsaw University of Life Sciences – SGGW, Forestry and Wood Technology No 93: 83–88

[14] **Roš M.** [1936]: Spannungsverteilung im gebogenen Balken (Stress distribution in bending beam) – based on Kollmann index. Das Holz als Baustoff (Wood as a building material). I. Schweiz. Kongress zur Förderung der Holzverwertung. Bern, 273–315

[15] **Štok B., Halilovič M.** [2009]: Analytical solutions in elasto-plastic bending of beams with rectangular cross section. Applied Mathematical Modelling 33: 1749–1760

[16] **Thunell B.** [1939]: Spannungsverteilung im gebogenen Balken (Stress distribution in bending beam) – based on Kollmann index. Ing. Vet. Akad. H. 3. Stockholm

[17] **Wagenführ R.** [2007]: Holzatlas. 6., neu bearbeitete und erweitere Auflage. Mit zahlreichen Abbildungen. Fachbuchverlag Leipzig im Carl Hanser Verlag

STANDARDS

[I] **GOST (ГОСТ) 6336-52** [1952]: Лесоматериалы. Методы физико-механических испытаний древесины (Forest materials. Methods of physical and mechanical testing of wood) (withdrawn)

[II] **GOST (ГОСТ) 16483.23** [1973]: Древесина. Метод определения предела прочности при растяжении вдоль волокон (Wood. Method for determination of ultimate strength in tension along the grain), (current)

[III] **ISO 13061-6** [2014]: Physical and mechanical properties of wood – Test methods for small clear wood specimens – Part 6: Determination of ultimate tensile stress parallel to grain (current)

[IV] **ISO/DIS 13061-17** [2015]: Physical and mechanical properties of wood – Test methods for small clear wood specimens – Part 17: Determination of ultimate stress in compression parallel to grain (current)

[V] **PN-D-04103** [1968]: Fizyczne i mechaniczne własności drewna. Oznaczanie wytrzymałości na zginanie statyczne (Physical and mechanical properties of wood. Determination of ultimate strength in static bending) (III-poit or IV-point) (not current)

[VI] **Warren W. H.** [1911]: The strength, elasticity, and other properties of New South Wales hardwood timbers (About old cylindrical tension test used by the Department of Forestry of New South Wales), pp. 58-62 (archetypal standard)

CHIP AND CHIPLESS WOODWORKING PROCESSES, 13(1): 59–64, 2022
Zvolen, Technical University in Zvolen, ISSN 1339-8350 (online), ISSN 2453-904X (print)

SAWDUST ANALYSIS USING MATLAB

Pavol Koleda – Mária Hrčková

Abstract

This article deals about the possibilities of obtaining information from a sawdust sample using the Matlab. Using sawdust analyzing during chip machining, it makes it possible to determine unsuitable conditions by cutting and woodworking, such as dulling of the tool, unsuitable cutting conditions, overheating of the tool and others. Such conditions can have negative effects on the operation and economics of the company. Commonly used sawdust sizing methods, such as sieving, obtain only partial information about a given sample. On the other hand, by means of image analysis of a sample, it is possible to find out much more, for example the largest and smallest dimension of each single particle, its circularity, area, perimeter, eccentricity, bounding box, major and minor axis length, or color of the particle.

Key words: *Matlab, sawdust, dimensional characteristics.*

INTRODUCTION

Nowadays woodworking with CNC technologies is an integral part of the woodworking industry. The range of used CNC machines is very wide in the so-called CNC machining centers (Korčok et al. 2018, Kos et al. 2004). Even with these modern computer-controlled machines, we cannot avoid the problem of removing secondary material, which arises during machining – chip (Kučerka, 2022). Measuring Sawdust dimensions measuring during chip machining enables monitoring and evaluation of the wood splitting process. A change in chip size may indicate blunting of the tool. Size, shape and density of the biomass particles affect the flow properties of the biomass particles (Rezaei, 2016).

MATERIAL AND METHODS

For wood dust analysis was used the Matlab. In it is first the image containing the measured sawdust loaded (Figure 1).

Technical University in Zvolen, T. G. Masaryka 24, 960 01 Zvolen
e-mail: pavol.koleda@tuzvo.sk

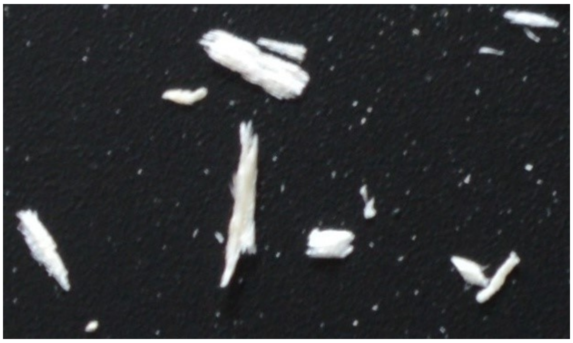

Figure 1 Picture with sawdust sample

For next analysis, this image is converted into binary form using a function:

$$im2bw(I, graythresh(I)) \tag{1}$$

I – a variable representing the loaded image.

Function *im2bw* converts the input image to a binary form in which the pixels belonging to the sawdust have the value 1 (white), the other pixels have a value 0 (black). The decision level for this transfer is calculated using a function *graythresh(I)*. This computes a global threshold T from grayscale image I, using Otsu's method. Otsu's method chooses a threshold that minimizes the intraclass variance of the thresholded black and white pixels (Otsu, 1979). The result of binarization is shown in the figure 2.

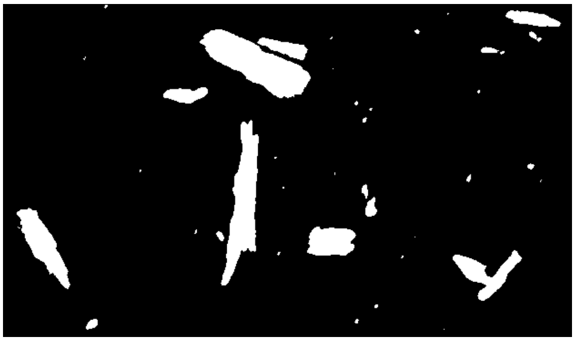

Figure 2 Binarized picture

During this binarization may be fictitious holes created, due to the structure of the sawdust. These are subsequently removed using the function:

$$imfill(BW,'holes') \tag{2}$$

BW – input binary image,
'holes' – parameter of the *imfill* function.

Function *imfill(BW,'holes')* fills holes in the input binary image *BW*. Using parameter *'holes'* are removed only holes in objects (Figure 3). Hole is a set of background pixels that cannot be reached by filling in the background from the edge of the image.

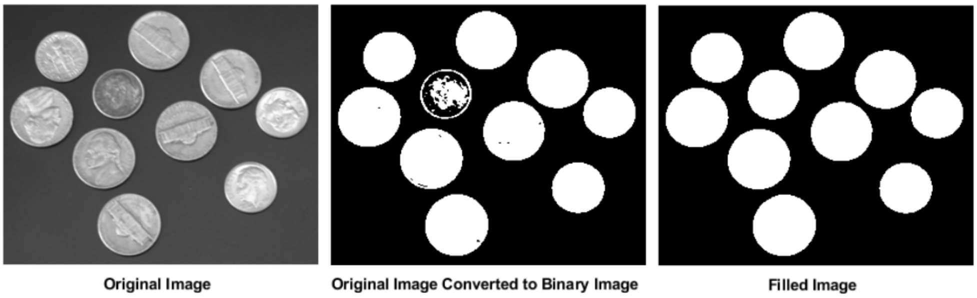

Figure 3 Removing holes in objects

It is possible to determine the dimensional parameters of the sawdust in the digital image modified in this way. In Matlab program were to determine sawdust parameters used functions

$$\begin{gathered} \textit{regionprops(BW,properties)} \\ \textit{bwferet(BW,properties)} \end{gathered} \qquad (3)$$

BW – input binary image,
properties – specified required calculated properties.

Using *regionprops* function are calculated the required characteristics of the found objects - sawdust. The list of these characteristics is specified as *Properties* in the function *regionprops*. To dimensions measure of the sawdust, the following were determined: Area, Perimeter, Centroid, Orientation, Circularity, Eccentricity and Bounding Box.

Function *bwferet* measures the Feret properties of objects in an image and returns the measurements in a table. The input properties specify the Feret properties to be measured for each object in input binary image *BW*. The measured Feret properties include the Major and Minor axis length, Feret angles, and endpoint coordinates of Feret diameters.

Area of individual sawdust is determined with a parameter *'Area'*. This parameter counts all pixels belonging to individual sawdust in the binary image.

The Perimeter measurement of sawdust is determined using a parameter *'Perimeter'*. Function *regionprops* computes the perimeter by calculating the distance between each adjoining pair of pixels around the border of the region.

The position of the center of sawdust is determined by a parameter *'Centroid'*, this detects the horizontal and vertical coordinates of the position of the center of particle in the image.

The rotation of sawdust in the image is detected by a parameter *'Orientation'*. It represents an angle between the x-axis and the major axis of the ellipse that has the same second-moments as the region, returned as a scalar. The value is in degrees, ranging from -90 degrees to 90 degrees.

Roundness of objects, returned as a structure with parameter *'Circularity'*. The structure contains the circularity value for each object in the input image. The circularity value is computed as

$$(4*\text{Area}*\text{pi})/(\text{Perimeter}^2) \qquad (4)$$

For a perfect circle, the circularity value is 1. The input must be a label matrix or binary image with contiguous regions.

Eccentricity of the ellipse that has the same second-moments as the region, is detected with parameter *'Eccentricity'*. The eccentricity is the ratio of the distance between the foci of the ellipse and its major axis length. The value is between 0 and 1. (0 and 1 are degenerate cases. An ellipse whose eccentricity is 0 is actually a circle, while an ellipse whose eccentricity is 1 is a line segment).

Position and size of the smallest box containing the region, detected with parameter *'BoundingBox'*. It's returned as a 1-by-(2*Q) vector. The first Q elements are the coordinates of the minimum corner of the box. The second Q elements are the size of the box along each dimension. For example, a 2-D bounding box with value [5.5 8.5 11 14] indicates that the (x,y) coordinate of the top-left corner of the box is (5.5, 8.5), the horizontal width of the box is 11 pixels, and the vertical height of the box is 14 pixels.

The largest and smallest dimensions of each sawdust are determined using parameters *'MajorAxisLength'* and *'MinorAxisLength'*.

RESULTS

The determined dimensional sawdust parameters are stored in an Excel table for further processing. Some of them can be graphically represented in a modified binary image with sawdust (Figure 4).

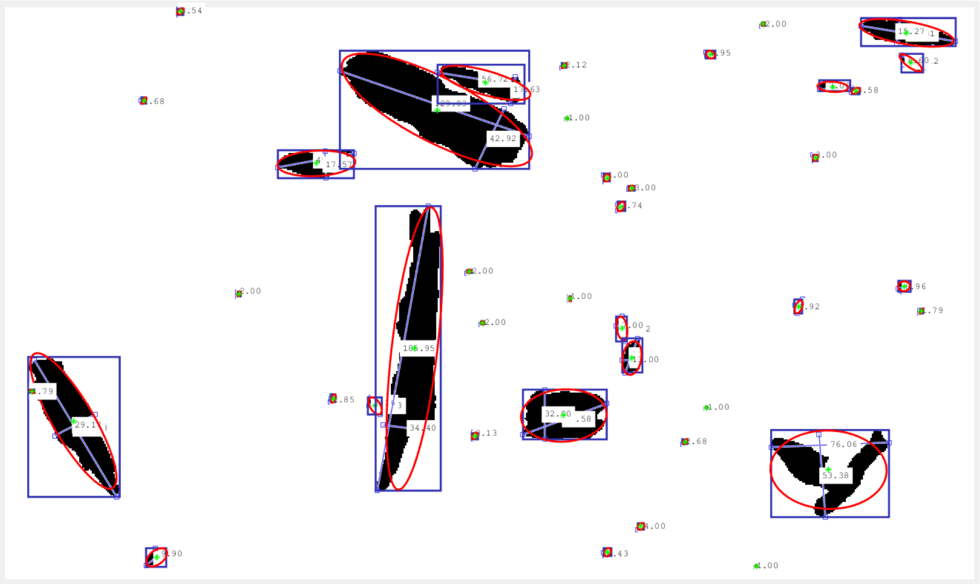

Figure 4 Graphic representation of the detected data

In Figure 4 are shown for individual sawdust Bounding box (blue rectangles), Major axis length and Minor axis length (blue lines with displayed length), Orientation (red ellipse) and position of sawdust center (green star).

The detected dimensional parameters of the measured sample can be displayed using histograms (Figure 5, Figure 6).

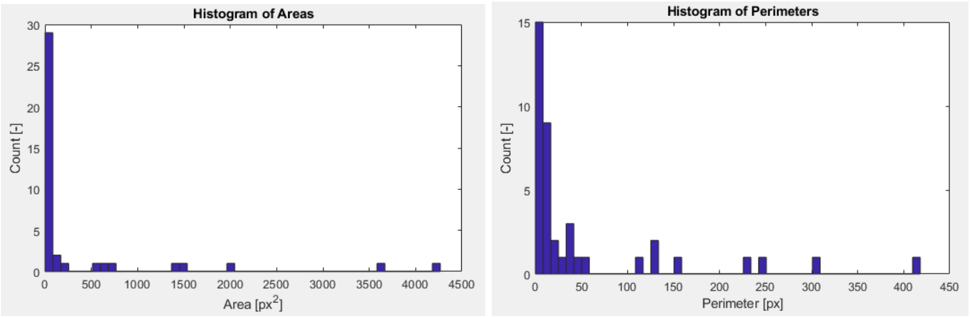

Figure 5 Histogram of Areas and histogram of Perimeters

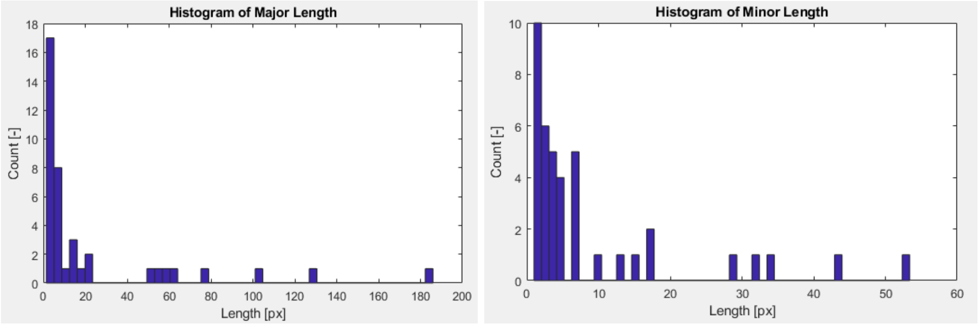

Figure 6 Histogram of Major and Minor wood chips length

CONCLUSION

As described in this article, detailed information of the dimensional characteristics of sawdust can be obtained using image analysis in Matlab. Compared to other methods, such as sieving, this method is non-destructive. However, the disadvantage is the need to separate the scanned sawdust from each other, otherwise they may overlap together. Such overlapped sawdust is subsequently evaluated as a one separate sawdust, what introduces error into the measurement. In addition to the obtained information in tabular form, matlab itself enables to statistical evaluation of the measured samples, for example using histograms.

ACKNOWLEDGMENTS

The paper was written with the support of project VEGA 1/0791/21 “Research of non-contact method of analysis of small and dust particles arising in the production process with a prediction of negative effects of dust particles”, project APVV-20-0403, “FMA analysis of potential signals suitable for adaptive control of nesting strategies for milling wood-based agglomerates,“ and thanks to support under the Operational Program Integrated Infrastructure for the project: National infrastructure for supporting technology transfer in Slovakia II – NITT SK II, co-financed by the European Regional Development Fund.

REFERENCES

KOLEDA, P.; BARCÍK, S.; KORČOK, M.; JAMBEROVÁ, Z.; CHAYEUSKI, V. Effect of Technological Parameters on Energetic Efficiency When Planar Milling Heat-treated Oak Wood. Bioresources 2021, 16, 515–528. DOI: 10.15376/biores.16.1.515-528

KORČOK, M., KOLEDA, P., BARCÍK, Š., VANČO, M. 2018. Effects of Technical and Technological Parameters on the Surface Quality when Milling Thermally Modified European Oak Wood. In: BioResources, 13(4): 8569-8577.

KOS, A., BELJO-LUČIĆ, R., ŠEGA, K., RAPP, A. O. 2004. Influence of woodworking machine cutting parameters on the surrounding air dustiness. In Holz als Roh-und Werkstoff 62(3): 169-176. DOI:10.1007/s00107-004-0473-2.

KUČERKA, M., OČKAJOVÁ, A., KMINIAK, R., PĘDZIK, M., ROGOZINSKI, T. 2022. The Effect of the Granulometric Composition of Beech Chips from a CNC Machining Center on the Environmental Separation Technique. In: Acta Facultatis Xylologiae. Zvolen, 2022. vol. 64(1), P 87-97. DOI: 10.17423/afx.2022.64.1.08.

INTERNATIONAL AGENCY FOR RESEARCH ON CANCER. 1995. Monographs on the Evaluation of Carcinogenic Risks to Humans: Volume 62 Wood Dust and Formaldehyde. Lyon, France. 1995. ISBN 92 832 1262 2.

OTSU, N., 1979. A Threshold Selection Method from Gray-Level Histograms. In: IEEE Transactions on Systems, Man, and Cybernetics. Vol. 9, No. 1, 1979, pp. 62–66.

REZAEI, H., LIM, C. J., LAU, A., SOKHANSANJ, S. 2016. Size, Shape and Flow Characterization of Ground Wood Chip and Ground Wood Pellet Particles. In: Powder Technology. Vol. 301. P. 737-746. DOI: 10.1016/j.powtec.2016.07.016.

CHIP AND CHIPLESS WOODWORKING PROCESSES, 13(1): 65–70, 2022
Zvolen, Technical University in Zvolen, ISSN 1339-8350 (online), ISSN 2453-904X (print)

INFLUENCE OF MECHANICAL OSCILLATIONS ON THE ACCURACY OF MAKING GROOVES IN SOLID WOOD

Georgi Kovatchev – Valentin Atanasov – Izabela Radkova

Abstract

This paper presents a study on the accuracy of the width of the groove channel depending on the magnitude of the mechanical oscillations. Details from Koto(Pterygotamacrocarpa) and Oak (Quercus petraea) were milled. The details are machined on a universal milling machine with bottom location of the working shaft model FD-3. The rotation frequency used for the experiments was 6000 min^{-1}*. During the research, attention is paid to some technological factors such as the feed speed of the processed material which is from 2m.min*$^{-1}$ *to 10m.min*$^{-1}$*, as well as milling area which ranges is from 48 mm*^{2} *to 144 mm*^{2}*. Measurements of the accuracy of the groove channel are made with an electronic caliper at a minimum of three points along its length. The investigation results can be used as a base for making some recommendations for the selection of technological factors.*

Key words: *wood shapers, milling, vibrations, accuracy;*

INTRODUCTION

The mechanical processing of wood details leads to certain deviations from their nominal dimensions. These deviations are due to a number of factors, some of which are inaccuracies in the cutting tools due to their wear, mechanical vibrations during operation, deformation of some of the machine parts, the elastic properties of wood and many factors related to the technology of processing details. The quality and accuracy of the obtained surfaces are also influenced by the different types of heat treatment of the wood as well as the choice of geometric parameters of the cutting tools (GOCHEV *et al.*2020, KORCOK *et al.*2018, KOVAC *et al.*2018). High rotation frequency of the milling machines combined with unbalanced or poorly prepared cutting tools are the reason for increasing the intensity of vibrations of any mechanical system (BREZIN *et al.*2015, VITCHEV *et al.*2019, VUKOV *et al.*2020). Important attention should be paid to the preparation of the cutting tools. The sharper, clearing the wood cutting tool after work and correct installation are factors that greatly affect the ability of each cutting tool to process the wood quality. Deviations from the exact dimensions of the parts cannot be unlimited, because this leads to inaccuracies in the structural elements in a product. The quality of processing of individual parts serves as an indicator of the quality of finished products. How well a particular part is processed can be determined by its deviations from those set in the drawing (KMINIAK *et al.*2018, OBRESHKOV 1997). It is known that the nature of the assembly between two connection sizes is determined by the joint between them. The joint is very important because it provides strength, solidity and the degree of mobility between the elements in assembly.

University of Forestry, 10 Kliment Okhridski Blvd., 1797 Sofia, , Bulgaria
e-mail: g_kovachev@ltu.bg; vatanasov_2000@ltu.bg; izabelarad@abv.bg

The aim of this work is measuring the accuracy of the groove width depending on the mechanical oscillations. The study was performed by milling specimens of Koto (*Pterygotamacrocarpa*) and Oak (*Quercus petraea*), changing various technological factors during the experiments. The investigation results can be used as a base for making some recommendations for the accuracy and shape of the details.

MATERIAL AND METHODS

To conduct the experimental part, a universal wood shaper with bottom location of the working shaft is selected Fig.1. The cutting mechanism is driven by an asynchronous electric motor with a power of 3 kW and rotation frequency of 2880 min^{-1}. The rotation frequency used for the experiments was 6000 min^{-1}. This is one of the most commonly used frequency in milling machines. The selected rotational speed is realized by pulleys mounted on the electric motor shaft and the machine shaft.

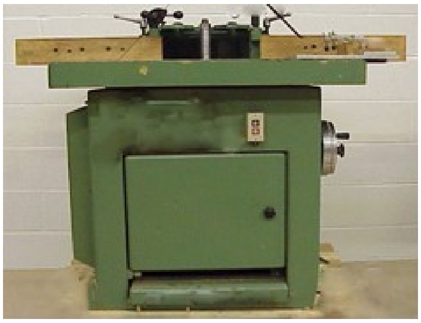

Figure 1. Wood shaper general view

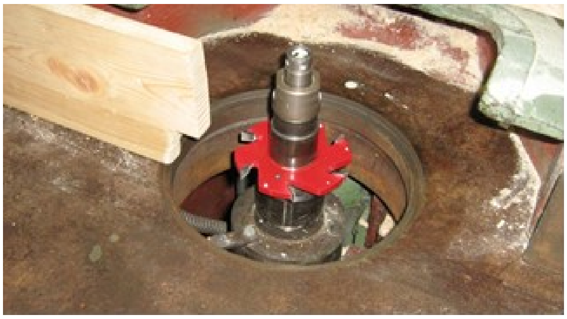

Figure 2. Groovecutter D=140 mm

A cutter with diameter D = 140 mm was used Fig 2. The technical data of the cutting tool are shown in Table 1.The inscriptions in the table are: *D* - diameter of the milling cutter,*d* – diameter of the bore, *B* – milling width, α – back angle of cutting, β – angle of sharpening, γ – front angle of cutting, *z* – number of teeth.

Table 1. Technical data of the cutting tool

Type of instrument	***D*** **mm**	***d*** **mm**	***B*** **mm**	**α** °	**β** °	**γ** °	**z** **бр**	**Material of the teeth**
Groovecutter	140	30	12	16	55	19	6	HM

The calculated cutting speed with the selected rotation frequency and diameter of the cutting tool is v=44 m/s. In the present work longitudinal milling of deciduous wood specimens which are used in the production of valuable furniture as well as other wood products – Koto (Pterygotamacrocarpa) and Oak (*Quercuspetraea*). The test samples are details with a cross-sectional dimension of 50x50 mm and a length of 1000 mm. Some of the wood test samples can be seen in Fig.3. Typically, the products made of deciduous wood are characterized by their high prices. Particular attention should be paid to the quality of the processing and production of these products. Feed speed and milling area have a direct effect on the vibration speed, and hence on the quality of the treated surfaces (KOVATCHEV *et al.*2018).

Figure 3. Wood test samples

The experiments were performed with feed speed from 2m.min^{-1} to 10m.min^{-1}, and milling area which ranges is from 48 mm^2 to 144 mm^2 shown in Table 2.

Table 2. Survey factors

Feed speed U, [$m.min^{-1}$]	2	6	10
Milling area A, [mm^2]	48	96	144

The dimensions of the milled channel are measured with a precision electronic caliper, whose measurement error is not greater than 0.01 mm Fig.4. The measurement is performed in at least three sections along the length of the sample at a distance of 20 mm from the beginning and end, also in the middle Fig.5 (БДС 3780-84).

Figure 4. Electronic caliper

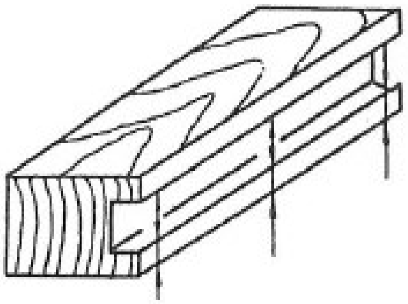

Figure 5. Measurement points

RESULTS AND DISCUSSION

The study was performed by milling specimens of Koto (*Pterygotamacrocarpa*) and Oak (*Quercus petraea*). The measurement of the vibration speed V (r.m.s) mm.s^{-1} was performed according to (BDS ISO 10816-1: 2002, KOVATCHEV *et al.*2018). Table 3 shows the values of the vibration speed according to (BDS ISO 10816-1: 2002), at milling width B = 12 mm, milling area 48 mm^2 and feed speed 2m.min^{-1} to 10m.min^{-1}.

Table 3. Vibration speed

Milling area *A*, [*mm*^{2}]	48		
Feed speed *U*, [*m.min*$^{-1}$]	2	6	10
V (r.m.s), mm.s^{-1} - *Комо (Pterygota macrocarpa)*	2,61	2,55	2,67
V (r.m.s), mm.s^{-1} - *Дъб (Quercus petraea)*	2,6	2,56	2,66

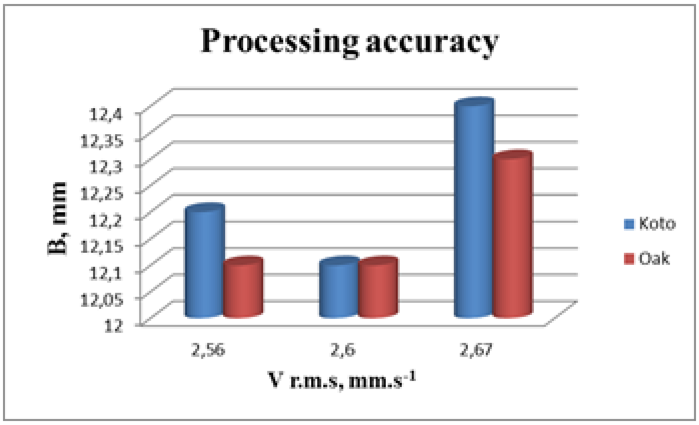

Figure 6. Accuracy of the groove channel with a milling area of 48 mm^2

Figure 6 shows that at milling area of 48 mm^2 and material feed speed 2m.min^{-1} and 6m.min^{-1} the change from the exact width of the groove channel is very small 0.1 - 0.2 mm. By increasing the feed speed to 10m.min^{-1} the deviation from the exact size is 0.4 mm. Table 4 shows the values of the vibration speed at milling width B = 12 mm, milling area 96 mm^2 and feed speed 2m.min^{-1} to 10m.min^{-1}.

Table 4. Vibration speed

Milling area *A*, [*mm*^{2}]	96		
Feed speed *U*, [*m.min*$^{-1}$]	2	6	10
V (r.m.s), mm.s^{-1} - *Комо (Pterygota macrocarpa)*	2,53	2,48	2,6
V (r.m.s), mm.s^{-1} - *Дъб (Quercus petraea)*	2,5	2,45	2,54

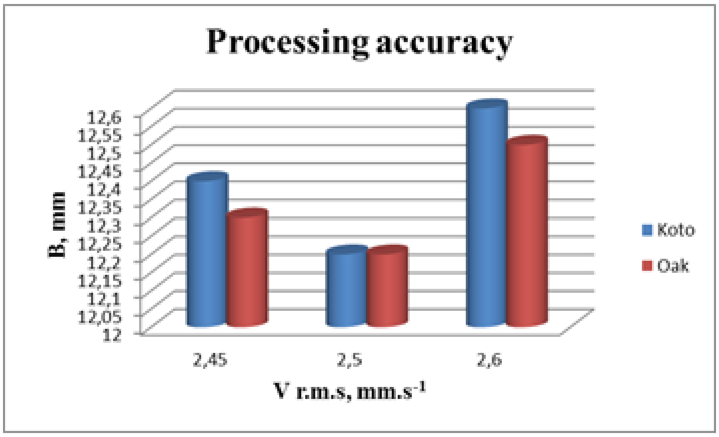

Figure 7. Accuracy of the groove channel with a milling area of 96 mm^2

Figure 7 shows that at feed speed $2 m.min^{-1}$ and $6 m.min^{-1}$ the maximum deviations reach to 0.3 - 0.4 mm. When the feed speed increases, the vibration also increases (KOVATCHEV *et al.*2018). The deviations from the exact size are reached to 0.5-0.6 mm.
Table 5 shows the values of the vibration speed at milling width B = 12 mm, milling area 144 mm^2 and feed speed $2 m.min^{-1}$ to $10 m.min^{-1}$.

Table 5. Vibration speed

Milling area *A*, [mm^2]	144		
Feed speed *U*, [$m.min^{-1}$]	2	6	10
V (r.m.s), $mm.s^{-1}$ - *Комо (Pterygota macrocarpa)*	2,2	2,2	2,33
V (r.m.s), $mm.s^{-1}$ - *Дъб (Quercus petraea)*	2,2	2,15	2,24

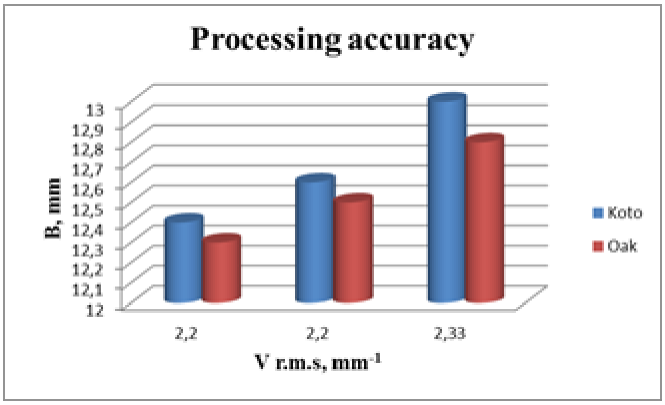

Figure 8. Accuracy of the groove channel with a milling area of 144 mm^2

Figure 8 shows that at feed rate of $2 m.min^{-1}$ the deviations from the accuracy are at least 0.3 - 0.4 mm. When the feed rate increases the vibrations also increase, the deviations start from 0.5 mm and reach up to 1 mm.

CONCLUSION

As a result of research and analysis of the results, the following conclusions can be made. When the test pieces are fed slowly the deviations from the exact dimensions during milling are not large. This is clearly visible in two milling areas 48 mm^2 and 96 mm^2 where the width of the grooves is in the range from 12.1 mm to a maximum of 12.4 mm. When the vibrations increase, they are directly dependent on the feed speed, the deviations increase to 12.6 mm. The most inaccurate grooves are made with a milling area of 144 mm^2. Even when the parts are fed with $2m.min^{-1}$ the deviations from the exact dimensions are from 12.3 - 12.4 mm. At higher vibrations the deviations reach up to 13 mm. This is 1 mm more than the width of the cutter.

REFERENCES

BREZIN,V., ANTON, P.2015. Engineering ecology, Sofia, ISBN 978-954-332-135-3, 259p.(in Bulgarian).

GOCHEV, Z., VITCHEV, P. 2020. Determination of performance indicators of PCD abrasive wheels for sharpening of tungsten carbide tools. Chip and Chipless Woodworking Processes 12 (1): 65-70, Zvolen, ISSN 2453-904X (print), ISSN 1339-8350 (online).

KMINIAK, R., SIKLIENKA, M., SUSTEK, J. 2018. Influence of the thickness of removed layer on the quality of created surface when milling oak blanks on the CNC machining center. Chip and Chipless Woodworking Processes 11 (1): 79-86, Zvolen, ISSN 2453-904X (print), ISSN 1339-8350 (online).

KORCOK, M., VANCO, M., BARCIK, S., GOGLIA, V. 2018. Influence of tool angular geometry on surface quality after milling of thermally modified oak wood. Chip and Chipless Woodworking Processes 11 (1): 87-96, Zvolen, ISSN 2453-904X (print), ISSN 1339-8350 (online).

KOVAC, J., KRILEK, J., HARVANEK, P. 2018. The analyse activity of cutting forces for the chipless cutting wood. Chip and Chipless Woodworking Processes 11 (1): 97-104, Zvolen, ISSN 2453-904X (print), ISSN 1339-8350 (online).

KOVATCHEV, G.,ATANASOV, V.2018.Determination of vibration during milling process of some deciduous wood species. In8th International Science Conference Hardwood Conference, Sopron, ISBN 978-963-359-095-9, ISSN 2631-004X, pp. 112–113.

OBRESHKOV P. 1997. Woodworking Machines, Sofia. 182 p.(in Bulgarian)

VITCHEV, P., ANGELSKI, D., MIHAILOV, V. 2019.Influence of the processed material on the sound pressure level generated by sliding table circular saw. In Acta Facultatis Xylologiae Zvolen, 61(2): 73−80, 2019, DOI: 10.17423/afx.2019.61.2.07.

VUKOV, G., SLAVOV, V., VITCHEV, P., GOCHEV, Z. 2020. Forced spatial vibrations of a wood shaper caused by the cutting forces on the worn cutting tool. Chip and Chipless Woodworking Processes 12 (1): 109-117, Zvolen, ISSN 2453-904X (print), ISSN 1339-8350 (online).

БДС 3780-84, Wood shaper with bottom location of the working shaft. Accuracy standards.

БДС ISO10816-1:2002, Evaluation Of Machine Vibration By Measurement On Non – Rotating Parts – Part 1: General Guidelines, 25 p.

CHIP AND CHIPLESS WOODWORKING PROCESSES, 13(1): 71–74, 2022
Zvolen, Technical University in Zvolen, ISSN 1339-8350 (online), ISSN 2453-904X (print)

ENERGY EFFICIENCY IN MASS CUSTOMIZED PRODUCTION OF WOODEN DOORS

Zdzisław Kwidziński[1,3] – Marcin Drewczyński[2] – Tomasz Rogoziński[3] – Marta Pędzik[3,4]

Abstract

Appropriate environmental policy management, including taking care of environmental aspects such as raw material consumption, energy consumption and waste management, is currently one of the most important areas for development and improvement in production plants. One way to achieve better resource management is to automate production. It is known that thanks to the use of automated devices, high precision and machining quality are ensured, as well as the possibility of customized production. In addition, a company can reduce the overmeasure of material for processing, reducing the consumption of raw material and the amount of generated waste. However, it is not known how much the automation of wooden door production line modules and the related efficiency increase has an impact on electricity consumption. Therefore, the aim of this article was to determine the influence of the operation of selected modules of the automated line for processing of TechnoPORTA door leaves on their energy consumption. The tested line modules have a lower energy demand than the previously used reference technological line. This also means that the automation of the technological line resulting from the introduction of the concept of mass customization has increased energy efficiency.

Key words: *efficiency indicator, wooden door factory, mass customization, production process*

INTRODUCTION

In order to meet consumer expectations and occupy a significant market position, companies must build their long-term competitive advantage (ANDÚJAR-MONTOYA et al., 2015). This is possible thanks to mass customization, i.e. adapting the company's offer to the individual needs of the consumer, producing smaller series with personalized features (CIECHOMSKI, 2015).

The product offerings of contemporary companies producing doors are characterized by enormous complexity and variability, which is possible on a large scale thanks to the dynamic development of production technology and is inextricably linked to the idea of Industry 4.0 (ESPINOZA PÉREZ et al., 2022). This ensures that standard products can be flexibly modified to enhance their features, which are of greater importance to consumers.

---

[1] Porta KMI Poland, Szkolna 54, 84-239 Bolszewo, Poland; Zdzislaw_Kwidzinski@porta.com.pl

[2] General Engineering Solutions, Al. Zwycięstwa 96/98, 81-451 Gdynia, Poland, m.drewczynski@ges.com.pl

[3] Poznań University of Life Sciences, Wojska Polskiego 38/42, 60-627 Poznań, Poland, tomasz.rogozinski@up.poznan.pl

[4] Lukasiewicz Research Network – Poznan Institute of Technology, Winiarska 1, 60-654 Poznań, marta.pedzik@pit.lukasiewicz.gov.pl

In addition, thanks to the automation of production lines and the introduction of advanced IT solutions, it is possible to freely make changes in order to improve the visual qualities of products. The production time is also reduced, making it possible to increase the efficiency of the entire line (TARIGAN et al., 2019). Automated systems allow to combine the central level of planning directly with production, where parameterized orders are sent to specific machines (KWIDZIŃSKI et al., 2021a; KWIDZIŃSKI et al., 2021b). Based on the data on material and labour costs incurred by Porta KMI Poland S.A., it can be concluded that the introduction of mass customization to the production of technical doors not only did not cause additional costs in this respect, but even allowed for significant savings on a yearly basis (PĘDZIK et al., 2020). What is more, thanks to the precise tools that are required by devices and machines in an automated production line, high precision and machining quality are ensured. Because of this, a company can reduce the overmeasure of material for machining, thus increasing its savings (KWIDZIŃSKI et al., 2021a). However, these figures do not take into account the costs incurred in reorganising the production process and the energy costs, which constitute an important economic indicator. Adequate environmental policy management, including taking care of environmental aspects such as raw material consumption, energy consumption, gas emissions and waste management, is currently one of the most important areas for development and improvement in manufacturing plants. It is industry that is the most energy-intensive sector, which is why manufacturers are increasingly focusing on the energy efficiency of production, which also provides them with cost optimization (HADDOUCHE and ILINCA, 2022). Perhaps the automation of the technological line resulting from the introduction of the concept of mass customization has an impact on increasing energy efficiency. The project of the TechnoPORTA technological line provides for low-emission production, which is associated with a reduction in energy consumption.

Therefore, the aim of this study is to preliminarily determine the influence of the operation of selected modules of the automated door leaf processing line on energy consumption. Energy-sustainable production can be a determining factor in the context of building long-term competitive advantage.

MATERIAL AND METHODS

Energy consumption was measured on selected modules of the TechnoPORTA line, which are most strongly associated with the customization of products. These were the SMM reference line, the Homag line for edgebanding, and the Masterwood line for milling and drilling holes. The SMM line includes operations of edgebanding, milling and drilling holes in door leaves. A representative batch of doors with identical technological features was prepared for each test. The same doors were used to measure energy consumption on the Masterwood line as on the Homag line.

A clamp meter for measuring power with the function of measuring the harmonic distortion of the UNI-Trend model UT243 (UNI-Trend Technology, China) was used for the measurement. The meter allows the measurement of power and three-phase energy with uneven load in three- and four-wire systems. The results of the individual phases were summarized. The results obtained in real-time were transferred to a PC, and then recorded in the form of a table and a graphic chart. In order to simplify the measurement method, the power recording took place on only one phase with sampling every 10 seconds.

For the measurement of the energy consumption of the SMM line, 3 pallets of test doors under the trade name Granit RC3 were prepared in the total amount of 28 pieces. An exemplary pallet is presented in Fig. 1. In the test in Homag line and in Masterwood line the same 47 door leaves were used.

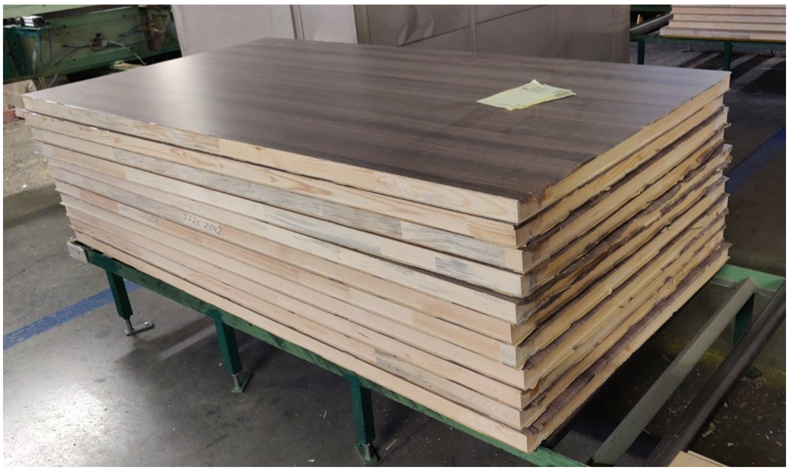

Fig. 1. Door leaves prepared for the test in SMM line

RESULTS AND DISCUSSION

The results of the measurement of energy consumption on the SMM reference line and on the individual processing lines of the TechnoPORTA project are presented in Table 1.

Table 1. Energy consumption of machining lines

Line	Number of door leaves [pcs]	Processing time [min]	Power consumed [kWh]	Power per product [kWh/pcs]
SMM	28	65	64.79	2.31
Homag	47	40	38.33	0.82
Masterwood	47	67	20.45	0.44

The energy consumption of the reference line is much higher compared to the successively tested lines of the TechnoPORTA project, as evidenced by the obtained results of the absorbed power. In no case during the performed tests were there any significant machine downtimes, which could have affected the results. After converting the power consumed in the specified time of operation on the lines into pieces of the product, we obtain the value of 2.31 kWh/pcs for the SMM line and 0.82 kWh/pcs and 0.44 kWh/pcs respectively for the Homag and Masterwood lines. The energy consumption results of both lines were 46% better than the SMM line, on which fewer pieces were made. The reduction of line energy consumption is influenced by the increase in process efficiency in relation to the current process carried out on the SMM reference line. Moreover, reducing downtimes by automating machine changeovers as much as possible could have also contributed to increasing the energy efficiency of the entire production process.

CONCLUSIONS

The above results clearly indicate that the tested TechnoPORTA design lines have a lower energy demand than the previously used technological line. This also means that the automation of the technological line resulting from the introduction of the concept of mass customization has increased the energy efficiency of the production in the form of lower energy demand in the production process of wooden technical leaves. Thus, based on these effects, long-term building of a company's competitive advantage can be expected.

REFERENCES

ANDÚJAR-MONTOYA, M., GILART-IGLESIAS, V., MONTOYO, A., MARCOS JORQUERA, D., 2015. A Construction Management Framework for Mass Customisation in Traditional Construction. Sustainability 7, 5182–5210.https://doi.org/10.3390/su7055182

CIECHOMSKI, W., 2015. Mass customization as a form of the market communication with consumers. Research Papers of Wroclaw University of Economics. https://doi.org/10.15611/pn.2015.414.06

ESPINOZA PÉREZ, A.T., ROSSIT, D.A., TOHMÉ, F., VÁSQUEZ, Ó.C., 2022. Mass customized/personalized manufacturing in Industry 4.0 and blockchain: Research challenges, main problems, and the design of an information architecture. Information Fusion 79, 44–57. https://doi.org/10.1016/j.inffus.2021.09.021

HADDOUCHE, M., ILINCA, A., 2022. Energy Efficiency and Industry 4.0 in Wood Industry: A Review and Comparison to Other Industries. Energies (Basel) 15, 2384. https://doi.org/10.3390/en15072384

KWIDZIŃSKI, Z., BEDNARZ, J., PĘDZIK, M., SANKIEWICZ, Ł., SZAROWSKI, P., KNITOWSKI, B., ROGOZIŃSKI, T., 2021a. Innovative line for door production TechnoPorta—technological and economic aspects of application of wood-based materials. Applied Sciences (Switzerland) 11. https://doi.org/10.3390/app11104502

KWIDZIŃSKI, Z., BEDNARZ, J., SANKIEWICZ, Ł., PĘDZIK, M., ROGOZIŃSKI, T., 2021b. TechnoPORTA intelligent, customized technological line for the automated production of technical doors - selected technical and economic indicators. Annals of WULS Forestry and Wood Technology 96–100. https://doi.org/10.5604/01.3001.0015.2383

PĘDZIK, M., BEDNARZ, J., KWIDZIŃSKI, Z., ROGOZIŃSKI, T., SMARDZEWSKI, J., 2020. The idea of mass customization in the door industry using the example of the company porta KMI Poland. Sustainability (Switzerland) 12. https://doi.org/10.3390/su12093788

TARIGAN, U., TARIGAN, U.P.P., SUKIRMAN, V., 2019. Integration of Lean Manufacturing and Group Technology Layout to increase production speed in the Manufacture of Furniture. IOP Conference Series: Materials Science and Engineering 528, 012058. https://doi.org/10.1088/1757-899X/528/1/012058

CHIP AND CHIPLESS WOODWORKING PROCESSES, 13(1): 75–80, 2022
Zvolen, Technical University in Zvolen, ISSN 1339-8350 (online), ISSN 2453-904X (print)

SUSTAINABLE MANUFACTURING PROCESS IN WOOD MACHINING

Alena Očkajová – Martin Kučerka – Adrián Banski

Abstract

The aim of this paper is to point out the importance of sustainability also in production processes. For the process of longitudinal sawing of beech, beech with a healthy false heart and spruce, we characterized the most important inputs and outputs of the given process based on the scheme from the viewpoint of sustainability. The aim of our investigation was the use of 2 different saw blades SB1 and SB2 and their effect on the granularity of sawdust from the viewpoint of dust particles ≤ 100 µm, which are dangerous for the operating personnel, because dust from hardwoods in particular is included among carcinogens. The proportion of individual sawdust fractions was obtained by sieve analysis. When sawing with the SB2 disc, 56.76 % ÷ 76.0 9% of dust particles ≤ 100 µm are produced compared to SB1 within the selected variants. When comparing woods, the proportion of dust particles ≤ 100 µm for spruce for all variants ranged from 7.95 ÷ 15.09 %, for beech from 10.52 ÷ 24.03 %, which is quite a high percentage, since it is a carcinogen. By choosing the right tool, we can reduce the share of the dust particles ≤ 100 µm, which is dangerous for the working environment.

Key words: *sustainability, manufacturing process, sawing, saw blade, airborne dust particles*

INTRODUCTION

In many our production facilities a solution of sustainable manufacturing process is not consider as urgent. In society still persists a view that it is an issue that affects primarily the environment (Potkány, Gejdoš and Debnár, 2018)] that was typical in previous period in the 1970s when the concept of sustainable development or sustainability have been defined, in relation to environmental issues (World Commission…, 1987). Only in 2015 the UN developed, within the Agenda 2030, the "Transformation of our world" programme: Sustainable Development Agenda 2030, which includes the first and separate "Sustainable consumption and production" (A/RES/70/1. 2015).

The "Sustainable production" is identified and analyzed at these three levels of (Haapala et al., 2013):

- products – 6R (reduce, reuse, recycle, redesign, recover, remanufacturing),
- processes – manufacturing cost, energy consumption, waste management, operational safety, personal health, environmental impact and,
- systems – planning methodology and an efficient supply chain system for all phases of the life cycle.

Matej Bel University, Tajovského 40, 974 01 Banská Bystrica
e-mail: alena.ockajova@umb.sk

In machining process, we used the scheme by (Lu et al., 2011), with the inputs (processing parameters, raw material, cutting tools, power supply, attachments) and outputs (finished products, chips, used cutting tools, other emission – dust, noise) for specific equipment – universal circular sawing machine and machining processes – longitudinal sawing. The result of this approach should be in the product quality, minimum energy consumption and other input materials, with a minimal impact on the working environment – and thus fulfill sustainability targets.

It is very important to implement such an approach also in woodworking enterprises, especially in woodworking secondary production. There is machining wood with moisture content of approx. 8 ÷ 12 % and during its processing, a large amount of wood dust is produced (depending on the technology) which poses a risk to the operating personnel, because it causes sinus cancer, adversely affects the skin and gradually weakens the entire respiratory system, (Očkajová et al., 2006, Beljo-Lučič et al., 2007, 2009, Dzurenda, Orlowski and Wasielewski, 2004).

The aim of this paper is to emphasize how the choice of selected parameters at the input – tools and material in the process of wood sawing will affect the output in the form of chips and other emission – dust.

MATERIAL AND METHODS

Sawing – the characteristic of input and output parameters are given in Fig.1.

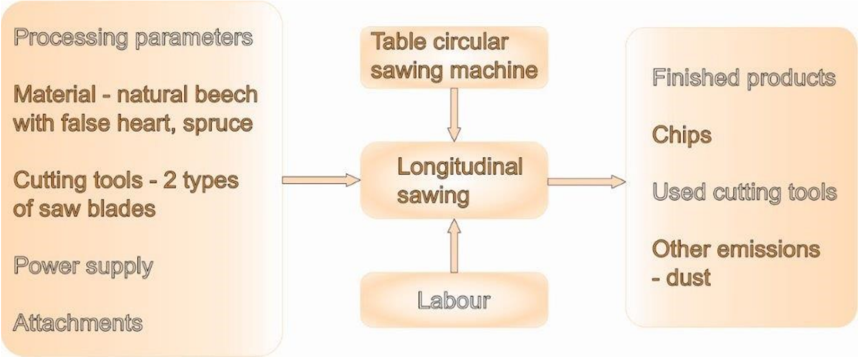
Processing parameters
Material - natural beech with false heart, spruce
Cutting tools - 2 types of saw blades
Power supply
Attachments
Table circular sawing machine
Longitudinal sawing
Labour
Finished products
Chips
Used cutting tools
Other emissions - dust

Fig.1 Input and output parameters from the viewpoint of sustainable wood machining process

Cutting material – natural beech, beech with false heart, spruce, humidity w = 12 %, dimensions of samples 20x100x1000 mm. Each sample was sawn 6 times to obtain the required amount of chips for sieving. Samples for particle size analysis of wood dust were taken isokinetically from the exhaust pipe in accordance with the (STN ISO 9096, 2004). A new bag was used for each variant of created chips.

Cutting tools – 2 types of saw blades (SB1, SB2)

SB1 the universal saw blade with triangular asymmetric spring set teeth, with the following characteristics:

- saw blade diameter 285 mm
- pitch of teeth 22 mm
- number of teeth 40
- tool geometry $\alpha = 21°$, $\beta = 37°$, $\gamma = 32°$
- calculated average chip thickness 0,045mm.

SB2 the saw blade with tipped swaged anti-kickback teeth, with chip breaker and optimal chip clearance with the following characteristics:

- saw blade diameter 300 mm
- pitch of teeth 52 mm
- number of teeth 18
- tool geometry $\alpha = 12°$, $\beta = 56°$, $\gamma = 22°$
- calculated average chip thickness 0,105 mm.

Universal circular sawing machine

- $v_c = 50$ m.s^{-1}
- rot = 3750 min^{-1}
- $v_{f\,1/f2} = 9/16$ m.min^{-1}

Granular analysis

For granular analysis was used a special set of sieves with dimensions of sieve mesh (1mm; 0.5 mm; 0.355 mm; 0.1 mm; 0.05 mm and bottom). These ones were placed on the vibrating stand of the sieving machine Retsch AS 200c. The sieving parameters were in accordance with (STN ISO 3310-1, 2000), sieving time $\tau = 15$ minutes, weight of samples 50 g. The share of particles remaining on the sieves after sieving were weighed on an electric laboratory balance Radwag 510/C/2, with accuracy 0.001 g. The result is average value of three sieving for each variant, (Landiga, 2005).

RESULTS AND DISCUSSION

Output parameter – chip and dust – the share of dust particles ≤ 100 µm, that are characterized as airborne dust particles. These ones very slowly sediment and stay a long time in atmosphere. The problem is that they are the risk for employees, because of their carcinogenicity, (especially the dust particles from hard wood, in our case – beech), (Government Decree of the Slovak Republic No. 471/2011 and No. 83/2015). Not only the smallest wood dust particles that get to the lung alveoli are dangerous but all particles we inhale, so we will consider the share of particles ≤ 100 µm.
The results are given in Table 1.

The comparison of dust particles ≤ 100 µm:

- **SB1 & SB2**

By using the SB2 disc, with a completely different input characteristic, with a lower number of teeth, twice the chip thickness than SB1, significant differences in the granular composition of the resulting sawdust were obtained. It can be clearly seen from the Table 1 that on a 1 mm screen, the proportions of sawdust are about 10 ÷ 15 % higher compared with SB2 saw blade, which means that the SB2 produces larger sawdust. It can also be seen in the proportion of sawdust on the 0.1 mm sieve, where the proportion of these smaller particles is higher in SB1 by about 5 ÷ 10 % compared to SB2. We evaluated particles with a size of ≤ 100 µm as problematic for the operating personnel, because the entire inhaled fraction is a risk with wood dust. For SB1, the share of these particles is in the interval from 17.62 ÷ 24.03 % for beech and from 12.61 ÷ 15.09 % for spruce. For SB2, these values are from 10.52 ÷ 16.68 % for beech and from 7.95 ÷ 11.07 % for spruce. In the Table 1, the percentages of particles ≤ 100 µm are compared for both discs (SB1 = 100 %) and the shares of these particles for SB2 range from 56.76 % ÷ 76.09 %, compared to SB1.

- **v_{f1} & v_{f2}**

The influence of a higher feeding speed on the granular composition of sawdust was manifested similarly to the influence of SB2, because even by increasing the feeding speed, the average thickness of the sawdust increases, and thus in all variants the proportion of particles with a size ≤ 100 mm is lower in v_{f2}, for beech it is in the interval from 3.12 to 5.95 % and for spruce it is from 2.48 to 3.12 % compared to v_{f1} (Očkajová et al., 2020, Beljo-Lučič et al., 2006)

Table 1 Granular analysis of dust particles from sawing of beech, beech with false heart and spruce

Dimension of sieve mesh	SB1/v_{f1} Beech	SB1/v_{f1} Beech – false heart	SB2/v_{f1} Beech	SB2/v_{f1} Beech – false heart	SB1/v_{f2} Beech	SB1/v_{f2} Beech – false heart	SB2/v_{f2} Beech	SB2/v_{f2} Beech – false heart	SB1/v_{f1} Spruce	SB2/v_{f1} Spruce	SB1/v_{f2} Spruce	SB2/v_{f2} Spruce
[mm]	[%]	[%]	[%]	[%]	[%]	[%]	[%]	[%]	[%]	[%]	[%]	[%]
1	48.07	52.63	65.26	60.99	54.71	58.54	71.12	67.40	52.80	69.02	55.31	70.27
0.5	18.28	17.69	14.91	15.44	19.92	16.26	13.01	15.04	21.86	13.94	22.94	15.82
0.355	9.62	7.76	6.22	6.89	7.29	7.58	3.35	5.79	10.25	5.97	9.14	5.96
0.1	21.24	19.28	11.56	14.76	15.94	16.07	9.23	10.20	13.64	9.71	11.47	7.36
0.05	2.51	2.53	1.60	1.84	1.88	1.48	1.19	1.51	1.39	1.35	1.12	0.58
bottom	0.28	0.11	0.45	0.08	0.26	0.07	0.10	0.06	0.06	0.01	0.02	0.01
Particles ≤ 100µm	24.03	21.92	13.64	16.68	18.08	17.62	10.52	11.77	15.09	11.07	12.61	7.95
SB1 to SB2	100%	100%	56.76	76.09	100%	100%	58.18%	66.79%	100%	73.35	100%	63.04%

- **Sound false heart of beech & beech**

When comparing the proportions of dust particles ≤ 100 μm arising in the process of sawing beech wood and beech wood containing a healthy false heart with the same input parameters – the same saw blade, the same feed speed, it can be concluded that the proportions of these particles are very similar, which can also be justified by the statements, that a healthy false heart has preserved physical-mechanical properties, only the colour of this wood changes and therefore there is no reason for the formation of a larger amount of dust particles (Požgaj et al., 1997).

- **Beech & spruce**

When sawing these two different types of wood (beech – broad-leaved ring-porous wood, spruce - coniferous wood) with different structures as well as structural cellular elements, differences in the proportion of dust particles ≤ 100 μm were obtained, always with a lower proportion for spruce, where for all variants ranged from 7.95 ÷ 15.09 %, for beech from 10.52 ÷ 24.03%. With a clear angular geometry of the saw blades and the same set conditions, we would assume the creation of the same or similar sawdust from the point of view of granular composition, which cannot be claimed e.g. when sanding, where each sanding grain works with a different angular geometry and always creates a different chip – size and shape, (Očkajová et al., 2016, 2021). A different proportion of particles ≤ 100 μm can be attributed to the structure and physical-mechanical properties of sawn wood, as beech is considered a less tough wood than spruce, (Požgaj et al., 1997).

CONCLUSION

From the point of view of sustainable manufacturing process we do not solve all input and output parameters only those that are the aim of our long-term interest. In real practice, such an approach is very important, because if the inputs are set correctly, we will also achieve high-quality outputs.

By choosing the right tool – saw blade SB2, we can influence the share of dust particles with a size ≤ 100 μm, whose share reaches 56.76 % ÷ 76.09 % compared to SB1 within the selected variants.

By setting a higher feed speed v_{f2}, the proportion of dust particles with a size ≤ 100 μm is lower for beech it is in the interval from 3.12 to 5.95 % and for spruce it is from 2.48 to 3.12 % compared to v_{f1}.

No difference in the proportion of dust particles with a size of ≤ 100 μm was obtained when sawing beech wood containing a healthy false heart.

A higher proportion of dust particles with a size ≤ 100 μm was obtained when sawing beech than spruce, which we attribute to its physical-mechanical properties, especially lower toughness. Solving this problem is important, because beech is classified as a category 1 carcinogen.

ACKNOWLEDGEMENT
This work was support by the grant agency KEGA under the project No. 026UMB-4/2021.

REFERENCES CITED

A/RES/70/1. 2015. Transforming Our World: The 2030 Agenda for Sustainable Development. 35.

BELJO-LUČIČ, R., ČAVLOVIČ, A., DUKIČ, I., IVANČAN, Ž. 2006. Influence of feed speed on emission of fine sawdust during circular sawing. In Trieskové a beztrieskové obrábanie dreva 2006. Zvolen: TU, 2006, s. 49-55.

BELJO-LUČIĆ, R., ČAVLOVIČ, A., DUKIČ, I., JUG, M., IŠTVANIČ, J., ŠKALJIČ, N. 2009. Machining properties of thermally modiefied beech-wood compared to steamed beech-wood. In Proceedings of the 3rd ISC-Woodworking technique, Zalesina. Zagreb: Faculty of Forestry, 2009.

BELJO LUČIČ, R., ČAVLOVIČ, A., IŠTVANIČ, J., DUKIČ, I., KOVAČEVIČ, D. 2007. Granulometric analysis of chips generated from planing of different species of wood. In Proceedings of the 2nd ISC-Woodworking technique, Zalesina. Zagreb: Faculty of Forestry, 2007, p. 207-213.

DZURENDA, L., ORLOWSKI, K., WASIELEWSKI, R. 2004. Granulometric analysys and separation options of dry sawdust exhausted from narrow - kerf frame sawing machines. Drvna industrija, Vol.56, No.1., pp 55-60.

Government Decree of the Slovak Republic n. 471/2011. Protection of employees against the risks associated with exposure to chemical agents at work. Government Office Slovakia.

Government Decree of the Slovak Republic n. 83/2015. Occupational protection of workers' health from risks associated with exposure to carcinogenic and mutagenic factors. Government Office Slovakia.

HAAPALA, K.R., ZHAO, F., CAMELIO, J., SUTHERLAND, J.W., SKERLOS, S.J., DORNFELD, D.A., JAWAHIR, I.S., CLARENS, A.F., RICKLI, J.L. 2013. A Review of Engineering Research in Sustainable Manufacturing. Journal of Manufacturing Science and Engineering, 135, doi:10.1115/1.4024040.

LANDIGA, M. 2005. Vplyv vybratých parametrov na tvorbu triesky pri pílení dreva na univerzálnej stolovej kotúčovej píle. Diplomová práca. TU Zvolen, 76 p. 10.

LU, T., GUPTA, A., JAYAL, A.D., BADURDEEN, F., FENG, S.C., JR., O.W.D., JAWAHIR, I.S. 2011. A Framework of Product and Process Metrics for Sustainable Manufacturing. In Proceedings of the Advances in Sustainable Manufacturing; Seliger, G., Khraisheh, M.M.K., Jawahir, I.S., Eds.; Springer: Berlin, Heidelberg; pp. 333-338.

OČKAJOVÁ A., KUČERKA M., KMINIAK R., BANSKI A. 2021. Sustainable Manufacturing Process in the Context of Wood Processing by Sanding. Coatings. 11(12):1463. https://doi.org/10.3390/coatings11121463

OČKAJOVÁ, A., KUČERKA, M., KMINIAK, R., KRIŠŤÁK, Ľ., IGAZ, R., RÉH, R. 2020. Occupational Exposure to Dust Produced When Milling Thermally Modified Wood. In International Journal of Environmental Research and Public Health [elektronický zdroj]: Open Access Journal. Basel: MDPI, 2020. ISSN 1661-7827. Vol. 17, no. 5 (2020), 1478.

OČKAJOVÁ, A., KUČERKA, M., KRIŠŤÁK, Ľ., RUŽIAK, I., AND GAFF, M. 2016. Efficiency of sanding belts for beech and oak sanding. *BioResources* 11(2), 5242-5254. DOI: 10.15376/biores.11.2.5242-5254.

OČKAJOVÁ, A., BELJO LUČIČ, R., ČAVLOVIČ, A., TEREŇOVÁ, J. 2006. Reduction of dustiness in sawing wood by universal circular saw. Drvna industrija. Vol.57, No.3., 2006, pp 119-126.

POTKÁNY, M., GEJDOŠ, M., DEBNÁR, M. 2018. Sustainable Innovation Approach for Wood Quality Evaluation in Green Business. Sustainability, 10, 2984, doi:10.3390/su10092984.

POŽGAJ, A., CHOVANEC, D., KURJATKO, S., BABIAK, M. 1997. *Štruktúra a vlastnosti dreva*; 2. vyd., Bratislava: Príroda, 1997, ISBN 80-07-00960-4.

STN ISO 9096 (83 4610): 2004. Ochrana ovzdušia. Stacionárne zdroje znečisťovania. Manuálne stanovenie hmotnostnej koncentrácie tuhých znečisťujúcich látok.

STN 1531 05/ STN ISO 3310-1: 2000. Súbor sít na laboratórne účely.

World Commission on Environment and Development Our Common Future; Oxford University Press: Oxford; New York, 1987; ISBN 978-0-19-282080-8.

CHIP AND CHIPLESS WOODWORKING PROCESSES, 13(1): 81–86, 2022
Zvolen, Technical University in Zvolen, ISSN 1339-8350 (online), ISSN 2453-904X (print)

PROVENANCE DEPENDENT OPTIMIZATION OF PINE TIMBER PROCESSING IN WOODEN BAD FRAME PRODUCTION

Bartosz Pałubicki [1,2] – Dariusz Orlikowski [2] – Witold Jarecki [2] –
Krzysztof Wiaderek [1,2] – Łukasz Matwiej [1,2] – Marek Wieruszewski [1,2]

Abstract

Pine timber from different European localizations and intended for the production of continental bed frames at Sun Garden Polska was analyzed. One of the available methods of processing sawn timber into intended friezes (frame semi-finished products) is its transverse or longitudinal-transverse cutting into ready-made elements and into cutouts of appropriate quality intended for joining lengthwise by means of finger joints. In the next stage of production, such boards are re-sawn into ready frame semi-finished products. As part of the research, the length shares of the quality classes KW, KS and KG in boards were determined. From the point of view of the final product, each of the frame components must meet the appropriate quality requirements, and hence the need to optimize the cutting not only based on maximizing the material efficiency of the process, but also taking into account the needs of elements in specific qualities. Merely increasing the quantitative efficiency in the production of dedicated wooden frames is pointless, because the performance indicators do not correspond to the fulfillment of production orders, leaving an excess of some components and a shortage of others. For this reason, it was proposed to parameterize the optimization process taking into account the filling of order baskets and the feedback based on them for timber of different provenances.

Key words: *Wood processing, production efficiency, timber quality, timber defects*

INTRODUCTION

The suitability of coniferous sawn materials obtained from Europe for the needs of the furniture industry is strongly dependent on its quality characteristics. The defects of sawn timber from the cross-section or length determine its strength and performance characteristics of wood and therefore on the final wooden products. Assumptions regarding the selection of boundary features are the basis of optimization processes, allowing a controlled production of furniture components. In the classification of coniferous wood, the origin of the raw material plays a significant role. In the classification systems, a decisive role is played by the identified defects, which include in particular: knots, twist of fibers, resin pockets, as well as defects of wood processing, i.e. cracks, discoloration, rot, and curvatures. Knots play a key role in the process of optimizing the acquisition of semi-finished products, accounting for up to 75% of defects (Purba 2019). Knots reduce the

---

[1] Poznan University of Life Sciences, ul. Wojska Polskiego 38/42, 61-627 Poznan, Poland
[2] Sun Garden Polska Sp. z.o.o sp.k., ul. Turecka 36, 62-709 MalanówSun, Poland
e-mail: bartosz.palubicki@up.poznan.pl

strength of the wood in zones (Baltrušaitis 2000;). Horizontal cracks along the sawn timber reduce the strength and technological quality (Buchelt et al. 2018).

Currently, modern optical systems with four-sided action are used to detect the defects. The assessment of the surface of the sawn timber on the basis of the image of the defect distribution improves the optimization of the sorting process of furniture elements. This stage requires assigning the zones of timber to the boundary quality characteristics determining the share of acceptable defects for the surface and the strength assessment (Schajer 2001; Roblot et all. 2010; Hu et all. 2018). Obtained range of occurrence of the identified defects in relation to their dimensions allows to obtain high efficiency of prefabrication by optimization (Klinea et al. 2001). Thanks to the automated systems (Microtec, Luxscan, Woodinsepctor, etc.), it is possible to determine the impact of both the quality of the raw material and its impact on the performance of furniture materials. Timber classification methods based on the occurrence of defects are related to its strength (Kozakiewicz and Krzosek, 2013). The knowledge of the rules of shaping technological processes by means of the boundary ranges of defect distribution allows to obtain the correct selection of sawn timber for semi-finished products and finished products in the furniture industry.

The aim of the research was to determine the suitability of coniferous sawn timber from two regions: Central and Northern Europe for the production of semi-finished products for the production of wooden bed frames. The work takes into account the automatic visual assessment of sawn timber, with the separation of strength zones that meet the requirements of the construction of final furniture. The aim was to evaluate the feasible technological processing efficiency in industrial practice with the applied softwood classification.

MATERIALS AND METHODS

Polish and Scandinavian sawn timber from Scots pine (*Pinus silvestris* L.) was used for the research. Based on the standard cross-sections of sawn elements, it was decided to choose a typical series of dimensions of the side trim, 19-25 mm thick and 2.5-6 m long. The sawn timber was obtained as a result of sawmill processing with the use of block band saws and the use of automatic side saws.

The timber was utilized to produce bed frames shown in Figure 1, consisting of the elements shown in Table 1. The frame consists of side (long) and head (short) rails. They consist of elements: long rail board (1), short rail board (6), long slat support (5), short slat support (not visible) and long slat support prolongation (2). The frame boards have a cross-section of 20x80mm, while the attached slat supports are 20x48mm. At the top 9 mattress slats (3) and at the bottom 2 leg supports slats (4) are mounted.

The manufacturing process of the frame elements was as follows. Dry sawn timber after destacking was planed on a Weinig Powermat 1200 four-sided moulder in order to adjust it to the net dimensions of the elements' cross-section and to prepare the surface for a reliable assessment of timber defects. Then, in the monitoring subassembly of the production line, with the use of the Luxscan CombiScan Sense C400 four-sided lumber scanner, the quality classification of lumber zones was performed according to visual classification based on PN 94021: 2013. Poor-quality zones - KG (C16 according to PN-EN 338), medium-quality KS (C24) and high-quality KW (C30) were separated and then optimization of the cross-cutting plan for frame elements (friezes) or shorter wood pieces was performed. These shorter pieces were then bundled, finger profiled on both ends and joined lengthwise. The glued frame elements were cut out from the prepared glued timber.

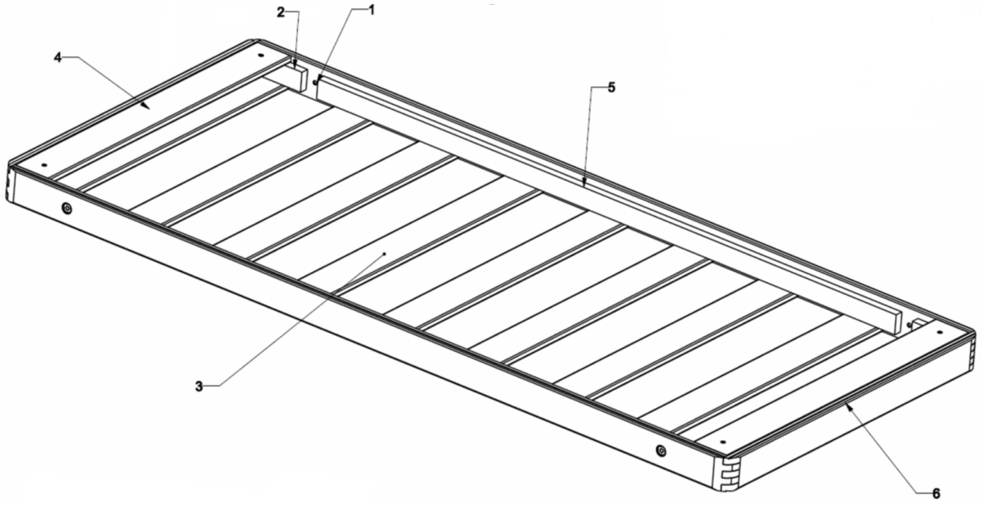

Figure 1. Design of the bed frame

The processing yield (W) of sawn timber in each cross-section (i) was determined by the volume of its successive stages as:

$$W_i = \frac{V_2}{V_1} \cdot \frac{V_3}{V_2} \cdot \frac{V_4 + V_5}{V_3}$$

where:
V_1 – timber volume (m^3)
V_2 – volume after planing (m^3)
V_3 - volume after cross-cutting (m^3)
V_4 - volume after elements formatting (if applied) (m^3)
V_5 – volume of glued boards after finger-jointing (m^3)

The operation of cutting the ends of the boards before planing was omitted in the analysis because it does not significantly affect the efficiency - the trade allowances on the length of the sawn timber cover the occasional cutting of its faces. The most flexible component, giving a lot of room for efficiency improvement, is the cross-cutting performed on the basis of the solutions of the optimizer. For each produced cross-section and for each element within the cross-section, the defects of sawn timber were determined in the optimization process according to predetermined normative requirements with an unacceptable proportion of wafers and blue stains. They specified both the quality in the middle zones and in the front zones intended for tenoning of elements. The optimization of cross-cutting was carried out not in terms of the usual maximization of production efficiency, but taking into account the shares of individual elements in the frames produced. Thus, the aim function of the optimization was the final efficiency of the frame production, not of the component production yield. Such configuration of the intended production does not cause excessive inventory of any of the elements.

Short and long rail boards with a cross-section of 80x20 mm

According to the assumptions formulated in the first stage of the project, the boards for the side rails should be made of KW class wood, and the head rail boards of the KS class wood.

The most important optimization task was to meet the material demand for the KW class for the production of long rail in such a way that there is no excess wood in lower quality. As part of the research for target cross-sections 80x20mm, side sawn timber with a nominal cross-section of 23x85mm was used.

Slat supports with a section of 48x20 mm

In the case of the production of slat supports with a cross-section of 20x48 mm, sawn timber with nominal dimensions of 23x105 mm (polish) and 25x112 (scandinavian) was used. In the technological process, longitudinal sawing of boards into two strips with target cross-sections was used in the processing subassembly (planer). The target elements were: long support for the side rail, short support for the side rail and short for the head rail. In the optimization task it was established that the end parts of the long slat supports (four pieces per frame) must be cut in the KW class in the amount corresponding to the production order for the frames.

Mattress and leg support slats with a cross-section of 95x16 mm

In addition to complete rails, the reference frame also includes mattress and leg support slats. From the point of view of their quality, these elements can be divided into three groups. The external mattress slats have much lower strength requirements than the others and can be made of KG wood. In turn, for the next two slats, a class of at least KS is required. The remaining slats constitute an important part of the frame strength and therefore must be separated from solid KW class timber or wood joined lengthwise. The algorithm optimizing the cross-cutting operation has therefore been configured to achieve these three classes: KW solid slats and KW, KS and KG cutouts in quantities satisfying the shares of the corresponding elements in the frame.

Table 1. Population of tested timber of polish and scandinavian provenances

		Number of boards	Total length of boards	Total volume tested
			m	m^3
Rail boards (20x80)	polish	4284	12729	20.5
	scandinavian	1511	4539	7.3
Slat supports (20x48)	polish	3434	11701	11.3
	scandinavian	3650	11602	11.2
Slats (16x95)	polish	4933	9882	16.9
	scandinavian	5043	19788	33.6

Complete frame production efficiency

For all optimized cutting solutions, the overall efficiency W_{Total} of sawn processing into ready-made bed upholstery frames was calculated as:

$$W_{Total} = \sum_{i=1}^{3} u_i \cdot W_i$$

taking into account the share (u_i) of components (rail boards, slat supports and slats) in the frame and their production efficiency W_i.

RESULTS AND DISSCUSSION

Figure 2 shows maximal efficiencies achievable for frame components and efficiencies for production of components in quantity proportional to their occurrence in the frame and hence filling the order basket. Both values for each component have been achieved by optimizing the unit values (weight coefficients) of each elements with specified quality class. In general proportional efficiency is only slightly lower than maximal with exception of Scandinavian rail boards and slat supports, where higher KS class shares did not allowed to obtain enough required KW elements. Slat supports scandinavian raw material showed clearly lower values compared to all other cases which was caused by higher initial nominal cross-section. Despite of higher maximal efficiency for scandinavian rail boards, polish timber is recommended for both rail boards and slat supports. For the slats scandinavian timber showed higher efficiency than polish.

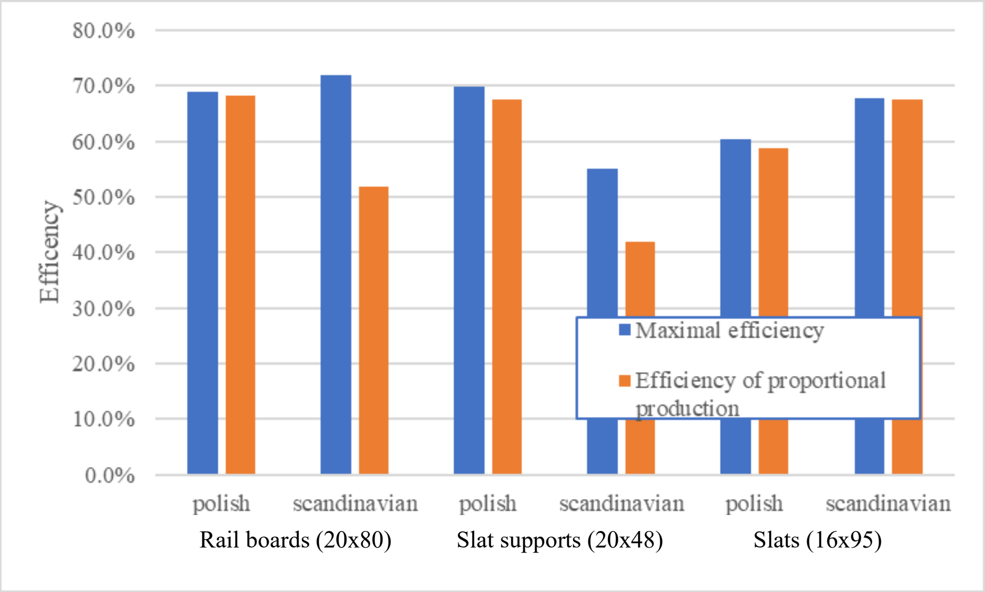

Figure 2. Efficiency of production bed frame components from polish and scandinavian timber

Table 1. Efficiency of production bed frames from polish and scandinavian timber

	Volume in the frame (m^3)	Share of frame volume	Frame production efficiency			
			polish	scandinavian	the worst case (mixed)	the best case (mixed)
Rail boards (20x80)	0.009184	32.1%	68.3%	51.7%	51.7%	68.3%
Slat supports (20x48)	0.005207	18.2%	67.5%	42.0%	42.0%	67.5%
Slats (16x95)	0.014212	49.7%	58.7%	67.5%	58.7%	67.5%
Total:	0.028603		**63.4%**	**57.8%**	**53.4%**	**67.7%**

Detailed results of production efficiency based on optimized cross-cutting of timber into requested bed frame elements are pointed in Table 2. For Scandinavian rail boards it is clear that they have better overall quality but polish allows better manipulation to achieve high quality elements. If one use only polish timber for bed frames production it would lead to over 63% efficiency, what is higher than fully scandinavian timber option (almost 58%). The most optimal solution (67.7%) includes mixing polish timber for rails and slat supports with scandinavian timber for the slats production.

CONCLUSIONS

Pine timber form two provenances (polish and scandinavian) shows different qualities and usability in upholstery wooden bed frame production. Using optimal timber setup increase overall efficiency from 57.8% for pure scandinavian and 63.4% pure polish timber to almost 68%.

REFERENCES

Baltrušaitis, A. (2000). Investigation of influence of knots on short – and long – term strength of glulam beams. World Conference on Timber Engineering 2000.

Buchelt, B.; Wagenführ, A.; Dietzel, A.; Raßbach, H. (2018). Quantification of cracks and cross-section weakening in sliced veneers. Eur. J. Wood Wood Prod., 76, 381–384. DOI:10.1007/s00107-017-1238-z.

Dahlen, J., Montes, C., Eberhardt, T.L., Auty, D. (2018). Probability models that relate nondestructive test methods to lumber design values of plantation loblolly pine. Forestry 91(3):295–306

Hu, M., Briggert, A., Olsson, A., Johansson, M., Oscarsson, J., Säll, H. (2018). Growth layer and fibre orientation around knots in Norway spruce: a laboratory investigation. Wood Sci Technol 52:7–27

Klinea D.E., Aramanb P., Surakc, C. (2001). Evaluation of an Automated Hardwood Lumber Grading System. Proceedings of ScanTech (2001). International Conference, Seattle, Washington, U.S.A.

Kozakiweicz P., Krzosek S. (2013). Technologia materiałów drzewnych. Wydawnictwo SGGW, Warszawa.

PN 94021: 2013 Tarcica iglasta konstrukcyjna sortowana metodami wytrzymałościowymi

PN-EN 338:2016-06 Drewno konstrukcyjne -- Klasy wytrzymałości

Purba, C.Y.C.; Pot, G.; Viguier, J.; Ruelle, J.; Denaud, L. (2019). The influence of veneer thickness and knot proportion on the mechanical properties of laminated veneer lumber (LVL) made from secondary quality hardwood. Eur. J. Wood Wood Prod. 77, 393–404. DOI: 10.1007/s00107-019-01400-3

Roblot, G., Bléron, L., Mériaudeau, F., Marchal, R. (2010). Automatic computation of the knot area ratio for machine strength grading of Douglas-fir and Spruce timber. Eur J Environmental Civil Eng 14(10):1317-1332

Schajer, G.S. (2001). Lumber strength grading using X-ray scanning. Forest Prod J 51(1):43-52.

Acknowledgement

Research conducted under the project POIR 01.01.01-00-802/19/ „The Development of an Original Technological Process Resulting in Higher Productivity, Efficiency and Quality of Wood Products“

CHIP AND CHIPLESS WOODWORKING PROCESSES, 13(1): 87–94, 2022
Zvolen, Technical University in Zvolen, ISSN 1339-8350 (online), ISSN 2453-904X (print)

THE INFLUENCE FALSE HEARTWOOD ON THE QUALITY OF BEECH STRUCTURAL TIMBER

Alena Rohanová

Abstract

The use of beech in building structures is conditioned by a complete assessment of its properties and their interaction with the specific structure and defects. The appearance of false heartwood in a beech tree is a natural defect. Knowledge about its influence on the use in building constructions is significant from the point of view of the structural timber quality. It is generally stated that false heartwood does not change the mechanical properties of wood. This knowledge is verified as part of structural timber research.

Using specimens of structural dimensions (50 × 150 × 2,700 mm, n = 52), the presence of fasle heartwood in the sawn timber surfaces was identified. For evaluation, three groups were created, one without false heartwood (0-0), second one with false heartwood on one surface (1-0) and third one with false heartwood on both surfaces (1-1). The modulus of elasticity, bending strength (MOR_{12}, MOE_{12}) and wood density (ρ_{12}) of the test specimens were determined by a bending destructive test (STN EN 408). The results from the experiments showed that the false heartwood does not significantly affect the values of MOR_{12} ($P = 0.811$); it is not significant (not significant) at ρ_{12} ($P = 0.301$). The influence of the false heartwood on MOE_{12} is at the limit of significance ($P = 0.058$); the highest values of MOE_{12} are at 0-0 (no core), medium at 1-0 and lowest at 1-1. The knowledge is in agreement with FRŮHWALD, 2008, CIBECCHINI et al. 2016.

Keywords: *beech structural timber, false heartwood, modulus of rupture, modulus of elasticity, wood density*

INTRODUCTION

Beech (*Fagus sylvatica L*) is the most widespread and economically strategic tree in Slovakia (approx. 34%). Long-term forestry planning assumes a lower representation of spruce and a higher representation of beech. It is a challenge for wood processors, who have to forecast their production and orient it towards final products with higher added value. This area of use can be significantly supported by structural products made of hardwood (including beech). Beech wood is generally considered an extremely active (living) material at all stages of its processing. It is very difficult to predict the shape changes and degradation defects caused by reaction wood, moisture, wood defects, etc. One of the typical defects of beech wood is false heartwood. Due to its red color, it is generally considered a lower quality raw material (FRŮHWALD, 2008). In the beech log processing chain false heartwood is specified in quality classes: roundwood, logs– STN 48 0056, sawn

---

Technical University in Zvolen, Faculty of Wood Sciences and Technology, T.G. Masaryka 24, 960 01 Zvolen
e-mail: rohanova@tuzvo.sk

timber – STN EN 978-1/AC. When evaluating the quality of structural timber (STN 49 1531), the false heartwood is not indicated. Only colorings (non-fungal, bluing) that are permissible for appearance reasons (STN 49 1531, DIN 4074-5) are allowed. Round reddish-brown to light brown false heartwood are considered healthy. With them, only the physical properties (color and permeability) change and the mechanical properties do not. KÚDELA, ČUNDERLÍK, 2012 state that unhealthy rotting beech false heartwood shows a significant reduction in mechanical properties in addition to a changed color and tarnishing.

Its use is not suitable for solid-wood semi-finished products and final products. Each product is specific and requires the interaction of properties (physical and mechanical) with quality parameters and usage requirements. The assessment criteria are mainly dominated by wood defects (e.g., even false heartwood).

Structural beech timber has a strategic position in building constructions, even from a global point of view. EU countries verify the properties of structural beech timber harvested in respective countries. The effects of wood structure and defects on quality are analyzed, represented by the following parameters: bending strength (*MOR*), modulus of elasticity (*MOE*) and wood density (ρ). This is also stated by the authors FRŰHWALD, 2008.

Currently, the so-called "Beech program" - structural timber intended for building elements is being dealt with. In accordance with EN, the quality of beech structural timber harvested in Slovakia is evaluated. During the evaluation, all factors that affect significantly the quality of structural timber are examined. Part of the research is also the natural occurrence of false heartwood nucleus.

MATERIAL AND METHODS

European beech (Fagus sylvatica L.) from the Horehronie region in Slovakia was used to prepare the test specimens. The number of trees was N = 15 and the number of sections was 30 (20.8 m^3). The length of the logs was 3,300 ÷ 3,500 mm. The quality of the logs was determined according to STN 48 0056. The logs were classified in class III. A. Structural timber was produced by segmental cutting. Segments were cut from each log: 1 central segment (thickness 80 mm) and side segment 2 pcs (thickness 160 mm), from which 60 × 160 x 3,100 mm (247 pcs) specimens were produced (BAJZA – ROHANOVÁ, 2018). After drying and visual sorting, the boards were intended for further experimental investigation (112 pcs). For the destructive bending test (N = 52), the test specimens had dimensions of 50 × 150 × 2,700 mm. The average moisture content of the specimens was determined to be 12 % in laboratory conditions. The moisture content was monitored and controlled by a Hydromette HT 85T.

The test specimens were marked in such a way that their source could be identified in the course of extensive experiments (number of roundwood, log, structural timber, position in the segment: e.g., 6/1/5 – Fig. 1). In each test specimen, the following was assessed:

a) False heartwood - identification of the shape and quality (healthy, rotting) according to POŽGAJ *et al.* 1997),
- occurrence on a wider surface of structural timber (0-0 – without, 1-0 – on one surface, 1-1 – on both surfaces (Fig. 1).

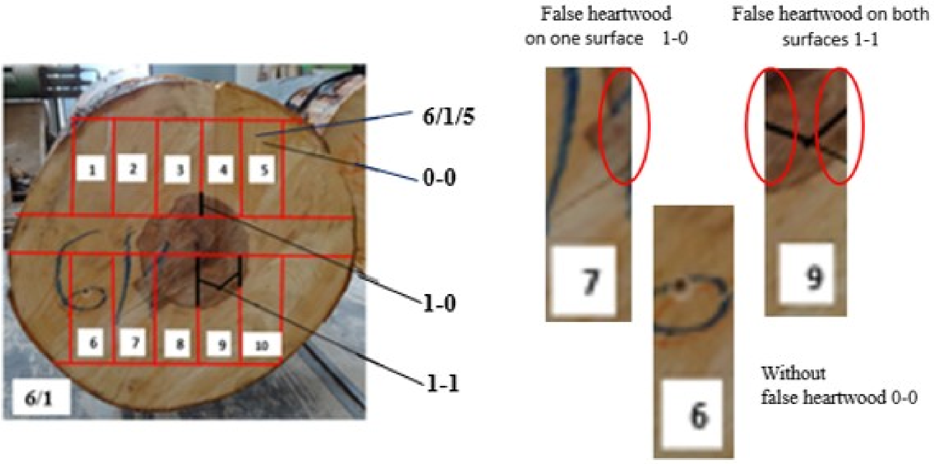
False heartwood
on one surface 1-0
False heartwood on both
surfaces 1-1
6/1/5
0-0
1-0
1-1
1
2
3
4
5
6
7
8
9
10
6/1
7
6
9
Without
false heartwood 0-0

Fig. 1 Beech log – wainscoting method (occurrence of false heartwood on the surfaces of structural timber) (ROHANOVÁ, 2021)

b) Quality parameters according to STN EN 408. In the test specimens, the bending strength (MOR_{12}), the modulus of elasticity in bending (MOE_{12}) and the wood density (ρ_{12}) were determined by a destructive bending test (ROHANOVÁ, KRÁL, 2021**)**.

RESULTS

Table 1 lists the basic statistical characteristics of the quality parameters (MOR_{12}, MOE_{12} and ρ_{12}) according to the occurrence of false heartwood on the surfaces of structural timber.

Table 1 Statistical characteristics of quality parameters (density of wood, modulus of rupture and modulus of elasticity) according to the occurrence of false heartwood in structural timber ((ROHANOVÁ, 2021**)**

Parameters	Statistical characteristics	Total	False heartwood on surface of structural timber		
			1-1 on both surfaces	1-0 on one surface	0-0 without
	n	52	20	21	11
Wood density (ρ_{12})	$\bar{x}$ (kg.m^{-3})	694	651	701	696
	x_{max} (kg.m^{-3})	745	742	745	740
	x_{min} (kg.m^{-3})	612	612	646	647
	V_x (%)	5	6	4	4
Modulus of rupture	$\bar{x}$ (MPa)	77	77	76	78
	x_{max} (MPa)	96	93	96	93

MOR_{12}	$x_{\min}$	(MPa)	52	57	52	62
	V_x	(%)	13	12	14	11
Modulus of elasticity MOE_{12}	$\bar{x}$	(MPa)	13,732	13,425	13,637	14,262
	$x_{\max}$	(MPa)	16,679	14,848	15,666	16,664
	$x_{\min}$	(MPa)	11,465	11,465	11,639	13,616
	V_x	(%)	8	8	7	7

For ρ_{12}, MOR_{12} and MOE_{12} – w (MC) = 12%; n- number of measurements; $\bar{x}$- mean value; $x_{\max}$- maximum value; $x_{\min}$- minimum value; and V_x - coefficient of variation

The influence of false heartwood was confirmed by the Duncan test only in the case of MOE. The highest *MOE* values are found in structural timber without false heartwood (0-0) and the lowest values are found in structural timber with false heartwood on both surfaces (1-1). The difference is at the limit of significance (p = 0.058), e.g at *MOR* (p = 0.811) and at ρ_{12} (p = 0.301).

Dependencies MOR_{12} - MOE_{12}, MOR_{12} - ρ_{12} and MOE_{12} - ρ_{12} (Fig. 2 to Fig. 4) compare the courses and correlation coefficients for different levels of evaluation of the occurrence of false heartwood (total n = 52, on both surfaces 1-1, on one surface 1 -0 and without 0-0). The agreement of the strength of dependence of the correlation coefficients between the parameters for all groups (p) was evaluated.

Fig. 2 – MOR_{12} - MOE_{12}

- total file (N = 52) , r = 0.41,
- in the three groups (0-0: N = 11, 1-0: N = 21, 1-1: N = 20) the difference between the correlation coefficients is non-significant, there is a high agreement between the MOR_{12} - MOE_{12} dependence strength for all groups, p = 0.688 – 0.965.

Fig. 3 – MOE_{12} - ρ_{12}

- total file (N = 52) , r = 0,47,
- in the three groups (0-0: N = 11, 1-0: N = 21, 1-1: N = 20) the difference between the correlation coefficients is non-significant, but the agreement between the dependence strength MOE_{12} - ρ_{12} is lower (for all groups), p 0.187 – 0.856.

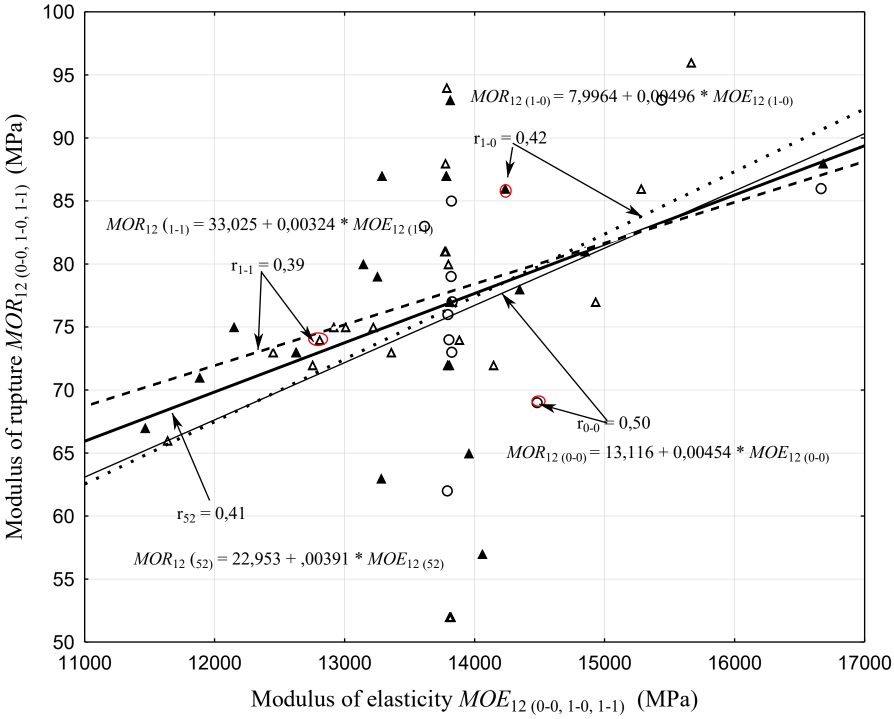

Fig. 2 Dependence of modulus of rupture on modulus of elasticity according to the occurrence of false heartwood in structural timber

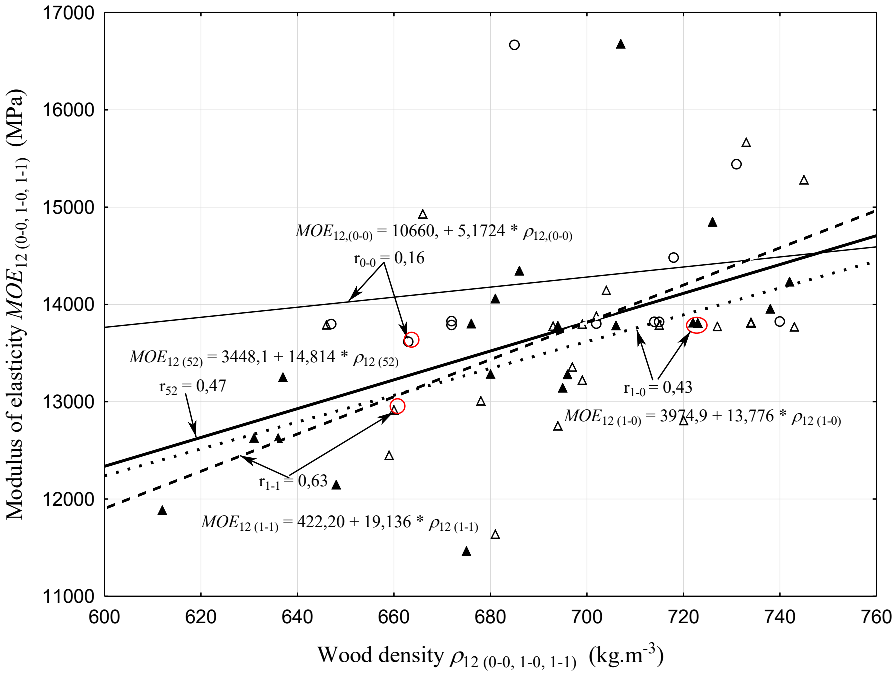

Fig. 3 Dependence of modulus of elasticity on wood density according to the occurrence of false heartwood in structural timber

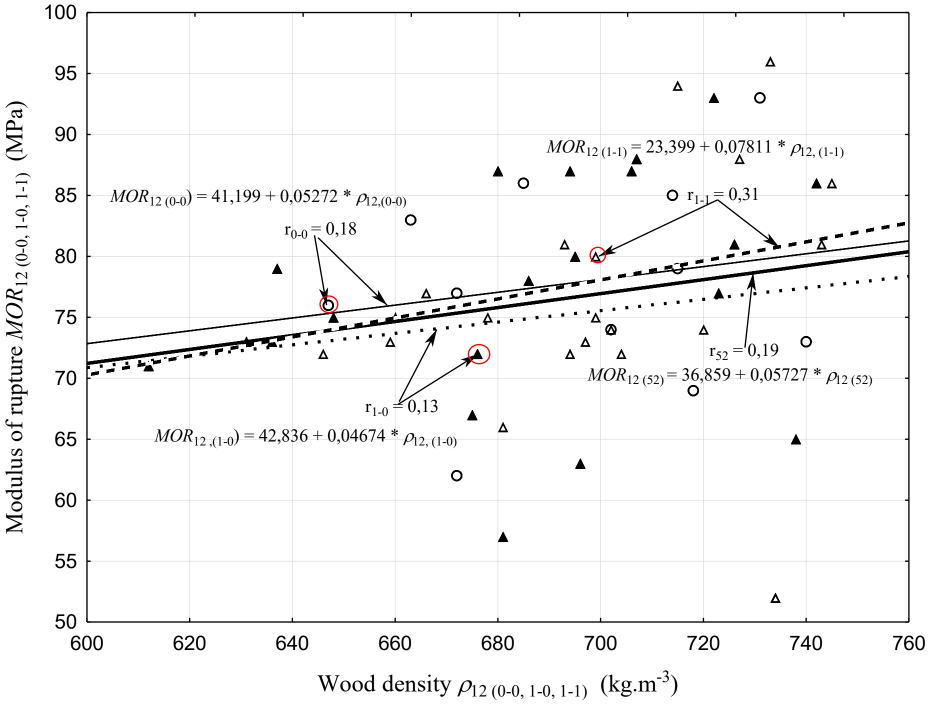

Fig. 4 Dependence of modulus of rupture on wood density according to the occurrence of false heartwood in structural timber

Fig. 4 – MOR_{12} - ρ_{12}

- total file (N = 52) , r = 0.19
- in the three groups (0-0: N = 11, 1-0: N = 21, 1-1: N = 20) the difference between the correlation coefficients is non-significant, high (highest) agreement between the dependence strength MOR_{12} - ρ_{12} (at all groups), p = 0.659 – 0.971.

DISCUSSION

The false heartwood was evaluated from the point of view of occurrence on wider surfaces of structural timber (0-0 without core, 1-0 on one surface and 1-1 on both surfaces). The influence of the false heartwood on the quality parameters (MOR_{12}, MOE_{12} a ρ_{12}) was verified. The analysis showed:
- false heartwood nucleus does non- significantly influence MOR_{12}, values (P = 0.811) and ρ_{12}, values (P = 0.301),
- the influence of the core on MOE_{12} is at the limit significantly (P = 0.058). Highest MOE12 values are at 0-0 (no false heartwood), medium at 1-0 and lowest at 1-1.

FRŰHWALD, 2008 presents the results of research into the properties of beech structural timber. *MOR* and *MOE* were evaluated on test specimens 30 x 150 x 2,500 mm (N=115 pcs.). During the analysis of the structure and defects of the wood, the occurrence of a false heartwood was also recorded. The results of the correlations of sorting characteristics are presented. For false heartwood and *MOR,* r = 0.00, for *MOE,* r = 0.28. It can be assumed that false heartwood has an influence on *MOE* (also at the limit of significance). DIN 4074-5:2003 e. g. states that discoloration caused by false heartwood does not affect strength and is therefore not a classification criterion. These findings need to be further analyzed.

CONCLUSIONS

False heartwood beech wood occurs naturally in all sawmill products (roundwood, logs, structural timber). The types of false heartwood despite the change in the color of the wood, predict the possibilities of using beech raw material in various types of products. Such wood is generally considered of lower quality. It is assumed that its occurrence is combined with other wood defects (e.g. wavy grain pattern), which limits its applicability, e.g. at the furniture (FRŰHWALD, 2008). POŽGAJ *et al.* (1997), KÚDELA, ČUNDERLÍK (2012) characterize the false heartwood in a wider context with the following knowledge. Healthy beech false heartwood (reddish-brown to light brown color) does not change the mechanical properties of wood. Rotting beech false heartwood (e.g. mosaic-like with contrasting border lines - tylated) can reduce some of the mechanical properties of wood. In the case of structural timber, assessing the influence of false heartwood on mechanical properties (quality parameters) it is more difficult. In the chain of technology for the production of sawmill products, important factors enter into the evaluation, e. g. log quality - cut, size and type of heartwood, position of the structural timber in the segmental section, occurrence of the false heartwood on the surfaces of the structural timber, etc. It affects the quality of structural timber, which is determined by the parameters MOR_{12}, MOE_{12} and ρ_{12}. During the experiments, the effect of healthy heartwood on MOE_{12} (lower values compared to healthy wood) was demonstrated. These findings are in agreement with the literature (FRŰHWALD, 2008, CIBECCHINI *et al.* 2016).

AKNOWLEDGMETS
This work was supported by the Scientific Grant Agency of the Ministry of Education, science, research and sport of the Slovak Republic and the Slovak Academy of Sciences - project VEGA No. 1/0063/22.

REFERENCES

BAJZA, O., ROHANOVÁ. A, 2018: Quantitative and Qualitative Yield of Beech Structural Timber (Fagus sylvatica, L.). In Annals of Warsaw University of Life Sciences. No 104 (2018) 290–294.

CIBECCHINI, A. - CAVALLI, A. - GOLI, G. - TOGNI, M. 2016: Beech sawn timber for structural use: A case study for mechanical characterization and optimization of the Italian visual strength grading rule . Florence : Journal of Forest Science, 62, 2016 (11): 521–528, 2016. DOI: 10.17221/93/2016-JFS.

FRŰHWALD, K. 2008: Procedure for determination of characteristic values of hardwood. Oslo - Frühwald. pdf, 2008. (Cit. 24.5.2018). Dostupné na internete: http:// www.coste53.net/downloads/Oslo/Oslo-WG3/COSTE53-MeetingOslo-WG3 Frühwald, K.,

KÚDELA, J.; ČUNDERLÍK, I. 2012. *Bukové drevo štruktúra, vlastnosti, použitie*. Zvolen: Vydavateľstvo Technickej univerzity vo Zvolene, 2012. ISBN 978-80-228-2318-0.

POŽGAJ, A., CHOVANEC, D., KURJATKO, S., BABIAK, M. 1997: Štruktúra a vlastnosti dreva. Príroda, a. s., Bratislava, 485 s., ISBN 80-07-00960-4.00.

ROHANOVÁ, A., KRÁL, Š. 2021: Proposal for redesign of characteristic values and strength classes for beech structural timber. In Materials, methods & technologies. Volume 15, 2021, 23rd International Conference 19-22 August, Burgas, Bulgaria. ISSN 1314-7269 (online), https://www.scientific-publications.net/en/open-access-journals/materials-methods-and-technologies/ (pages: 318-333).

ROHANOVÁ, A. 2021. Buk v drevených stavebných konštrukciách. Monografia.1. vyd. Zvolen: Technická univerzita vo Zvolene, 2021. 103 s. ISBN 978-80-228-3285-4.

STN 48 0056. 2007. *Kvalitatívne triedenie listnatej guľatiny.* Bratislava: SÚTN, 2007.

STN EN 975-1/AC (2011). Appearance grading of hardwoods. Part 1: Oak and beech. Slovak Institute of Technical Standardization Bratislava, Slovakia.

STN 49 1531/Z1. **2006.** *Drevo na stavebné konštrukcie.Vizuálne triedenie podľa pevnosti.* Bratislava: SÚTN. 2006.

DIN 4074, **Teil 5:2003**, Sortierung von Holz nach der Tragfähigkeit, Teil 5: Laubschnittholz. German Committee for Standardization.

CHIP AND CHIPLESS WOODWORKING PROCESSES, 13(1): 95–99, 2022
Zvolen, Technical University in Zvolen, ISSN 1339-8350 (online), ISSN 2453-904X (print)

OVERALL SET OF BANDSAW TEETH VERSUS METHODS OF MEASUREMENTS

Dawid Stenka – Kazimierz A. Orlowski – Daniel Chuchała

Abstract

This article deals with the impact of the manual methods of measurement on the overall set measurement results. It describes the results of the measurement of bandsaw teeth kerf with the use of a micrometer and a digital calliper.

It is commonly known that the cutting process causes the wear of cutting tools. The wear of the cutting edge depends on the cutting conditions as well as on the mechanical properties of the processed material.

One of the methods used to estimate the state of saw teeth uses kerf measurements. The overall set of teeth of the bandsaw Prime ST 0.8/1.2 by Wintersteiger, which was used in the oak wood re-saving process, was measured using a micrometer and a digital calliper. The results of different measurements were compared to estimate the accuracy and precision of those methods. It was shown that micrometer measurements were much more precise than calliper measurements. It was also noted that the kerf varied between two tooth ranges.

Key words: *Bandsaw, Overall set (kerf), tool wear, digital calliper, micrometer*

INTRODUCTION

The saw's teeth become blunt during use. A lot of research has focused on the cutting edge wear problem. They showed that the wear of the cutting edge depends on the cutting conditions as well as on the mechanical properties of the processed material. For wood, there are more factors than for metals, e.g. defects (knots), annual rings, moisture content, etc. (Csanady and Magoss, 2020; Klamecki,1979).

The impact of saw blade override on cutting-edge radius and recession was demonstrated by Šustek and Siklienka (2012). A decrease in the override from 5 to 50 mm resulted in a decrease in edge recession and cutting edge radius.

The dependence of tool wear on surface quality was studied by Kminiak et al. (2015, 2016). The articles have not proven any direct relationship between tool wear and surface quality.

Orlowski et al. (2021) used a NIKON ECLIPSE Ti-S microscope equipped with a NIKON DS-Fi2 recording camera to take pictures of teeth, which were then analysed in a graphical software to measure the radii of the main cutting edges. Currently, to estimate the state of a bandsaw teeth most often micrometer are used in measurements.

Faculty of Mechanical Engineering and Ship Technology, and EkoTech Center - Gdańsk University of Technology, 11/12 Gabriela Narutowicza Street, 80-233 Gdańsk, Poland
email: stenkadawid@yahoo.com, kazimierz.orlowski@pg.edu.pl, daniel.chuchala@pg.edu.pl

An innovative way to determine the wear of a cutting tool was proposed by Brili et al. (2021). In the model, a cutting tool was monitored with an infrared (IR) camera immediately after the cut and for the following 60 s. Thanks to deep learning algorithms, this model allowed over 96% accuracy of assessment.

The goal of this papier was the comparison of measurements accuracy of bandsaw teeth with a digital calliper and a micrometer. The latter methods seem to be appropriate for industrial condition and simultaneously be much simpler to realize in industrial conditions in comparison to complicated instrumentation such as a microscope.

MATERIALS AND METHODS

The object of the measurements was Prime ST 0.8/1.2 by Wintersteiger (Innkreis, Austria). The examined saw was used in the re-sawing process of oak (*Quercus* L.) "wet" boards (average MC = 32,9% with standard deviation SD_{MC} = 2,1%) and was waiting for the regeneration process (re-griding). The saw blade's technical specifications were as follows: saw thickness s = 0.8 mm, overall set (kerf) S_t = 1.2 mm, tooth pitch P = 25 mm, number of teeth n = 220, rake angle γ_f = 20°, blade angle β_f = 60°, tooth type - stellite tipped.

Four measurement series of the overall set were made, two using a digital calliper (type Gedore No. 711, 0–150 mm, UK), and two with the use of a micrometer. Then, the results of those measurements were analysed and compared.

RESULTS AND DISCUSSION

The results of the measurements were analysed. The digital calliper measurement series were named C1 and C2, whereas the micrometer measurement series were named M1 and M2. Arithmetic means series of calliper and micrometer measurements were named C and M. The arithmetic mean and standard deviation of every series were determined and compared (Table 1). The values of the mean series (C and M) are shown in Figure 1.

Table 1. Differences between arithmetic mean and standard deviation of measurement series

Series Code	Standard Deviation	Arithmetic Mean	Percentage Standard Deviation
	[µm]	[mm]	[%]
M1	9.40	1.209	0.78
M2	9.51	1.209	0.79
M	9.45	1.209	0.78
C1	13.53	1.184	1.14
C2	10.11	1.195	0.85
C	13.13	1.189	1.10

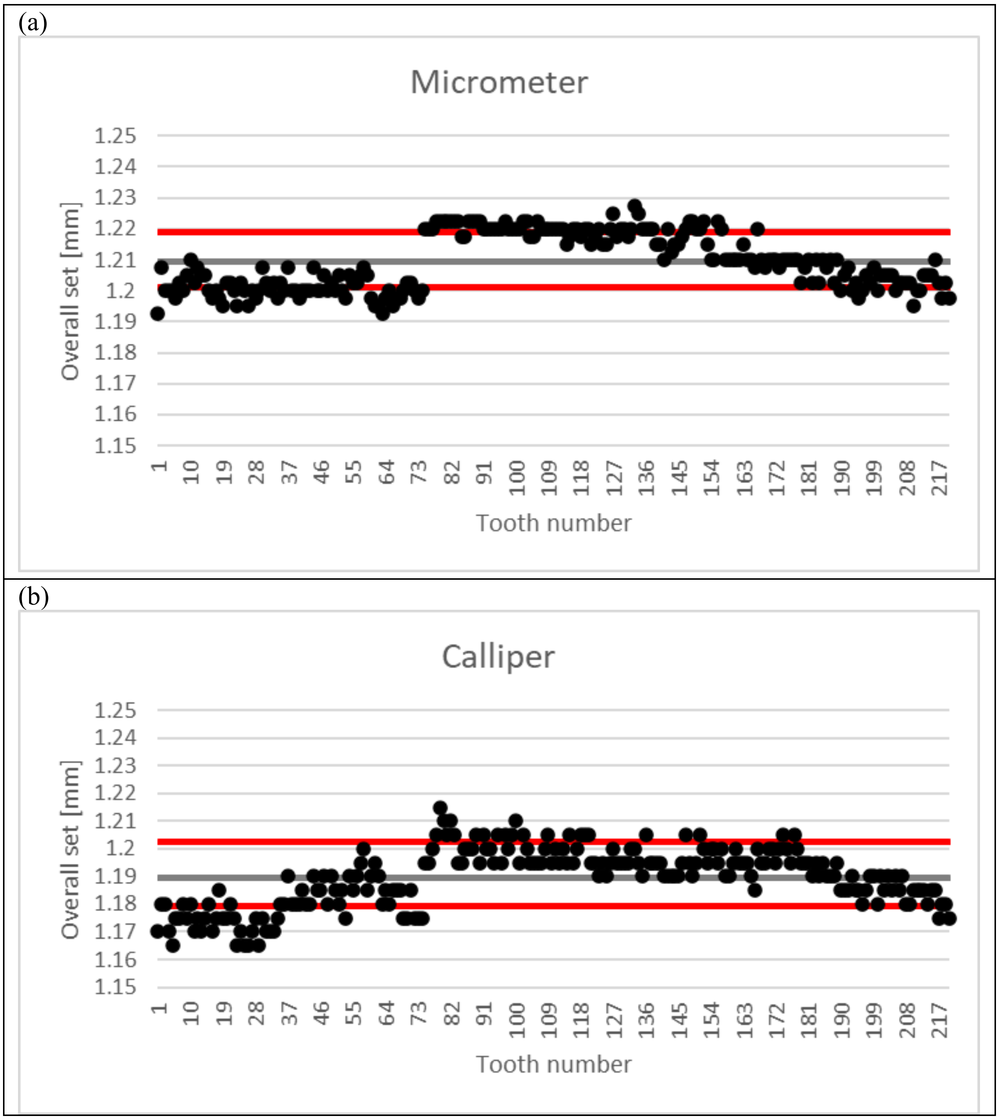

Figure 1. The overall set of bandsaw teeth, measured with: a micrometer (series M) (a); a digital calliper (series C) (b)

The measurement series were statistically compared. The differences between values from series M2-M1, C2-C1, C-M were shown in Figure 2. The standard deviation, arithmetic mean of differences between those series were calculated. Also, the differences between arithmetic means of those series were determined. Those values were shown in Table 2.

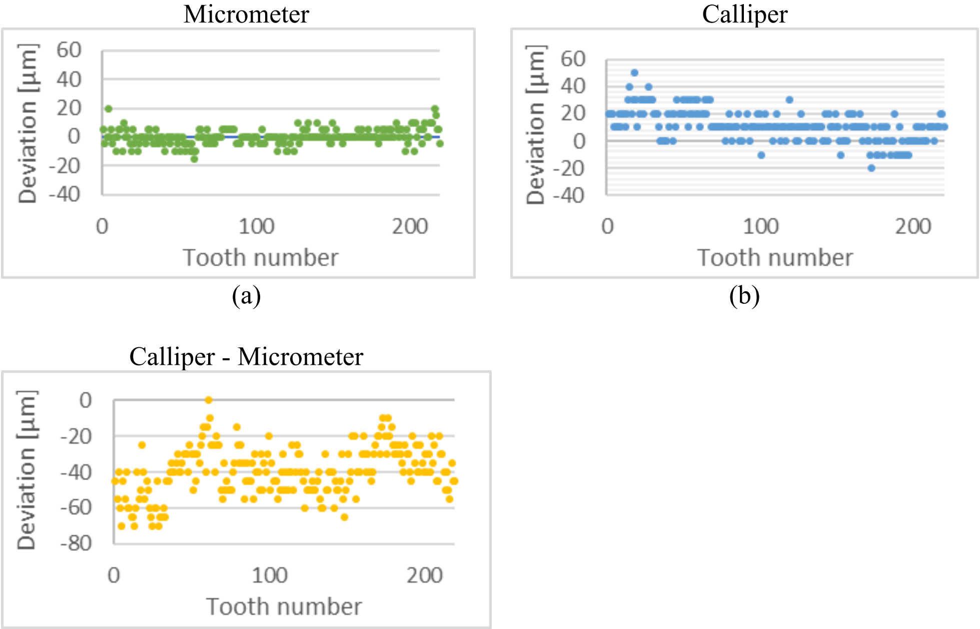

(a) (b)

(c)

Figure 2. Tooth kerf measurements deviation between: M2 and M1 series (a); C2 and C1 series (b); C and M series (c)

Table 2. Statistical parameters of differences between measurement series

Series Code	Standard Deviation	Mean Deviation	Difference of Arithmetic Means
	[µm]	[µm]	[µm]
M2 to M1	5.4	3.6	0.1
C to M	13.4	10.6	-39.6
C2 to C1	11.0	8.2	10.9

CONCLUSIONS

The comparison of saw overall set measurement methods has allowed for following conclusions:

- The arithmetic mean of micrometre measurements (M_M=1,209 mm) is higher than the arithmetical mean of calliper measurements (M_C=1,189 mm) and exceeds the assumed value. This size is even greater than the standard kerf of the new bandsaw, which leads to the conclusion that probably the micrometer could not be correctly calibrated.
- The percentage standard deviation of micrometre measurements ($SD_{M\%}$ = 0,78%) are smaller than the percentage standard deviation of calliper measurements ($SD_{C\%}$ = 1,10%). Also the standard deviation between M2 and M1 series ($SD_{M2\text{-}M1}$ = 5,4 µm)

is lower than between C2 and C1 ($SD_{C2\text{-}C1}$ =11 μm). That means, the micrometer measurements are more precise.

- Both type of measurements have shown the difference of tool wear between two teeth intervals.

REFERENCES

1. Orlowski, K.A.; Chuchala, D.; Przybylinski, T.; Legutko, S. Recovering Evaluation of Narrow-Kerf Teeth of Mini Sash Gang Saws. Materials 2021, 14, 7459.
2. Brili, N.; Ficko, M.; Klančnik, S. Tool Condition Monitoring of the Cutting Capability of a Turning Tool Based on Thermography. Sensors 2021, 21, 6687.
3. Csanady, E.; Magoss, E. Mechanics of Wood Machining, 3rd ed.; Springer: Cham, Switzerland, 2020.
4. Klamecki, B.E. A review of wood cutting tool wear literature. Holz Roh Werkst. 1979, 37, 265–276.
5. Kminiak, R., Gašparík, M., Kvietková, M., The dependence of surface quality on tool wear of circular saw blades during transversal sawing of beech wood. BioResources, 2015, 10: 7123–7135. https://doi.org/10.15376/biores.10.4.7123-7135
6. Kminiak, R., Siklienka, M., Šustek, J., Impact of tool wear on the quality of the surface in routing of mdf boards by milling machines with reversible blades. 2016. https://doi.org/10.17423/afx.2016.58.2.10
7. Šustek, J., Siklienka, M., Effect of saw blade overlap setting on the cutting wedge wear. Acta Facultatis Xylologiae Zvolen. 2012, 54(1): 73−79.

ACKNOWLEDGMENTS

Financial support of these studies from Gdańsk University of Technology by the DEC – 4/2022/IDUB/III.4.1/Tc grant under the Technetium Talent Management Grants - ‘Excellence Initiative - Research University’ program is gratefully acknowledged.

Authors would like to acknowledge the sawmill Łączy–Kołczygłowy spółka z o.o. (Poland) for their support of the experiment.

CHIP AND CHIPLESS WOODWORKING PROCESSES, 13(1): 101–108, 2022
Zvolen, Technical University in Zvolen, ISSN 1339-8350 (online), ISSN 2453-904X (print)

MILLING OF PLYWOOD WITH A SHAPER ORIGIN HANDHELD CNC ROUTER

Pavlin Vitchev – Zhivko Gochev – Engindzhan Halim

Abstract

SHAPER ORIGIN combines computer-guided accuracy with hand-held feed. This article presents the sequence of work, the software of the CNC router SHAPER ORIGIN, and the used router bits. Experimental studies have been carried out on the milling processes of plywood and MDF, taking into account the spindle speed, the depth of cut and the quality of the resulting surfaces. Practical recommendations have been made for efficient operation of the SHAPER ORIGIN handheld CNC router.

Key words*:* *CNC router, SHAPER ORIGIN, router bits, spindle speed, wood, wood-based materials, surfaces quality.*

INTRODUCTION

With the advancement of technological development, in human life and in industry alike, machines with Computer Numerical Control (CNC) become an indispensable part of any modern furniture production. Due to their technological and functional features they are used in numerous technological operations in the production of almost all types of furniture and wood products (Angelski, 2014; Gochev, 2018).

The CNC machine is a complex hardware and software system based on the use of digital electronic devices in the control system. In fact, CNC can be considered as a computerized complex that controls the working modules of the machine and precisely executes the programmed task. All movements of the executive parts of the machine are set by a special control digital program (NC program).

As a result of the increasing variety and application of CNC machines in the furniture industry, there are many scientific and applied studies in the literature that investigate and present the technological capabilities, software provision, operating modes, cutting tools and quality of the processed surfaces when working with this type of machines (Karagos et al., 2011, Pinkowski et al., 2013; Kminiak & Šustek, 2016; Palubicki & Rogozinski, 2016; Kminiak & Banski, 2017; Kminiak et al., 2017; Nemec et al., 2017).

The CNC technology is also used in manual routers. This type of machine is often used in smaller productions, in finishing and assembly work or for making templates and prototypes.

An example of one of the first manual CNC routers is the CNC Shaper Origin model.

Although the machine has been available, mostly in the American market for more than five years, it still counts as innovative technology.

Department of Woodworking Machines, University of Forestry, 10 Kl. Ohridski Blvd., 1797 Sofia
e-mail: p_vitchev@ltu.bg; zhivkog@ltu.bg; arsenal7@abv.bg

The objective of the current work is to investigate the main functional and technological capabilities of a hand-guided CNC milling machine, model Shaper Origin during processing of plywood and MDF parts.

TECHNOLOGICAL AND SOFTWARE CAPABILITIES OF CNC SHAPER ORIGIN

One of the main advantages of the CNC Shaper Origin in terms of construction is that the parts processed by it can be placed on any horizontal flat surface, i.e. there are no requirements for a specific work table. The general appearance of the machine is presented in Figure 1. Its relatively small overall dimensions (197 x 299 x 350 mm) and weight (6.6 kg) allow to be easily transported and carried.

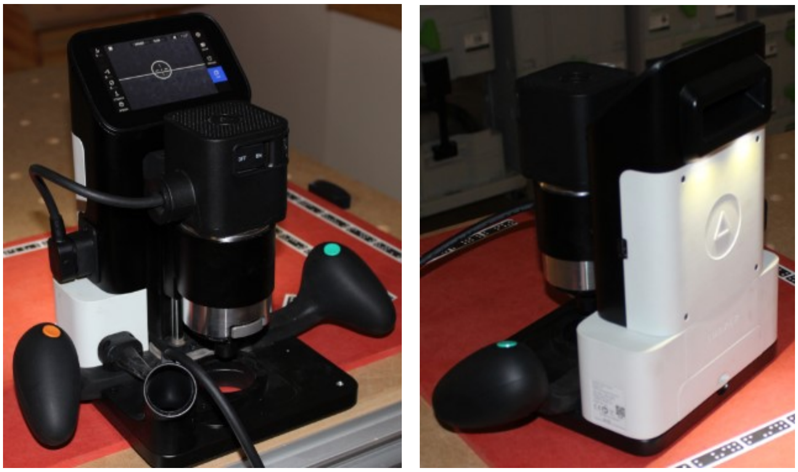

Figure 1. CNC Shaper Origin – general view

The machine tracks its position in the workpiece thanks to a pre-glued marker tape (Shaper Tape), developed and offered by the manufacturer (Fig. 1). A random unique code is printed on the tape, which is read by the forward-facing camera (9) (Fig. 2) located on the front panel of the machine. The scanned information is fed into the machine's software.

The main elements of the machine are presented in Fig. 2. By using the touch display (1), the control program is entered, and the trajectory and the cutting process are monitored. The spindle (2) can be removed from the holder (4) for easier and faster changing of the cutting tool. The machine is guided by the operator by means of the two handles (5), each of which has a multifunctional button with functions depending on the specific menu in which the machine's software is located. The machine has three software-controlled axes – *X*, *Y* and *Z*. After each change of the cutting tool, the machine has to be calibrated along the *Z*-axis using the "*z*-touch" function. The movement (l) along *Z*-axis is set in the machine software and during the machining, the spindle moves at a distance (h), $h = z\text{-touch} + l$.

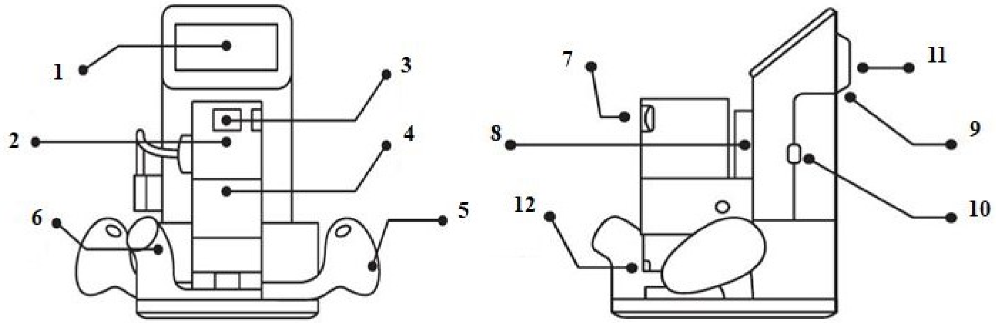
1
2
3
4
5
6
7
8
9
10
11
12

Figure 2. Basic elements of CNC Shaper Origin:
1 – multitouch LCD display; 2 – spindle; 3 – on/off button of spindle; 4 – spindle holder; 5 – multi-functional handles; 6 – aspiration; 7 – speed control; 8 – movement along z; 9 – scanning camera; 10 – USB port; 11 – back handle; 12 – collet retainer.

During machining, the cutting geometry that must be followed by the operator, the axis of rotation of the cutting tool and the self-correcting area of the spindle along the X and Y axes are visualized on the machine's display (Fig. 3). In case the operator deviates from the cutting geometry more than the self-adjusting zone (i.e. a radius of 10 mm plus the radius of the cutting tool), the machine spindle retracts automatically.

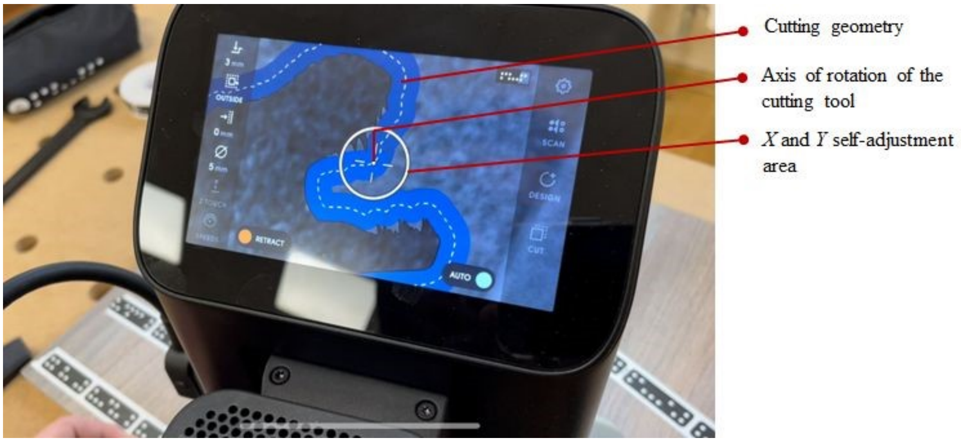
3 mm
OUTSIDE
0 mm
5 mm
Z TOUCH
SPEED
RETRACT
AUTO
SCAN
DESIGN
CUT
Cutting geometry
Axis of rotation of the cutting tool
X and Y self-adjustment area

Figure 3. Software interface in cutting process (CNC Shaper Origin)

The programming process passes sequentially through the three main menus: *Scan; Design; Cut*, located in the right-hand side of the LCD multitouch display (fig. 3). After applying a Shaper Tape to the worksurface, the operator scans the surface by moving the machine facing the taped field to capture the markers. The scanned quality is visualized in the upper right corner of the screen by the corresponding graphic image (Fig. 4).

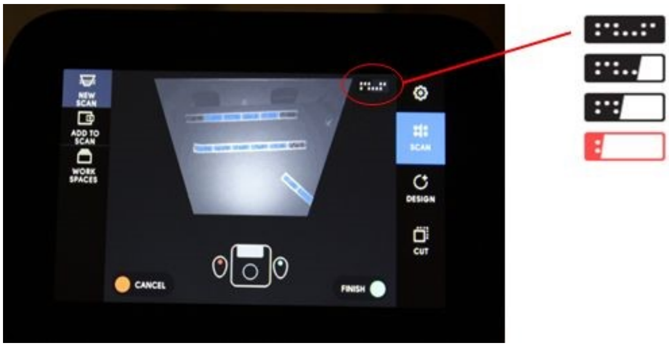

Figure 4. Software interface in scanning process (CNC Shaper Origin)

The machine's software can store a number of scanned surfaces whose names can be entered by the operator. In the work process, a different scanned surface can be selected, if necessary. In the "*Design*" menu, the operator enters the cutting geometry. It can also be created in the machine software if not too complex (Fig. 5). However, if the cutting geometry is more complex, it can be created using external software, such as Adobe Illustrator, Corel Draw etc. and then the file, that has to be saved in a svg (Scalable Vector Graphics) format, can be imported back in the CNC software by the portable USB drive.

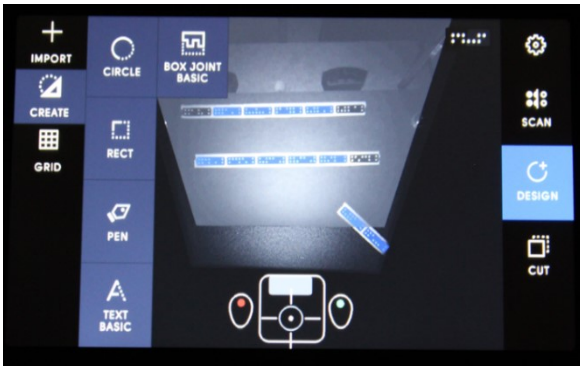

Figure 5. Software interface in design process (CNC Shaper Origin)

The software positioning of the cutting geometry on the machined surface can be done arbitrarily by positioning the image visually on the machine screen and activating the "*Place*" button. In this case, the machine itself plays the role of a computer mouse. For more precise positioning, it is necessary to create a grid on the scanned worksurface with a zero point – one of the corners of the processed surface. In this case, the exact positioning of the geometry along the X and Y axes is set in the machine software.

In the third main menu "*Cut*", the information about the specific technological operation - cutting or engraving – is entered, setting the processing depth along the Z axis (Fig. 6). The tool correction is selected according to the entered machining geometry – external (1), internal (2) and central (3). It is possible to cut the entered geometry as a pocket (4).

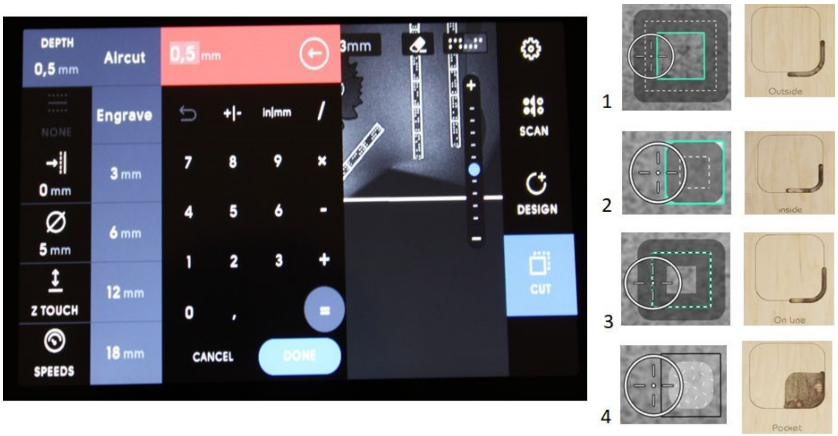

Figure 6. Software interface of menu of cutting (CNC Shaper Origin)
1 – external correction; 2 – internal correction; 3 – central correction;
4 – cutting of “pocket“.

In the "*Cut*" menu, the information about the cutting tool is entered, the machine is calibrated along the *Z* axis.

After entering all the necessary parameters in the control program, the actual cutting process along the corresponding lines is started. The machine spindle is activated by a switch (3) located on its front panel (Fig. 2). The operator positions the CNC milling machine on the contour to be milled. It "lights up" on the machine screen. To start the cutting process, the button on the right handle of the machine is activated. The spindle moves down the "*z*- touch" distance + the set milling depth.

The geometry to be machined, the direction in which the operator must move the machine, the axis of rotation of the spindle (the center of the milling tool) and the self-adjustment zone of the tool along the *X* and *Y* axes are visualized on the CNC display (Fig. 3). Pressing the green button again, activates the automatic cutting mode, in which the spindle will automatically move along the *X* and *Y* axes within the self-adjustment zone. This feature is very useful when contours with small radii are being machined and it excludes the potential for human mistakes.

EXPERIMENTAL STUDY ON THE OPERATION OF THE CNC SHAPER ORIGIN

The current study investigates the functional capabilities of CNC Shaper Origin machine during milling of surfaces with a complex two-dimensional geometry (along the *X* and *Y* axes) (Fig. 7a). The machine does not allow for changes along the *Z* axis during the cutting process. Two cabinet doors (fig. 7-a) made out by plywood, 18 mm thick, from birch (*Betula pendula*) (fig. 7-b) were manufactured. The decorative dinosaur figures are made of 12 mm thick volume colored MDF (Valchromat, Portugal) (fig. 7-c). For the manufacturing of the doors, eight programs were created to control the CNC machining: 4 programs for cutting each decorative figure from MDF and 4 programs for milling the doors in order to insert the decorative figures into them. The characteristics of the control program are summarized in Table 1. Adobe Illustrator was used to design the dinosaurs’ figures with different shape and dimension. Then the *svg* file was imported back to the CNC software.

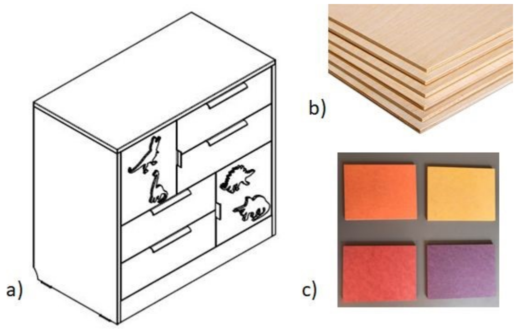

Figure 7. Product and materials used: a) – the two cabinet doors are made; b) – plywood for the base of the doors; c) – volume colored MDF – for the decorative figures.

In the current study, the location of the figures on the workplace of the pre-scanned surface were positioned visually using the "*Place*" function.
As a result of the conducted experiments, the optimal parameters of the cutting mode when milling the plywood and MDF parts were established and are presented in Table 1. Table 2 gives the characteristics of the used cutting tools.

Table 1. Data entered in "*Cut*" menu

Characteristics of the control program	**Parameter values**	
	Milling of MDF	**Milling of playwood**
Milling depth	4, 8, 12 mm	2, 4, 6 mm
Type of milling	Outside	Pocket
Tool shift	Without	Without
Z-axis calibration (*z*-touch)	Yes	Yes
Plunge speed of the tool	400 mm·min^{-1}	400 mm·min^{-1}
Rotational speed	16 400 min^{-1}	16 400 min^{-1}

Table 2. Characteristics of the cutting tool

Parameters	**Milling of MDF**	**Milling of chipboard**
Outer diameter *D*	5 mm	3 mm
Tail diameter *d*	8 mm	8 mm
Total lenght *L*	50 mm	45 mm
Working length *I*	12 mm	10 mm
Number of cutting edges *z*	2	2
Maximum rotation frequency *n*	24 000 min^{-1}	27 000 min^{-1}

Figure 8 presents part of the stages of generating the control program and the generated figures.

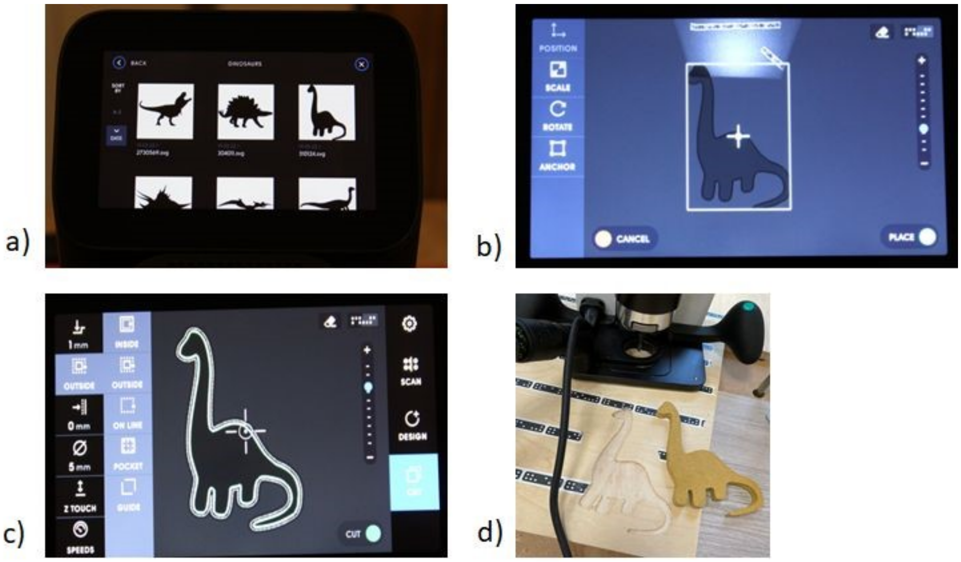

Figure 8. Process of creating the program and processing the materials a) – import the files; b) – positioning the geometry on the working surface; c) – settings in the “Cut” menu; d) – milled figure from plywood and MDF.

CONCLUSIONS AND RECOMMENDATIONS

Based on the results from this preliminary experimental study, performed with the Shaper Origin CNC milling machine, the following observations and recommendations can be made:

- a stable fixation of the machined workpiece to the worktable, to exclude or minimize any displacement, is strongly recommended;
- when placing the marker tape (Shaper Tape), no tape overlap or folded section of the tape should be allowed, as this leads to an error in the process of scanning the workspace;
- the possibility to use different software products (e.g. Adobe Illustrator) to design more complex geometry for milling or engraving, gives the operator relative freedom to choose the software of his preference; what should be remembered is that the file has to be saved in *svg* format in order to be imported back to the SNC software;
- despite the well-developed and intuitive software of the machine, it is necessary for the operator to have good knowledge about the technological processing of wood and wood-based materials, the cutting modes and the cutting tools used;
- the lack of possibility to change the position of the cutting tool along the *Z* axis during the cutting process, can be pointed out as one of the technological deficiencies of the machine;
- when processing parts with a greater thickness, the milling is recommended to be carried out in several passes. The milling depth should not be greater than 2 mm for a cutting tool with a diameter of 3 mm and grater than 3 mm for a cutting tool with a diameter of 5 mm.

- our experiment confirmed the high processing precision of the machine, even for counters with small cutting radius. The roughness of the treated surfaces of plywood and MDF parts is of the required quality.

The specific change in the quality of the machined surfaces, as a function of the cutting mode and the cutting tool, is not an object of this paper. These results are discussed in another paper by the authors.

REFERENCE

Gochev Zh., 2005. Manual of cutting wood and wood cutting tools, Publishing House of University of Forestry, ISBN 954-332-007-1, Sofia, pp. 29-39 (in Bulgarian).
Gochev, Zh., 2018. Wood cutting and cutting tools. Avangard Prima, ISBN 978-619-239-047-1, Sofia, pp. 43-50 (in Bulgarian).
Karagoz, U., Akyildiz, MH., Isleyen, O., 2011. Milling of wood materials with computerized numerically controlled (CNC) router. Proceedings of the 4th International science conference woodworking techniques, September 07-10, 2011, Czech Republic, pp. 132-138.
Kavalov, A., Angelski D., 2014. Technology of furniture. Publishing house of University of Forestry, Sofia, 390 pp. ISBN 978-954-332-115-5 (in Bulgarian).
Kminiak, R., Šustek, J., 2016. The suitability of repeated machining in nesting milling on CNC machining centers. Chip and chipless woodworking processes, Technical University in Zvolen, pp. 101-114.
Kminiak, R., Banski, A., 2017. Variability of surface quality of MDF boards at nesting milling on CNC machining centers. Acta facultatis xylologiae Zvolen, 59(1): 121-130, DOI10.17423/afx.2017.59.1.12.
Kminiak, R., Banski, A., Chakhov, DK., 2017. Influence of the thickness of removed layer on the quality of created surface during milling the MDF on CNC machining centers. Acta facultatis xylologiae Zvolen, 59(2): 137-146, DOI10.17423/afx.2017.59.2.13.
Nemec, M., Kminiak, R., Danihelova, A., Gergel', T., Ondrejka, V., 2017. Vibrations and workpiece surface quality at changing fed sped of CNC machine. Akustika,Volume 28: 117-123.
Palubicki, B., Rogozinski, T., 2016. Efficiency of chips removal during CNC machining of particleboard. Wood research 61(5): 811-818.
Pinkowski, G., Szymanski, W., Krauss, A., 2013. Mallung quality of sweet cherry (Prunus avium L.) wood on a CNC woodworking machine. In: Annals of Warsaw University of Life Sciense, No. 84: 36-41.

Acknowledgements: This paper is supported by the Scientific Research Sector at the University of Forestry – Sofia, Bulgaria, under contract № НИС-Б-1046/05.04.2021.

TO NAJLEPŠIE Z DREVA

reddot winner

PYTHAGORAS

INDEWO®

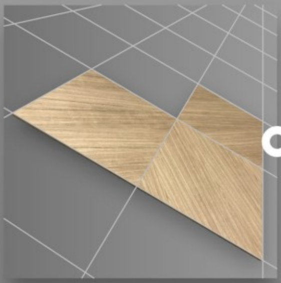

WOOD'N TILES

INOIS®MICRO

SPICA

europlac.sk

europlac
...das beste aus holz

SECTION

THERMAL TREATMENT OF WOOD

CHIP AND CHIPLESS WOODWORKING PROCESSES, 13(1): 113–121, 2022
Zvolen, Technical University in Zvolen, ISSN 1339-8350 (online), ISSN 2453-904X (print)

THICKNESS SWELLING AND WATER ABSORPTION OF PLA-BASED COMPOSITES FILLED WITH BARK

Piotr Borysiuk – Radosław Auriga

Abstract

As part of this study, the effect of the addition of bark to the PLA matrix on the thickness swelling and water absorption of WPC composites was determined. For comparison, analogous WPC composites were made based on a polyethylene (HDPE) matrix. Three levels of the composite filling and optional addition of additives (CaO in the case of composites based on PLA and MAHPE in the case of composites based on HDPE) were investigated. The composites were produced in two stages by means of extrusion and flat pressing. For the produced composites, the density, the density profile as well as the swelling and water absorption after 2 and 24 hours of soaking in water were examined. The investigation has shown that PLA-based composite boards are generally characterized by higher swelling and water absorption values, especially after 24 h of soaking in water compared to analogous HDPE-based composite boards. Moreover, the matrix / filler has the greatest influence on the resistance of composites to moisture. The addition of CaO in the case of PLA-based composites, and MAHPE in the case of HDPE-based composites reduced water absorption.

Key words: *PLA composites, bark, swelling, water absorption*

INTRODUCTION

The genesis of the creation of wood-polymer composites, commonly known as WPC (wood plastic composites), is related to the development of thermoplastics and the use of natural fibrous materials as fillers for their production (Wolcott and Englund 1999, Clemons 2002). Currently, traditional WPC composites are produced, depending on their application, on the basis of such polymers as polyethylene PE (decking & construction, consumer goods), polypropene PP (automotive, construction, consumer goods) or polyvinyl chloride PVC (decking & construction) (Partanen and Carus 2019). It is worth noting that a significant advantage of wood-polymer composites over other wood and wood-based materials is their resistance to water (Falk *et al.* 1999, Sellers *et al.* 2000). Additive synthetic polymers are generally characterized by a low (less than 1%) water absorption (Saechtling 2000) and in WPC composites they constitute a natural hydrophobic agent. It blocks the access of moisture to the wood particles included in the composite in a mechanical way. The hydrophobic properties generally deteriorate with an increase in the proportion of wood particles in the composite (Zajchowski *et al.* 2005) and an increase in the porosity of its structure (e.g. as a result of foaming). Increasing the share of wood

Institute of Wood Sciences and Furniture, Warsaw University of Life Sciences – SGGW, ul. Nowoursynowska 159, 02-776 Warsaw, Poland

particles results in their greater availability on the surface of the composite, and therefore their greater exposure to water.

Currently, in the production of WPC composites, biodegradable thermoplastics can also be used, among which poly (lactic acid) PLA is the most popular (Borysiuk *et al.* 2021, Borysiuk *et al.* 2022). It can be easily disposed of by composting without negative environmental effects (Markarian 2008). PLA is by far the most widely researched and used biodegradable aliphatic polyester in the history of mankind. Due to its advantages, PLA is a leading biomaterial for many applications in medicine, as well as in the industry replacing conventional petrochemical polymers (Farah *et al.* 2016). Among the WPC fillers the foremost is wood in the form of flour or wood fibers, - the size of these particles depends on the purpose of the composites (Kuciel *et al.* 2010). Also bark particles can be used as a filler for WPC composites (Harper and Eberhardt 2010; Yemele *et al.* 2010, Safdari *et al.* 2011, Gozdecki *et al.* 2009, Gozdecki *et al.* 2010, Borysiuk *et al.* 2021, Borysiuk *et al.* 2022). In general, researchers pointed a decrease in the mechanical properties of WPC composites when using bark as a filler. On the other hand, with regard to the physical properties, Gozdecki *et al.* (2009) reported the beneficial effect of the substitution of wood flour with bark particles on the reduction of swelling and water absorption of the tested polypropylene-based composites. Andrzejewski *et al.* (2019) showed a beneficial effect of cork filler (up to 30%) on the dimensional stability of PLA composites under the influence of moisture. On the other hand, the use of wood flour or bark as a filler deteriorates the resistance of PLA composites to the effects of moisture (Kamau-Devers *et al.* 2019, Borysiuk *et al.* 2021).

As part of this study, the effect of the addition of a filler (bark or sawdust) to the PLA matrix on the swelling and water absorption of the obtained composites was determined. For comparison, similar composites were made based on a matrix of high-density polyethylene (HDPE).

MATERIAL AND METHODS

As part of the research, 12 variants of WPC composites were produced (Table 1) based on two types of polymer matrices: polylactic acid - PLA (Ingeo ™ Biopolymer 2003D, NatureWorks LLC, Minnetonka, MN, USA) and high density polyethylene - HDPE (Hostalen GD 7255, Basell Orlen Polyolefins Sp.z o.o., Płock, Poland). The bark of coniferous trees was used as filler (P.P.H.U. TARTAK IMPORT-EXPORT Jerzy Abramczyk, Wólka-Folwark, Poland). In the production of composites an additional substance was also used, such as: calcium oxide CaO (Avantor Performance Materials Poland S.A., Gliwice, Poland) in the case of composites based on PLA and polyethylene-graft-maleic anhydride MAHPE (SCONA TSPE 2102 GAHD, BYK-Chemie GmbH, Wesel, Germany) in HDPE composites.

The bark was dried to 5% moisture and then mechanically ground and sorted into particles passing through a 0.49 mm sieve (above 35 mesh).

The composites were produced in two stages.

First stage. WPC granules were produced with an appropriate formulation (Table 1) - using the Leistritz Extrusionstechnik GmbH, Nürnberg, Germany extruder (temperatures in individual sections of the extruder were 170ºC - 180ºC), a continuous composite band was obtained, which was then shredded on a DS-2/OBR shredder (OB-RPPD in Czarna Woda, Poland);

Second stage. The obtained granulate was used to produce boards with nominal dimensions 300x300x2.5 mm^3 by flat pressing in a mold, using a one-shelf press (AB AK Eriksson, Mariannelund, Sweden) at a temperature of 200°C and a maximum unit pressing pressure of Pmax = 1.25 MPa (the pressure during pressing, along with the plasticization of the material, was gradually increased from 0 to Pmax). The pressing time was 6 minutes. After hot pressing, the boards were cooled in the mold for 6 minutes in the cold press.

Table 1. Characteristics of the composition of individual variants of composites.

Variant	Matrix	Share of the matrix	Additvies	Share of the filler
1P	PLA	60		40
2P	PLA	50		50
3P	PLA	40		60
4P	PLA	57	3	40
5P	PLA	47	3	50
6P	PLA	37	3	60
1H	HDPE	60		40 b
2H	HDPE	50		50 b
3H	HDPE	40		60 b
4H	HDPE	57	3	40 b
5H	HDPE	47	3	50 b
6H	HDPE	37	3	60 b

After production, the composites were conditioned for 7 days under laboratory conditions (20 ± 2°C, 65 ± 5% humidity).

The following physical properties of the boards were tested:

- density according to EN 323:1999 and density profile using Laboratory Density Analyzer DAX GreCon (Fagus-Grecon Greten GmbH & Co. KG, Alfeld, Germany). Density measurement was made every 0.02 mm at the measurement speed of 0.05 mm/s;
- thickness swelling (TS) and water absorption (WA) after 2h and 24h immersion in water - according to EN 317:1999

Determinations of the tested properties were made for each variant of the composites in at least 10 repetitions. Statistical analysis of the results was carried out in Statistica version 13 (TIBCO Software Inc., CA, USA). Analysis of variance (ANOVA) were used to test ($\alpha = 0.05$) for significant differences between factors. A comparison of the means was performed by Tukey test, with $\alpha = 0.05$.

RESULTS AND DISCUSSION

The tested boards were characterized by densities in the range of 1114 - 1232 kg/m^3 for the PLA matrix and 1040 - 1105 kg/m^3 for the HDPE matrix. The values of average densities for individual variants of composites boards are presented in Table 2. Density differentiation for individual variants within the same matrix (PLA or HDPE) did not exceed 10%. The effect of the addition of additional substances was not reported in this respect. It should be noted, that the composites made on the basis of PLA with the same proportion of filler and additive were characterized by 1 to 15% higher density, depending on the variant.

Table 2. Board density values for individual board variants.

Matrix	Share of the filler [%]	Additvies P [kg/m³]	Additvies σ [kg/m³]	Without additvies ρ [kg/m³]	Without additvies σ [kg/m³]
PLA	40	1180	34	1171	41
PLA	50	1232	62	1114	46
PLA	60	1123	54	1123	51
HDPE	40	1040	39	1053	26
HDPE	50	1043	27	1105	27
HDPE	60	1093	25	1077	38

ρ – mean, σ – standard deviation

This is due to the higher density of the PLA matrix compared to the HDPE matrix. Similar correlations were obtained by Andrzejewski *et al.* (2019) investigating WPC composites based on PLA and PP. All variants of the tested boards were characterized by a generally uniform density distribution on the cross-section (Figs. 1, 2). Density variation in the thickness of individual boards did not exceed 60 kg/m^3 in the case of PLA-based boards and 178 kg/m^3 in the case of HDPE-based boards. This proves a good homogenization of composite components and an even distribution of the filler particles in the polymer matrix. Borysiuk *et al.* (2019) found that in the case of HDPE boards filled with sawdust, an increase in the filler content reduces the density in the core zone of the board. A similar correlations was not observed in this study in the case of the use of bark particles as a filler.

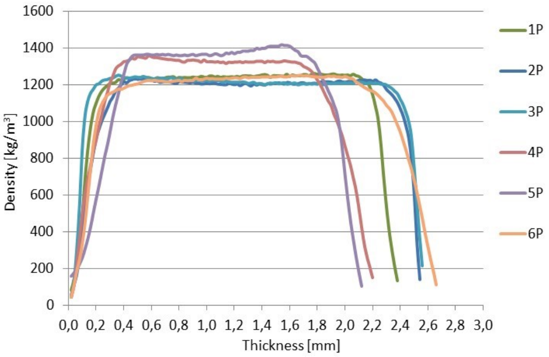

Figure 1. Density profile of PLA based composites board

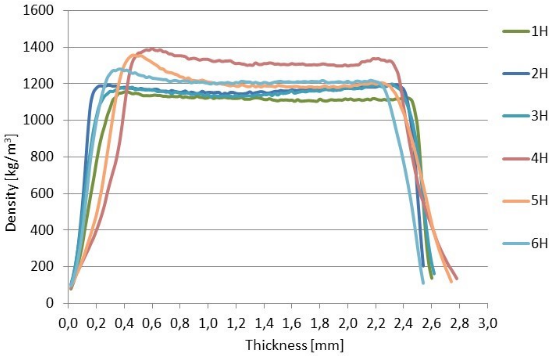

Figure 2. Density profile of HDPE based composites board

Table 3. The results of the composites boards thickness swelling test

Matrix	Variant	Share of the matrix	Additives	Thickness swelling after 2 h [%]		Thickness swelling after 24 h [%]	
				ρ	σ	ρ	σ
PLA	1P	60	-	$0.82^{d,e}$	0.14	$2.98^{A,B}$	0.57
	2P	50	-	$1.62^{a,b}$	0.31	4.20^{E}	0.82
	3P	40	-	$1.44^{a,b}$	0.26	5.18^{F}	0.78
	4P	57	3	1.70^{a}	0.23	$3.23^{A,B}$	0.50
	5P	47	3	0.54^{d}	0.16	1.63^{C}	0.24
	6P	37	3	2.19^{f}	0.36	6.62^{G}	1.20
HDPE	1H	60	-	$1.04^{c,e}$	0.20	$1.72^{C,D}$	0.28
	2H	50	-	$1.42^{a,b,c}$	0.23	$2.47^{A,C,D}$	0.32
	3H	40	-	$1.49^{a,b}$	0.25	$2.74^{A,B}$	0.44
	4H	57	3	2.12^{f}	0.37	$3.37^{A,B,E}$	0.53
	5H	47	3	$1.23^{b,c}$	0.22	$2.55^{A,D}$	0.37
	6H	37	3	1.64^{a}	0.29	$3.65^{B,E}$	0.55

a,b,c,d,e,f A,B,C,D,E,F,G – homogeneous groups by Tukey test (α = 0.05)

Table 4. The results of the composites boards water absorbtion test

Matrix	Variant	Share of the matrix	Additives	Water absorption after 2 h [%]		Water absorption after 24 h [%]	
				ρ	σ	ρ	σ
PLA	1P	60	-	$0.52^{a,b}$	0.08	2.75^{B}	0.33
	2P	50	-	1.08^{c}	0.20	4.23^{C}	0.65
	3P	40	-	3.70^{e}	0.67	11.15^{E}	1.45
	4P	57	3	0.34^{a}	0.05	1.09^{A}	0.07
	5P	47	3	0.40^{a}	0.07	1.39^{A}	0.21
	6P	37	3	2.17^{d}	0.36	5.27^{D}	0.65
HDPE	1H	60	-	$0.64^{a,b}$	0.15	1.05^{A}	0.15
	2H	50	-	$0.83^{b,c}$	0.13	2.43^{B}	0.34
	3H	40	-	$0.82^{b,c}$	0.15	2.88^{B}	0.39
	4H	57	3	0.39^{a}	0.08	0.81^{A}	0.11
	5H	47	3	$0.59^{a,b}$	0.12	0.94^{A}	0.12
	6H	37	3	0.45^{a}	0.09	0.70^{A}	0.10

a,b,c,d,e,f A,B,C,D,E,F,G – homogeneous groups by Tukey test (α = 0.05)

The results of the thickness swelling and water absorption test are presented in Tables 3 and 4. Regardless of the share of the matrix and the additive (CaO in the case of PLA-based composites, MAHPE in the case of HDPE-based composites), PLA-based panels are generally characterized by higher values of thickness swelling and water absorption, especially after soaking in water for 24 hours. Similarly, the increase in the content of filler particles (decrease in the share of the thermoplastic matrix) in most variants influenced on the increase in the thickness swelling and water absorption values of the composites (Table 3 and 4). It is worth noting that greater changes were recorded in the case of PLA-based boards. This is evidenced by various homogeneous groups presented in tables 3 and 4 relating to composites with similar formulation. Similar dependencies were obtained by Borysiuk *et al.* (2021), investigating PLA composites filled with bark of varying degrees of fragmentation. The increase in the content of lignocellulosic filler in the composite results in its greater "availability" for moisture, which translates into an increase in the swelling and absorbability of composites (Klysov 2007). Among the analyzed factors (Tables 5 and 6), the type of matrix and its share as well as the interaction between these factors were characterized by a statistically significant main percentage effect on the studied values of swelling and buoyancy after 24 hours of soaking in water (respectively X = 61.6% and 70.9%). The influence on the values of swelling and soreness of the factors not included in the study was much smaller, Error = 15.1% and 3.1%, respectively (Table 5 and 6).

Table 5. Analysis of variance for selected factors and interactions between factors influencing the thickness swelling of the manufactured composite boards

Factors	Thickness swelling after 2h		Thickness swelling after 24h	
	p	X	p	X
Matrix (M)	0.0314	1.0	0.0000	17.0
Share of matrix (SM)	0.0000	14.5	0.0000	32.1
Additives (Add)	0.0000	6.4	0.0097	1.0
M x SM	0.0000	5.9	0.0000	12.5
M x Add	0.0863	0.6	0.0000	3.9
SM x Add	0.0000	40.9	0.0000	13.5
M x SM x Add	0.0000	8.4	0.0000	4.9
Error		22.4		15.1

p – probability of error, X – percentage of contribution

Table 6. Analysis of variance for selected factors and interactions between factors influencing the water absorption of the manufactured composite boards

Factors	Water absorption after 2h		Water absorption after 24h	
	p	X	p	X
Matrix (M)	0.0000	14.7	0.0000	24.1
Share of matrix (SM)	0.0000	34.2	0.0000	27.8
Additives (Add)	0.0000	7.7	0.0000	16.9
M x SM	0.0000	31.8	0.0000	19.0
M x Add	0.0000	1.7	0.0000	3.5
SM x Add	0.0000	2.5	0.0000	4.8
M x SM x Add	0.0000	1.7	0.0000	0.9
Error		5.7		3.1

p – probability of error, X – percentage of contribution

Considering the addition of additional substances: CaO in the case of composites based on PLA and MAHPE in the case of composites based on HDPE, it should be noted that their appliaction generally increased the swelling of the composites boards with a simultaneous decrease in their absorbability. It is worth noting that with regard to the swelling value (especially for HDPE-based composites), the observed changes were often statistically insignificant (the same homogeneous groups - table). It should also be added that while in the case of swelling after 24h, the percentage effect of adding the additive was only X = 1% (Table 5), in the case of water absorption after 24h, the percentage effect of introducing the additive was much greater and amounted to X = 16.9% (table 6). With regard to composites based on PE or PP, it is generally indicated that the addition of a compatibilizer has a positive effect on reducing moisture penetration (Klysov 2007, Yeh *et* *al.* 2021). With regard to PLA-based composites, the addition of CaO, which is actually a moisture absorbing and biocidal agent (Commission 2014), resulted in a reduction in the absorbability of the composites.

CONCLUSION

1. Composite boards made on the basis of PLA are generally characterized by higher swelling and water absorption values, especially after 24 hours of soaking in water compared to analogous HDPE-based composite panels.
2. Regardless of the matrix type (PLA or HDPE), the matrix / filler has the greatest impact on the resistance of composites to moisture.
3. An increase in the content of bark particles from 40 to 60% (regardless of the type of matrix: PLA or HDPE) generally increases the swelling and absorbability of composites.
4. The addition of CaO in the case of PLA-based composites reduces water absorption.
5. The addition of MAHPE in the case of HDPE based composites reduces water absorption.
6. Regardless of the matrix type (PLA, HDPE), composite panels based on them are characterized by a similar average density and the course of the density profiles.

ACKNOWLEDGMENTS
The presented research was financed under the "Strategic research and development program: environment, agriculture, and forestry" (BIOSTRATEG, GrantNo. BIOSTRATEG3/344303/14/NCBR/2018). The funding institution was The National Centre for Research and Development.

REFERENCES

1. ANDRZEJEWSKI J., SZOSTAK M., BARCZEWSKI M., ŁUCZAK P., 2019: Cork-wood hybrid filler system for polypropylene and poly(lactic acid) based injection molded composites. Structure evaluation and mechanical performance. Composites Part B: Engineering, 163:655-668. https://doi.org/10.1016/j.compositesb.2018.12.109
2. BORYSIUK P., AURIGA R., KOŚKA P., 2019: Influence of the filler on the density profile of wood polymer composites. Annals of Warsaw University of Life Sciences - SGGW. Forestry and Wood Technology, 106/2019, 31-37
3. BORYSIUK P., BORUSZEWSKI P., AURIGA R., DANECKI L., AURIGA A., RYBAK K., NOWACKA M., 2021: Influence of a bark-filler on the properties of PLA biocomposites. Journal of Materials Science, https://doi.org/10.1007/s10853-021-05901-6
4. BORYSIUK P., KRAJEWSKI K., AURIGA A., AURIGA R., BETLEJ I., RYBAK K., NOWACKA M., BORUSZEWSKI P., 2022: PLA Biocomposites: Evaluationof Resistance to Mold. Polymers 2022, 14, 157. https://doi.org/10.3390/polym14010157
5. CLEMONS C., 2002: Wood-Plastic Composites in the United States. The Interfacing of Two Industries. Forest Products Journal, 52 (6), 10-18

6. COMMISSION, D., 2014. Regulation (EU) No 1062/2014. Off. J. Eur. Union 294, 20–30.
7. EN 317:1999 Particleboards and fibreboards - determination of swelling in thickness after immersion in water. Brussels
8. EN 323:1999 Wood-based panels - determination of density.
9. FALK R. H., VOS D., CRAMER S. M., 1999: The comparative performance of woodfiber-plastic and wood-based panels. 5th International Conference on Woodfiber - Plastic Composites, 270-274, www.fpl.fs.fed.us/documnts/pdf1999/falk99f.pdf
10. FARAH S., ANDERSON D. G., LANGER R., 2016: Physical and mechanical properties of PLA, and their functions in widespread applications — A comprehensive review. Advanced Drug Delivery Reviews 107, 367-392 https://doi.org/10.1016/j.addr.2016.06.012
11. GOZDECKI C., KOCISZEWSKI M., MIROWSKI J., WILCZYŃSKI A., ZAJCHOWSKI S., 2009: Effect of wood bark on wood-plastic composite properties. Annals of Warsaw University of Life Sciences, Forestry and Wood Technology, 68, 278-282
12. GOZDECKI C., KOCISZEWSKI M., WILCZYŃSKI A., MIROWSKI J., 2010: Effect of wood bark content on mechanical properties of wood-polyethylene composite. Annals of Warsaw University of Life Sciences, Forestry and Wood Technology, 71, 203-206
13. HARPER D. P., EBERHARDT T. L., 2010: “Evaluation of micron-sized wood and bark particles as filler in thermoplastic composites,” 10th International Conference on Wood & Biofiber Plastic Composites. Madison, WI: Forest Prod. Soc., 248-252.
14. KAMAU-DEVERS K., KORTUM Z., MILLER S. A., 2019: Hydrothermal aging of bio-based poly(lactic acid) (PLA) wood polymer composites: Studies on sorption behavior, morphology, and heat conductance. Construction and Building Materials 214:290-302. https://doi.org/10.1016/j.conbuildmat.2019.04.098
15. KLYSOV A. A., 2007: Wood-Plastic Composites. Wiley-Interscience, 728p., ISBN-13: 978-0470148914
16. KUCIEL S., LIBER-KNEĆ A., MIKUŁA J., KUŹNIAR P., KORNIEJENKO K., ŻMUDKA S., ŁAGAN S., RYSZKOWSKA J., GAJEWSKI J., SAŁASIŃSKA K., TOMASZEWSKA J., ZAJCHOWSKI S., 2010: Kompozyty polimerowe na osnowie recyklatów z włóknami naturalnymi. Praca pod redakcją S. Kuciela, Politechnika Krakowska, Kraków
17. MARKARIAN J., 2008: Biopolymers present new market opportunities for additives in packaging. Plastics, Additives and Compounding; 10(3):22–25. https://doi.org/10.1016/S1464-391X(08)70091-6
18. PARTANEN A, CARUS M., 2019: Biocomposites, find the real alternative to plastic – An examination of biocomposites in the market. Reinforced Plastics 63(6), 317-321 https://doi.org/10.1016/j.repl.2019.04.065
19. SAECHTLING H., 2000: Tworzywa sztuczne. Wydawnictwa Naukowo-Techniczne, Warszawa
20. SAFDARI V., KHODADADI H., HOSSEINIHASHEMI S. K., GANJIAN E., 2011: The effects of poplar bark and wood content on the mechanical properties of wood-polypropylene composites. BioResources 6(4), 5180-5192

21. SELLERS T. JR., MILLER G. D. JR., KATABIAN M., 2000: Recycled thermoplastics reinforced with renewable lignocellulosic materials. Forest Products Journal, 50 (5), 24-28
22. WOLCOTT M. P., ENGLUND K., 1999: A Technology Review of Wood-Plastic Composites. 33rd International Particleboard / Composite Materials Symposium, April 13-15, Washington State University, Pullman, WA, USA, 103-111
23. YEH S. -K., HU CH. -R., RIZKIANA M. B., KUO CH. -H., 2021: Effect of fiber size, cyclic moisture absorption and fungal decay on the durability of natural fiber composites. Construction and Building Materials, 286, 122819. https://doi.org/10.1016/j.conbuildmat.2021.122819
24. YEMELE M. C. N., KOUBAA A., CLOUTIER A., SOULOUNGANGA P., WOLCOTT M., 2010: "Effect of bark fiber content and size on the mechanical properties of bark/HDPE composites," Composites Part A: Applied Science and Manufacturing 41(1), 131-137. https://doi.org/10.1016/j.compositesa.2009.06.005
25. ZAJCHOWSKI S., GOZDECKI C., KOCISZEWSKI M., 2005: Badania właściwości fizycznych i mechanicznych kompozytów polimerowo-drzewnych (WPC). Kompozyty, 5, 45-50

Našu ponuku nájdete na:
www.areko.sk

25.80
°C
18.43°C
Fühler
Anzeige
Logger

ARECO

CHIP AND CHIPLESS WOODWORKING PROCESSES, 13(1): 123–128, 2022
Zvolen, Technical University in Zvolen, ISSN 1339-8350 (online), ISSN 2453-904X (print)

CHANGE IN THE ENERGY FOR WARMING UP OF WOODEN PRISMS DURING AUTOCLAVE STEAMING AT DISPATCHING INTERFERENCES IN PRODUCTION OF VENEER

**Nencho Deliiski[1] – Ladislav Dzurenda[2] – Pavlin Vitchev[1] –
Natalia Tumbarkova[1] – Dimitar Angeski[1]**

Abstract

An approach for computing and research of the energy needed for warming up of wooden prisms during their steaming in autoclaves for the cases of dispatching interferences into the steaming process in order to obtain a duration that is suitable for the subsequent cutting of the veneer from the heated plasticized wood has been suggested. Using two own coupled 2D unsteady models implemented in the approach, calculations of the change of this energy during steaming and plasticizing of non-frozen beech prisms in an autoclave have been carried out. The calculations were made at initial wood temperature of 0 °C, wood moisture content of 0.6 kg·kg^{-1}*, cross-section dimensions of the prisms 0.4 × 0.4 m; steaming autoclave with a diameter of 2.4 m, length of 9.0 m, and loading level of 50%; heat power of the steam generator, equal to 500 kW for the cases of reducing by the dispatcher the maximum temperature of the basic steaming regime from 130* ^{o}*C to 120, 110, and 100* ^{o}*C in the 3rd, 5th, and 7th hour of this regime.*

Key words: *wooden prisms, autoclave steaming, warming up, energy expenditure, dispatching interference, veneer production*

INTRODUCTION

During the process of veneer cutting, the wood should be in good plasticizing condition. For heating in order to plasticize prismatic wood materials in the production of veneer, the prisms are very often subjected to steaming in pits, chambers or autoclaves (Chudinov 1968; Lawniczak 1995; Trebula – Klement 2002; Pervan 2009; Deliiski – Dzurenda 2010).

The plasticizing of wood materials under increased pressure and temperature of the steaming medium in autoclaves is used in many applications due to its greater energy efficiency and shorter duration in comparison with the plasticizing at atmospheric pressure (Shubin 1990; Videlov 2003; Deliiski 2003, 2013; Sokolovski et al. 2007).

---

[1] Faculty of Forest Industry, University of Forestry, Kliment Ohridski Bd. 10, 1797 Sofia, Bulgaria
e-mails: deliiski@netbg.com, p_vitchev@ abv.bg, ntumbarkova@abv.bg, d.angelski@gmail.com
[2] Faculty of Wood Sciences and Technology, Technical University of Zvolen, T.G.Masaryka 24,
96001 Zvolen, Slovakia
e-mail: dzurenda@tuzvo.sk

In the specialized literature sources (Chudinov 1968; Shubin 1990; Trebula – Klement 2002; Deliiski – Dzurenda 2010) completely lack any information about the temperature and energy parameters of steaming regimes in case of dispatcher intervention in them.

That is why this article considers an approach based on two personal mathematical models to compute the energy needed for warming up of non-frozen wooden prisms during their steaming in autoclaves for the cases when the dispatcher at a certain moment decides that it is necessary to extend the time for obtaining such a duration of the steaming that is suitable for the subsequent cutting of the veneer from the heated plasticized prisms.

MATERIAL AND METHODS

Mathematical model of the 2D temperature distribution in wooden prisms during their steaming

When the length of the prisms, *l*, is larger than their thickness, *d*, at least more 4 ÷ 5 times, and simultaneously with this the width, *b*, does not exceed the thickness more than 3 times, for computing the temperature field in the prism's cross section, which is equally distant from the frontal sides (i.e. along the coordinates *x* and *y* of this section) during heating and cooling in steaming or air medium the following 2D mathematical model can be used (Deliiski 2003):

$$c_{\mathrm{w}} \cdot \rho_{\mathrm{w}} \frac{\partial T}{\partial \tau} = \mathrm{div}\ \left(\lambda_{\mathrm{w-cr}} \mathrm{grad}\ T\right) \tag{1}$$

at

$$T(x, y, 0) = T_{\mathrm{w0}} \tag{2}$$

and boundary conditions:

$$T(x, 0, \tau) = T(0, y, \tau) = T_{\mathrm{m}}(\tau), \tag{3}$$

where c_{w} is the specific heat capacity of the wooden prisms during their steaming, $\mathrm{J \cdot kg^{-1} \cdot K^{-1}}$; ρ_{w} – wood density, $\mathrm{kg \cdot m^{-3}}$; $\lambda_{\mathrm{w\text{-}cr}}$ – thermal conductivity of the wood cross sectional to the fibers, $\mathrm{W \cdot m^{-1} \cdot K^{-1}}$; x – coordinate along the prism's thickness of the separate points of the calculation mesh for numerical solving of the model: $0 \le x \le d$, m; d – thickness of the prism, m; y – coordinate along the prism's width of the separate points of the calculation mesh: $0 \le y \le b$, m; b – width of the prism, m; τ – time, s; T – temperature, K; T_{w0} – initial average mass temperature of the prism subjected to steaming, K; T_{m} – processing medium temperature during the steaming of the prisms, K.

Mathematical descriptions of c_{w}, ρ_{w}, and $\lambda_{\mathrm{w\text{-}cr}}$ have been suggested in (Deliiski 2003, 2013; Deliiski – Dzurenda 2010) as a function of the temperature, *T,* and wood moisture content, *u*.

Mathematical model of the heat energy consumption and heat balance of steaming autoclaves

The non-stationary heat balance of the steaming autoclave is mathematically presented by the following model, which has been experimentally verified in (Deliiski 2003):

$$Q_{\mathrm{a}}^{n} = Q_{\mathrm{w}}^{n} + Q_{\mathrm{mb}}^{n} + Q_{\mathrm{il}}^{n} + Q_{\mathrm{e}}^{n} + Q_{\mathrm{fv}}^{n} + Q_{\mathrm{cw}}^{n}, \tag{4}$$

where Q_{a}^{n} is the specific (for 1 $\mathrm{m^3}$ wood materials) heat energy, which is supplied into the autoclave by the introduced in it water steam, $\mathrm{kWh \cdot m^{-3}}$.

The meaning of the indices of the variables in Equation (4) is, as follows: a – autoclave; w – wood of the prisms; mb – metal body of the autoclave; il – insulating layer of the autoclave; e – heat emission of the autoclave; fv – free (unoccupied by prisms) volume; cw – condense water; n – current number of the step along the time coordinate, $\Delta\tau$, with the help of which the joint solving of the models is carried out: $n = 0, 1, 2, 3, \ldots$.

Dependences of all components of the heat balance in Equation (4) on the influencing factors have been given in (Deliiski 2003; Deliiski – Dzurenda 2010).

Change in T_m in regimes for steaming of prisms in an autoclave without and in the presence of dispatching interventions

The typical temperature time profiles of these regimes include the following 5 stages: • Intensive increasing of T_m during the time $0 \div \tau_1$ caused by the opening the valve directing the water steam in the autoclave; • Constant T_m of the steaming medium during $\tau_1 \div \tau_2$ of the basic (without dispatching interference) regime, caused by dosed introduction of steam in the autoclave. In the regimes with dispatcher intervention after a certain time interval $\Delta\tau_a$, $\Delta\tau_b$, or $\Delta\tau_c$ from their beginning the maximum regime temperature T_{m1} decreases with $\Delta T_{m1\text{-}a}$, $\Delta T_{m1\text{-}b}$, or $\Delta T_{m1\text{-}c}$ respectively and remains unchanged until the time $\tau_2 = \tau_{steam}$ is reached. Upon reaching $\tau_{2\text{-}a} = \tau_{steam\text{-}a}$, $\tau_{2\text{-}b} = \tau_{steam\text{-}b}$, or $\tau_{2\text{-}c} = \tau_{steam\text{-}c}$, the supply of steam to the autoclave is stopped; • Decreasing T_m of the steaming medium during $\tau_2 \div \tau_3$ caused by using the already accumulated heat in the autoclave for futher warming up of the prisms; • Decreasing T_m of the steaming medium during $\tau_3 \div \tau_4$, which is caused by the opening the valves directing the residual steam and condensed water out of the autoclave; • Decreasing T_m near the steamed prisms out of the autoclave during $\tau_4 \div \tau_f$.

RESULTS AND DISCUSSION

Computation of the 2D temperature distribution in prisms during steaming

Using own software package for joint solving of the models (1) – (3) and (4) in the calculation environment of Visual FORTRAN, simulations were made to compute the T_m and also the 2D non-stationary change in the temperature field in the square cross section of the studied beech prisms during their steaming in an autoclave. The coordinates of the representative points of the prisms, in which the change in T was recorded, were equal, as follows: Point 1 with T_1: $d/8$, $b/8$ and Point 2 with T_2: $d/2$, $b/2$ (center of the prisms).

During simulations the following values of the parameters of T_m, which influence the temperature distribution in the prism's cross section of autoclave steaming regimes both without and in the presence of dispatching interference, were set: • Initial value of T_m: $T_{m0} = 273.15$ K (i.e. $t_{m0} = 0$ °C); • Maximal value of the temperature of the basic steaming regime without dispatcher's intervention: $T_{m1} = 403.15 \text{ K} = \text{const}$ (i.e. $t_{m1} = 130\ °\text{C} = \text{const}$); • Steps of change in the basic value of $T_{m1} = 403.15$ K at despatching interventions: $\Delta T_{m1\text{-}a} = 10 \text{ K} = 10$ °C, $\Delta T_{m1\text{-}b} = 20 \text{ K} = 20$ °C, and $\Delta T_{m1\text{-}c} = 30 \text{ K} = 30$ °C; • Temperature of the second stage of the basic steaming regime with constant value of $T_{m1} = 403.15$ K: $T_{m2} = 383.15$ K (i.e. $t_{m2} = 110$ °C); • Temperature of the third stage of the basic steaming regime with constant value of $T_{m1} = 403.15$ K: $T_{m3} = 353.15$ K (i.e. $t_{m3} = 80$ °C); • Temperature of the air near the steamed prisms during conditioning: $T_{m\text{-}cond} = 293.15$ K (i.e. $t_{m\text{-}cond} = 20$ °C).

During the simulation the following in total of 9 combinations between ΔT_{m1} and $\Delta\tau$ have been applied: • $\Delta T_{m1\text{-}a}$ with $\Delta\tau_a$, $\Delta\tau_b$, and $\Delta\tau_c$; • $\Delta T_{m1\text{-}b}$ with $\Delta\tau_a$, $\Delta\tau_b$, and $\Delta\tau_c$; • $\Delta T_{m1\text{-}c}$

with $\Delta\tau_a$, $\Delta\tau_b$, and $\Delta\tau_c$, where $\Delta\tau_a = 3$ h, $\Delta\tau_b = 5$ h, and $\Delta\tau_c = 7$ h are time intervals between the beginning of the steaming regimes and the occurrence of the dispatching intervention.

During the computations the following values of the factors influencing the duration τ_{reg} of the prisms' steaming regimes were set: • Dimensions of the square cross section of beech prisms: 0.4 × 0.4 m; • Initial temperature t_{w0} of the prisms subjected to autoclave steaming: 0 °C; • Moisture content u of the prisms: 0.6 kg·kg^{-1}; • Basic density of 560 kg·m^{-3} for the beech wood; • Inner diameter of 2.4 m, length of the cylindrical part of 9.0 m of the autoclave; • Loading level γ of the autoclave with filled in wooden prisms for steaming: $\gamma = 50\%$; • Limited heat power $q_{source} = 500$ kW of the steam generator.

On Fig. 1, as an example, the calculated change in the surface temperature, t_s, average mass temperature, $t_{w\text{-}avg}$, and t of 2 representative points t_1 and t_2 of the beech prisms with $d \times b = 0.4 \times 0.4$ m, moisture content $u = 0.6$ kg·kg^{-1}, and loading level of the autoclave $\gamma = 50\%$ during their autoclave steaming in total of 3 types of dispatcher's intervention at 7th hour and subsequent air conditioning is presented. In addition, this figure shows the change of the same variables in the basic regime, in which there is no dispatcher intervention.

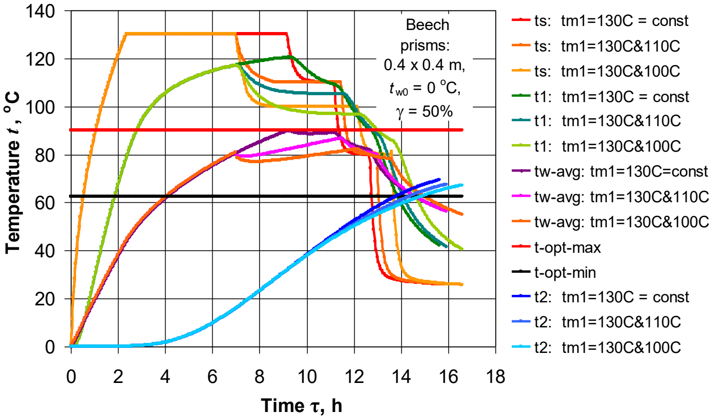

Figure 1. Changes in t_s, $t_{w\text{-}avg}$, t_1, and t_2 of non-frozen beech prisms during their steaming in an autoclave at dispatching interferences in 7th h of the steaming regimes and subsequent air conditioning, depending on $\Delta t_{m1} = 20$ °C, $\Delta t_{m1} = 30$ °C, and τ.

On this figure the minimal and maximal values of the optimal wood temperature, $t_{opt\text{-}min} = 62$ °C and $t_{opt\text{-}max} = 90$ °C, respectively, are also shown. For the obtaining of quality veneer from plasticized beech wood it is needed that the temperature of all points of the prisms during the veneer cutting process stays between these optimal values of the temperature (Deliiski 2003; Deliiski – Dzurenda 2010).

Computing the energy needed for warming up of the prisms during steaming in an autoclave without and in the presence of dispatching interventions

On Figures 2 and 3 the change in the energy Q_w during the regimes for autoclave steaming of the studied prisms at $t_{m1} = 130$ °C = const and at $t_{m1} = 130$ °C & 120 °C and $t_{m1} = 130$ °C & 100 °C is shown. In order to facilitate the analysis of the graphs for Q_w, these figures also show the change in the steaming medium temperature, t_{m1}, in the basic regime and in the regimes with dispatch interventions at $\Delta\tau_a = 3$ h, $\Delta\tau_b = 5$ h, and $\Delta\tau_c = 7$ h.

The analysis of the obtained results allows for making the following statements:

1. At the moment $\tau_2 = \tau_{\mathrm{steam}}$= 9.15 h when the supply of steam to the autoclave is stopped, the largest value $Q_{\mathrm{w\text{-}max}}$ = 65.35 kWh·m^{-3} has the basic steaming regime, conducted only at constant value of t_{m1} = 130 °C.

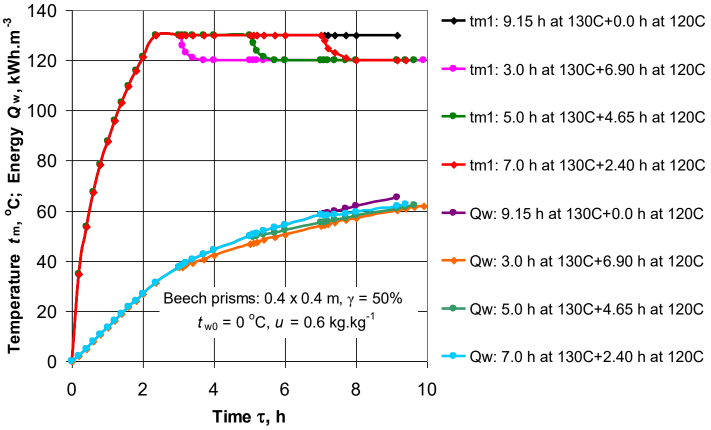

Figure 2. Changes in t_{m} and Q_{w} of the beech prisms during steaming at t_{m1} = 130 °C and t_{m1} = 130 °C & 120 °C with dispatching interferences in 3rd h, 5th, and 7th h, depending on τ.

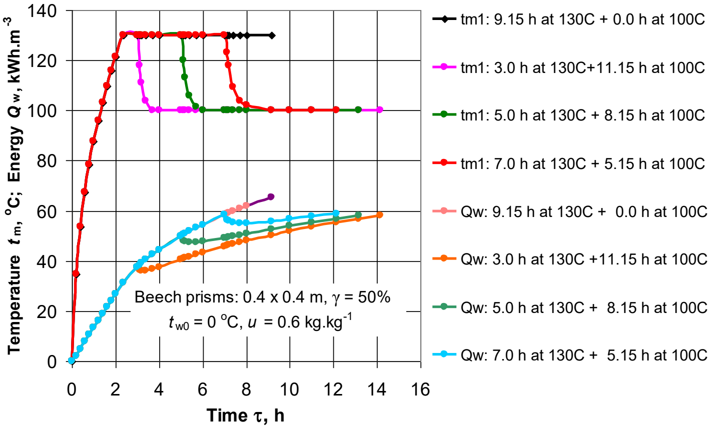

Figure 3. Changes in t_{m} and Q_{w} of the beech prisms during steaming at t_{m1} = 130 °C and t_{m1} = 130 °C & 100 °C with dispatching interferences in 3rd h, 5th, and 7th h, depending on τ.

2. In the cases when after dispatching intervention the temperature of the steaming medium, t_{m1}, decreases from 130 to 120 °C, the energy consumption Q_{w} reach the following maximum values: 62.06 kWh·m^{-3} at $\tau_2 = \tau_{\mathrm{steam}}$ = 9.90 h and $\Delta\tau$ = 3 h; 62.18 kWh·m^{-3} at $\tau_2 = \tau_{\mathrm{steam}}$ = 9.65 h and $\Delta\tau$ = 5 h; 62.81 kWh·m^{-3} and $\tau_2 = \tau_{\mathrm{steam}}$ = 9.40 h and $\Delta\tau$ = 7 h.

3. When after dispatching intervention t_{m1} decreases from 130 to 110 °C, the energy Q_{w} reach the following maximum values: 61.91 kWh·m^{-3} at $\tau_2 = \tau_{\mathrm{steam}}$ = 12.70 h and $\Delta\tau$ = 3 h; 61.97 kWh·m^{-3} at $\tau_2 = \tau_{\mathrm{steam}}$ = 12.10 h and $\Delta\tau$ = 5 h; 62.29 kWh·m^{-3} and $\tau_2 = \tau_{\mathrm{steam}}$ = 11.70 h and $\Delta\tau$ = 7 h.

4. When after dispatching intervention t_{m1} decreases from 130 to 100 °C, the energy Q_{w} reach the following maximum values: 57.96 kWh·m^{-3} at $\tau_2 = \tau_{\mathrm{steam}}$ = 14.15 h and $\Delta\tau$ = 3 h; 58.15 kWh·m^{-3} at $\tau_2 = \tau_{\mathrm{steam}}$ = 13.15 h and $\Delta\tau$ = 5 h; 58.84 kWh·m^{-3} and $\tau_2 = \tau_{\mathrm{steam}}$ = 12.15 h and $\Delta\tau$ = 7 h.

CONCLUSIONS

The present paper describes an approach for computing the energy Q_w needed for warming up of wooden prisms during their steaming in autoclaves for the cases of dispatching interventions into the steaming regimes in order to obtain a duration that is suitable for the subsequent cutting of the veneer from the heated plasticized wood

It was determined that the maximum value of energy $Q_{w\text{-max}}$ = 65.35 kWh·m^{-3} has the basic steaming regime in autoclave conducted only at maximum temperature t_{m1} = 130 °C for beech prisms with cross section of 0.4 × 0.4 m and moisture content of 0.6 kg·kg^{-1}.

The influence of the following variables of dispatching interventions in autoclave steaming process on the energy Q_w was studied during the computer simulations with two own models: time interval $\Delta\tau$ = 3, 5, and 7 h between the beginning of the steaming regimes and the moment when the dispatcher decides to intervene; temperature range Δt_{m1} = 10, 20, 30 °C between the basic regime's maximum value of t_{m1} = 130 °C and the new values of t_{m1} after the intervention, which are equal to 120, 110, 100 °C, respectively.

It has been determined that $Q_{w\text{-max}}$ in all regimes with dispatching intervention are smaller than those indicated for the basic steaming regime. The smallest value of $Q_{w\text{-max}}$ = 57.96 kWh·m^{-3} was found in regime with $\Delta\tau$ = 3 h and Δt_{m1} = 30 °C.

The suggested approach presented above can be applied in the software for systems used for computing and model-based automatic realization of energy-efficient regimes for autoclave steaming of different wood materials with desired duration set by the dispatcher.

REFERENCES

1. CHUDINOV, B. S. 1968: Theory of Thermal Treatment of Wood. Nauka, Moscow, 255 p. (in Russian).
2. DELIISKI, N. 2003: Modelling and Technologies for Steaming Wood Materials in Autoclaves. Dissertation for DSc., University of Forestry, Sofia, 358 p. (in Bulgarian).
3. DELIISKI, N. 2013: Modelling of the Energy Needed for Heating of Capillary Porous Bodies in Frozen and Non-Frozen States; Lambert Academic Publishing, Scholars' Press: Saarbrücken, Germany, 2013; 106 p.
4. DELIISKI, N., DZURENDA, L. 2010: Modelling of the Thermal Processes in the Technologies for Wood Thermal Treatment. TU Zvolen, Slovakia, 224 p. (in Russian).
5. LAWNICZAK, M. 1995: Hydrothermal and Plasticizing Treatment of Wood. Part I. Boiling and Steaming of Wood, Agricultural Academy, Poznan, Poland, 149 p. (in Polish).
6. PERVAN, S. 2009: Technology for Treatment of Wood with Water Steam. University in Zagreb (in Groatian).
7. SHUBIN, G. S. 1990: Drying and Thermal Treatment of Wood. Lesnaya promyshlennost, Moscow, URSS, 337 p., 1990 (in Russian).
8. SOKOLOVSKI, S., DELIISKI, N., DZURENDA, L. 2007: Constructive Dimensioning of Autoclaves for Treatment of Wood Materials under Pressure. In Proceedings of the 2nd International Scientific Conference "Woodworking techniques", Zalesina, Croatia, 11–15 September 2007, pp. 117–126.
9. TREBULA, P., KLEMENT, I. 2002: Drying and Hydrothermal Treatment of Wood, TU in Zvolen, Slovakia, 449 p. (in Slovak).
10. VIDELOV, H. 2003: Drying and Thermal Treatment of Wood, University of Forestry in Sofia, Bulgaria, 335 p. (in Bulgarian).

CHIP AND CHIPLESS WOODWORKING PROCESSES, 13(1): 129–136, 2022
Zvolen, Technical University in Zvolen, ISSN 1339-8350 (online), ISSN 2453-904X (print)

GRANULOMETRIC COMPOSITION OF CHIP FROM THE PROCESS OF MACHINING STEAMED AND UNMAMMED BEECH WOOD ON THE CNC MACHINING CENTER

Ladislav Dzurenda

Abstract

The paper presents information on the grain size and shape of chips formed in the process of machining steamed and unsteamed beech wood on a CNC machining center. Chips were taken from the wood milling process with a single-blade shank milling cutter under machining conditions: feed rate $v_f = 2$ *m.min*$^{-1}$*,* $v_f = 4$ *m.min*$^{-1}$ *and* $v_f = 6$ *m.min-1 and removal:* $e = 1$*mm,* $e = 3$ *mm and* $e = 5$ *mm.*

The granulometric analysis of the chips shows that the majority of 60 to 80% of the formed chip from steamed beech wood consists of a coarse fraction of fibrous chips with a significant elongation in one direction. In the case of unsteamed wood, the share of the coarse fraction is about 10% higher.

The proportion of medium-coarse fractions with dimensions of 1.0 - 0.125 mm is 2 to 3.5 times lower compared to the coarse fraction.

Dust fractions with dimensions below 125 μm are isometric grains, i. chips having approximately the same dimensions in all three directions. Their representation is on average 2.5 to 3%.

Chips in unsteamed as well as steamed beech wood with dimensions below 32 μm were not measured, so it can be stated that no respirable dust particles with dimensions below <10 μm are formed.

Key words: beech wood, steaming, milling, CNC machining center, particle size distribution.

INTRODUCTION

CNC woodworking technologies have become an integral part of the woodworking industry. The range of used CNC machines is wide and CNC machining centers are among the most used in secondary wood processing plants. The chip produced from the milling process in the CNC machining center is a polydisperse bulk material of various grain sizes from coarse, medium coarse and dust fractions: *Kminiak - Dzurenda (2019), Očkajová et al. (2020).* The representation of individual fractions from milling processes on CNC depends on the properties of the processed raw material, tool parameters as well as technical-technological parameters of the machining process. Coarse with medium-coarse chips formed by milling on CNC centers, as reported by the works: *Banski - Kminiak (2018), Kminiak et al. (2020)* are fibrous, the length of which is several times greater than the width and thickness. Fine fractions smaller than 125 μm are isometric chips that are approximately the same size in all three dimensions.

Technical University in Zvolen, T. G. Masaryka 24, 960 01 Zvolen
e-mail: dzurenda@tuzvo.sk

Wood dust with a grain size in the range of 1 ÷ 500 µm: *Hejma et al. (1981), Dzurenda (2002), Dzurenda et al.(2010)* is a hygroscopic, low-abrasive, explosive bulk material. From the point of view of the influence of dust particles with dimensions below 100 µm on the human respiratory system, the dust particles are divided into:

- respirable (inhalable) mass fraction <100 µm,
- thoracic 5 ÷ 10 µm,
- tracheobronchial (respirable mass fraction) 2.5 ÷ 5µm,
- highly respirable mass fraction <2.5 µm.

Dust fraction particles (> 10 µm), according to *Buchancova (2003), do* not sediment rapidly in the working environment and are inhaled by humans if the airways are not protected. They are trapped in the upper respiratory tract and, together with mucus and the action of the ciliated epithelium, move into the nasopharynx, from where they can enter the digestive tract or be eliminated from the body by coughing. Smaller particles (0 <5 µm) are especially problematic - the so-called respirable fraction. They penetrate into the pulmonary alveoli, where they are phagocytosed by alveolar macrophages. Here they can remain deposited and cause local biological effects, or they can penetrate the blood and lymph.

Recently, the focus of research in the field of thermal treatment of wood has focused on steaming with steam for the purpose of targeted wood color in non-traditional wood shades *Trebula (1986), Tolvaj et al. (2009), Dzurenda (2014, 2018, 2022).* This creates a wider space for designers and designers to use the excellent mechanical properties of beech wood in other colors and color shades without its surface treatment by staining or dyeing. The dried beech wood, after drying, is used as a construction material and is mechanically machined with milling cutters on CNC machining centers.

The aim of this work is to determine the effect of thermal treatment of beech wood with saturated steam on the particle size distribution in the process of milling steamed beech blanks on the CNC machining center SCM Tech Z5 and comparison of the grain size of chips with unsteamed beech wood formed in the milling process on a CNC machining center under the same milling conditions.

MATERIAL AND METHOD

***Material*:** blanks were machined in the experiment:

- unsteamed beech wood with dimensions: 50 x 80 x 500 mm,
- steamed beech wood saturated with steam with temperature t = 135 ° C for τ = 9 hours. with dimensions: 50 x 80 x 500 mm,
- wood moisture of steamed and uncooked blanks w = 10 ± 2%.

CNC machining center: the experiment was performed on a 5-axis CNC machining center SCM Tech Z5 (Figure 1).

The milling of blanks was carried out with a single-knife end mill with the type designation KARNED 4451 from the manufacturer Karned Tools s.r.o., Prague, Czech Republic. The reversible knife HW 49.5 / 9 / 1.5 made of sintered carbide T10MG was fitted in the end mill. Technological conditions of milling:

- cutter speed n = 20,000 rpm,
- sliding speed vf = 2 m.min^{-1}, v_f = 4 m.min^{-1} and v_f = 6 m.min^{-1}
- at removal e = 1 mm, e = 3 mm, e = 5 mm.

Sampling and particle size analysis of chips: Chips from the work area of the CNC machining center were sucked out by a local suction source STILER model FM 470 with a filter bag made of Finet PES 4 filter fabric.

Fig.1 CNC machining center SCM Tech Z5

The granulometric composition of the chip was determined by sieving. For this purpose, special sets of stacked screens (2 mm, 1 mm, 0.5 mm, 0.25 mm, 0.125 mm, 0.063 mm, 0.032 mm and bottom) placed on the vibrating stand of the Retsch AS 200c screening machine from the company were used. Retsh GmbH, Germany. The parameters of the Retsch AS 200c screening machine were set for screening at a screening interruption frequency of 20 seconds, screening time τ = 15 minutes, weight 50 g. The granulometric composition was obtained by weighing the proportions remaining on the sieves after sieving on a Radwag 510 / C / 2 electric laboratory balance from Radwag Balances and Scales, Radom, Poland, with a weighing accuracy of 0.001 g. Screening was performed on three samples for each chip taken.

In order to refine the chip shape information, an optical analysis of the largest coarse chips and the smallest fine chips was performed. Microscopic analysis of the fine fraction with dimensions below 125 μm was performed by an optical method - analysis of a microscopic image obtained on a Nikon Optiphot-2 microscope with a Nikon 4x objective. The chips were scanned with a 3-chip television CCD camera HITACHI HV-C20 (RGB 752 - 582 pixels), with a horizontal resolution of 700 TV lines and evaluated by the LUCIA-G 4.0 program. The LUCIA-G image analysis program makes it possible to identify individual chip particles in the image with basic data such as: length, width and circularity, i. roundness expressing the degree of deviation of the projection of a given chip shape from the projection of the circle shape ψ according to the equation:

$$\psi = \frac{4 \cdot \pi \cdot S}{O^2}$$

where: S - particle surface [m^2],
O - particle circumference [m].

RESULTS AND DISCUSSION

Treasure for chips formed in the process of machining unsteamed beech wood on the CNC machining center at removal e = 3 mm and a feed rate $v_f = 4$ m.min^{-1} is shown in Fig. 2.

Results of sieve analyzes of chips created for sliding speeds $v_f = 2$ m.min^{-1}, $v_f = 4$ m.min^{-1} and $v_f = 6$ m.min^{-1} and chip removal e = 1 mm, e = 3 mm, e = 5 mm for unsteamed and steamed beech wood are given in Table 1.

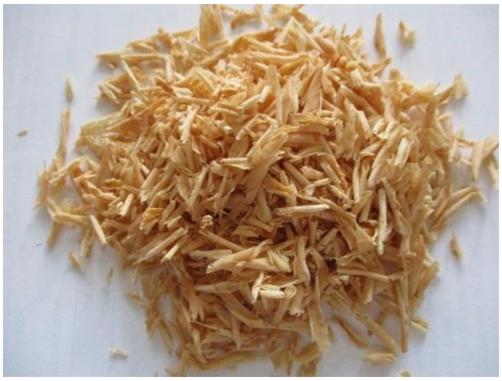

Fig. 2. A look at the chips from milling beech wood at the CNC machining center.

Tab. 1. Granulometric composition of chips from the process of milling unsteamed and steamed beech wood on a CNC machining center.

Layer e [mm]	**Mesh sieves [μm]**	**Factions**	**Chip fraction percentage [%]**					
			Unsteamed beech wood			**Steamed beech wood**		
			Feed speed v_f [m.min^{-1}]			**Feed speed v_f [m.min^{-1}]**		
			2	**4**	**6**	**2**	**4**	**6**
1 mm	2 mm	hrubé	83.56	71.86	65.49	75.64	60.23	50.23
	1 mm		7.70	18.19	22.26	9.20	20.46	24.69
	500 μm	stredne hrubé	3.06	4.52	8.55	6.54	8.47	10.02
	250 μm		2.01	3.11	5.81	4.54	6.48	9.48
	125 μm		1.98	1.62	2.32	1.99	2.18	3.86
	63 μm	**jemné**	1.27	0.54	0.59	1.64	1.83	1.46
	32 μm		0.42	0.16	0.00	0.45	0.35	0.27
	< 32 μm		0.00	0.00	0.00	0.00	0.00	0.00
3 mm	2 mm	hrubé	87.28	84.12	66.89	67.28	64.37	58.78
	1 mm		1.26	1.98	13.17	13.25	12.37	11.73
	500 μm	stredne hrubé	3.30	5.64	9.76	8,66	12.69	14.62
	250 μm		3.26	4.33	5.48	5.39	6.09	8.12
	125 μm		2.64	2.52	3.23	3.64	3.24	5.13
	63 μm	jemné	1.76	1.16	1.19	1.36	0.99	1.32
	32 μm		0.50	0.26	0.27	0.41	0.25	0.30
	< 32 μm		0.00	0.00	0.00	0.00	0.00	0.00
5 mm	2 mm	hrubé	78.87	62.24	54.29	66.73	62.44	51.94
	1 mm		1.78	12.88	15.51	9.80	10.16	12.75
	500 μm	stredne hrubé	5.92	11.79	13.26	9.62	12.16	17.49
	250 μm		6.11	7.77	8.84	6.65	8.28	8.96
	125 μm		4.45	4.80	5.63	4.77	5.75	9.89
	63 μm	jemné	2.33	2.03	2.05	1.93	1.02	1.02
	32 μm		0.53	0.48	0.43	0.50	0.20	0.20
	<32 μm		0.00	0.00	0.00	0.00	0.00	0.00

In FIG. 3 and FIG. 4 show the proportion of coarse, medium-coarse and fine chip fractions from the milling of unsteamed and steamed beech wood as a function of the feed rate and removal at the SCM Tech Z5 CNC machining center.

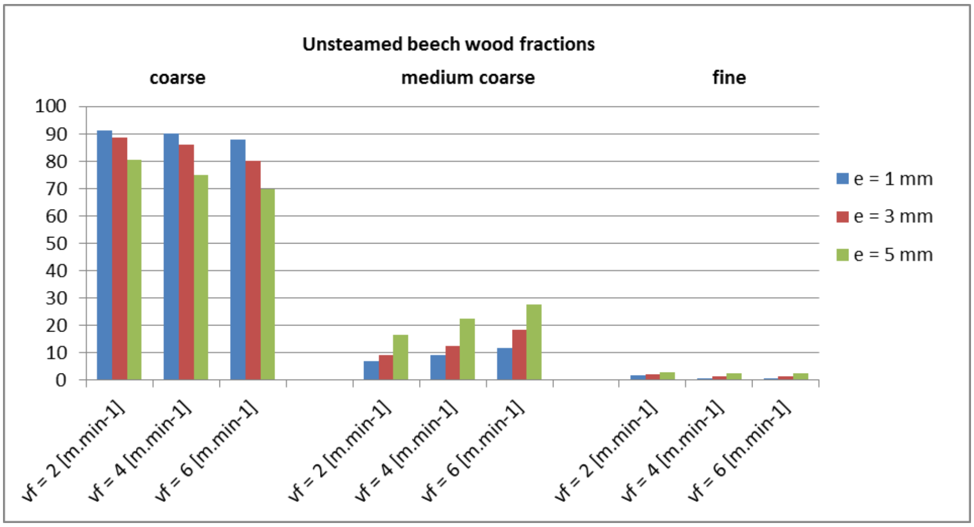

FIG. 3. Comparison of coarse, medium coarse and fine fractions of unsteamed beech wood depending on the sliding speed of milling and removal.

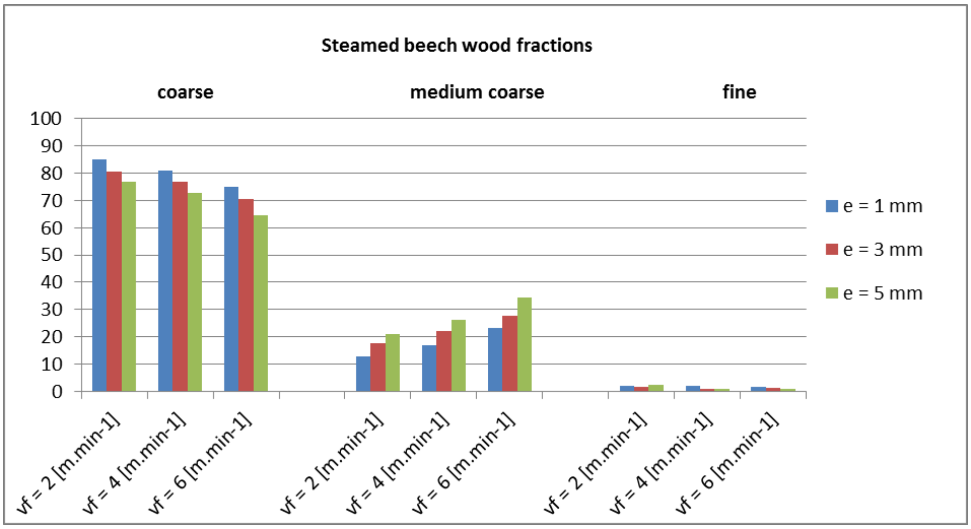

FIG. 4. Comparison of coarse, medium coarse and fine fractions of steamed beech wood depending on the sliding speed of milling and removal.

From the chip size analyzes generated in the milling process at the SCM Tech Z5 CNC machining center shown in Table 1, FIG. 3. and 4. it follows that the majority of the formed in the loose wood mass of both unsteamed and steamed beech wood are the chips of the coarse fraction. The share of the coarse fraction of chips from the milling of unsteamed beech wood is in the range of 70 to 90% and for steamed wood the share of the said fraction is about 10% lower. The proportion of this chip fraction in both types of beech wood decreases with increasing removal and increasing sliding speed.

The proportion of medium-coarse fractions with dimensions of 1.0 - 0.125 mm is 2 to 3.5 times lower compared to the coarse fraction.

Dust fractions with dimensions below 125 μm are isometric grains, i. chips having approximately the same dimensions in all three directions. Their representation is on average 2.5 to 3%.

The chips of both unsteamed and steamed beech wood with dimensions below 32 μm were not measured and it can be stated that no respirable (thoracic and tracheobronchial) dust particles with dimensions below <10 μm are formed.

According to the shape of the chips, the chips generated by wood milling on a CNC machining center, as evidenced by the data with the dimensions of the largest and smallest beech uncooked and steamed wood chips at removal e = 1 mm, feed rates v_f = 2 m.min^{-1} and v_f = 6 m.min^{-1} and under the same feeding conditions at removal e = 5 mm are given in Tables 2 and 3, they are a mixture of fibrous and isometric chips.

Tab. 2: Area dimensions of the largest and smallest chips from beech wood milling on the CNC machining center SCM Tech Z5

Unsteamed beech wood	Maximum chip dimensions [mm]			Minimum chip dimensions [μm]		
	sample 1	sample 2	sample 3	sample 1	sample 2	sample 3
e = 1 mm, v_f = 2m.min^{-1}	2.2 x 19.3 2.3 x 23.1 1.9 x 16.8	1.8 x 19.8 2.3 x 22.7 1.8 x 18.8	2.8 x 21.3 1.9 x 23.1 2.3 x 18.8	37.1 x 43.6 39.6 x 45.3 40.8 x 46.8	39.5 x 42.6 42.8 x 44.2 43.2 x 44.2	41.7 x 44.3 42.6 x 44.9 44.7 x 45.2
e = 1 mm, v_f = 6 m.min^{-1}	1.8 x 20.1 2.2 x 15.1 3.3 x 23.0	2.1 x 22.1 2.2 x 18.1 1.9 x 22.5	1.9 x 18.1 1.8 x 19.1 2.5 x 22.2	39.1 x 43.6 40.6 x 45.3 42.8 x 46.8	38.9 x 42.6 42.6 x 44.2 43.8 x 44.6	40.5 x 42.3 42.6 x 43.9 44.5 x 45.1
e = 5 mm, v_f = 2m.min^{-1}	1.9 x 19.3 3,3 x 23.8 2.8 x 21.1	1.9 x 21.3 2.5 x 19.8 3.1 x 25.1	2.2 x 20.5 2.3 x 24.4 2.1 x 21.7	37.1 x 43.6 40.6 x 45.3 44.8 x 46.8	39.6 x 42.6 42.5 x 44.4 43.4 x 44.8	42.7 x 43.3 44.6 x 44.8 44.6 x 45.3
e = 5 mm, v_f = 6 m.min^{-1}	2.1 x 20.8 2.2 x 18.6 2.6 x 24.0	2.2 x 20.9 1.8 x 19.8 2.2 x 26.2	2.3 x 21.8 1.8 x 19.9 2.6 x 23.8	40.1 x 43.6 39.9 x 45.3 42.8 x 46.8	39.9 x 42.6 42.8 x 44.4 43.5 x 44.1	41.5 x 44.1 42.6 x 44.2 44.3 x 45.2

Tab. 3: Area dimensions of the largest and smallest chips from the milling of steamed beech wood on the CNC machining center SCM Tech Z5.

Steamed beech wood	Maximum chip dimensions [mm]			Minimum chip dimensions [μm]		
	sample 1	sample 2	sample 3	sample 1	sample 2	sample 3
e = 1 mm, v_f = 2 m.min^{-1}	2.2 x 21.3 2.0 x 23.3 2.1 x 19.8	1.8 x 20.8 2.3 x 22.7 2.3 x 19.8	1.8 x 21.9 2.3 x 24.1 1.9 x 21.8	38.1 x 41.6 39.2 x 44.3 41.8 x 44.8	39.8 x 41.6 40.8 x 42.2 41.2 x 43.2	42.7 x 44.3 41.6 x 44.9 43.7 x 45.2
e = 1 mm, v_f = 6 m.min^{-1}	1,8 x 20.1 2.2 x 17.1 1.9 x 23.2	2.1 x 22.1 1.8 x 18.1 1.9 x 22.5	2.6 x 20.1 1.8 x 19.8 2.5 x 21.2	40.1 x 43.6 42.6 x 45.3 41.8 x 45.8	38.9 x 42.6 42.6 x 44.2 43.8 x 44.6	39.5 x 42.3 40.6 x 44.1 40.5 x 43.1
e = 5 mm, v_f = 2 m.min^{-1}	2.1 x 19.3 1.9 x 21.8 1.8 x 22.1	1.9 x 21.9 2.5 x 20.8 2.1 x 23.1	2.2 x 20.5 2.3 x 22.4 2.1 x 20.7	39.1 x 43.6 42.6 x 45.3 41.8 x 42.8	40.6 x 42.6 41.5 x 44.8 43.4 x 44.6	41.7 x 43.3 44.1 x 44.8 44.2 x 45.3
e = 5 mm, v_f = 6 m.min^{-1}	2.1 x 20.8 1.8 x 21.6 2.6 x 24.8	1.8 x 21.9 2.2 x 19.9 2.6 x 23.2	2.3 x 21.8 1.8 x 21.9 3.3 x 22.8	37.1 x 38.6 39.9 x 44.3 42.6 x 46.8	39.9 x 43.6 42.2 x 44,4 41.5 x 44.1	42.5 x 44.1 40.6 x 40.8 43.3 x 45.3

The coarse fraction chips are rolled into a roll and, from an aerodynamic point of view, can be characterized as fibrous chips, characterized in that the length significantly exceeds its width. After unrolling the roll, the area dimensions of the chips are: 6.2 x 15.1 mm, 5.2 x 19.3 mm, 4.8 x 18.6 mm, 4.4 x 16.8 mm, 3.9 x 21 , 8. Coarse fraction chips are cut layers of milled wood. At lower feed rates, the chips are solid. As the sliding speed increases, the amount of bent chips breaks. After unrolling the roll, these chips have squares, resp. circularity rectangle in the interval $\Psi = 0.7 \div 1.0$ thus meeting the criteria of leaf chips in the developed state.

Chips of fine fractions with dimensions below 125 μm are chips belonging to the category of isometric chips, i. chips with the same dimensions in all three dimensions. This finding follows from the fact that the chip plan determined by the optical method is square, resp. the value of the circularity in the interval $\Psi = 0.7 \div 1.0$ and assuming that the third dimension of loose three-dimensional objects on a horizontal surface is smaller than its largest dimension.

CONCLUSION

Based on the performed experiments we can draw the following conclusions about the influence of thermal treatment of beech wood with saturated steam with temperature t = 135 ° C on the particle size distribution in the process of milling steamed beech blanks on CNC machining center SCM Tech Z5:

- The majority of 60 to 80% of chips from the milling of steamed beech wood are chips of coarse fraction with dimensions over 1 mm. In the case of unsteamed wood, the share of the coarse fraction is about 10% higher
- The coarse chips are rolled into a roll and, from an aerodynamic point of view, they can be characterized as fibrous chips, i. their length significantly exceeds the thickness and width (diameter of the roll).
- Chips of fractions with dimensions below 125 μm of steamed and unsteamed beech wood are chips belonging to the category of isometric chips, i. chips with the same dimensions in all three dimensions.
- The proportion of the inhalable dust fraction of steamed and unsteamed wood milling did not exceed 3%.
- The presence of thoracic and tracheobronchial dust fractions has not been demonstrated.

LITERATURE

BANSKI A., KMINIAK R. (2018). *Influence of the thickness of removed layer on granulometric composition of chips when milling oak blanks on the CNC machining center.* In: Trieskové a beztrieskové obrábanie dreva 11(1), 23-30. ISSN 2453-904X.

BUCHANCOVÁ, J. a kol. (2003): *Pracovné lekárstvo a toxikológia*. Martin: Osveta. 2003.ISBN 80-8063-113-1.

DZURENDA. L. (2002). *Vzduchotechnická doprava a separácia dezintegrovanej drevnej hmoty.* Zvolen: TU vo Zvolene, 2002. ISBN 80-228-1212-9.

DZURENDA, L., ORLOWSKI, K., GRZESKIEWICZ, M., (2010): *Effect of thermel modification of oak wood on sawdust granularity*. In: Drvna industrija, 2010, 61(2): 89–94.

DZURENDA, L., (2014): *Sfarbenie bukového dreva v procese termickej úpravy sýtou vodnou parou.* In: *Acta Facultatis Xylologiae Zvolen*, 56(1), 41-50.

DZURENDA, L., (2018): *Netradičné farebné odtiene dreva roztrúseno-pórovitých listnatých drevín nadobudnuté procesom termickej úpravy sýtou vodnou parou.* In: Nábytok a výrobky z dreva, 66-71 s. ISBN 978-80-228-3089-8.

DZURENDA, L., (2022*): Range of Color Changes of Beech Wood in the Steaming Process.* In: BioResources 17(1), 1690-1702. doi: 10.15376/biores.17.1.1690-1702

HEJMA J. a kol., (1981): *Vzduchotechnika v dřevozpracovávajícím průmyslu*. Praha, SNTL, 398s.

KMINIAK, R., DZURENDA, L., (2018): *Granulometric composition of chips from the milling process of spruce on a CNC machining center.* In: Annals of Warsaw University of Life Sciences. Forestry and Wood Technology. No. 104 (2018), p. 45-52. ISSN 1898-5912.

KMINIAK, R., ORLOWSKI, K. A., DZURENDA, L., CHUCHALA, D., BANSKI, A. (2020). *Effect of Thermal Treatment of Birch Wood by Saturated Water Vapor on Granulometric Composition of Chips from Sawing and Milling Processes from the Point of View of Its Processing to Composites*. In: *Applied Sciences* 10, no. 21: 7545. https://doi.org/10.3390/app10217545.

OČKAJOVÁ, A., KUČERKA, M., KMINIAK, R., ROGOZIŃSKI, T. (2020). *Granulometric composition of chips and dust produced from the process of working thermally modified wood.* In Acta Facultatis Xylologiae Zvolen, 62(1): 103-111, DOI: 10.17423/afx.2020.62.1.09.

TOLVAJ, L., NEMETH, R., VARGA, D., MOLNAR, S., (2009): *Colour homogenisation of beech wood by steam treatment.* In: Drewno. No. 52 vol. 181. 5 – 17 s.

TREBULA, P., (1986): *Sušenie a hydrotermická úprava dreva. časť Hydrotermická úprava dreva parením a varením*. Technická univerzita vo Zvolene, 255 s.. ISBN 80-228-0574-2.

Acknowledgments:

This experimental research was carried out under the grant project VEGA 1/0324/21 "Analýza rizík zmeny materiálovej skladby a technologického zázemia na kvalitu pracovného prostredia v malých a stredných drevospracujúcich firmách“ and the grant project APVV-17-0456 “Termická modifikácia dreva sýtou vodnou parou za účelom cielenej a stabilnej zmeny farieb drevnej hmoty” as the result of work of author and the considerable assistance of the VEGA and APVV agency.

CHIP AND CHIPLESS WOODWORKING PROCESSES, 13(1): 137–145, 2022
Zvolen, Technical University in Zvolen, ISSN 1339-8350 (online), ISSN 2453-904X (print)

THE EFFECT OF CO_2 LASER ENGRAVING ON THE COLOUR MODIFICATIONS OF BIRCH PLYWOOD IN DIFFERENT MODES OF USE

Zhivko Gochev – Pavlin Vitchev

Abstract

The paper presents the results of a study on the processes of laser surface treatment of plywood samples. The change in colour when exposed to CO_2 laser beam, under different exposure modes, was studied with a SC-30 calorimeter. The difference in colour shades of plywood samples was measured in the colour space L, a* and b*. The results allow to offer modes for surface treatment with laser beam in the construction of complex graphic images on plywood products.*

Key words: *CO_2 laser beam, calorimeter, colour space, plywood, surface treatment*

INTRODUCTION

CNC machines for CO_2 laser cutting and engraving are becoming more and more popular not only among companies from the woodworking and furniture industry (WWFI), but also among individual and small producers of wood products and wood-based materials (WBM).

CO_2 laser devices with low power, up to 80 W, are compact and can be placed and used in small workshops, even at home. The modern market gives a wide choice of machines with an affordable price, which is influenced by many factors, but there are Chinese machines on the market with a power of 40 W to 150 W, with a price of 1 000 to 6 000 EUR.

The electromagnetic radiation of the CO_2 laser beam, with a wavelength of 10.6 μm, is absorbed by the wood and WBM from 80% to 90% and is transformed into thermal energy capable of instantly heating and vaporizing the surface layer of the material (in the case of an unfocused laser beam) or cut it (with a focused laser beam) (Gochev 1996).

Laser engraving is a process in which, as a result of the carbonization of wood, a part of the surface layer is removed, at a certain width and depth. By controlled variation of the parameters of the laser radiation, even very small images and inscriptions can be engraved, but with great precision in detail, and amazing results can be achieved with exceptional levels of contrast, creating an almost three-dimensional effect.

The literature provides different information on engraving or decorating with a CO_2 laser beam, as well as with semiconductor lasers and it changes in the color of wood from beech, oak, ash, linden, spruce, etc. tree species (*Petutschnigg at al. 2013; Gurau et al. 2017; Vidholdová et al. 2017; Sikora at al. 2018; Jurek et al. 2021 and others*).

A number of publications have investigated the effect of laser power intensity on the resulting modification of the engraved material (*Pagano et al. 2009; Eltawahni et al. 2013;*

Department of Woodworking Machines, University of Forestry, 10 Kl. Ohridski Blvd., 1797 Sofia
e-mail: zhivkog@ltu.bg p_vitchev@ltu.bg

Hernández-Castañeda et al. 2011; Martinez-Conde et al. 2017). However, the color change created by the impact of the laser beam does not depend only on the intensity (power) and profile (cross-section) of the laser beam. The impact of the environment (air) also has an influence on the colour shades of the material. Therefore, the type of wood, its temperature (and the ambient temperature), its humidity (and the ambient humidity), the hardness and the current chemical composition of the engraved layers (the age of the wood and its surface treatment) are also important for colour change.

The aim of the present work is to study the influence of the CO2 laser beam parameters, power and scanning speed, on the changes in the colour of birch plywood samples and its use in the engraving of complex graphic images, based on which to formulate the relevant conclusions and recommendations.

MATERIALS AND METHODS

The experimental studies were carried out with a FormaTec CO2 laser machine, model K40 (China) (Fig. 1).

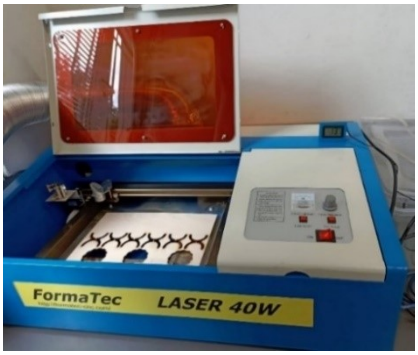

Figure 1. CO_2 laser machine for engraving and cutting

The changes that occur in the colour of the surface layer of the material were studied on plywood samples - ordinary birch (Petula pendula Roth.) with dimensions 200 x 200 x 3 mm, density $\rho = 400$ kg/m^3 and humidity W = 6%.

The selection of initial parameters and levels of the variable factors influencing the changes in the colour of the surface layer of the studied material is based on the analysis of literature studies and preliminary experimental studies. The dispersion analysis methodology was used to evaluate the results of the two-factor experiment (Vuchkov at. al. 1986). The regression equation for two variation factors is of the form

$$y_{pr.v.} = b_o + b_1x_1 + b_2x_2 + b_{11}x_1^2 + b_{22}x_2^2 + b_{12}x_1x_2 \quad (1)$$

Where $y_{pr.v}$ is the predicted value of the output quantity;
b_o – coefficient before the free member;
b_1 and b_2 – coefficients before the linear member; b_{11} and b_{22} – coefficients before the non-linear members of the equation.

The values of the variable factors – power of the laser beam (P, W) and speed of scanning (feed) of the laser beam (V_f, mm/s) in explicit and coded form are given in table 1.

Table 1 Variable factor values

Variable factors	**Minimum value**		**Average value**		**Maximum value**	
	open form	**coded form**	**open form**	**coded form**	**open form**	**coded form**
$x_1 = P$, W	4,0	-1	5,6	0	7,2	+1
$X_2 = V_f$, mm/s	250	-1	260	0	270	+1

The matrix of the planned two-factor experiment is shown in Table 2.

Table 2 The matrix of the planned two-factor experiment

№ of the experiment	**Variable factors**			
	$x_1 = P$, W		**$X_2 = V_f$, mm/s**	
1.	-1	4.0	-1	250
2.	+1	7.2	-1	250
3.	-1	4.0	+1	270
4.	+1	7.2	+1	270
5.	-1	4.0	0	260
6.	+1	7.2	0	260
7.	0	5.6	-1	250
8.	0	5.6	+1	270
9.	0	5.6	0	260
Experiments in the middle of the factor space				
10.	0	5.6	0	260
11.	0	5.6	0	260
12.	0	5.6	0	260

To measure the difference in colours of a standard sample (without laser exposure) and on the examined sample (after exposure to a laser beam) a portable colorimeter for colour difference, model SC-30 (China) was used, shown in fig. 2 . The device allows measurements in two colour spaces *L*a*b** and *L*c*h**. To measure the temperature in the scanning area of the laser beam, an IR-thermometer, model KIRAY for non-contact measurement of surface temperature.

RESULTS AND DISCUSSION

The difference in colour shades of the plywood samples is measured in a three-dimensional colour model, as a reference standard e CIELAB (*L*a*b**). CIE (in French – *Commission Internationale de l'Eclairade*; in English – *International Commission on Illumination*). The *L*a*b** colour space uses three axes to represent the nearly uniform distribution of perceived colour difference. The vertical axis L represents lightness/darkness where at $L = 100$ we have white and at $L = 0$ we have black and shows differences between dark colours and lighter pastels. The horizontal and mutually perpendicular axes, „*a*" and „*b*", represent the primary colour coordinates in the red-green, yellow-blue range.

It is known that wood is composed of cellulose, lignin, hemicellulose and extractive substances, which are thermally unstable. The cellulose content in wood reaches up to 50%, and lignin and hemicellulose from 20 to 30%.

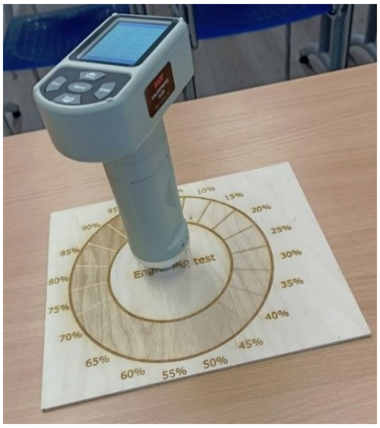

Figure 2. Colorimeter, model SC-30;

Heat transfer in the horizontal direction is carried out by thermal radiation (TR) from the laser beam. The investigated material – ordinary birch plywood – receives the heat in a thin surface layer (1 μm ~ 1 mm) and begins to heat up. Depending on the heat dissipation and the specific heat capacity of the material, the temperature starts to rise, being highest in the surface layer receiving the radiation. Deep in the body, heat spreads through thermal conduction.

Between 120 and 200 °C, in addition to dehydration, the release of non-combustible gases - CO2, formic acid, acetic acid and water vapour - begins. At a temperature higher than 120 °C, structural changes begin with the main component of wood - cellulose - destruction, which is accompanied by the formation and release of volatile substances. Above 200 °C, the rate of pyrolysis increases, with hemicellulose (200-260 °C) decomposing first, followed by cellulose (240-300 °C) and finally lignin (280-500 °C) (*Poletto and al. 2013*).

A system of isolated zones with different colours from dark brown to light, approaching the natural colour of birch plywood, is engraved on the surface of the samples. Specialized software "Inkscape" was used to conduct this research (https://wikibgbg.top/wiki/Inkscape; https://paradacreativa.es/bg/que-es-inkscape-y-como-funciona/).

To estimate the difference between two colours, the total color difference ΔE^* is used, which is estimated according to BDS EN ISO 11664-6:2016) and is calculated by the formula

$$\Delta E^* = \sqrt{(\Delta E^*)^2 + (\Delta a^*)^2 + (\Delta b^*)^2} \qquad (2)$$

Where ΔL^*, Δa^* and Δb^* are differences in individual axes (difference between values measured after laser exposure and reference sample).

Based on the conducted experimental studies and after mathematical processing of the data, with the help of specialized software Q-StatLab, the regression equation was derived

$$Y_1 = 70{,}004-5{,}600X_1+1{,}617X_2+1{,}837X_1^2+1{,}188X_2^2-1{,}450X_1.X_2 \qquad (3)$$

Where Y_1 is the expected variation in the color shade of the surface of the machined parts, L^* in coded form;
X_1 – the power of the laser beam (P) in coded form;
X_2 – feed rate (V_f) in coded form.

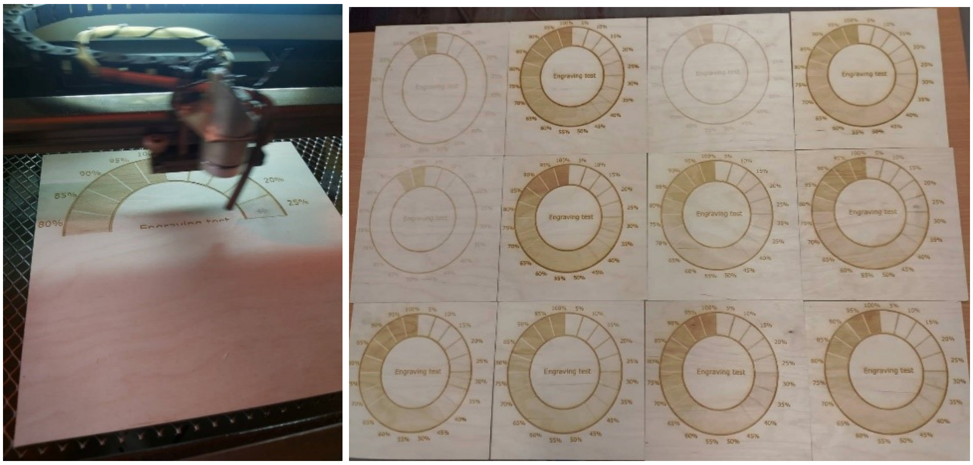

Figure 3. Results of an engraving test and changes in the colour of birch plywood

This equation can be used to predict the variation in surface colour, relative to the base colour (standard), as a function of variation in laser beam power (*P*) and scan speed (V_f). Table 3 presents the coefficients of the regression equation. From the values of the regression coefficients, it is clear that the power of the laser radiation (b_1 = 5.056) has a greater influence than the two investigated factors, and the second most important factor is the scanning speed factor (b_2 = 2.594).

Figure 4 graphically presents the variation of the value of the L^* axis (illuminance) depending on the power of the laser beam (*P*) at three different scanning speeds (V_f), and in fig. 5 – depending on V_f, at different laser beam powers.

As a result of the experimental studies, a regression equation (4) was derived, on the basis of which the total colour difference ΔE^* can be estimated depending on the change in the power of the laser beam (*P*) and the feed rate (V_f).

$$Y_2 = 23.196+6.317X_1-1.750X_2-2.688X_1^2-1.288X_2^2+1.450X_1.X_2 \qquad (4)$$

Where Y_2 is the expected change in the indicator E^* in coded form;

X_1 – the power of the laser beam (P) in coded form;

X_2 – feed rate (V_f) in coded form.

Table 3 presents the coefficients of the regression equation.

Table 3. Regression coefficients

Coefficient	Coded value	Coefficient	Coded value
b_1	5.056	b_{22}	6.597
b_2	2.594	b_{12}	3.734
b_{11}	1.487		

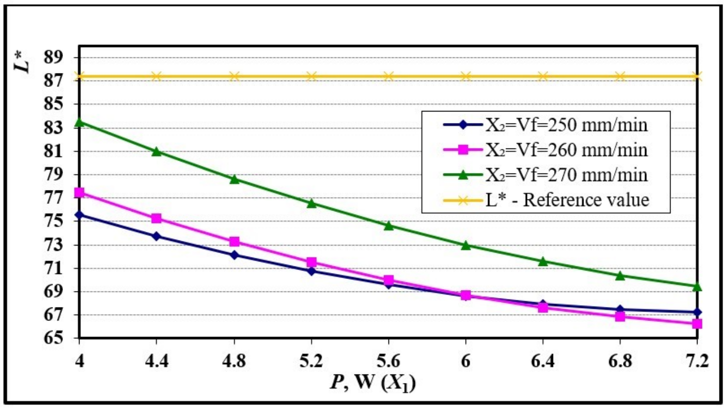

Figure 4. Graphic representation of L* axis values as a function of laser beam power (*P*) at different feed rates (V_f)

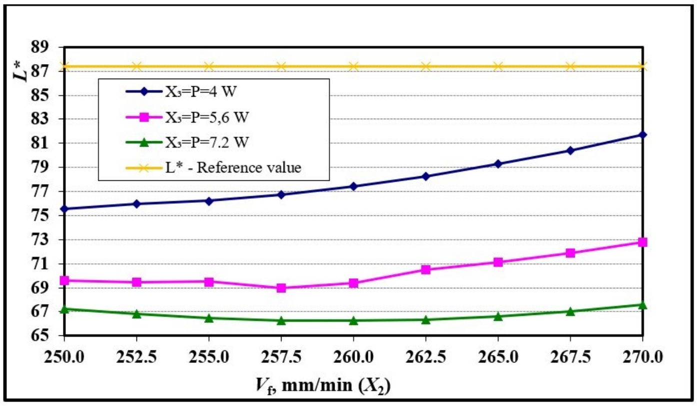

Figure 5. Graphical representation of *L** axis values as a function of scan speed (V_f) at different laser beam powers (*P*)

The values of the regression coefficients confirm the greater influence of the laser radiation power ($b_1 = 6.317$) compared to the scanning speed ($b_2 = 1.750$).

Figure 6 graphically presents the variation of Δ*E** values depending on the power of the laser beam (*P*) at the three different scanning speeds (V_f), and in fig. 7 – depending on Vf at different laser beam powers.

Table 4. Regression coefficients

Coefficient	Coded value	Coefficient	Coded value
b_1	6.317	b_{22}	1.288
b_2	1.750	b_{12}	1.450
b_{11}	2.688		

The measured value of the *L** axis (luminance) of the standard (reference) sample is 87.4%, the difference to absolute white (100%) is 12.6%.

The *L** axis values (74.2%; 82.1% and 78.4%) are very close to that of the standard sample of 87.4% (№ of the experiment 1; 2 and 3, Fig. 3), i.e. changes in shades when building complex graphic images, photography type will not be well noticeable.

The total colour difference ΔE^* varies significantly with increasing laser beam power with maximum values at № of the experiment 2; 4 and 6 (Fig. 3).

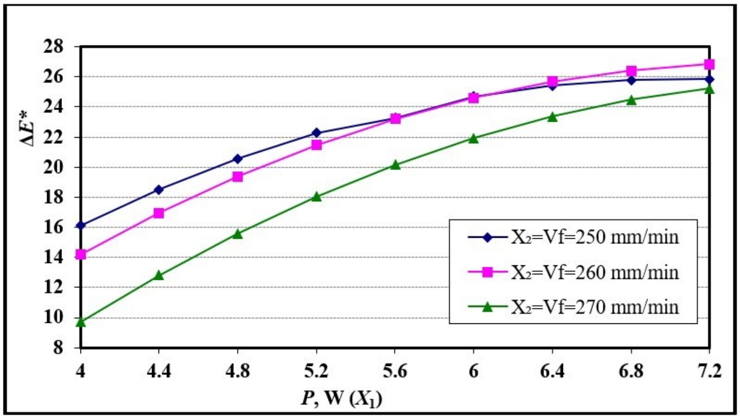

Figure 6. Graphical presentation of ΔE^* values as a function of laser beam power (P) at different feed rates (V_f)

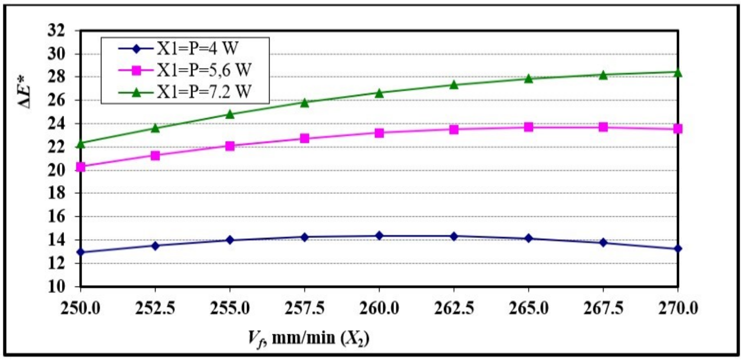

Figure 7. Graphic representation of the dependence of ΔE^* values depending on the scanning speed (V_f) at different laser beam powers (P)

At the focus point, the laser beam has the greatest density and falling as a TR, the greatest accumulation of heat is concentrated perpendicular to the processed material and, accordingly, the fastest rise in temperature. It is in the area of this point that the processes related to heating the material and the structural changes that occur in it, related to a change in the colour of the surface layers and pyrolysis processes take place first.

The measured temperatures in the scanning area of the laser beam using an IR-thermometer were in the range of 210 to 290 ºC. This interval corresponds to the thermal decomposition of hemicellulose and cellulose and the initial stage of lignin decomposition.

The change in colour of the surface layers of the plywood, resulting from the degree of their carbonization, is also influenced by the contact with air and the O_2 content.

CONCLUSION

As a result of the conducted research and analysis, the following more important conclusions and recommendations can be made:

1. CIE *L*a*b** colour analyses show a gradual darkening of the laser-treated samples with increasing laser beam power, the influence of which is more pronounced than the scanning speed.
2. The *L** axis values, at laser beam power ≤ 4 W and scan speeds of ≥ 250 mm/s, are very close to that of the standard sample of 87.4%, i.e. changes in shades when building complex graphic images, photography type, will not be well noticeable.
3. The *L** (illuminance) axis values show the most significant variation at laser beam power *P* = 7.2 W and scan speeds from 250 to 270 mm/s, which correspond to dark brown.
4. Larger values of laser beam power produce a greater degree of carbonation and colour saturation, while smaller values produce a lighter shade in the graphic layout of complex photographic images.
5. The measured temperatures in the scanning area of the laser beam are in the range of 210 to 290 °C. This interval corresponds to the thermal decomposition of hemicellulose and cellulose and the initial stage of lignin decomposition.
6. According to the specifics of the material, the engraved image becomes more pronounced and detailed, or in other cases fainter. Depending on the desired effect and contrast, the operating modes of the machine are selected.
7. The colour change created by the effect of the laser beam on the wood also depends on the effect of the environment (air and O_2 content), which is recommended to be investigated.

REFERENCES

1. BDS EN ISO 11664-6:2016 (in Bulgarian).
2. Gochev Zh., 1996. Investigation of the laser cutting process of furniture details from wood particle boards, Ph.D thesis for awarding an educational and scientific degree „Doctor“, LTU Printing Base, Sofia, p. 200 (in Bulgarian).
3. Gurau L., A. Petru, A. Varodi, M. Timar, 2017. The Influence of CO2 Laser Beam Power Output and Scanning Speed on Surface Roughness and Colour Changes of Beech (Fagus sylvatica), BioResources 12(4):7395-7412, ISSN: 1930-2126, DOI: 10.15376/biores.12.4.7395-7412.
4. Eltawahni H., N. Rossini, M. Dassisti, K. Alrashed, T. Aldaham, K. Benyounis, A. Olabi, 2013. Evaluation and optimization of laser cutting parameters for plywood materials. Opt. Lasers Eng., 51(9):1029-1043, ISSN: 0143-8166, https://doi.org/10.1016/j.optlaseng.2013.02.019.
5. Hernández-Castañeda J., H. Kursad, L. Li, 2011. The effect of moisture content in fibre laser cutting of pine wood. Opt. Lasers Eng., 49(9-10):1139–1152, ISSN: 0143-8166 https:// doi.org/10.1016/j. optlaseng. 2011.05.008.
6. Jurek M., R. Wagnerová, 2021, Laser beam calibration for wood surface colour treatment, European Journal of Wood and Wood Products, 79(5):1097–1107, ISSN: 1436736X, doi.org/10.1007/s00107-021-01704-3.
7. Martinez-Conde A., T. Krenke, S. Frybort, U. Müller, 2017. Review: Comparative analysis of CO_2 laser and conventional sawing for cutting of lumber and wood-based

materials. Wood Sci. Technol., 51:943–966., ISSN: 1432-5225, https://doi.org/10.1007/s00226-017-0914-9.

8. Pagano N., S. Genna, C. Leone, V.Lopresto, 2009. Wood Laser machining using CO_2 30W laser in CW and pulse regime, In book: Innovative production machines and systems. LAPT, Napoli, pp. 145-150, ISBN-10:1849950067.
9. Petutschnigg A., M. Stöckler, F. Steinwendner, J. Schnepps, H. Gütler, J. Blinzer, H. Holzer, Th. Schnabel1, 2013. Laser Treatment of Wood Surfaces for Ski Cores: An Experimental Parameter Study, Advances in Materials Science and Engineering, Volume 2013(11), Article ID 123085, pp 1-7, ISSN: 1687-8434 (Print), ISSN: 1687-8442 (Online), DOI: 10.1155/3013/123085.
10. Poletto M., V. Pistor, A. Zattera, 2013. Structural Characteristics and Thermal Properties of Native Cellulosep - Cellulose - Fundamental Aspects (Edited by Theo van de Ven and Louis Godbout). InTech, p. 378, ISBN 978-953-51-1183-2.
11. Sikora A., F. Kačík, M. Gaff, V. Vondrová, T. Bubeníková, I. Kubovský, 2018. Impact of thermal modification on color and chemical changes of spruce and oak wood, Journal of Wood Science, Volume 64, pp. 406-416, https://doi.org/10.1007/s10086-018-1721-0, ISSN: 1611-4663 (electronic).
12. Vidholdová Z., L. Reinprecht, R. Igaz, 2017. The Impact of Laser Surface Modification of Beech Wood on its Color and Occurrence of Molds, 12(2):7395-7412, ISSN: 1930-2126, DOI: 10.15376/biores.12.2.4177-4186.
13. Vuchkov I., S. Stoyanov, 1986. Mathematical modeling and optimization of technological objects, SPH Tehnika, Sofia, p. 341 (in Bulgarian).
14. https://wikibgbg.top/wiki/Inkscape
15. https://paradacreativa.es/bg/que-es-inkscape-y-como-funciona/

Acknowledgements: This paper is supported by the Scientific Research Sector at the University of Forestry – Sofia, Bulgaria, under contract № НИС-Б-1046/05.04.2021.

Chip and chipless woodworking processes, 13(1): 147–150, 2022
Zvolen, Technical University in Zvolen, ISSN 1339-8350 (online), ISSN 2453-904X (print)

STUDY OF MAPLE WOOD MODIFIED BY SATURATED WATER STEAM

Peter Jurkovič[1] – Ján Sedliačik[2] – Igor Novák[3] – Ján Matyašovský[1] – Angela Kleinová[3]

Abstract

The treatment of maple (Acer pseudoplatanus) wood by saturated water steam consists of a hydrothermal modification of wood with effective heat transfer, that can reached industrially significant properties of wood. The maple wood was modified by steam at 125 °C during 8 hours, and at pressure 0.18 MPa. The water contact angle of saturated steam-treated maple wood increased from 44.9° (for native wood) to 55.3° (for steam-treated wood), and the stability of water drop on steam-treated maple wood surface increased. FTIR spectra show an increase in C=O and glycoside bonds concentration on the surface of steam-treated maple wood, but the concentration of C–O–C groups decreased

Key words: *maple wood, saturated water steam, contact angle, hydrophilicity, FTIR-ATR*

INTRODUCTION

Wood modification is term describing the application of chemical, mechanical, physical, or biological methods to alter the properties of the material. The modified wood should itself be nontoxic under service conditions, and furthermore, there should be no release of any toxic substances during service, or at end of life, following disposal or recycling of the modified wood. To modify wood (1-4), four main types of processes can be implemented:
(1) chemical treatment,
(2) thermo-hydro and thermo-hydro-mechanical treatments,
(3) treatments based on biological processes,
(4) physical treatment with the use of electromagnetic irradiation or plasma.
The treatment of wood using various modification methods, e.g. corona discharge or low temperature plasma, can change the chemical and physical properties of wood. In water steam treating process steam alter chemically and physically properties of the wood. The treatment with water steam represents the hydrothermal method of modification. This method can change hydrophilicity as well as dimensional stability of wood.
The thermos-physical properties of wood-based materials have been widely studied in the literature (1-4). The heat transfer in wood depends on the geometry of the wood sample, as well as porosity, moisture content, and many other factors, e.g. wood after thermal modification (5-8). Because wood is a hygroscopic material, it mostly contains water in the form of bonded water or free water. The amount of water has a profound effect on almost all properties of wood, including its thermal properties.

---

[1] VIPO, a.s., Gen. Svobodu 1069/4,958 01 Partizánske, Slovak Republic
[2] Technical University in Zvolen, T. G. Masaryka 24, 960 01 Zvolen, Slovak Republic
[3] Slovak Academy of Sciences, Polymer Institute, Dúbravská cesta 9, 845 41 Bratislava 45
e-mail: pjurkovic@vipo.sk

The aim of this investigation was to study the effects of saturated water steam-treatment process on the chemical changes in the wood components as well as study of their correlation with surface properties od modified wood.

MATERIAL AND METHODS

The samples of wood species as maple (*Acer pseudoplatanus*) with dimensions 50×15×5 mm (Technical University in Zvolen, Slovakia) with the moisture content of 8 % were pre-treated with water steam at these conditions: the temperature was 125 °C, treatment time 8 hours and pressure 0.18 MPa.

The physical and chemical changes were observed using measurements of water contact angles by contact angle meter, ATR-FTIR, XPS for all investigated maple wood samples. The drops of testing liquid (re-distilled water, $V = 20\ \mu L$) were placed on the wood surface with a micropipette (Biohit, Finland), and the stable value of contact angle, due to penetration of water into wood, was determined. The contact angles measurements of maple wood with water were carried out using professional SEE (Surface Energy Evaluation) system completed with a web camera (Advex, Czech Republic) and necessary PC software.

Fourier Transform Infrared - Attenuated Total Reflectance (FTIR-ATR) spectroscopy measurements were performed with the FTIR NICOLET 8700 spectrometer (Thermo Scientific, UK) using a single bounce ATR accessory equipped with a Ge crystal. For each measurement, the spectral resolution was 2 cm^{-1} and 64 scans were performed. From each sample type, 20 spectra were taken at different points – 10 from both sides (the locations were selected at random).

RESULTS AND DISCUSSION

The water contact angle (WCA) on the investigated pristine maple wood surface is relatively small and it is equal 44.9 (Table 1). After modification of maple wood with steam ($T = 125$ °C, $t = 8$ hours, and $p = 0.18$ MPa) the value of WCA increased to value $\theta = 55.3$ due to higher hydrophobicity of steam-treated maple wood surface.

Table 1. Water contact angle of native maple wood and saturated steam-treated maple wood

Native sample No.	WCA (°)	Steam-treated sample No.	WCA (°)
1	46.2	1	54.8
2	45.4	2	55.4
3	44.5	3	54.0
4	42.2	4	54.6
5	44.2	5	56.0
6	45.0	6	53.8
7	46.2	7	54.8
8	45.6	8	55.2
9	43.8	9	56.0
10	45.4	10	56.8
11	44.6	11	57.2
12	45.4	12	54.8
	Mean = 44.9		**Mean = 55.3**

The increase of WCA for steam-treated maple wood can be explained by chemical and chemical changes on/in steam modified maple wood. The hydrophilicity of the wood surface depends on the amount of polar oxygenic functional groups creating using modification of maple wood with steam.

Figure 1 illustrates the FTIR-ATR spectra of pristine maple wood (blue) and saturated steam-treated maple wood (red), the entire middle infrared region and Figure 2 shows the FTIR-ATR spectra of pristine maple wood (green) and steam-treated maple wood (red), area of deformation vibrations.

From FTIR-ATR spectra shown in Figure 1 and 2 could be found following regions:

- C = O vibration region (1710-1697 cm^{-1}), maximum absorbance at about 1738-1726 cm^{-1}. In some cases, there is a double in this area,
- C-O-C bond region (1190-920 cm^{-1}), undifferentiated multi-peak band: 1160, 1110, 1056 and 1033 cm^{-1}) and (although this band is not very pronounced but is characteristic of cellulose),
- band with a maximum at 896 cm^{-1} (β (1,4) glycoside bond).

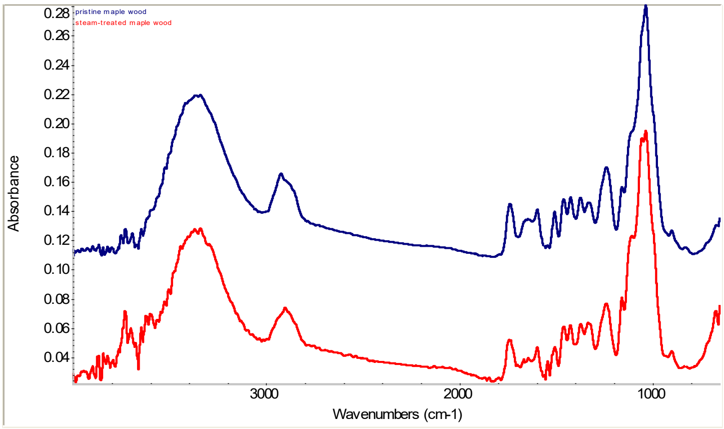

Figure 1. FTIR-ATR spectra of pristine maple wood (blue) and steam-treated maple wood (red), the entire middle infrared region.

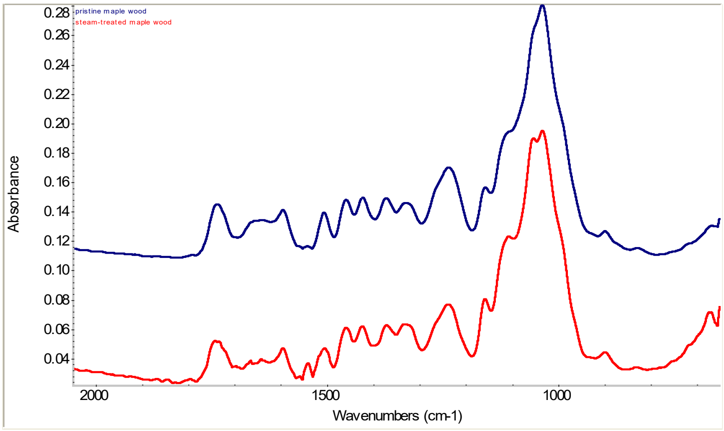

Figure 2. FTIR-ATR spectra of pristine maple wood (blue) and steam-treated maple wood (red), area of deformation vibrations.

CONCLUSION

The influence of steam treatment on the surface properties of maple wood was investigated. The increase of hydrophobicity of maple wood has been found after saturated steam modification. The increase of water contact angle on the surface of steam-treated maple wood surface was confirmed. FTIR-ATR measurements results of steam-treated maple wood confirmed a decrease in oxygenic functional groups content as well as an increase in carbon content on the steam-treated maple wood surface.

ACKNOWLEDGEMENTS

This work was supported by the Slovak Research and Development Agency under the contracts No. APVV-16-0177, APVV-17-0456, APVV-20-0159 and APVV-21-0051. This work was supported by the project VEGA 1/0264/22.

REFERENCES

1. Bekhta, P., Mamoňová, M., Sedliačik, J., Novák, I. (2016). Anatomical study of short-term thermo-mechanically densified alder wood veneer with low moisture content. European Journal of Wood and Wood Products 74(5), 643-652.
2. Bekhta, P., Proszyk, S., Krystofiak, T., Sedliačik, J., Novak, I., Mamoňová, M. (2015). Effects of short-term thermomechanical densification on the structure and properties of wood veneers. Wood Material Science and Engineering 12(1), 40-54.
3. Kol, H.Ş. (2009a). The transverse thermal conductivity coefficients of some hardwood species grown in Turkey. Forest Products Journal 59(10), 58-63.
4. Kol, H. Ş. (2009b). Effect of some chemicals on thermal conductivity of impregnated laminated veneer lumbers bonded with polyvinyl acetate and melamine-formaldehyde adhesives. Drying Technology 27(9), 1010-1016.
5. Gaff, M., Babiak, M., Vokatý, V., Gašparík, M., Ruman, D. (2017a). Bendability characteristics of hardwood lamellae in elastic region. Composites Part B: Engineering 116, 61-75.
6. Gaff, M., Gašparík, M., Babiak, M., Vokatý, V. (2017b). Bendability characteristics of wood lamellae in plastic region. Composite Structures 163, 410-422.
7. Adl-Zarrabi, B., Boström, L. (2004). Determination of thermal properties of wood and wood based products by using transient plane source. In: Proceedings of the 8th World Conference on Timber Engineering, WCTE 2004, Lahti, Finland, pp. 604.
8. Akoshima, M., Baba, T. (2006). Study on a thermal-diffusivity standard for laser flash method measurements. International Journal of Thermophysics 27(4), 1189-1203.
9. TenWolde, A., McNatt, J. D., Krahn, L. (1988). Thermal properties of wood and wood panel products for use in buildings. INC. DOE/USDA-21697/1, USDA Forest Service, Madison, USA.
10. Kvietková, M., Gaff, M., Gašparík, M., Kaplan, L., Barcík, Š. (2015). Surface quality of milled birch wood after thermal treatment at various temperatures. BioResources 10(4), 6512-6521.
11. Yin, Y., Berglund, L., Salmen, L. (2010). Steam-Treatment Effects on Wood Cell Walls. Biomacromolecules 12(1), 194-202.

CHIP AND CHIPLESS WOODWORKING PROCESSES, 13(1): 151–159, 2022
Zvolen, Technical University in Zvolen, ISSN 1339-8350 (online), ISSN 2453-904X (print)

EFFECT OF PRESS DRYING ON DIMENSION STABILITY AND DENSITY OF BEECH WOOD

Ivan Klement[1] – Peter Vilkovský[1] – Tatiana Vilkovská[1] – Jacek Barański[2] – Aleksandra Suchta[2]

Abstract

Timber is traditionally dried in kilns by processes that often take several days or weeks to complete. At present, it is possible to apply several methods of rapid drying of timber, including, for example, press drying. This research is based on the use of this process. Drying was performed using the heating plates with a temperature of 160 °C. Three pressures were compared in the research 1.0 MPa, 1.4 MPa, and 1.8 MPa. The density of the samples remarkably increased during press drying. The pressure of the heating plates had a substantial effect. The difference in the average density between the pressure of 1.0 MPa and 1.8 MPa was more than 92 kg.m^{-3}. A larger increase in density was discovered for radial samples (ranging between +95.31 to+110.85). The difference in the change of sample thickness was larger in the case of the tangential samples. For both groups of samples (radial, tangential) and all pressures, the samples dried by the contact method were more stable during swelling than the samples dried by the convection method.

Key words: press drying; beech wood; density, dimension stability, pressure

INTRODUCTION

The timber is traditionally dried in kilns by processes often taking several weeks. According to the research [1] should press drying understood as a method of rapidly removing water from the wood. The process of press drying can be defined as the application of heat to the opposite surfaces of timber by heating plates to remove moisture from the timber. Temperatures for press drying range from 130 up to 190 °C. During drying, the heat is transferred, mainly by conduction [2]. However, this rapid removal of water and the high-temperature cause modification in the wood such as darkening of natural colour in the case of some tree species. Press drying offers many advantages such as keeping the wood flat during drying, short time of drying, etc. Based on the research [3] the sawing pattern did not affect the drying time to a large extent. Following the paper showing [4] that a 10-minute difference can occur between a quarter-sawn board and flatsawn. The author of [5] mentioned in his work that drying time for beech wood was only 2 hours from 80% to 3% of moisture content (MC). In addition, contact drying can affect the dimensional stability or density of dried samples, as evidenced by several studies [6,7]. According to work [6] was performed on 24 mm-thick specimens from three species of coniferous wood

---

[1]Technical University in Zvolen, T. G. Masaryka 24, 960 01 Zvolen
e-mail: peter.vilkovsky@tuzvo.sk, klement@tuzvo.sk
[2]Gdansk University of Technology, G. Narutowicza 11/12, 80-233 Gdansk, Poland
e-mail: aleksandra.konopka@pg.edu.pl, jacek.baranski@pg.edu.pl

(pitch pine, larch, and white pine) where press dried under two-platen pressures of 0.17 and 0.34 MPa to obtain drying information regarding drying rate, thickness shrinkage, and drying defects. The influence of platen pressure on drying fare in the range of moisture content (30 to 10%) increased for pitch pine and larch but reduced for white pine at higher pressure. Thickness shrinkage was increased at the higher pressure, and estimated thickness shrinkage at final MC of 10 percent became unrealistically greater for specimens containing higher final moisture content under the influence of compressive strain. Comparable observations [7] were researched density profiles by hot-press drying. Specimens were oven-dried temperatures at 115, 135, 160, 185, and 205°C, respectively. The thickness of the sample was dimensions of 50 mm (longitudinal) by 50 mm (tangential). Drying was under way placed between two plates with a pressure of 3.5 MPa applied in the radial direction. Hot-press drying created an M-shaped curve of density: high density at the two surface regions that gradually decrease toward the core region. During hot-press drying, wood became plastic and could undergo large deformation under the combined effect of moisture, high temperature and mechanical compression. As the drying process progressed, heat and water evaporation gradually moved inwards and resulted in the densification of the core layer. Consequently, surface regions in the timber were compressed more than core regions and a density profile is created. Surface regions had a density from 600 to 850 $kg.m^{-3}$ and the core regions had a density only ranging between 400-450 $kg.m^{-3}$.

Next observations [8] investigated the effect of heating platens temperature on the temperature and pressure inside poplar timber was investigated. Samples of poplar timber were with dimensions 400 × 120 × 25 mm (l × t × r). Results showed when the heating platens' temperature increase from 120 to 140 °C, the maximum values of temperature and pressure also increase by 14.5 and 26.2%, respectively. Moisture at the centre layer of poplar timber with MC above FSP was in a liquid state, i.e., unsaturated water under overpressure conditions in the hot-press drying process. Flashing occurred to the unsaturated water in poplar timber during the opening period of heating platens and resulted in the decrease in MC. This phenomenon was the main moisture transfer mode in the wood hot-press drying process with MC above FSP.

The objective of this research was to evaluate the effect of press drying process on the density and dimensional stability of beech wood with the use of different pressures.

MATERIAL AND METHODS

Beech wood (*Fagus sylvatica* L.) were used for the experimental measurements. The Sample were chosen from two beech logs with a diameter of 40 cm and the length of 300 cm. The forest located in the part called Môťová (475 m.a.s.l.) belonging to the University Forest Enterprise of the Technical University in Zvolen, Slovakia.

Radial and tangential samples were cut out (*longitudinal and cross section sawing)* from the log, according to sawing patterns (Fig. 1). Dimensions of drying samples were 120×800×30 mm (w × l × t).

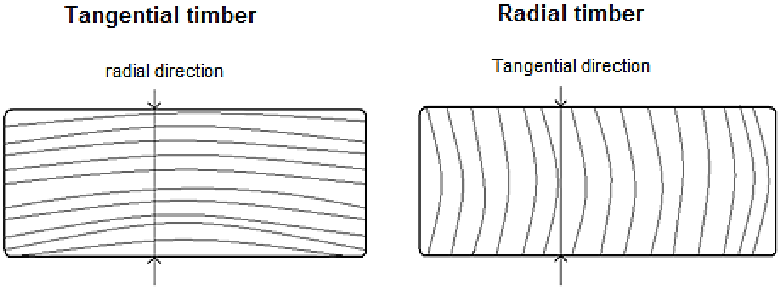
Tangential timber

Radial timber

Fig. 1 Radial and tangential samples used in contact drying

The process of press drying was conducted in hydraulic single storied press type CBJ 500 - 5 (TOS RAKOVNIK). Temperature of the heating plates was 160 °C. Used were three specific plate pressures of 1.0, 1.4 and 1.8 MPa. The group of samples were dried until the temperature measured in the centre of the sample reached the temperature of the pressing plate (t_p = 5°C). The press drying in the was completed at that time. One filling always consisted of samples from one radial and one tangential log (R and T).

The regime of contact drying was consisting of three phases (I - III.). Samples were dried at a constant temperature (II.) after gradual rise in temperature (I.) to 160 °C. The cooling phase was (III.) after reaching the desired temperature in the centre of the samples. The last phase was air conditioning at 20 °C.

Convection hot air drying in the Memmert HCP laboratory dryer was used to compare the changes in the monitored properties of the sample groups. The standard drying regime according to ON 490651 for the given wood species, thickness, and initial moisture were used. The samples were also cut to determine initial moisture content and density as well (Fig. 4). Initial MC and final MC of wood was determined using the gravimetric method according to STN EN 49 0103. The moisture content was calculated using Eq. 1,

$$MC = \frac{m_w - m_0}{m_0} \cdot 100 \ (\%) \qquad (1)$$

Where: mw is the weight of the wet sample (g) and m0 is the weight of the absolutely dry sample (g)

Density in oven-dried state was measured before and after drying. The measurement was performed under laboratory conditions. The density (ρ_0) of wood at 0% moisture content was measured according to STN EN 49 0108. The oven-dried density was calculated using Eq. 2,

$$\rho_0 = \frac{m_0}{V_0} \ (\text{kg.m}^{-3}) \qquad (2)$$

Where: m_0 is the weight of oven-dried moisture samples (kg) and V_0 is the volume of oven-dried moisture samples (m^{-3}).

Thickness and width of the samples were measured before and after every contact drying with an accuracy of 0.01 mm. The samples were placed in an air-conditioning chamber at a temperature of 20 °C and a relative humidity of 60% after contact drying. Similarly, samples after convection drying were measured and conditioned. The dimensions of the samples were measured again after conditioning (Fig. 2).

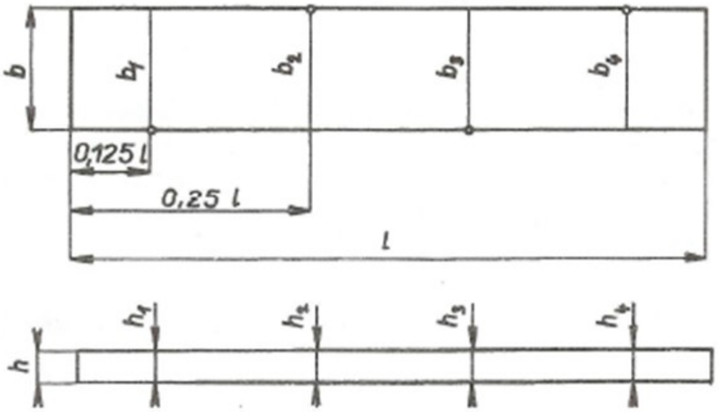

Fig. 2 Scheme of measuring the thickness and width of samples

All samples were still conditioned to an equilibrium moisture content of ≈20% and then the thicknesses and widths of the samples were measured (Fig. 4 and 5). From these values, the stabilizing effect of contact drying on the width using the anti-drying factor was evaluated:

$$F_b = \frac{b_{KV} - b_{KT}}{b_{KV}} \cdot 100 \qquad (\%) \tag{3}$$

Where: b_{KV} swelling of wood in width, dried by convection, transferred from one state of moisture balance to another (%),

b_{KT} - swelling of wood in width, determined by the contact method, transferred from one wood state of moisture balance to another (%).

Effect of contact drying on thickness:

$$F_h = \frac{h_{KV} - h_{KT}}{h_{KV}} \cdot 100 \qquad (\%) \tag{4}$$

Where: h_{KV} Swelling of wood in thickness, dried by convection, transferred from one state of moisture balance to another (%),

h_{KT} - Swelling of wood in thickness, dried by the contact, method transferred from one state of moisture balance to another (%).

RESULTS AND DISCUSSION

Table 1 shows the measured average values of the initial and final humidity of individual groups of samples and the total time of contact drying. The average values of the density of the samples in the dry state before and after drying and the increase in the average density of the samples due to contact drying are also shown here.

Tab. 1 Initial and final moisture of the samples, drying time, and density of the samples

Type of samples	Pressure of plates (MPa)	MC (%)		Drying time (min)	Density ρ0 (kg.m-3)		
		Initial	Final		Before drying	After drying	Change of density (kg.m-3)
Radial	**1.0**	77.48	3.95	80	675.61	770.92	+95.31
	1.4	80.27	6.08	80	684.16	785.15	+100.99
	1.8	69.5	5.52	90	675.62	786.47	+110.85
Tangential	**1.0**	71.87	5.78	100	669.93	722.07	+52.14
	1.4	54.14	5.37	110	663.08	752.35	+89.27
	1.8	55.54	4.87	90	666.95	774.85	+107.90

It can be seen from the measured data that the initial moisture content of the samples was from 54.14 to 80.27% and the final moisture content was from 3.95 to 6.08%. Drying time was shorter for radial samples, while plate pressure had no effect on drying time, nor was the effect of sample type significant. As a result of contact drying, the density of the samples increased by an average of 92 kg.m^{-3}, while the influence of plate pressure on the density value was confirmed. A larger increase in density was discovered for radial samples (ranging between +95.31 to +110.85 kg.m^{-3}). This difference was caused by the direction of the plate pressure. In the case of radial samples, the direction of the pressure was tangential, the densification, and thus the increase in density was greater. For tangential samples was an increase ranging from +52.14 to +107.90 kg.m^{-3}. Similarly, observations [7] were researched density profiles by hot-press drying at temperatures of 115, 135, 160, 185, and 205°C, respectively, and a pressure of 3.5 Mpa which was applied in the radial direction. Results showed that drying for these conditions creates an M-shaped curve of density: high density at the two surface regions that gradually decreased toward the core region. Surface regions had a density from 600 to 850 kg.m^{-3} and the core regions had a density only ranging between 400-450 kg.m^{-3} The next study [6] similarly discovered that contact drying can affect the density of dried samples.

The change in the dimensions of the samples depending on the drying time is shown in Figures 3, 4 and 5.

The impact of plate pressure during contact drying was more remarkable for tangential samples, where a thickness change of 6.75% was measured at a pressure of 1.0 Mpa and a 23.3% change in thickness at a pressure of 1.8 Mpa (Fig. 4). In the case of radial samples, the impact of plate pressure was almost insignificant and the differences in the change in the thickness of the samples, at individual pressures, were less than 1.0% (Fig. 3). The differences in the change of the thickness of the samples were caused by the fact that the direction of the pressure is in the tangential direction for the radial samples and in the radial direction for the tangential samples. The values of the change in the width of the samples are significantly smaller than the change in thickness (less than 3%). The effect of pressure on the change in width was confirmed for both radial and tangential samples (Fig. 5). However, the effect of plate pressure is opposite to the change in thickness. As the pressure of the plates increased, the change in the width of the samples was smaller. Greater values of the change in width were observed when evaluating the change in this dimension after conditioning the samples to a humidity of 12%. Research [6] was performed on 24 mm-thick specimens using three species of coniferous wood (pitch pine, larch, and white pine) where press dried under two-platen pressures of 0.17 and 0.34 Mpa. The initial moisture content of samples was from 30 to 89%. Results confirmed that thickness shrinkage was caused by increased at the higher pressure.

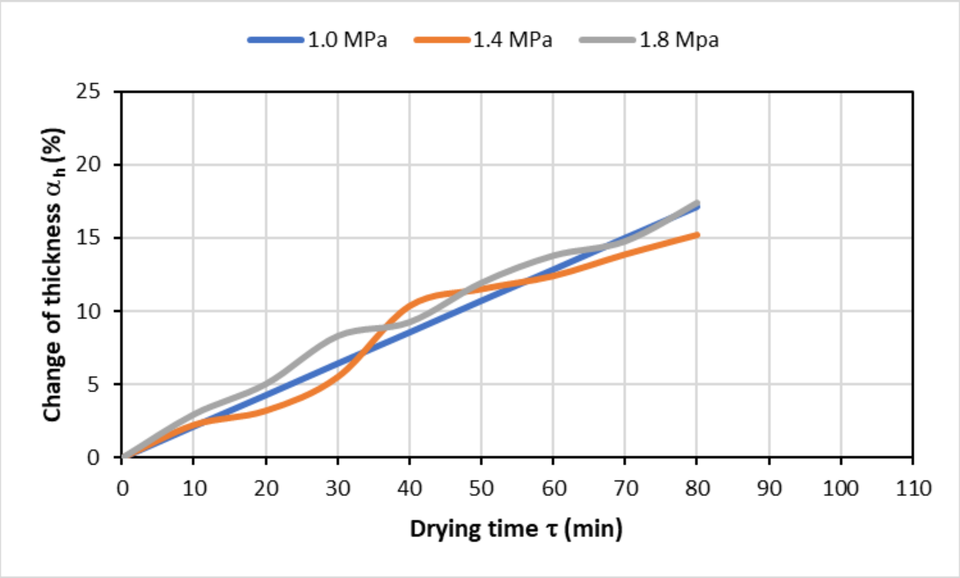

Fig. 3 Thickness change at different contact drying pressures – radial samples

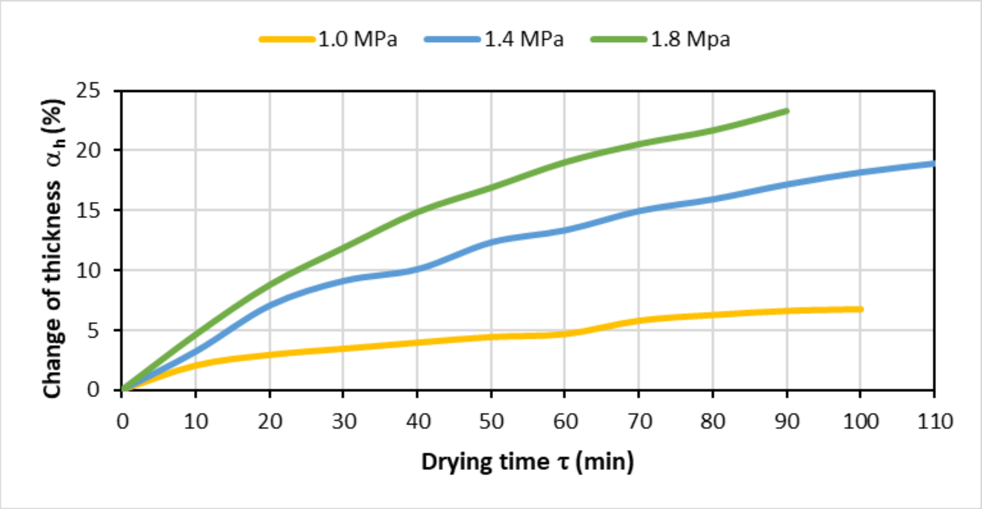

Fig. 4 Thickness change at different contact drying pressures – tangential samples

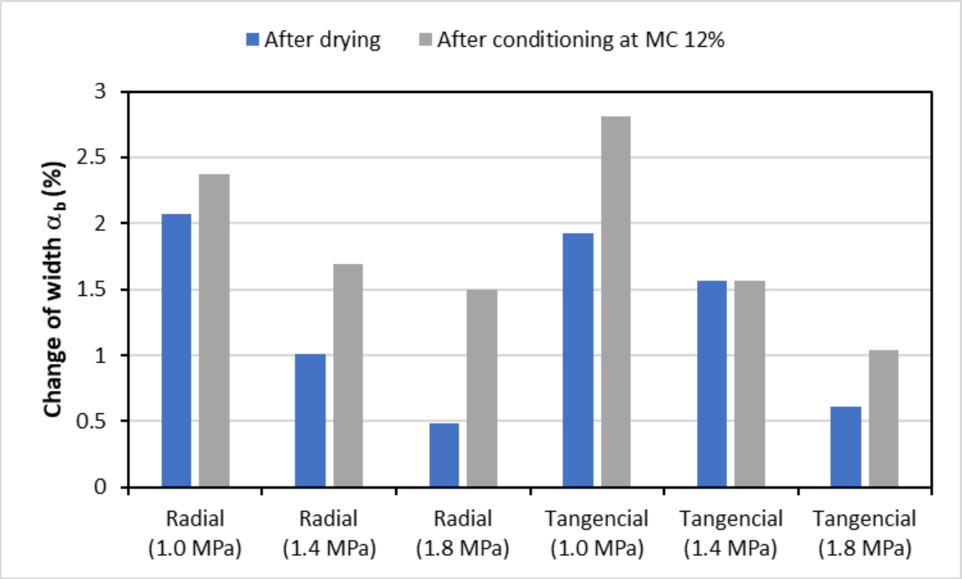

Fig. 5 Width change at different contact drying pressures and samples

Based on the measured changes in the dimensions of the group of samples during contact and convection drying, the values of the anti-drying factor were calculated (tab. 2 and 3).

Tab. 2 Dimensional change during contact and convection drying and anti-drying factor: radial samples

Measurements	Press drying						Convection drying	
	Pressure 1.0 Mpa		Pressure 1.4 Mpa		Pressure 1.8 Mpa			
	Thickness	Width	Thickness	Width	Thickness	Width	Thickness	Width
Before drying (mm)	30.19	110.39	31.10	111.37	30.19	110.66	30.91	110.45
After drying (mm)	25.03	108.10	26.45	110.25	24.83	110.12	28.24	107.61
After air conditioning MC=12% (mm)	25.82	107.77	26.65	109.49	25.09	109.00	27.37	105.59
After air conditioning MC=20% (mm)	28.09	109.56	29.32	111.59	27.74	111.21	28.42	109.42
The difference before and after drying (%)	17.09	2.07	14.95	1.01	17.75	0.49	8.64	2.57
Difference after air conditioning from 12% to 20% (%)	8.08	1.63	9.12	1.88	9.54	1.99	3.70	3.50
Factor F_h / F_b (%)	**-118.3784**	**53.4286**	**-146.4865**	**46.2857**	**-157.8378**	**43.1429**	**-**	**-**

Tab. 3 Dimensional change during contact and convection drying and anti-drying factor: tangential samples

Measurements	**Press drying**						**Convection drying**	
	Pressure 1.0 Mpa		**Pressure 1.4 Mpa**		**Pressure 1.8 Mpa**			
	Thickness	**Width**	**Thickness**	**Width**	**Thickness**	**Width**	**Thickness**	**Width**
Before drying (mm)	30.3	110.68	30.41	110.65	29.97	110.51	30.61	110.55
After drying (mm)	26.96	108.55	25.03	108.92	23.47	109.84	29.38	106.25
After air conditioning MC=12% (mm)	27	107.57	24.95	108.92	23.19	109.36	28.59	105.03
After air conditioning MC=20% (mm)	28.77	108.78	26.63	110.30	24.88	110.95	29.69	110.09
The difference before and after drying (%)	11.02	1.92	17.69	1.56	21.69	0.61	4.02	3.89
Difference after air conditioning from 12% to 20% (%)	6.14	1.11	6.32	1.25	6.81	1.43	3.7	4.6
Factor F_h / F_b (%)	**-65.95**	**75.87**	**-70.81**	**72.83**	**-84.05**	**68.91**	-	-

The anti-drying factor F inform the stabilizing effect of contact drying compared to convection drying. The results of F_b mean that for both groups of samples and all pressures. The samples dried by the contact method are more dimension stable in swelling than the samples dried by the convection method. For thickness swelling. The calculated F_h values were negative.

This means that the thickness swelling of the samples during contact drying was greater by the indicated F_h values at all pressures compared to convection drying. The bigger difference was at the radial samples.

CONCLUSION

The aim of the work was to determine the effect of contact drying on the change in thickness and width of the samples. well as the overall dimensional stability and change in density due to the different pressure used during contact drying. Samples with a thickness of 30 mm with radial and tangential course of annual rings were used for drying. Drying was carried out at a temperature of heating plates of 160 °C and a pressure of 1.0 MPa. 1.4 MPa and 1.8 MPa. The results were compared with classic hot air drying.

The following conclusions can be drawn from the measured data:

- Contact drying is very intensive, and a low final moisture was achieved in a short drying time.
- Radial samples dried faster than tangential ones. while plate pressure did not have a significant effect on drying time. during contact drying. the density of the samples increased significantly. the pressure of the plates had a significant effect on the density increase.
- In radial samples. the density increased by an average of 102 kg.m^{-3} and in tangential samples by 83 kg.m^{-3}.
- The average thickness change for radial samples was 16.6%. while plate pressure had no significant effect. In the case of tangential samples. the influence of plate pressure was significant and the change in the thickness of the samples was in the interval from 7 to 23%.
- The change in width of the samples during contact drying was almost the same for radial and tangential samples. with the largest values at the lowest plate pressures.

- For both groups of samples (radial. tangential) and all pressures. the samples dried by the contact method were more stable during swelling than the samples dried by the convection method.
- Thickness swelling of the samples during contact drying was greater compared to convection drying. The bigger difference was with the radial samples.

ACKNOWLEDGEMENTS

This work was supported by the Scientific Grant Agency of the Ministry of Education. science. research and sport of the Slovak Republic and the Slovak Academy of Sciences - project VEGA No. 1/0063/22.

This work was supported by the Slovak Research and Development Agency under the Contract no. APVV-21-0049.

REFERENCES

1. Hittemeier. M.E.. Comstock G.L.. and Hann. R.A.. (1968). Press drying nine species of wood. Forest Product Journal. 1968. 18(9):91-96.
2. Heebink. B. G.. Compton. K. C. (1966). Paneling and flooring from low-grade hardwood logs. Forest Product Laboratory. 1966. Note FPL-0122. pp. 23
3. Simpson. T. W. (1983). Maintaining timber quality in press drying by manipulating sawing patterns. Wood and Fiber Science. 1984. 16(3): 411-426.
4. Schmitdt. J. (1967) Press drying of wood. Forest product journal 8(4) pp71-76
5. Chen. P. Y. S.. Biltonen. F. E. 1979. Effect of Prefreezing on Press-Drying of Black Walnut Heartwood. Forest Product Journal. 1979. 29(2): 48−51.
6. Jung. S. H.. Lee. H. N.. Yeo. H. (1993). Press-drying of Plantation Softwood Lumber. Journal of the Korean Wood Science and Technology 21(3)
7. Zhou. F.. Gao. X.. Fu. Z.. Zhou. Y. (2018). Drying kinetics of poplar lumber during periodic hot-press drying. Drying Technology. DOI: 10.1080/07373937.2018.1426597
8. Hou. J.. Yi. S.. Zhou. Y.. Pin. B. (2018). Moisture state variety in poplar lumber with moisture content above fibre saturation point during hot-press drying. Journal of Wood Science. (2018) 64:730–737 DOI: 10.1007/s10086-018-1759-z

NORMS:

STN 490 108 (1993). “Wood. Determination of density.” Slovak Standards Institute. Bratislava. Slovakia.

STN 490 103 (1993). “Wood. Determination of the moisture content of the physical and mechanical testing.” Slovak Standards Institute. Bratislava. Slovakia.

Spoločnosť AREKO, s.r.o. a Technická univerzita vo Zvolene majú dlhodobú spoluprácu v rámci dodávania záznamových a meracích prístrojov, senzorov, softvéru a kalibrácií. V rámci drevárskej fakulty sa prístroje využívajú napr. na katedre drevených stavieb pre výskum vlhkostných a tepelných vlastnosti drevených konštrukcií, tepelno-technických vlastností okien na báze dreva, energetickej náročnosti stavieb a kvality vnútorného prostredia drevostavieb.

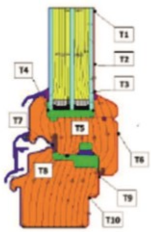

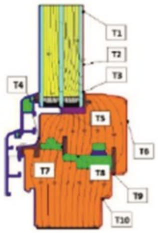

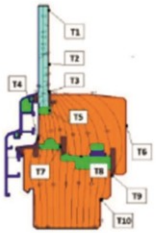

Využívané sú prístroje ako ALMEMO typ MA 5690 – 1 , snímač teploty, vlhkosti a tlaku vzduchu FHAD46C0, snímač koncentrácie CO2 FYA600CO2, snímač koncentrácie formaldehydu vo vzduchu FYA600CH2O, ALMEMO METEO-MULTISENZOR FMD760, ALMEMO 202 a iné. Pomocou prístrojového vybavenia Areko bol zrealizovaný napr. aj výskum vplyvu konštrukcie drevených a drevo-hliníkových okien na povrchové teploty.

V súčasnosti prebiehajú v dlhodobom horizonte výskumy vlhkostných a tepelných vlastností obalových konštrukcií na báze dreva v referenčnom výskumnom objekte v areáli TU vo Zvolene, ako aj na reálnych obývaných stavbách. Taktiež dôležitým prebiehajúcim výskumom je aj mapovanie parametrov obytnej vnútornej klímy ako teplota, vlhkosť, stav CO2 a formaldehydu.

tzv. syndróm chorých budov

ALMEMO® 2490
M 0
°C
15.3
MAX
M▲
MIN
MEM
ON OFF
CLR
M▼

CHIP AND CHIPLESS WOODWORKING PROCESSES, 13(1): 161–168, 2022
Zvolen, Technical University in Zvolen, ISSN 1339-8350 (online), ISSN 2453-904X (print)

INFLUENCE OF HEAT TREATMENT OF WOOD ON CHIP SIZE DURING MILLING

Martin Kučerka[1] **– Alena Očkajová**[1] **– Richard Kminiak**[2]

Abstract

The aim of the paper is to determine and compare the particle size analysis of chips resulting from the milling process of natural and heat-treated oak and spruce wood at different temperatures (160 °C, 180 °C, 200 °C and 220 °C). The individual percentages were divided according to the mesh size of the sieves into a coarse fraction using a mesh size of 2 mm and 1 mm, a medium coarse fraction with a mesh size of 0.5 mm and 0.250 mm and a fine fraction with a mesh size of 0.125 mm; 0.08 mm; 0.063 mm; 0.032 mm and the bottom of the screening machine, depending on the type of wood and the treatment temperature. When milling oak, the highest proportion of fine particles was recorded at a treatment temperature of 220 °C - 13.18 %. In this way, we can state that the milling showed the effect of a decrease in the mechanical properties of wood with increasing treatment temperature, which is more brittle. The percentage of the finest particles in spruce wood increases with increasing treatment temperature, from 0.53 % in the milling of natural wood to 11.29 % in the milling of heat-treated wood at 220 °C.

Key words: *thermowood, milling, wood dust, granular analysis, fine particles*

INTRODUCTION

Thermowood is a heat-treated wood with specific and very interesting properties, which are studied from many points of view. It is examined from the point of view of changes in physical-mechanical properties, chemical properties (Reinprecht & Vidholdová, 2008; Kačíková & Kačík, 2011; ThermoWood Handbook, 2003; Čabalová, et al. 2016), the quality of the obtained surface (Kvietková et al. 2015, Vančo et al., 2017), wood colors, machinability (Očkajová et al., 2020a; Očkajová et al., 2020b; Kráľ & Hrázský, 2005; Sandak et al., 2017), machinability in the context of energy consumption (Kubš et al., 2016), weather effects, granulometry of the resulting chips (Barcík & Gašparík, 2014), resp. sawdust (Dzurenda et al., 2010), etc. To make the use of heat-treated wood adequate, it is necessary to know its behavior in all possible areas of use. It is not enough to have information only about the change in its properties due to heat treatment, but also about the technologies of its treatment and possible risks (Rogozinski et al., 2017; Marková et al., 2016; Martinka & Rantuch, 2013; Kminiak et al., 2020).
The essence of heat, steam, and water treatment is that no harmful chemicals are used to change the properties of wood, and the result is wood, with new physicomechanical properties, which are reflected in increased dimensional stability and biological resistance and other performance properties of tropical woods (Hlásková et al., 2015; Igaz et al., 2019;

---

[1] Matej Bel University, Tajovského 40, 974 01 Banská Bystrica
[2] Technical University in Zvolen, T. G. Masaryka 24, 960 01 Zvolen
e-mail: martin.kucerka@umb.sk, alena.ockajova@umb.sk, richard.kminiak@tuzvo.sk

Očkajová & Kučerka, 2018; Očkajová et al., 2019; Mikušová et al., 2019; Kučerka & Očkajová, 2018; Tepelně upravené dřevo Thermo Wood, 2013).

In terms of machining, heat-treated wood has no limitations compared to natural wood. The only problem can be that the processing of wood (whether natural or heat-treated) is always accompanied by the formation of dust particles (Marková et al., 2007; Rogozinski, 2016), which are smaller and therefore more dangerous. When heat-treated wood is used, the formation of a fine fraction of dust is caused by an increase in its brittleness and a decrease in some mechanical properties (Reinprecht & Vidholdová, 2008; Kráľ & Hrázský, 2005; Očkajová et al., 2018; Korčok et al., 2019).

The purpose of the work is to determine the particle size distribution of chips formed from the oak and spruce wood depending on the heat treatment (160 °C, 180 °C, 200 °C and 220 °C), in selected parameters of cutting speed 40 $m.s^{-1}$ and feed rate 15 $m.min^{-1}$, focusing on the fine fraction of the chips formed.

MATERIAL AND METHODOLOGY

Experimental samples:

Winter oak (Quercus petraea) and Norway spruce samples (Picea abies) measuring 20 x 100 mm with a length of approximately 700 mm came from the location Vlčí jarok (Budča). They were dried to a moisture content of 8%. The drying process was carried out in the Research and Development Institutions of the Technical University of Zvolen.

Furthermore, the samples were heat treated in the FLD Arboretum (Czech University of Agriculture in Prague) in the town of Kostelec nad Černými lesy. Chamber S400 / 03 (LAC Ltd., Czech Republic) was used for heat treatment, Fig. 1, designed for the heating (treatment) of wood with ThermoWood technology. Five samples of each tree were prepared for the experiment.

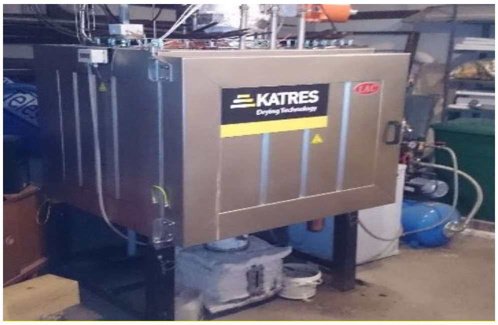

Fig. 1 Chamber S400/03

The thermal modification took place at selected temperatures in six phases:

- phase 1 - raising the temperature to 40 °C,
- phase 2 - raising the temperature to 130 °C, drying,
- phase 3 - heat treatment - heating to working temperature,
- phase 4 - heat treatment - working temperature for 3 hours,
- phase 5 - cooling to 130 °C and humidity adjustment,
- phase 6 - cooling to a temperature of 60 °C with humidity adjustment at the level of 4 – 8 %.

After reaching a temperature of 60 °C, the entire process was completed.

Machinery

The experiment was carried out on the spindle milling machine ZDS-2 (Liptovské strojárne) with the Frommia ZMD 252/137 feed mechanism.

Equipment - milling head FH 45 Stanton SZT (Turany, Slovakia), with the parameters: diameter of milling head - 125 mm, diameter of milling head with protruding blade 130 mm, thickness of milling head 45 mm, number of blades 2, cutting material – steel MAXIMUM SPECIAL 55: 1985/5, front rake angle $\gamma = 25$ °.

Cutting conditions:
cutting speed $v_c = 40$ m.s^{-1}
feed rate $v_f = 15$ m.min^{-1}
thickness of the cut layer = 1 mm

Granulometric analysis

The granulometric composition of the sawdust was determined by sieve analysis. For this purpose a special set of sieves on top of one another was used (2 mm; 1mm; 0.5 mm; 0.25 mm; 0.125 mm; 0.080 mm; 0.063 mm; 0.032 mm and the bottom), placed on the vibration stand of a sieving machine (Retsch AS 200c), with a settable frequency for interrupting the sieving (20 seconds) and with an amplitude for deviating the sieves (2mm/g), in line with the STN 153105/ STN ISO 3310-1.

Granulometric composition was obtained by weighing the shares remaining on the sieves after sieving on an electronic laboratory Radwag WPS 510/C/2 scale (Radwag Balances and Scales, Radom Poland), with a capacity of 510 g and a precision of weighing of 0.001g. For each variant three sievings were done and the results are given as their average value.

RESULTS AND DISCUSSION

The results of granulometric analyzes are given in Tables 1 and Table 2, on the basis of which the residue curves are constructed according to the methodology (Kučerka & Šustek, 2006). Individual percentages were divided according to the mesh size of the sieves, namely the coarse fraction using a mesh size of 2 mm and 1 mm, the medium coarse fraction using a mesh size of 0.5 mm and 0.250 mm and the fine fraction, using a mesh size of 0.125 mm; 0.08 mm; 0.063 mm; 0.032 mm and the bottom of the screening machine, depending on the type of wood and the treatment temperature.

Tab. 1 Granulometric analysis of natural and heat-treated oak wood according to heat treatment

Mesh size [mm]	Percentage of fractions [%]				
	Winter oak				
	natural	**160 °C**	**180 °C**	**200 °C**	**220 °C**
2	46	7,97	6,12	7,92	6,36
1	33,6	33,56	26,12	26,92	20,91
0,5	14,4	36,45	40,82	38,69	32,27
0,25	4,8	17,08	20,82	20,36	27,27
0,125	0,8	3,8	4,49	4,75	9,55
0,08	0,4	0,76	0,82	0,9	2,27
0,063	0	0,38	0,41	0,23	0,91
0,032	0	0	0,41	0,23	0,45
dno	0	0	0	0	0
particles < 100 μm	1,2	4,94	6,13	6,11	13,18

In the case of oak longitudinal milling chips (Table 1), with increasing treatment temperature, an increased proportion of mainly medium-sized chips (sieves of 0.5 and 0.25 mm) and also a proportion of fine chips, particles of size 0.125 mm. The highest proportion of fine fraction was recorded at a treatment temperature of 220 °C - 13.18 %. Natural oak is dominated by chips in the sieves (2 mm 1 mm and 0.5 mm) and the proportion of fine fraction and dust is approximately 1.2 %, so it can be stated that the grinding showed a decrease in the mechanical properties of wood with increasing treatment temperature, which is more fragile and manifested itself only in the formation of the dust fraction (Reinprecht & Vidholdová, 2008). This change occurs immediately with a treatment temperature of 160 °C.

Tab. 2 Granulometric analysis of natural and heat-treated spruce wood depending on heat treatment

Mesh size [mm]	Percentage of fractions [%]				
	Norway spruce				
	natural	**160 °C**	**180 °C**	**200 °C**	**220 °C**
2	73,16	76,4	51,05	17,01	4,03
1	20,53	18,63	34,97	32,65	25
0,5	4,21	3,11	11,19	29,93	35,48
0,25	1,58	1,24	2,1	14,97	24,19
0,125	0,53	0,62	0,7	4,08	6,45
0,08	0	0	0	1,36	2,42
0,063	0	0	0	0	1,61
0,032	0	0	0	0	0,81
dno	0	0	0	0	0
particles < 100 μm	0,53	0,62	0,7	5,44	11,29

In the case of coniferous spruce wood and in the chips from the milling process of this wood, the particle size distribution of the sawdust is different from that of the oak. Similar values of chip percentages from the milling process were obtained in 2 and 1 mm sieves (the so-called coarse fraction) at natural spruce and treatment temperatures of 160 and 180 °C, where the coarse fraction was approximately 86.02 ÷ 95.03 %. A significant difference was recorded at a treatment temperature of 200 °C, where the share of the coarse fraction dropped by approximately half compared to natural wood, and at a temperature of 220 °C, the value of the coarse fraction dropped to one third. At treatment temperatures of 200 and 220 °C, the percentages of medium-thick chips on the 0.5 mm and 0.250 mm sieves increase significantly. At a treatment temperature of 200 °C, the percentage in this sieve is 44.90 % and at a temperature of 220 °C this proportion is up to 59.67 %, compared to the proportion of this fraction 13.29 % (treatment temperature 180 °C).

The percentage of fine fraction, particles with a size ≤ 0.125 mm, ranges from 0.53 % to 0.70 % for natural wood and treatment temperatures of 160 and 180 °C, this value is 5.44 % for a treatment temperature of 200 °C, and at a treatment temperature of 220 °C it increases 2-fold.

Although 0.08 mm dust particles did not appear in natural spruce and treatment temperatures of 160 and 180 °C, at treatment temperatures of 200 and 220 °C, their percentage ranges from 1.36 % to 4.64 %, and again we can conclude a similar conclusion as for chips from the oak milling process that at higher wood treatment temperatures the proportion of medium-coarse chips, fine fraction and wood dust increases, but significant changes were recorded from 200 °C, which correlates with the authors' claims. that changes due to rising temperatures take place in conifers later than in deciduous trees due to a higher proportion of lignin (Reinprecht & Vidholdová, 2008). Kačíková & Kačík, (2011) when examining the thermal effect on spruce, state that lignin up to 180 °C first plasticizes and cellulose begins to degrade rapidly to form volatile products above 200 °C.

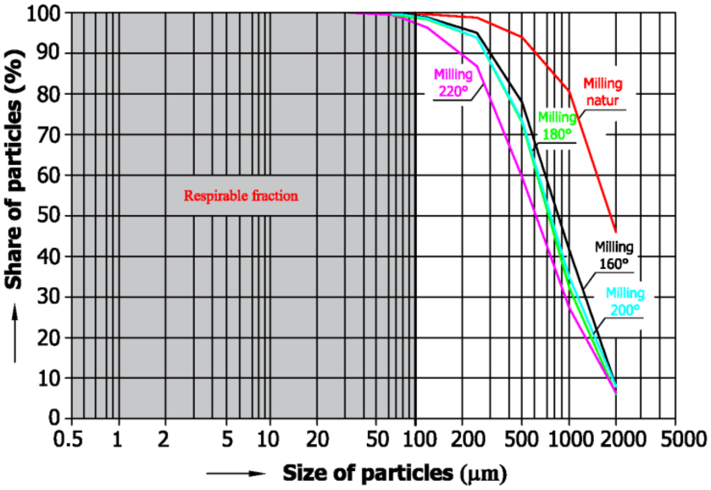

Graph 1 Residue curves for oak, depending on the treatment temperature

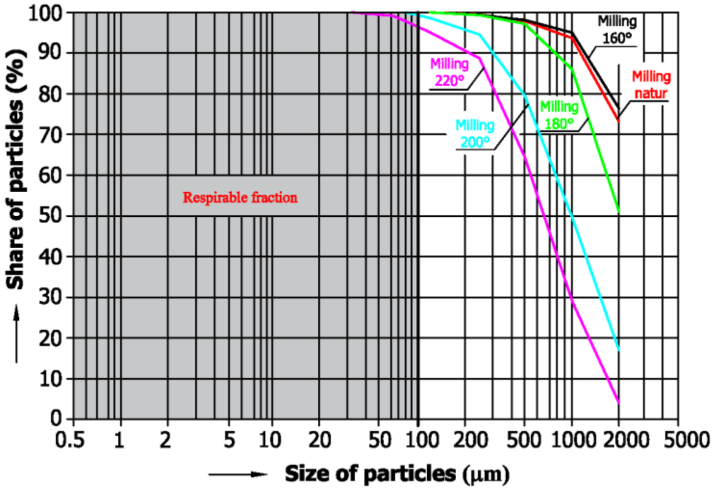

Graph 2 Residue curves for spruce wood as a function of treatment temperature

The residue curves give us a clear idea of the particle size distribution depending on the treatment temperature as well as the technology of mechanical woodworking itself. In this case, it is the technology of woodworking by milling at a feeding speed of 15 m.min^{-1}. It is clear from the residue curves that in both cases, both in the case of deciduous oak wood and in the case of coniferous spruce wood, they shift to the left to the finer particles due to the increased treatment temperature.

CONCLUSION

The results of the experimental measurements can be summarized as follows:

- with increasing oak treatment temperature, an increased proportion of mainly medium-sized chip fractions is formed in the longitudinal milling process, the proportion of fine chips, particles with a size ≤ 0.125 mm, has also increased,
- the milling of oak wood showed the effect of a decrease in the mechanical properties of the wood with increasing treatment temperature, when the wood is more brittle, and this resulted in an increase in the proportion of fine fraction up to 13.18 % at a treatment temperature of 220 °C,
- in the case of spruce wood, the proportion of fine chips increased only at a treatment temperature of 200 °C, confirming the theory of some authors that changes due to increasing temperatures take place in conifers later than in deciduous ones due to a higher proportion of lignin,
- we assume that the main factor influencing the particle size analysis of heat-treated wood in the milling process is the reduced mechanical properties of thermally modified wood, which becomes more brittle,
- the proportion of dust particles ≤ 0.08 mm in oak gradually increases from the treatment temperature of 160 °C and in the case of spruce up to the temperature of 200 °C.

This work was support by the grant agency KEGA under the project No. 026UMB-4/2021.

REFERENCES CITED

BARCÍK, Š., GAŠPARÍK, M. 2014. Effect of Tool and Milling Parameters on the Size Distribution of Splinters of Planed Native and Thermally Modified Beech Wood. In BioResources, 9(1): 1346-1360.
ČABALOVÁ, I., KAČÍK, F., ZACHAR, M., DÚBRAVSKÝ, R. 2016. Chemical changes of hardwoods at thermal loading by radiant heating. In Acta Facultatis Xylologiae. Zvolen: Technical University in Zvolen, 58(1): s. 43-50.
DZURENDA, L., ORLOWSKI, K., GRZESKIEWICZ, M. 2010. Effect of thermal modification of oak wood on sawdust granularity. In Drvna Industrija, 61(2): s. 89-94.
HLÁSKOVÁ, Ľ., ROGOZINSKI, T., DOLNY, S., KOPECKÝ, Z., JEDINÁK, M. 2015. Content of respirable and inhalable fraction in dust created while sawing beech wood and its modifications. Drewno 2015, 58, 135-146.
IGAZ, R., KMINIAK, R., KRIŠŤÁK, L., NĚMEC, M., GERGEĽ, T. 2019. Methodology of Temperature Monitoring in the Process of CNC Machining of Solid Wood. Sustainability 2019, 11(1): 95, DOI: 10.3390/su11010095.
KAČÍKOVÁ, D., KAČÍK, F. 2011. Chemical and mechanical changes during thermal treatment of wood. (Chemické a mechanické zmeny dreva pri termickej úprave). TU vo Zvolene. ISBN 978-80-228-2249-7
KMINIAK, R., SIKLIENKA, M., IGAZ, R., KRIŠŤÁK, Ľ., GERGEĽ, T., NĚMEC,M., RÉH, R., OČKAJOVÁ, A., KUČERKA, M. 2020. Effect of Cutting Conditions on Quality of Milled Surface of Medium-density Fibreboards. In BioResources. Raleigh: NC State University, 2020. ISSN 1930-2126. Vol. 15, no. 1 (2020), pp. 746-766
KORČOK, M., KOLEDA, P., BARCÍK, Š., OČKAJOVÁ, A., AND KUČERKA, M. 2019. Effect of technological and material parameters on final surface quality of machining when milling thermally treated spruce wood. In BioResources. Raleigh: North Carolina State University, 2019. ISSN 1930-2126. Vol. 14, no. 4 (2019), pp. 10004-10013

KUBŠ, J., GAFF, M., BARCÍK, Š. 2016. Factors Affecting the Consumption of Energy during the Milling of Thermally Modified and Unmodified Beech Wood. In BioResources, 11(1): 736-747.

KUČERKA, M., OČKAJOVÁ, A. 2018. Thermowood and granularity of abrasive wood dust. In Acta Facultatis Xylologiae Zvolen. Zvolen: Technická univerzita vo Zvolene, 2018. ISSN 1336-3824. roč. 60, č. 2 (2018), s. 43-51

KUČERKA, M., ŠUSTEK, J., 2006. Spracovanie a vyhodnotenie údajov sitovej analýzy v programe Excel 2000. In: Trieskové a beztrieskové obrábanie dreva 2006. V. MVK, Tatry 2006, Vydavateľstvo Technickej univerzity vo Zvolene. 2006, ISBN 80-228-1674-4, 179 – 184.

KVIETKOVÁ, M., GAFF, M., GAŠPARÍK, M., KAPLAN, L., BARCÍK, Š. 2015. Surface Quality of Milled Birch Wood after Thermal Treatment at Various Temperatures. In BioResources, 10(4): 6512-6521.

MARKOVÁ, I., VLADÁROVÁ, M., FILIPI, B., 2007. Sledovanie správania sa usadeného drevného prachu duba pri jeho teplotnom zaťažení. In: Požární ochrana, Ostrava, 12.–13. září 2007. Ostrava: SPBI, 2007, s. 322–332. ISBN 978-80-7385-009-8.

MARKOVÁ, I., MRAČKOVÁ, I., OČKAJOVÁ, A., LADOMERSKÝ, J. 2016. Granulometry of selected wood dust species of dust from orbital sanders. In Wood research, 61(6): 983-992. ISSN 1336-4561.

MARTINKA, J., RANTUCH, P., 2013. Posúdenie vplyvu veľkosti častíc dubového dreva na teplotu vznietenia rozvíreného prachu. Acta Facultatis Technicae, XVIII, 2013 (2), pp. 75–82.

MIKUŠOVÁ, L., OČKAJOVÁ, A., DADO, M., KUČERA, M., DANIHELOVÁ, Z. 2019. Thermal Treatment´s Effect on Dust Emission During Sanding of Meranti Wood. In BioResources 14(3), 5316-5326

OČKAJOVÁ, A., KUČERKA, M. 2018. Čo je Thermowood = What is Thermowood. In Technika a vzdelávanie: časopis zameraný na technické vzdelávanie v základných, stredných, i na vysokých školách, na oblasť základného a aplikovaného výskumu, aplikáciu informačných technológií vo výučbe odborných predmetov. Banská Bystrica: Vydavateľstvo Univerzity Mateja Bela - Belianum, 2018. ISSN 1338-9742. roč. 7, č. 2 (2018), s. 32-35

OČKAJOVÁ, A., KUČERKA, M., KRIŠŤÁK, Ľ., IGAZ, R. 2018. Granulometric analysis of sanding dust from selected wood species. In BioResources. 13(4), 7481-7495

OČKAJOVÁ, A., BARCÍK, Š., KUČERKA, M., KOLEDA, P., KORČOK, M., VYHNÁLIKOVÁ, Z. 2019. Wood Dust Granular Analysis in the Sanding Process of Thermally Modified Wood versus its Density. In BioResources 14(4), 8559-8572

OČKAJOVÁ, A., KUČERKA, M., KMINIAK, R., KRIŠŤÁK, Ľ., IGAZ, R., RÉH, R. (2020a). Occupational Exposure to Dust Produced When Milling Thermally Modified Wood. In International Journal of Environmental Research and Public Health [elektronický zdroj]: Open Access Journal. Basel: MDPI, 2020. ISSN 1661-7827. Vol. 17, no. 5 (2020), 1478.

OČKAJOVÁ, A., KUČERKA, M., KMINIAK, R., ROGOZIŃSKI, T. (2020b). Granulometric composition of chips and dust produced from the process of working thermally modified wood. In Acta Facultatis Xylologiae Zvolen. Zvolen: Technická univerzita vo Zvolene, 2020. ISSN 1336-3824. roč. 62, č. 1, s. 103-111.

REINPRECHT, L., VIDHOLDOVÁ, Z. 2008. ThermoWood - preparing, properties and applications. Thermodrevo - príprava, vlastnosti a aplikácie. TU Zvolen. ISBN 978-80-228-1920-6

ROGOZINSKI, T., WILKOWSKI, J., GORSKI, J., SZYMANOWSKI, K., PODZIEWSKI, P., CZARNIAK, P. 2017. Technical note: Fine particles content in dust created in CNC milling of selected wood composites. In Wood and Fiber Science, 49(4): 461-469.

SANDAK, J., GOLI, G., CETERA, P., SANDAK, A., CAVALLI, A., TODARO, L. 2017. Machinability of Minor Wooden Species before and after Modification with Thermo-Vacuum Technology. Materials 2017, 10, 121; DOI: 10.3390/ma10020121.

STN 1531 05/ STN ISO 3310-1: 2000. Súbor sít na laboratórne účely.

VANČO, M., MAZÁN, A., BARCÍK, Š., RAJKO, Ľ., KOLEDA, P., VYHNÁLIKOVÁ, Z., SAFIN, R. F. 2017. Impact of Selected Technological, Technical, and Material Factors on the Quality of Machined Surface at Face Milling of Thermally Modified Pine Wood. In BioResources, 12(3): 5140-5154.

Tepelně upravené dřevo Thermowood [online]. Opava: Specialista na finské stavební materiály, © 2013. Posledná zmena 14.6.2017 13:21 [cit. 10.4.2018].

ThermoWood Handbuch [online]. © 2003. [cit. 2010-04-10]. Dostupné z: https://asiakas.kotisivukone.com/files/en.thermowood.palvelee.fi/downloads/ThermoWood_Handbuch.pdf

CHIP AND CHIPLESS WOODWORKING PROCESSES, 13(1): 169–174, 2022
Zvolen, Technical University in Zvolen, ISSN 1339-8350 (online), ISSN 2453-904X (print)

WOOD-BEECH PANELS WITH LOW FORMALDEHYDE EMISSION

Ján Matyašovský[1] – Ján Sedliačik[2] – Igor Novák[3] – Peter Jurkovič[1] – Peter Duchovič[1] – Mariana Sedliačiková[2]

Abstract

Modification of polycondensation resins were directed to urea-formaldehyde adhesives with the application in woodworking industry. Fibril proteins of skin, mainly collagen and keratin, polymer polyphenolic molecules of vegetable tannins are significant and perspective biopolymers for selected technical applications e.g., bonding and lowering of formaldehyde from wood-beech panels. Tested modifications confirmed the influence of additives on viscosity of adhesive mixtures and their applicability for gluing of wood-based panels with enhanced bonding quality and formaldehyde emissions. Formaldehyde emissions were evaluated from five-layer plywood according to JIS A 1460 (2001): "Building boards. Determination of formaldehyde emission. Desiccator method". The gluing quality has been assessed according to standards EN 314-1 and EN 314-2 and the tested plywood meet the requirements of the standard for Class 1 – suitable for application in the interior.

Key words: *beech plywood, UF adhesive, modifier, biopolymers, gluing, formaldehyde*

INTRODUCTION

In woodworking industry, at present, polycondensation urea-formaldehyde (UF) resins are the most used adhesives for wood-based panels. Their wide utilization is allowed by their relative low price, high reactivity, availability of raw material and easy applicability, after hardening they provide transparent, but fragile bond. UF adhesives are thermo-reactive resins hardening in wide interval of temperatures with short time of condensation and they are resistant against micro-organisms. A major disadvantage is their low water and moisture resistance and consequent toxicity caused by the hydrolysis and release of formaldehyde (fd) from finished products.

Formaldehyde adversely affects the respiratory system, eyes, skin, genetic material, reproductive organs, and has a strong effect on the central nervous system (Příhoda 1988).

On the market, there is large number of biopolymers, which as secondary raw material can be used for modification of adhesives with the aim to keep and/or increase the quality of adhesives and glued joints. Leather and food industry produces amount of different biopolymer waste, which pollutes the environment (Buljan et al. 1997, Matyašovský et al. 2011). Modification of wood properties has been in the center of attention globally, and the research has been especially focused on modification of an entire volume thermo wood and change color, adhesion and liquid penetration (e.g., Kúdela et al. 2018). Thermo-oxidative

---

[1] VIPO, a.s., Gen. Svobodu 1069/4,958 01 Partizánske, Slovak Republic
[2] Technical University in Zvolen, T. G. Masaryka 24, 960 01 Zvolen, Slovak Republic
[3] Slovak Academy of Sciences, Polymer Institute, Dúbravská cesta 9, 845 41 Bratislava 45

stability of different materials and biopolymers was tested by differential scanning calorimetry (DSC) (Matyašovský *et al.* 2019). The research aimed not only on the study of properties of wood and adhesives, but as glued products are also the subject exposed to the environment in which they are located, and to study their interactions (Šmidriaková *et al.* 2011).

Glutaraldehyde (GA) is chemical matter, which is often tested for modification of hardeners; there is the assumption, which is completely cross-linked into the structure of the adhesive. Maminski *et al.* (2006) investigated melamine-urea-formaldehyde (MUF) adhesive, they added GA into the hardener in form of 50 % water solution. Shear strength of birch samples glued with modified adhesive was significantly higher in comparison with the reference sample. Also, there is a direct bond of GA with chemical compounds of wood, what significantly increase the strength of glued joint.

MATERIAL AND METHODS

In the experimental research, there were applied:

- UF resin KRONORES CB 1639F,
- hardener RODA M 210 pH = 7.4, overall nitrogen as N weight 21.5 %, amidic nitrogen weight 4.5 % (Duslo Šaľa, Slovakia).

For modification of UF resin, activators and selected modifiers were applied:

0. reference sample of UF resin – KRONORES CB 1639F,
1. collagen hydrolysate – prepared from leather collagen waste in VIPO,
2. starch – native corn starch MERIZET® 100,
3. mimosa extract – WEIBULL TANAC polyphenolic molecules of vegetable tannins,
4. quebracho extract – UNITAN polyphenolic condensed tannins,
5. glutaraldehyde 50% (GLT) – PROTECTOL GA-50, pH = 3.7,
6. methylol derivate (MOD) – pre-condensate prepared in VIPO,
7. lecithin from soy – phospholipids, (lecithin – phosphatidyl choline),
8. methyl ester fat 99.8% (MEKT)– prepared in VIPO,
9. extract from olive leaves – oleuropein, phenylethanoid, polyphenolic compounds,
10. keratin hydrolysate – prepared from sheep wool in VIPO.

Quality of gluing was tested according to standards EN 314-1 and EN 314-2. Three-layer plywood of beech (*Fagus sylvatica*) veneer was prepared for determination of physical and mechanical properties at following conditions: pressing pressure 1.8 MPa, temperature 105 °C, time 5 resp. 6 min. Plywood were conditioned at the temperature of 20 ± 2 °C and relative humidity 65 ± 5 %. Tested pieces were pre-treated for the class 1:

- immersion in water 20 °C for 24 hours,
- constant rate loading,
- disruption after 30 ± 10 seconds,
- accuracy of 1 N.

Formaldehyde emissions from five-layer plywood of beech were tested according to the test method JIS A 1460 “Building boards. Determination of formaldehyde emission. Desiccator method” according to following conditions:

- volume of desiccator: 9-11 dm^3,
- loading coefficient: 1800 cm^2,
- temperature of 20 ± 0.5 °C,
- test duration 24 h,
- the analytical method: acetylacetone method with spectrophotometric evaluation.

Experimental research was aimed on preparation of adhesive mixtures and testing their influence on viscosity, thickness swelling, strength of glued joint and formaldehyde emission.

Adhesive mixtures were prepared according to following scheme:
0 – Reference sample – 100% UF resin + 20% technical flour + 4% hardener
1 – UF resin + 18% technical flour + 2% collagen + 4% hardener
2 – UF resin + 18% technical flour + 2% native starch + 4% hardener
3 – UF resin + 18% technical flour + 2% mimosa powder + 4% hardener
4 – UF resin + 18% technical flour + 2% quebracho powder + 4% hardener
5 – UF resin + 20% technical flour + 2% glutaraldehyde 50 % + 4% hardener
6 – UF resin + 20% technical flour + 2% methylol pre-condensate + 4% hardener
7 – UF resin + 20% technical flour + 2% lecithin from soy + 4% hardener
8 – UF resin + 20% technical flour + 2% methyl ester fat + 4% hardener
9 – UF resin + 20% technical flour + 2% extract from olive + 4% hardener
10 – UF resin + 20% technical flour + 2% keratin + 4% hardener

RESULTS AND DISCUSSION

For determination of applicability of proposed additives into UF resin KRONORES CB 1639F, adhesive mixtures were prepared with parameters comparable to reference sample.

Determination of viscosity

The influence of addition of modified additives on the viscosity of UF adhesive mixture is graphically presented in Figure 1.

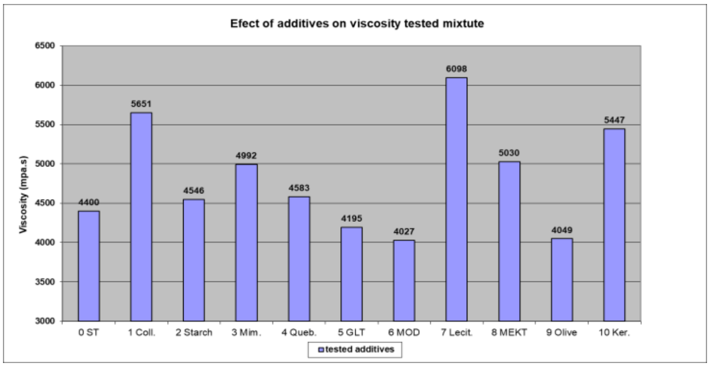

Figure 1. Viscosity of UF adhesive mixture

Results of dynamic viscosity of UF adhesive mixtures confirmed:

- additives starch, quebracho, GLT, MOD and extract from olive leaves are suitable for modification viscosity,
- additives lecithin, collagen and keratin increase viscosity – there is necessary lowering amount of technical flour added into UF resin.

–

Determination of thickness swelling

The influence of addition of modified additives on the thickness swelling of prepared plywood is presented in Table 1.

Table 1. Thickness swelling of test pieces of plywood after 2 and 24 h

Sample No.	Thickness swelling after 2h	Thickness swelling after 24 h
0 standard	20.61	40.84
1 collagen	23.50	42.62
2 starch	23.70	43.76
3 mimosa	14.97	32.21
4 quebracho	19.08	37.14
5 GLT	19.21	37.83
6 MOD	19.16	36.83
7 lecithin	20.43	38.52
8 MEKT	26.57	44.10
9 olive	22.95	40.64
10 keratin	17.80	35.31

From measured values of thickness swelling of plywood test pieces after 2 and 24 h follow, that thickness swelling is improved by modifiers:
3 – UF resin + 18% technical flour + 2% mimosa powder + 4% hardener
4 – UF resin + 18% technical flour + 2% quebracho powder + 4% hardener
5 – UF resin + 20% technical flour + 2% glutaraldehyde 50 % + 4% hardener
6 – UF resin + 20% technical flour + 2% methylol pre-condensate + 4% hardener
7 – UF resin + 20% technical flour + 2% lecithin + 4% hardener
10 – UF resin +18% technical flour + 2% keratin hydrolysate + 4% hardener

Quality of gluing
Obtained results of the influence of modifications on shear strength of plywood test pieces are presented in Table 2.

Table 2. Shear strength of plywood test pieces

Sample No.	Shear strength					
	Avg. **x** (MPa)	St. dev. **s** (MPa)	variability **v_k** (%)	value **min.** (MPa)	value **max.** (MPa)	n
0	**1.92**	0.18	9.3	1.61	2.19	15
1	**2.05**	0.19	9.0	1.84	2.44	15
2	**2.63**	0.20	7.6	2.40	3.07	15
3	**2.41**	0.14	5.8	2.19	2.64	15
4	**2.41**	0.16	6.7	2.19	2.74	15
5	**2.80**	0.20	7.2	2.45	3.11	15
6	**2.60**	0.14	5.3	2.45	2.84	15
7	**1.26**	0.18	14.5	0.99	1.56	15
8	**1.98**	0.20	10.3	1.69	2.23	15
9	**2.11**	0.15	7.0	1.85	2.34	15
10	**1.76**	0.09	5.2	1.58	1.92	15

Note. EN 314-2 requires the value of shear strength 1.0 MPa.

Tested plywood fulfils requirement of the standard for class of gluing 1 – they are suitable for application in normal interior environment. The highest shear strength (2.8, 2.6 and 2.6)

MPa were obtained for samples of glutaraldehyde 50% – PROTECTOL GA-50, native corn starch and methylol derivate – pre-condensate prepared in VIPO.

Formaldehyde emission

Obtained results of the influence of modifications on formaldehyde emission of tested samples are graphically presented in Figure 2.

Measured values of extinctions of formaldehyde tested samples confirmed decreasing of emissions for each additive in comparison with reference sample. The most significant decrease of formaldehyde emission down to 30% was obtained for modification No. 6 – UF resin + 20% technical flour + 2% methylol pre-condensate + 4% hardener and No.10 biopolymer Keratin - samples were prepared in VIPO.

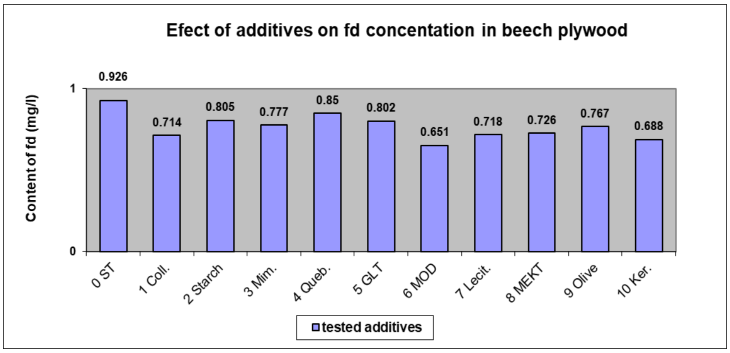

Figure 2. Results of formaldehyde emission by desiccator method

CONCLUSION

1. Lecithin from soy, collagen and keratin are mostly increasing the viscosity of UF adhesive mixtures in comparison with the reference sample from the value 4400 mPa.s up to 6098 mPa.s. There is necessary lowering of application of technical flour into UF adhesive mixtures.
2. The influence of addition of modified additives on the thickness swelling of prepared plywood was stated and the thickness swelling is improved by mimosa, keratin, quebracho, glutaraldehyde, methylol pre-condensate and lecithin.
3. Plywood fulfils requirements of the standard for class of gluing 1 – they are suitable for interior applications. Highest shear strengths (2.8, 2.6 and 2.6) MPa were obtained for samples of glutaraldehyde 50%, native corn starch and methylol derivate prepared in VIPO.
4. Measured values confirmed the decrease of formaldehyde emissions for all additives in comparison with the reference sample. The most significant decrease of formaldehyde emission down to 30% was obtained for modification No. 6 – UF resin with methylol pre-condensate.

ACKNOWLEDGEMENTS

This work was supported by the Slovak Research and Development Agency under the contracts No. APVV-14-0506, APVV-18-0378, APVV-19-0269, APVV-21-0051. This work was supported by the project VEGA 1/0264/22.

REFERENCES

1. Příhoda, P., Jech, L. 1988. Hygienické aspekty problematiky formaldehydu unikajícího z výrobků dřevozpracujícího průmyslu. In Syntema – Chemizace dřevo průmyslu. Dom techniky ČSVTS Brno. 1988, p. 45-53.
2. Buljan, J., Reich, G., Ludvik, J. 1997. Mass balance in leather processing. Proceedings of the Centenary Congress of the IULCS, London, 138-156.
3. Matyašovský, J., Sedliačik, J., Jurkovič, P., Kopný, J., Duchovič, P. 2011. De-chroming of Chromium Shavings without Oxidation to Hazardous Cr^{6+}. The journal of the American Leather Chemists Association 106(1), 8-17.
4. Matyašovský, J., Sedliačik, J., Šimon, P., Novák, I., Krystofiak, T., Jurkovič, P., Duchovič, P., Sedliačiková, M., Cibulková, Z., Mičušík, M., Kleinová, A. 2019. Antioxidant Activity of Keratin Hydrolysates Studied by DSC. The journal of the American Leather Chemists Association 114(1), 20-28.
5. Kúdela, J., Andor, T. 2018. Beech wood discoloration induced with specific modes of thermal treatment. Annals of Warsaw University of Life Sciences 103, 64-69.
6. Šmidriaková, M., Sedliačik, J., Matyašovský, J. 2011. Prírodné polyméry na báze modifikovaného kolagénu ako čiastočná náhrada UF lepidla. In: Adhesives in Woodworking Industry. Zvolen, 14-20.
7. Maminski, M.L., Pawlicki, J., Parzuchowski, P. 2006. Improved water resistance and adhesive performance of a commercial UF resin blended with glutaraldehyde. The Journal of Adhesion 82(6), 629-641.

CHIP AND CHIPLESS WOODWORKING PROCESSES, 13(1): 175–181, 2022
Zvolen, Technical University in Zvolen, ISSN 1339-8350 (online), ISSN 2453-904X (print)

EFFECT OF HYDROTHERMAL TREATMENT ON SURFACE QUALITY OF BEECH WOOD AFTER PLANE MILLING

Ľubomír Rajko – Peter Koleda – Štefan Barcík – Vlado Goglia

Abstract

This article deals with issues of influence of selected technical, technological and tools factors during face milling of beech wood which is modified by saturated water steam with emphasis on surface quality. Experiments were conducted on samples which were modified by saturated water steam at temperatures (T=105, 125 and 135 °C) however one of them was in native state, feed rate was (6, 10, 15 m.min^{-1}), cutting speed was (20, 40, 60 m.s^{-1}) and rake angle was (20, 25, 30°). Experimental measurement of surface quality was conducted via laser device LPM – 4. In the article, the effect of the thermal modification mode and cutting speed on the resulting surface quality was investigated.

Key words: *roughness, hydrothermal treatment, cutting speed, feed rate, beech wood, milling*

INTRODUCTION

Wood and its use are of great importance to humanity, whether it is the use of wood for exterior or interior. Due to outer influences, the mechanical and aesthetic properties of wood can be reduced (Kokutse *et* al. 2006, Kaplan *et* al. 2018). The inactivated wood surface also presents smaller roughness, reducing losses in planning machine and high-quality wood surfaces, which may be important for many wood applications.

There are currently several types of thermal treatment of wood, the principle of which is different depending on the medium and temperature used (Navi and Sandberg 2012, Dzurenda and Deliiski, 2019). The most well-known types of thermal treatment are ThermoWood in Finland, Plato Wood in the Netherlands, oil-heat treatment (OHT) in Germany, and Les Bois Perdure and retification process (Retiwood) in France (Esteves and Pereira 2011; Sandberg and Kutnar 2016). In general, thermal treatment can be defined as a process in which high temperatures ranging between 150 and 260 °C are applied to wood in an environment with different types of media (steam, nitrogen, oil, etc.) without chemical substances (Sandberg and Kutnar 2016).

Nowadays, milling as a machining of the material is process which is come to the fore. Milling is the process of machining using rotary cutters to remove material by advancing a cutter into workpiece. The milling process uses a rotary tool called a milling cutter. (Sedlecký *et* al. 2018; Siklienka *et al*. 2013; Lisičan 1996).

The precision of surface roughness is a result of repetitive cutting edge activity on the workpiece surface, it depends mainly on cutting speed, depth of cut, feed rate and geometry

Technical University in Zvolen, T. G. Masaryka 24, 960 01 Zvolen
e-mail: peter.koleda@tuzvo.sk

of cutting tool. The precision of surface roughness of the milled parts requires increased attention for the following surface technological treatment. Suitable cutting conditions can achieve an improved surface quality during woodworking (Prokeš 1982; Kačíková and Kačík 2011, Budakçı *et al.* 2013) and optimization of energy consumption (Kubš *et al.* 2017; Koleda *et al.* 2018).

The aim of the study was to determine the influence of the heat treatment temperatures of beech wood and cutting speed during milling on the quality of milled surface. This research is part of a study of the properties of woodworking thermally modified beech wood by saturated water steam that is focused on measuring the quality and energy of the machining process.

MATERIALS AND METHODS

The milling blades which were used for experimental milling had dimensions 45 × 35 × 6 mm (h × w × t) (Fig. 1), which were made of tool steel HSS 18 % W with AlTiCrN surface induction hardened. The milling blades were coated by the method PVD (Physical Vapor Deposition). The coating process of the blades was carried out in the company WOOD – B s.r.o in Nové Zámky, Slovakia. The chemical composition of the milling blades is shown in Tab. 1.

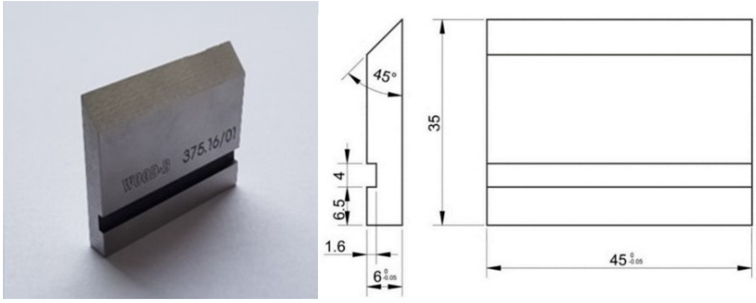

Fig. 1 Changeable milling blade

Table 1 Chemical Composition of Used Milling Blades

Blade from the tool steel 19 573							
Co	**Mn**	**Si**	**P**	**S**	**Cr**	**Mo**	**V**
1,4 ÷ 1,65	0,2 ÷ 0,45	0,2 ÷ 0,45	0,03	0,035	11 ÷ 12,5	0,6 ÷ 0,95	0,8 ÷ 1,20

The blades were clamped in the milling heads marked FH 45 STATON made in SZT – machines Turany, with parameters mentioned in the table 2.

Table 2 Parameters of Milling Head

Diameter of the Cutter Body	125 [mm]
Diameter of the Cutter Body with Blades	130 [mm]
Thickness of the Cutter Body	45 [mm]
Number of Blades	2 [pc]
Maximum speed	8000 (min^{-1})
Rake Angle	$\gamma = 20°, 25°, 30°$

Beech wood (*Fagus sylvatica*) was used as a material for the samples. From the logs, the boards of the radial medial timber with a thickness of 25 mm were first manipulated on a band saw. Moisture of boards were w > 45%. The boards were dried to 12 % moisture content in a wood drying kiln in KAD 1x6 (KATRES s.r.o.) at the company Sundermann spol. s.r.o (Banská Štiavnica Slovak republic). Subsequent processing of the boards, samples were obtained by circular saw DMMA 35 (Rema s.a., Reszel, Poland) and wood thickness planer machine F2T80 (TOS Svitavy, Czech Republic). Samples with dimensions of 600 mm × 100 mm × 20 mm were heat – treated in an APDZ 240 autoclave at a higher saturated water steam pressure than atmospheric pressure. The process of thermal treatment of the material was carried out at the company Sundermann spol. s.r.o (Banská Štiavnica Slovak republic). Fig. 2 shows the course of heat treatment of samples.

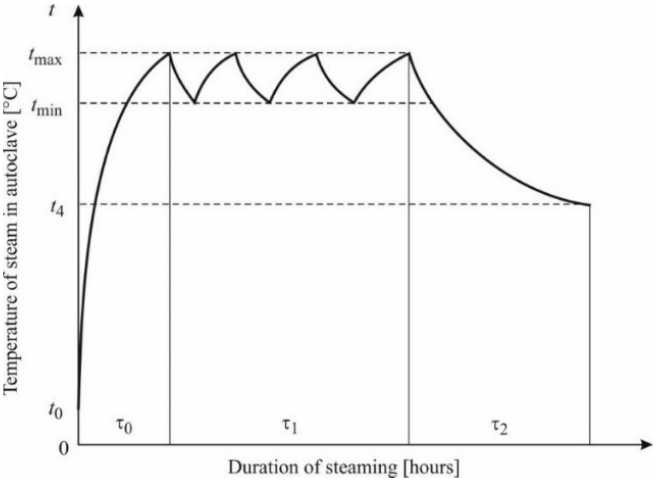
t
t_max
t_min
t_4
t_0
0
Temperature of steam in autoclave [°C]
τ0
τ1
τ2
Duration of steaming [hours]

Fig. 2 Time course of heat-treatment

Table 3 Modes of thermal treatment of beech wood with saturated steam

Modes	Temperature of saturated steam [°C]			Steaming time in hours [hours]			
	t_{max}	t_{min}	t_4	τ_0 - heating	τ_1 - phase I	τ_2 - phase II	Total time
Steaming mode I.	107.5	102.5	100	≈1.5	3.5	1.0	≈ 6.0
Steaming mode II.	130.0	125.0	100		4.0	1.0	≈ 6.5
Steaming mode III.	140.0	135.0	100		4.5	1.0	≈ 7.0

The density measurement of the experimental samples was conducted according to the STN 49 0108 standard. All samples were weight by laboratory scale with a measuring accuracy of 0,01 g and subsequent measurement by a calliper with an accuracy of 0,01 mm. The resulting values of dimensions and weights of the samples were processed and the measured values of the density was calculated according to $\rho_w = m_w/V_w$.. The average density values which are calculated from obtained values and percentage change compared to native wood are shown in the table 4.

Table 4 Measured Values of the Bulk Density of Beech Wood

Thermal Treatment [°C]	**Density [kg.m^{-3}]**	**Percentual change [%]**
Native Wood	683,5	-
105 °C	671,8	-1,74%
125 °C	691,9	1,21%
135 °C	705,1	3,05%

The milling process was performed on the lower spindle miller ZDS-2 (Liptovské strojárne, Slovakia). The feeding was ensured by the feeding device Frommia ZMD 252/137 (Maschinenfabrik Ferdinand Fromm, Fellbach, Germany) (Fig. 3). The cutting conditions were as follow: cutting speed: 20, 40 a 60 m.s^{-1}, feed rate: 6, 10 a 15 m.min^{-1}, rake angle: 20°, 25° and 30°.

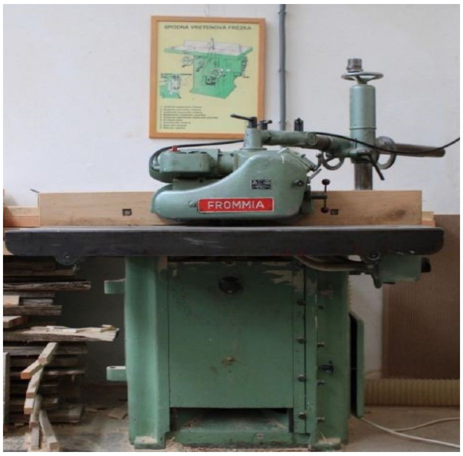

Fig. 3 Lower spindle milling machine FVS and feeder mechanism Frommia ZMD 252/137

The measurement of the surface quality was conducted after the milling of experimental samples by laser device LPM – 4 (Fig. 4). A digital camera captured images of the laser line at an angle and, based on the scanned image, the object profile in the cross-section was evaluated. The roughness measurement was made on three points of the sample; on the entrance of the sample into the cut, on the center of sample, and on the output of sample of the cut to monitor the changing of surface roughness on the input of the tool. This was measured after stabilization and on the output of tool of the cut, as well as in three wide zones on the edges and in the middle of sample thickness. The bottom spindle milling machine which is equipped by a three phase asynchronous engine was controlled via a frequency changer UNIFREM 400 007M (Vonsch s.r.o., Brezno, Slovak Republic). Frequency changer was connected to computer via USB serial converter USB. The program LPM - View was used to graphically display of the resulting values and then this values were saved to program Excel to another processing by STATISTICA 12.

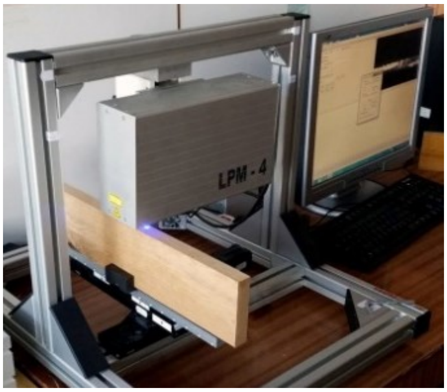

Fig. 4 Laser device LPM – 4

RESULTS AND DISCUSSION

From the Fig. 5 the highest surface roughness depending on the temperature of thermal modification was achieved during heat treatment of the sample at 125 °C. The subsequent decrease of surface roughness was occurred with thermally treated samples to 135 °C and by samples without thermally modification and so in native state. According to the graph, it can be claimed that the lowest achieved value of surface roughness was at the heat treatment at 105 °C.

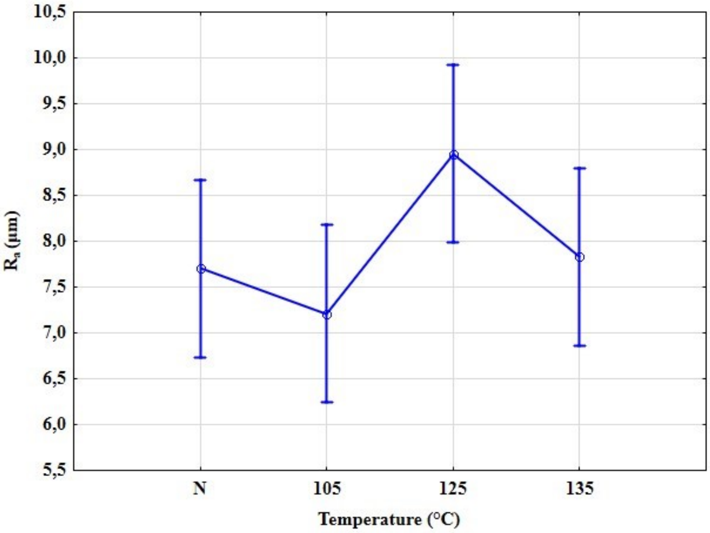

Fig. 5 Effect of thermal treatment on the surface quality

The results of the experiment can be compared with ThermoWood technology which is similar with PlatoWood. Regarding research on the roughness of heat-treated wood, it is possible to compare this work with Barcík *et al.* (2014) and Kvietková *et al.* (2015), who studied pine, beech and birch wood. For the roughness evaluation in their experiments, the contact method was used for the surface roughness measurement. Considering these results, it was justified in stating that it is possible to draw on the knowledge and laws of the work to understand the issue.

According to Kaplan *et al.* (2018) who examined oak wood, proclaimed that thermal modification of wood does not affect the average roughness values after machining. Based on results was discovered that the difference between the measured roughness values of treated and untreated wood was negligible.

CONCLUSIONS

Thermal modification by water saturated steam affected the surface quality; the best quality was achieved for the sample treated at 105 °C. By increasing the temperature, the surface roughness was increased, and the worst results were at the thermal treatment at 125 °C. Thermal treatment at 135 °C caused an increase in the surface roughness compared to the natural material.

ACKNOWLEDGMENTS

The paper was written with the support of project APVV-20-0403, “FMA analysis of potential signals suitable for adaptive control of nesting strategies for milling wood-based agglomerates,“ project APVV 17/0456 “Thermal modification of wood with water vapor for purposeful and stable change of wood colour,“ and thanks to support under the Operational Program Integrated Infrastructure for the project: National infrastructure for supporting technology transfer in Slovakia II – NITT SK II, co-financed by the European Regional Development Fund.

REFERENCES

Barcík, Š., Gašparík, M., Houska, A., Razumov, E. Y., Sedlecký M. 2014. „Vliv technologických faktorů na kvalitu opracování povrchu při frézováni termicky modifikovaného borovicového dřeva“ [Influence of technological factors on surface finish quality during milling of thermally modified pine wood], In: Trieskové a beztrieskové obrábanie dreva 2014. Zborník prednášok 9(1): 11–22, 2014, ISSN 1339-8350

Budakçı, M., İlçe, A. C., Gürleyen, T., Utar. M. 2013. Determination of the surface roughness of heat-treated wood materials planed by the cutters of a horizontal milling machine.

Dzurenda, L., Deliiski, N. 2019. Tepelné procesy v technológiách spracovania dreva. Zvolen: TU vo Zvolene, 283 s. ISBN 978-80-228-3192-5.

Esteves, B. M., and Pereira, H. M. 2009. “Wood modification by heat treatment: A review,” BioResources 4(1), 370-404. DOI: 10.15376/biores.4.1.370-404

Kačíková, D., Kačík, F. 2011. Chemické a mechanické zmeny dreva pri termickej úprave. Zvolen: Technická univerzita vo Zvolene.

Kaplan, L., Kvietková, MS., Sikora, A., Sedlecký, M. 2018. “Evaluation of the effect of individual parameters of oak wood machining and their impact on the values of waviness measured by a laser profilometer,“ *WoodRessearch* 63(1), 127-140

Kokutse, A.D., Stokes, A., Bailléres, H., Kokou, K., Baudasse, Ch. 2016 Decay resistance of togolese teak (Tectona grandis L.f) heartwood and relationship with colour. Trees 20(2), 219-223. DOI: 10.1007/s00468-005-0028-0

Kvietková M., Gaff M., Gašparík, M., Kaplan, L., Barcík, Š. 2015. Surface quality of milled birch wood after thermal treatment at various temperatures. BioResources 10(4), 6512-6521. DOI:10.15376/biores.10.4.6512-6521 ISSN: 1930-2126.

Lisičan, J. (1996). *Teória a Technika spracovania dreva* [*Theory and technique of wood processing*], Matcentrum, Zvolen (in Slovak).

Reinprecht, L., Vidholdová, Z. 2008. *Termodrevo – príprava, vlastnosti a aplikácie*. Zvolen, Technical University in Zvolen, ISBN 978-80-228-1920-6.

Prokeš, S. 1982. *Obrábění dřeva a nových hmot ze dřeva* [*Machining of wood and new wood materials*], SNZI, Prag, Czech Republic

Sandberg, D., Kutnar, A. 2016. Thermally modified timber: recent developments in Europe and North America. Wood and fiber Science: journal of the Society of Wood Science and Technology 48, 28-39

Sedlecký, M., Kvietková, M., Kminiak, R., Kaplan, L. 2018. Medium-density fiberboard and edge-glued panel after edge milling - surface waviness after machining with different parameters measured by contact and contactless method. Wood Research 63(4), pp 683-698

Siklienka, M., Kminiak, R. 2013. *Delenie a obrábanie dreva. 1. vyd.* [Cutting and machining of wood. 1st edition] Zvolen, Technical University in Zvolen, 207 s. ISBN 978-80- 228-2618- 1

CHIP AND CHIPLESS WOODWORKING PROCESSES, 13(1): 183–188, 2022
Zvolen, Technical University in Zvolen, ISSN 1339-8350 (online), ISSN 2453-904X (print)

EVALUATION OF PROPERTIES OF DATE PALM WOOD COMPOSITES WITH POLYOLEFIN

Ján Sedliačik[1] – Peter Jurkovič[2] – Igor Novák[3] – Igor Krupa[4] – Ján Matyašovský[2]

Abstract

Low-density polyethylene (LDPE) was blended with date palm (Phoenix dactylifera) wood powder to prepare composites with various concentrations of filler ranging from 10-70 wt. %. The Young´s modulus of the composites significantly increased with an increase of the filler content in the entire concentration range. The maximum value for the composite filled with 70 wt. % of the filler is approximately 13 times higher than that for the pristine LDPE. The incorporation of date palm wood into the LDPE matrix led to a significant increase in the polarity of composites and to an increase in their adhesion to polar substrates.

Key words: *date palm wood, polyethylene, wood/polyolefin composite, adhesion*

INTRODUCTION

Polyethylene based matters were successfully used for a dimensional stabilization of wood (1), bonding of veneer (2) or investigated epoxy resins reinforced with long date palm fibres (3). The authors searched the optimum length of embedded fibres that have controlled interfacial adhesion properties and determined that 10 mm was the optimum length. Similar research focused on the effect of diameters and alkali treatments on the tensile properties of date palm fibre reinforced epoxy composites was performed by some authors (4). The alkali treatment of date palm fibres was able to provide good adhesion within the matrix and the tensile strength, elastic modulus and the fibre-matrix interaction of the composite were improved. Date palm wood powder/glass fibres reinforced hybrid composites of recycled polypropylene were investigated by many researchers (5, 6).

Wetting of wood based materials by standard liquids is a complex process controlled by chemical composition of the liquids used, properties of the substrate, interactions among unsaturated force fields across the phase boundary between wood and liquid, as well as by secondary effects of a range of factors implied by specific properties of the wood and the liquids used (8).

The aim of this contribution was evaluation of selected mechanical properties (static and dynamic) of composites based on low-density polyethylene and date palm wood powder. The polarity and adhesive properties of the prepared composites was also studied.

---

[1] Technical University in Zvolen, T. G. Masaryka 24, 960 01 Zvolen, Slovak Republic
[2] VIPO, a.s., Gen. Svobodu 1069/4,958 01 Partizánske, Slovak Republic
[3] Slovak Academy of Sciences, Polymer Institute, Dúbravská cesta 9, 845 41 Bratislava 45,
[4] QAPCO Polymer Chair Center for Advanced Materials, Qatar University, Quatar
e-mail: sedliacik@tuzvo.sk

MATERIAL AND METHODS

Low density polyethylene was used as the matrix (melting point = 110.6 ± 0.1 °C and date palm wood powder was used as the filler.

The majority of the filler particles had sizes ranging from 0.25 to 1 mm. The composites of polyethylene with date palm wood (DW) were prepared by mixing both components in the 30 ml mixing chamber of a Brabender Plasticorder PLE 331 at 140 °C for 10 minutes at a mixing speed of 35 rpm. 1-mm thick slabs were prepared by compression moulding in laboratory press at 140 °C for 1 minute. Dog-bone shaped specimens with a working area of 30×4×1 mm were cut from the slabs. The mechanical properties were measured at room temperature using an Instron 3365 universal testing machine at a deformation rate of 50 $mm.min^{-1}$.

For adhesive tests Epoxy resin CHS-Epoxy 531, polyamine hardener Telalit 410 (Spolchemie), mixing ratio of epoxy resin to hardener = 4 : 1 weight parts, dichloromethane (Merck) have been used.

The surface properties of the polyethylene (PE) were determined by measuring the contact angles of re-distilled water using a Surface Energy Evaluation (SEE) system coupled with a web camera (Advex) and PC software. The drops of water, which was used as a testing liquid (V = 3 μl), were placed on the polymeric surface with a micropipette (0 - 5 μl, Biohit), and the contact angle of the testing liquid was measured.

RESULTS AND DISCUSSION

Surface and adhesive properties

The surface and adhesive properties of the LDPE/DW composites were investigated. The dependence of the water contact angle on composite surface vs. the filler content in PE is shown in Figure 1.

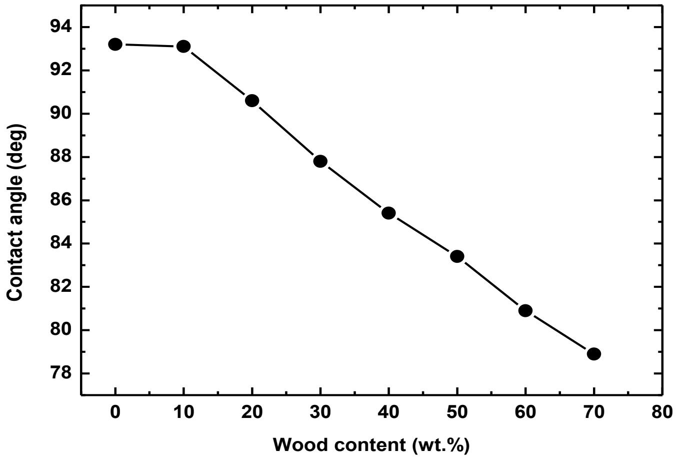

Figure 1. Water contact angle on the LDPE/DW surface vs. DW filler content.

The increase in the filler content results in a more polar nature of the composite material. The dependence of the water contact angle vs. the wood content decreases nonlinearly. The water contact angle on the LDPE/DW composite surface significantly decreases with the DW concentration from 93.2 deg (unfilled polyethylene) to 87.8 deg (30 wt. % of wood in composite), and to 78.9 deg (70 wt. %. of the filler). For the surface properties, it can be concluded that the water contact angles on the surface of the LDPE/DW composites decreased from 93.2 deg (unfilled polyethylene) to 78.9 deg (LDPE/DW composite filled with 70 wt. % of the filler).

The results of the shear strength in the adhesive joint LDPE/DW composite – epoxy vs. filler content are shown in Figure 2. Figure 2 reveals an increase in the shear strength of the adhesive joint between the LDPE/DW composite and the epoxy substrate with an increase of the filler content. As shown in Figure 2, the shear strength of the adhesive joint significantly increased from 0.62 MPa (unfilled PE) to 1.37 MPa if filled with 70 wt. % of DW. The shear strength of the adhesive joint between the LDPE/DW composite and the epoxy resin significantly increased from 0.62 MPa (unfilled PE) to 1.37 MPa (LDPE/DW composite with 70 wt.% of the filler).

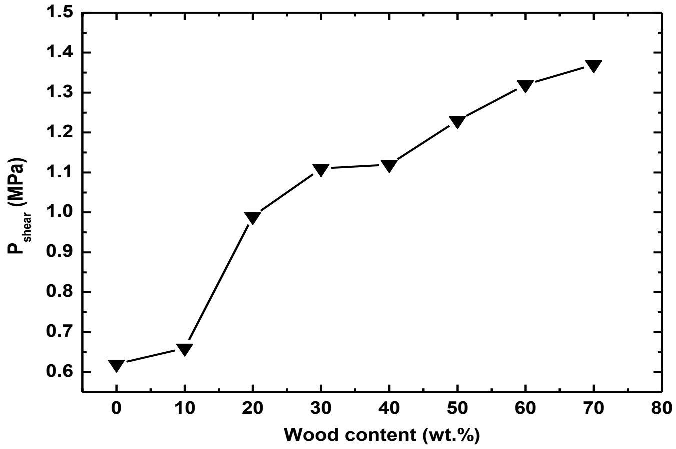

Figure 2. Shear strength of adhesive joint LDPE/DW composite – epoxy adhesive vs. DW filler content.

Mechanical properties

The mechanical properties of the composites tested in the tensile mode at room temperature (25 °C) were characterised. The static mechanical properties evaluated from the stress-strain curves included the yield point, stress and elongation at break and Young's modulus. The stress-strain curve of LDPE is shown in Figure 3.

Figure 3 reveals significant cold drawing and good deformability up 650%. The materials also undergo strain (orientation) hardening, which results in a high strength at break. There are also two distinguished yield points in the curve, which is a common behaviour for polyolefin, that have a broad size distribution of crystallites. A yield point in polymers is conventionally accepted as being the point where the stress-strain curve exhibits a local maximum.

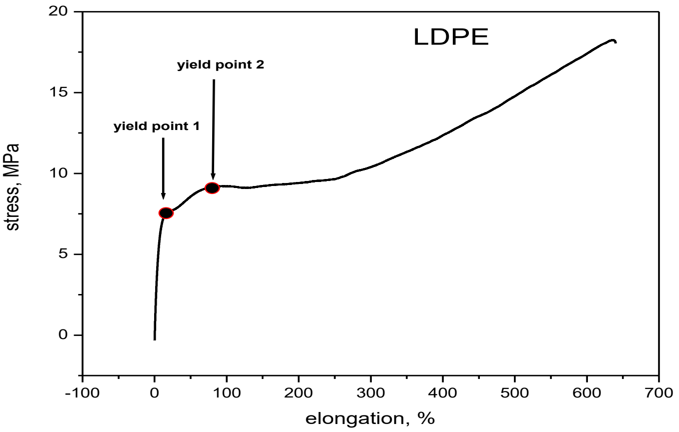

Figure 3. The stress-strain curve of pristine LDPE.

For samples that initially deform homogeneously, this maximum occurs as a result of the internal plastic strain rate of the material increasing to a point where it becomes equal to the applied strain rate. In some cases, a maximum in the force also relates to the onset of necking, where the strain hardening of the necked materials is not sufficient to counteract the reduction of the cross-sectional area, which leads to a reduction in load. This maximum may become less defined as the testing temperature is increased or as the strain rate is decreased, until it disappears. The temperature where the local maximum disappears is lowest for the most branched material and highest for the unbranched, high-density material. The yielding phenomenon of semi-crystalline polymers has been associated with a change in the morphology of the material, where a spherulitic structure transforms into a fibrillar one. During stretching, this change occurs through shearing and fragmentation of the crystalline lamellae into blocks that rearrange into the form of parallel microfibrils. The stress-strain curve of composite consisting of 10 wt.% of PWP is shown in Figure 4.

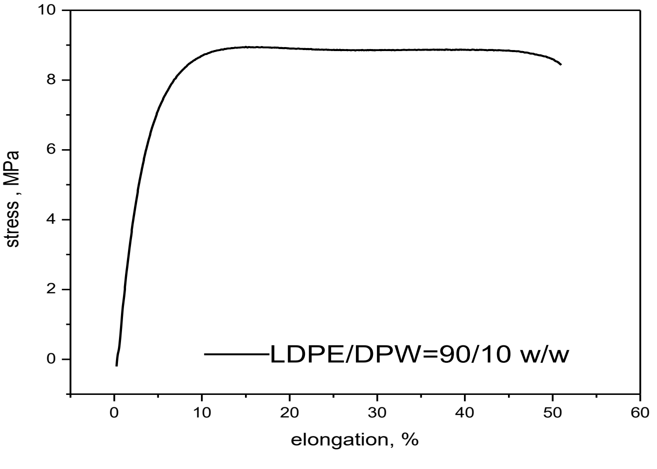

Figure 4. The stress-strain curve of LDPEV/DPW=90/10 w/w.

A dramatic decrease in drawability is observed, even at this very low filler content. The filler particles represent defects and stress concentrators and significantly reduce the drawability of the matrix. The orientation hardening is completely suppressed; however, the material exhibits some extent of plastic deformation. In this case, the rupture is not brittle. The behaviours of the composites filled with 20 and 30 wt.% of wood are similar. However, if the matrix is filled with 40 wt.% of the filler and greater, the material becomes brittle. The mechanical properties of the composites are summarised in Table 1.

Table 1. Mechanical properties of the composites at 25 °C. The x/y notation represents the LDPE/DPW w/w ratio.

Sample	φ	$\varepsilon_y \pm S\varepsilon_y$ (%)	$\sigma_y \pm S\sigma_y$ (MPa)	$\varepsilon_b \pm S\varepsilon_b$ (%)	$\sigma_b \pm S\sigma_b$ (MPa)	$E \pm S_E$ (MPa)
LDPE	0	15.5[a] (0.3)	8.0 (0.2)	633 (20)	18.5 (0.7)	150 (7)
90/10	0.069	15.2 (0.3)	9.2 (0.2)	22.0 (19)	9.0 (0.3)	285(22)
80/20	0.142	br	br	8.8 (0.6)	9.2 (0.4)	376 (22)
70/30	0.221	br	br	4.8 (0.6)	9.4 (0.2)	562 (71)
60/40	0.306	br	br	3.2 (0.3)	9.3 (0.5)	800 (42)
50/50	0.398	br	br	2.1 (0.1)	9.7 (0.5)	1064 (83)
40/60	0.498	br	br	1.4 (0.1)	10.2 (0.4)	1457 (122)
30/70	0.608	br	br	1.1 (0.1)	11.1 (0.6)	1933 (124)

Where:

ε_y, σ_y, ε_b, σ_b, E – elongation at yield, yield stress, elongation at break, stress at break, and Young's modulus of elasticity,

$S\varepsilon_y$, $S\sigma_y$, $S\varepsilon_b$, $S\sigma_b$, S_E – standard deviations,

φ – the volume portion of the filler,

br – refers to the brittle rupture.

The stiffness and hardness of the composites, which are characterized by the Young´s modulus, significantly increase with an increase in the filler content in the entire concentration region. The maximum value of 1933 MPa for the specimen filled with 70 wt.% of the filler is approximately 13 times greater than the one of the LDPE. This result indicates that the filler has a very strong reinforcing effect. Similar results were achieved by AMMAR et al. (2019) who obtained results showed that the sample made from date palm fibers and bio-matrix from lignin-glyoxal-resin thermo pressed in the ratio of 50/50 wt.% has the best mechanical properties.

The stress at the break of the composites and the dependence on the filler fraction varies nonlinearly. We have considered two influences of the filler on the stress at the break. On the one hand, we have to consider that the reinforcing effect of the filler leads to an increase in the tensile stress values with an increase of the filler fraction and, on the other hand, that the orientation strengthening occurs for semi-crystalline polymers at high deformation. The latter effect is indirectly negatively influenced by the filler presence and by a steep decrease in the deformation such that orientation of the matrix cannot occur. At low filler fractions, the deformation is sufficiently low to prevent the orientation, but the reinforcing effect of the filler presence is marginal. The particles of the filler represent defects and stress concentrators. The behavior of the stress-strain curve is changed; orientation hardening and cold flow are suppressed. The samples break close to the yield point. Therefore, an initial dramatic decrease of tensile strength has been observed. The initial stress at the break of

LDPE (18.5 ± 0.7 MPa) decreased to a value of 9.0 ± 0.3 when it was filled with 10 wt. % of the filler. However, in this case, only the orientation hardening was suppressed. The cold flow occurs only up to 10 wt.% of the filler. After this level, if the filler content increases, material becomes brittle. The slight increase in the stress at break at higher filler contents is caused by the reinforcing effect of the filler.

CONCLUSION

A fine powder with a fibrous shape was prepared from date palm wood by grinding in a high energy mill. The prepared fibers have a broad size distribution; the majority of the fibers have a length between 1 and 3 mm. Low density polyethylene was used as the matrix for preparing LDPE/DPW composites. The filler concentration ranged from 10 to 70 wt.%. The stiffness and hardness of the composites, which were characterized by the Young´s modulus, significantly increased with an increase in the filler content in the entire concentration range. The maximum value of 1933 MPa for the composite filled with 70 wt.% of the filler is approximately 13 times greater than that for the LDPE. This result indicates that the filler has a strong reinforcing effect and that there is a good distribution of the filler. Furthermore, the stress at the break of the composites and its dependence on the filler fraction varies nonlinearly. The material becomes brittle if filled with more than 10 wt. % of the filler. The incorporation of DPW into the LDPE matrix led to a significant increase in the polarity of composites and to an increase in their adhesion to polar substrates.

ACKNOWLEDGEMENTS

This work was supported by the Slovak Research and Development Agency under the contracts No. APVV-16-0177, APVV-17-0583 and APVV-18-0378. This work was supported by the project VEGA 1/0264/22.

REFERENCES

1. Repák, M., Reinprecht, L. 2020. Physico-mechanical properties of thermally modified beech wood affected by its pre-treatment with polyethylene glycol. In Acta Facultatis Xylologiae Zvolen 62(1), 67-78.
2. Bekhta, P., Sedliačik, J. 2019. Environmentally-friendly high-density polyethylene-bonded plywood panels. Polymers 11(7), 1166.
3. Alsaeed, T., Yousif, B.F., Ku, H. 2013. The potential of using date palm fibres as reinforcement for polymeric composites. Materials & Design 43, 177-184.
4. Abdal-Hay, A., Suardana, N.P.G., Choi, K.S., Lim, J.K. 2012. Effect of diameters and alkali treatment on the tensile properties of date palm fiber reinforced epoxy composites. International Journal of Precision Engineering and Manufacturing 13(7), 1199-1206.
5. Wolcott, M.P., Adcock, T. 2000. New advances in wood-fiber polymer formulations. In Proceedings of Wood-Plastic Conference. Plastics Technology Magazine and Polymer Process Communications. p. 107-114.
6. Mirski, R., Bekhta, P., Dziurka, D. 2019. Relationships between thermoplastic type and properties of polymer-triticale boards. Polymers 11(11), 1750.
7. Al-Otaibi, M.S., Alothman, O.Y., Alrashed, M.M., Anis, A., Naveen, J., Jawaid, M. 2020. Characterization of date palm fiber-reinforced different polypropylene matrices. Polymers 12(3), 597.
8. Kúdela, J. 2014. Wetting of wood surface by a liquids of a different polarity. In Wood Research 59(1), 11-24.

ISSN 2453-904X (print) ISSN 1339-8350 (online)